The Design and Synthesis of High Affinity Ligands for Cyclophilin A

Kirk James Malone

A thesis submitted for the degree of
Doctor of Philosophy

University of Edinburgh

November 2005

Acknowledgments

I would like to thank my supervisor Professor Nick Turner for all his help, encouragement and football banter during the time of my PhD research. I would also like to thank my collaborators on this project; Professor Malcolm Walkinshaw, Dr. Martin Wear, Dr. Brian McHew, Alan Patterson, Dr. Perdi Barran, Dr. Sally Shirran, and Hannah Florance; without their hard work and great support this thesis would not have been possible. I'd like to especially thank the two fellow chemists on the project, Dr. Kevin "Molerat" Bailey and Dr. Colin "Tiger" Dunsmore. Dimedone chemistry isn't that bad when you've got great mates to battle with you!

I'd like to really thank all the members of the Turner/Flitsch research group past and present for being brilliant people to work with and ensuring some fun nights out. I'd like to especially thank the gentlemen of Lab 25A; Tiger, Pigeon, Bear, TSC and Rooby-Dooby; for being great mates and making coming to work a pleasure.

I would like to say a special thank-you to my friends & family for all their help and support over the years. Finally I'd like to really thank Rachel for always being there for me despite us being at opposite ends of the country during our PhDs, and for all her continuing love and affection.

Contents

Abstract 9

Abbreviations 10

1 Introduction

1.1 Drug discovery 13

1.1.1 Historical drug discovery 13

1.1.2 Structure-based design 15

1.1.3 Peptidomimetic design 18

1.1.4 Chemical genetics 19

1.1.5 Conclusions 22

1.2 Peptidyl-prolyl *cis/trans* isomerases 24

1.2.1 PPIase activity 26

1.2.2 Cyclosporin A 28

1.2.3 Mechanism of immunosuppression 29

1.3 Involvement of cyclophilin in other disease areas 30

1.3.1 Cyclophilin A as an anti-HIV drug target 30

1.3.2 Cyclosporin A rheumatoid arthritis therapy 33

1.3.3 Anti-parasitic activity of cyclosporin A 34

1.4 Review of cyclophilin A ligands 35

1.4.1 Cyclosporin A derivatives 35

1.4.2 Sanglifehrins 37

1.4.3 Peptide ligands 39

1.4.4 Non-peptide ligands 41

1.5 Previous ligand design and lead discovery 43

1.5.1 Initial lead compound - dimedone 45

1.5.2 Lead optimisation 46

2 Results and Discussion I - Ligand Design and Synthesis

2.1 *O*-acylated dimedone enol esters 53

2.2 Alkyl-dimedone derivatives....56
2.3 Amide-linked derivatives....61
2.4 C-6 alkylated amide-linked derivatives....75
2.5 Alternate dimedone-based ligands....81
2.6 Ligand Optimisation....83
2.6.1 Lead compound selection....83
2.6.2 Alternate amino acids....86
2.6.3 Hydrophilic ligands....87
2.6.4 Cbz group replacement....88
2.6.5 Fluorescently labelled ligands....90

3 Results and Discussion II - Mass Spectrometry Screening
3.1 Introduction....96
3.2 Mass Spectrometry....96
3.2.1 Ionisation....96
3.2.2 Analysers....100
3.2.3 Tandem mass spectrometry....101
3.2.4 Detectors....102
3.3 Detection of protein complexes by ESI-MS....103
3.4 Analysis of Cyclophilin A by ESI-MS....106
3.5 Analysis of Cyclophilin A complexes by ESI-MS....108
3.5.1 Cyclophilin A:cyclosporin A....108
3.5.2 Cyclophilin A:synthetic ligands....112
3.5.3 Measuring dissociation constants by mass spectrometry....117
3.5.4 High throughput ligand screening....120
3.6 Conclusions....123

4 Results and Discussion III - Biological Assays
4.1 Introduction....127
4.2 Intrinsic fluorescence binding assay....127
4.2.1 Experimental methods....128
4.2.2 Results and discussion....130

4.3 Peptidyl-prolyl cis-trans isomerase (PPIase) assay....132
4.3.1 Experimental methods....133
4.3.2 Results and discussion....134
4.4 *In vivo* activity assay....135
4.5 Conclusions....139

5 Experimental
5.1 General techniques....143
5.2 Experimental procedures....144
5.2.1 *N-benzyloxycarbonyl-L-valinyl fluoride*....144
5.2.2 *3-(N-benzyloxycarbonyl-L-valinyl-oxy)-5,5-dimethyl -cyclohex2-enone*....145
5.2.3 *N-allyloxycarbonyl-L-phenylalanine*....146
5.2.4 *N-allyloxycarbonyl-L-phenylalaninyl fluoride*....147
5.2.5 *3-(N-allyloxycarbonyl-L-phenylalaninyloxy)-5,5 -dimethyl-cyclohex-2-enone*....147
5.2.6 *N-allyloxycarbonyl-1-amino-1-cyclopentanecarboxylic acid*....148
5.2.7 *N-allyloxycarbonyl-1-amino-1-cyclopentyl fluoride*....148
5.2.8 *3-(N-allyloxycarbonyl-L-phenylalaninyl-oxy)-5,5-dimethyl -cyclohex-2-enone*....149
5.2.9 *4-benzyl-5,5-dimethyl-cyclohexane-1,3-dione*....149
5.2.10 *5,5-dimethyl-3-methoxy-cyclohexe-2-enone*....151
5.2.11 *3-methoxy-5,5,6-trimethyl-cyclohex-2-enone*....151
5.2.12 *6-allyl-5,5-dimethyl-3-methoxy-cyclohex-2-enone*....152
5.2.13 *6-benzyl-5,5-dimethyl-3-methoxy-cyclohex-2-enone*....153
5.2.14 *5,5-dimethyl-3-methoxy-6-((E)-3-phenyl-allyl)-cyclohex -2-enone*....153
5.2.15 *(6,6-dimethyl-4-methoxy-2-oxo-cyclohex-3-enyl)-acetic acid tert-butyl ester*....154
5.2.16 *6-benzyl-3-(N-benzyloxycarbonyl-L-valinyl-oxy)-5,5 -dimethyl-cyclohex-2-enone*....155
5.2.17 *3-amino-5,5-dimethyl-cyclohex-2-enone*....156

5.2.18 *Attempted preparation of 3-(N-benzyloxycarbonyl -L-valinyl-amino)-5,5-dimethyl-cyclohex-2-enone* 157
5.2.19 *3-(N-benzyloxycarbonyl-L-valinyl-amino)-5,5 -dimethyl-cyclohex-2-enone* 158
5.2.20 *3-(N-allyloxycarbonyl-L-phenylalaninyl-amino)-5,5 -dimethyl-cyclohex-2-enone* 159
5.2.21 *3-(N-allyloxycarbonyl)-1-amino-1-cyclopentyl-amino)-5,5 -dimethyl-cyclohex-2-enone* 160
5.2.22 *5,5-dimethyl-3-(methylamino)-cyclohex-2-enone* 161
5.2.23 *3-(N-allyloxycarbonyl-L-phenylalaninyl-methylamino) -5,5-dimethyl-cyclohex-2-enone* 161
5.2.24 *4,5,5-trimethyl-cyclohexane-1,3-dione* 162
5.2.25 *4-allyl-5,5-dimethyl-cyclohexane-1,3-dione* 163
5.2.26 *5,5-dimethyl-4-((E)-3-phenyl-allyl)-cyclohexane-1,3-dione* 164
5.2.27 *(6,6-dimethyl-2,4-dioxo-cyclohexyl)-acetic acid tert -butyl ester* 164
5.2.28 *3-amino-4,5,5-trimethyl-cyclohex-2-enone* 165
5.2.29 *6-allyl-3-amino-5,5-dimethyl-cyclohex-2-enone* 166
5.2.30 *3-amino-6-benzyl-5,5-dimethyl-cyclohex-2-enone* 166
5.2.31 *4-amino-6-((E)-3-phenyl-allyl)-5,5-dimethyl-cyclohex -2-enone* 167
5.2.32 *(4-amino-6,6-dimethyl-2-oxo-cyclohex-3enyl)-acetic acid tert-butyl ester* 168
5.2.33 *6-allyl-3-(N-benzyloxycarbonyl-L-valinyl-amino)-5,5 -dimethyl-cyclohex-2-enone* 168
5.2.34 *3-(N-benzyloxycarbonyl-L-valinyl-amino)-5,5-dimethyl -6-((E)-3-phenyl-allyl)-cyclohex-2-enone* 170
5.2.35 *6-benzyl-3-(N-benzyloxycarbonyl-L-valinyl-amino) -5,5-dimethyl-cyclohex-2-enone* 171
5.2.36 *N-allyloxycarbonyl-1-amino-1-cyclopentanecarboxylic acid* 172
5.2.37 *Valine template library (3x6) synthesis* 173
5.2.38 *5,5-dimethyl-3-(L-phenylalanine methyl ester)-cyclohex*

-2-enone.....179
5.2.39 *5,5-dimethyl-3-(L-valine methyl ester)-cyclohex-2 enone*.....179
5.2.40 *5,5-dimethyl-3-(L-tyrosine methyl ester)-cyclohex-2-enone*.....180
5.2.41 *(6,6-dimethyl-4-methoxy-2-oxo-cyclohex-3enyl)-acetic acid*.....181
5.2.42 *(6,6-dimethyl-4-methoxy-2-oxo-cyclohex-3enyl)-acetyl-L-valinyl methyl ester*.....182
5.2.43 *2-(6,6-dimethyl-4-methoxy-2-oxo-cyclohex-3-enyl)-N-((S)-1-phenyl-ethyl)-acetamide*.....183
5.2.44 *5,5-dimethyl-3-methoxy-6-(2-(2-methyl-piperidin-1-yl)-2-oxo-ethyl)-cyclohex-2-enone*.....184
5.2.45 *6-allyl-3-(N-benzyloxycarbonyl-D-valinyl-amino)-5,5-dimethyl-cyclohex-2-enone*.....184
5.2.46 *6-allyl-3-(N-benzyloxycarbonyl-L-leucyl-amino)-5,5-dimethyl-cyclohex-2-enone*.....185
5.2.47 *6-allyl-3-(N-benzyloxycarbonyl-L-isoleucyl-amino)-5,5-dimethylcyclohex-2-enone*.....186
5.2.48 *6-allyl-3-(N-α-benzyloxycarbonyl-N-ε-tert-butoxycarbonyl-L-lysyl-amino)-5,5-dimethyl-cyclohex-2-enone*.....187
5.2.49 *6-allyl-3-(N-benzyloxycarbonyl-L-prolyl-amino)-5,5-dimethyl-cyclohex-2-enone*.....188
5.2.50 *(4-(N-benzyloxycarbonyl-L-valinyl-amino)-6,6-dimethyl-2-oxo-cyclohex-3-enyl)-acetic acid*.....189
5.2.51 *3-(N-benzyloxycarbonyl-L-valinyl-amino)-6-(2,3-dihydroxy-propyl)-5,5-dimethyl-cyclohex-2-enone*.....190
5.2.52 *(4-(N-benzyloxycarbonyl-L-valinyl-amino)-6,6-dimethyl-2-oxo-cyclohex-3-enyl)-acetaldehyde*.....190
5.2.53 *6-allyl-3-(L-valinyl-amino)-5,5-dimethyl-cyclohex-2-enone*.....191
5.2.54 *Reductive amination array (1x9) synthesis*.....192
5.2.55 *Attempted preparation of 6-allyl-3-(N-fluorescein-thiourea-L-valinyl-amino)-5,5-dimethyl-cyclohex-2-enone*.....195
5.2.56 *6-allyl-3-(N-dansyl-L-valinyl-amino)-5,5-dimethyl-cyclohex-2-enone*.....196

Abstract

Cyclophilin A (CypA) is a member of the immunophilin family of proteins and receptor for the immunosuppressant drug cyclosporin A (CsA). CypA also catalyses the *cis-trans* isomerisation of peptidyl-prolyl (Xaa-Pro) amide bonds, biologically important in protein folding. CypA is a potential therapeutic target for areas including HIV replication and parasitic development. Although many natural and synthetic CsA derivatives are known to bind to and inhibit CypA, there are relatively few examples of small-molecule CypA ligands reported.

A number of low molecular weight ligands have been synthesised based upon *O*-acylated 5,5-dimethyl-1,3-cyclohexanedione and *N*-acylated 3-amino-5,5-dimethyl-cyclohex-2-enone. Routes to C-6 alkylated derivatives were also investigated and derivatives synthesised. Mass spectrometry was initially used to identify CypA:ligand complexes, and was developed into a high-throughput primary assay. Ligands were ranked in order of their relative CypA dissociation constants, and this approach identified ligand **I** as a lead compound.

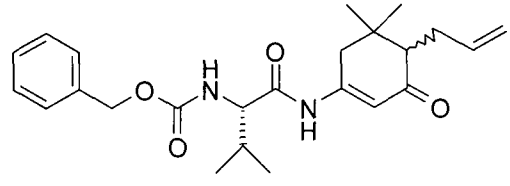

I

Further biological *in vitro* assays supported the relative ligand rank order of selected ligands, and *in vivo* studies using the nematode *C. elegans* revealed ligand **I** to have anti-parasitic activity. A fluorescently-labelled ligand derivative was synthesised that showed similar anti-parasitic properties upon screening, and revealed strong fluorescent staining of the gut lumen and surrounding tissues when the *C. elegans* nematodes were visualised under ultra-violet light.

Abbreviations

Aib	α-aminoisobutyric acid
Ala	alanine (A)
Alloc	allyloxycarbonyl
Arg	arginine (R)
Asn	asparagine (N)
Asp	aspartic acid (D)
Boc	*tert*-butoxycarbonyl
BOP	1-benzotriazolyoxytris(dimethylamino)phosphonium hexafluorophosphate
br	broad
CaM	calmodulin
Cbz	carbobenzyloxy
CID	collision induced dissociation
CN	calcineurin
Cys	cysteine (C)
CsA	cyclosporin A
Cyp	cyclophilin
DAPI	4',6-diamidino-2-phenylindole
DAST	diethylaminosulfur trifluoride
DCC	dicyclohexylcarbodiimide
DCM	dichloromethane
DIC	diisopropylcarbodiimide
DIPEA	*N*,*N*-diisopropylethylamine
DCU	dicyclohexylurea
DMAP	4-dimethylaminopyridine
DMPU	*N*,*N'*-dimethylpropyleneurea
DMSO	dimethylsulfoxide
DOS	diversity-orientated synthesis
EDCI	1-(3-dimethylaminopropyl)-3-ethylcarbodiimide

EI	electron impact
ELISA	enzyme-linked immunosorbent assay
ESI	electrospray ionisation mass spectrometry
FAB	fast atom bombardment
FITC	fluorescein isothiocyanate
FKBP	FK-binding protein
Gln	glutamine (Q)
Glu	glutamic acid (E)
Gly	glycine (G)
HATU	O-(7-azabenzotriazol-1-yl)-*N*,*N*,*N*',*N*'-tetramethyluronium hexafluorophosphate
HBTU	*O*-(benzotriazol-1-yl)-*N*,*N*,*N*',*N*'-tetramethyluronium hexafluorophosphate
His	histidine (H)
HIV	human immunodeficiency virus
HMPA	hexamethylphosphoric triamide
HOBt	1-hydroxybenzotriazole
HPLC	high performance liquid chromatography
HRMS	high resolution mass spectrometry
HTS	high throughput screening
Hz	hertz
IL-2	interleukin-2
Ile	isoleucine (I)
J	coupling constant
LDA	lithium diisopropylamine
Leu	leucine (L)
LIDAEUS	ligand design at Edinburgh University
Lys	lysine (K)
MALDI	matrix assisted laser desorption ionisation
Met	methionine (M)
mp	melting point
MS	mass spectrometry

NF-AT	nuclear factor of activated T-cells
NMM	*N*-methylmorpholine
NMR	nuclear magnetic resonance
PBB	protein database
Phe	phenylalanine (F)
PPIase	peptidyl-prolyl *cis/trans* isomerase
PPL	porcine pancreas lipase
Pro	proline (P)
PS-CBH	polymer-supported cyanoborohydride
PyBOP	benzotriazole-1-yl-oxy-tris-pyrrolidino-phosphonium hexafluorophosphate
PyBroP	bromo-tris-pyrrolidino-phosphonium hexafluorophosphate
Rf	retention factor
Ser	serine (S)
SAR	structure-activity relationships
SBD	structure-based design
TBDMS	*tert*-butyldimethylsilyl
TBTU	2-(1*H*-benzotriazole-1-yl)-1,1,3,3-tetramethyluronium tetrafluoroborate
TOS	target-orientated synthesis
TOF	time of flight
TFA	trifluoroacetic acid
THF	tetrahydrofuran
Thr	threonine (T)
TNBS	trinitrobenzenesulfonic acid
Trp	tryptophan (W)
p-TSA	*para*-toluene sulfonic acid
Tyr	tyrosine (Y)
Val	valine (V)
Xaa	generic peptide

1. Introduction

This thesis is concerned with the design and synthesis of high affinity ligands for cyclophilin A (CypA). The project incorporated aspects of structure-based design, medicinal chemistry and the emerging field of chemical genetics. As an introduction to the project these areas are discussed below, along with an overview of the functions of cyclophilin A. The previous work done on the project is also outlined, concerning the discovery of the original lead compound, dimedone, and subsequent ligand optimisation.

1.1 Drug discovery

1.1.1 Historical drug discovery

Drug research is a relatively new area, as a multidisciplined industrial endeavour it is not much older than a century. The field began in the late 19th century when chemistry was starting to advance and pharmacology had become a separate scientific discipline in its own right. By this stage some of the key principles of chemical theory had been established, Avogadro's atomic hypothesis had been accepted and the periodic table had been determined. Initially, it was the expansion in synthetic dye production that marked the first step in the industrialisation of organic chemistry. Coal tar, a previously inconvenient by-product of the manufacture of coke and town gas, was used as the starting material for a range of silk dyes[1] that were a commercial success and went on to have a profound influence on contemporary medicine.

It was the evolution of dye chemistry that led to some of the key principles of modern biology being discovered. Paul Ehrlich noted that biological tissue had a selective affinity for dyes, thus leading him to postulate the existence of "chemoreceptors". He went on to pioneer immunological studies, claiming that differences in chemoreceptors between parasites, micro-organisms and host tissues

could be exploited to treat illnesses.[2] Clearly this was the starting point for modern receptor theory, and his contribution to the field of medicine was recognised by the award of the Nobel Prize in 1908.

The isolation and purification of the active ingredients of known medicinal plants was another key driving force in early drug discovery. Morphine was isolated from opium extract in the early 1800s by Friedrich Sertürner[3] and sparked the study into natural product chemistry. A host of other alkaloids were subsequently isolated, including caffeine and quinine in 1820, codeine and atropine in the 1830s and cocaine in 1860.[4] During the first half of the 20th century, the field of medicinal natural products continued to expand through the discovery of antibiotics. Penicillin was isolated by Alexander Fleming in 1929[5] and ushered in a new era in the treatment of bacterial infections. The emerging pharmaceutical industry that had grown out of pharmacies and dye companies embraced this new direction and started to include microbiology as a means of drug discovery.[2] Of relevance to this project, the immunosuppressants cyclosporin A (CsA), FK506 and rapamycin were all discovered through such microbial screening.[6]

The modern pharmaceutical industry approaches drug discovery in a multidisciplinary fashion. Chemistry, biochemistry, pharmacology and microbiology all interact to investigate biological processes and to discover new therapeutic drug candidates. Technological advances such as combinatorial chemistry and high-throughput screening (HTS) have allowed the synthesis and testing of an unprecedented number of new chemical entities against a broad range of targets. The drug discovery process often commences from research into a particular disease area leading to selection of a therapeutic target, followed by chemical lead compound selection and optimisation. This discovery period, if successful, is followed by a scale-up of drug production and in-depth *in vitro* and *in vivo* biological testing. Although drug development can be outlined as a linear process (Figure 1.1), in reality the process is based on cycles of synthesis and screening to obtain analogues with improved efficacy and selectivity, and reduced side-effects.

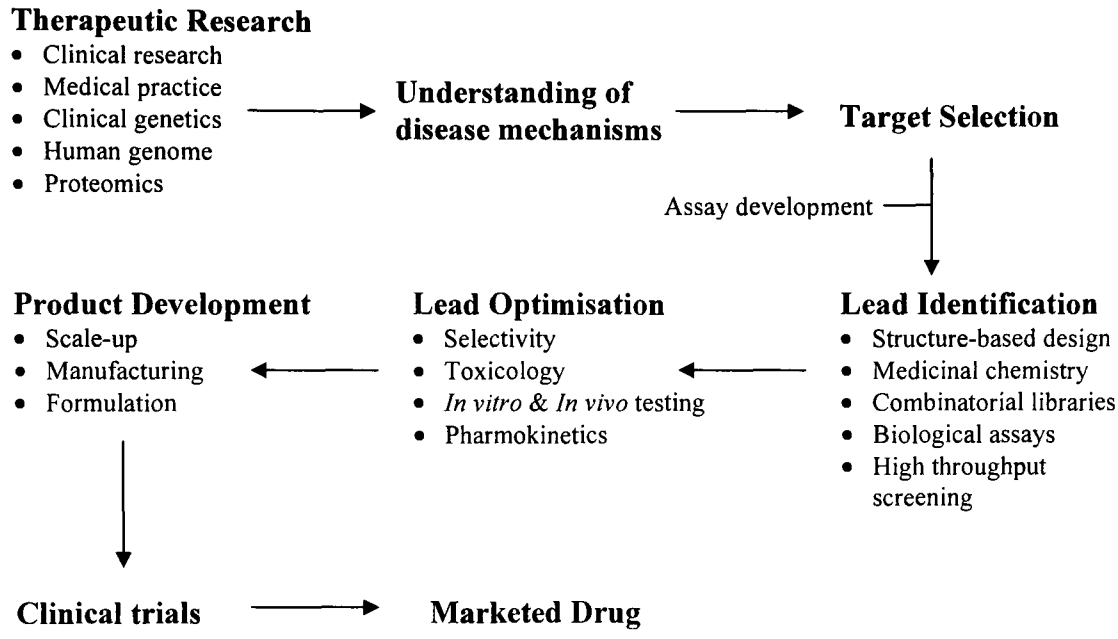

Figure 1.1: Simplified chart of successful drug discovery in the pharmaceutical industry.[7]

1.1.2 Structure-based design

Structure-based design has emerged over the last few years to become a key tool in medicinal chemistry. Greater understanding of molecular recognition in protein-ligand complexes has led to the expansion in the area, aided by the exponentially increasing amount of information on the three-dimensional structure of proteins. If the three-dimensional structure of a given protein is known, this information can be exploited for the tailored optimisation of a known lead structure, or even applied to the *de novo* design of new ligands.

Structure-based ligand design is an iterative process. The process starts with an analysis of the binding site of the target protein, ideally with a ligand bound in place. Structural determination is accomplished mainly by X-ray crystallography,[8] or by multidimensional NMR spectroscopy,[9] and the number of solved protein structures has increased exponentially over the last ten years. In 1995 there were just over 4,000 entries in the Research Collaboratory for Structural Bioinformatics (RCSB) Protein Database (PDB), the worldwide repository for the three-dimensional

structure of proteins. There are now over 31,000 solved protein structures listed.[10] The three-dimensional protein-ligand structure is analysed to identify the binding mode and conformation of the ligand as well as the key protein-ligand interactions. This knowledge can then be used to modify an existing lead compound, or to design a new series of ligands. The proposed ligands are then synthesised and assayed using biochemical, spectroscopic and crystallographic methods. The next cycle of ligand design and optimisation is commenced upon analysis of these results (Figure 1.2).[11]

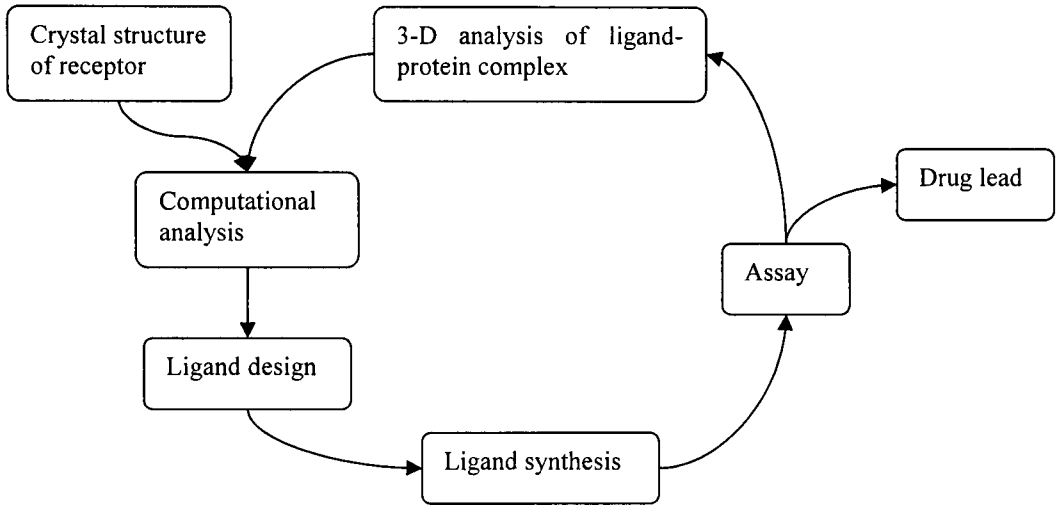

Figure 1.2: The iterative process of structure-based design.[12]

Structure-based design can still be of relevance in the absence of crystallographic data. If the crystal structure of a particular protein-ligand complex is unobtainable a comparative analysis of known binding ligands can often reveal the key binding features. Ligands can then be designed to optimise these protein-ligand interactions. The ensuing assay results will validate the design if the binding affinity is increased, or lead to a new ligand design hypothesis if the new compounds are less active.

The vast majority of ligands bind to protein active sites through non-covalent interactions. Usually, opposite charged functional groups of the protein and ligand are paired, hydrogen bonds are formed and lipophilic ligand moieties are found in hydrophobic pockets of the protein. The binding affinity of a ligand is expressed in

terms of the equilibrium constant, K, which is thermodynamically related to the Gibbs free energy, ΔG (Equation 1.1). This in turn is composed of enthalpic and entropic contributions (Equation 1.2). Combining these two equations gives the van't Hoff equation (Equation 1.3), which shows that the binding affinity of a ligand is driven by both enthalpic and entropic factors.[13]

Equation 1.1: $\Delta G = -RT\ln K$

Equation 1.2: $\Delta G = \Delta H - T\Delta S$

Equation 1.3: $\ln K = \Delta H/RT + \Delta S/R$

The enthalpic component of the above equations is determined principally by electrostatic and van der Waals interactions, and the entropic portion measures the order of the entire system. The majority of this entropic portion correlates with the lipophilic surface, that of the ligand and the section of the protein that becomes buried upon binding.[11]

Water often plays a key role in protein-ligand interactions with both the ligand and protein being solvated before complex formation. They lose part of their hydration shell upon binding, this having both enthalpic and entropic repercussions. If the binding of a ligand merely replaces tightly bound water molecules without yielding additional electrostatic interactions the desolvation effects can equal the new ligand-protein interactions, resulting in the net enthalpic contributions being close to zero. However, the replacement of loosely bound water molecules by a ligand can have a positive enthalpic effect due to the stronger protein-ligand interactions and the released water now being able to hydrogen bond with the bulk water.[14] The entropic repercussions arise from lipophilic interactions between the ligand and protein. Such hydrophobic interactions are beneficial to ligand binding mainly due to the replacement and release of ordered water molecules. Water molecules at hydrocarbon surfaces have been shown to be more ordered than water molecules in the bulk solvent,[15] therefore the release of water upon ligand binding would have a positive entropic effect. There are also enthalpic contributions to lipophilic

interactions as water molecules in protein hydrophobic areas are unable to form hydrogen bonds, upon release the molecules can hydrogen bond with the bulk solvent.

The flexibility of the ligand is another important factor in determining the strength of protein-ligand interactions. Generally, the formation of a non-covalent bond between a protein and a ligand corresponds to a favourable negative contribution to the enthalpy, favouring the binding process. However, this is often accompanied by a restriction of the translational and rotational motion of the ligand, corresponding to a negative change in entropy, this being unfavourable to the binding. This opposing interplay is known as enthalpy/entropy compensation, and is a fundamental property of non-covalent protein-ligand interactions.[13] Conformationally constrained ligands are often designed to limit this loss of entropy on binding. The binding affinities of ligands are increased if the ligands can be pre-organised into the conformation of that of the bound state. Ligands are often constrained by the replacement of open alkyl chains by ring structures, or the introduction of conformational locking groups into the ligand structure.[16] Macrocyclic and intramolecular hydrogen bonding structures have also been exploited to similarly enhance the pre-organisation.[17]

1.1.3 Peptidomimetic design

The biological activity of peptides is of enormous interest to the pharmaceutical industry, but endogenous peptides have limited medicinal potential. Peptides and small proteins are generally easily proteolysed, rapidly excreted and have poor bioavailability, making them unsuitable candidates for pharmaceutical development. Peptidomimetics are peptide derived compounds that resemble peptides in some way and are designed to mimic the binding of the peptide to the receptor, but have enhanced drug profiles compared to peptides.

Three distinct classes of peptidomimetics have been described in the literature.[18] Early peptidomimetics focussed on the geometry of the peptide bond and secondary structural feature of proteins such as α-helices and β-turns and are referred to as

type-I mimetics.[19] Often these mimetics match the peptide backbone and focus on the replacement of the amide functionality with such groups as amines, α-difluoroketones and ethylene and ketomethylene isosteric groups.[20] The second type of mimetic is called the functional mimetic, or type-II mimetic. This is a small non-peptide molecule that does not necessarily mimic the structure of the original peptides and binds to a subsite on the protein that is different from the original peptide receptor. The last class of peptidomimetics, type-III, are in some ways the ideal peptidomimetic as they are novel templates that are structurally unrelated to the original peptides, but mimic key features that allows the ligand to bind to the peptide functional site.

There is no standard systematic way of transforming the structure of an enzyme bound substrate into a peptidomimetic. A number of different techniques have been used including the replacement of amino acids in the peptide backbone with unnatural analogues, and the use of cyclic or bridging dipeptides to conformationally constrain the structure. Structure-based design techniques are also often used to design *de novo* type-III peptidomimetics in which the key peptide binding moieties are mimicked by the ligand. In this way peptidomimetic ligands are often structurally smaller than the original peptide as often only a few peptide residues make energetically significant contact to the protein binding site.

1.1.4 Chemical genetics

Chemical genetics is the name given to the study of biological systems through the interaction of exogenous ligands, instead of using genetic intervention. The area was founded in the mid-1990s by Stuart Schreiber[21] and Timothy Mitchison[22] as a method of emulating the principles of genetics with organic chemistry. Genetics has been traditionally used to study biological systems through perturbing the function of proteins by manipulation at the gene level. This is generally achieved by the mutation of a gene followed by observation of the physiological effect this has on the system, the phenotype. Chemical genetics uses small molecule ligands instead of mutations to alter the function of proteins in a similar manner.

Genetics can be divided into two categories: forward genetics that entails random mutagenesis followed by phenotypic screening and mutant gene identification; and reverse genetics that introduces a mutation into a specific gene of interest and is followed by a study of the phenotypic consequences.[23] Thus forward genetics is from phenotype to gene, in reverse it is from gene to phenotype. A chemical genetics approach can be similarly sub-divided. Forward chemical genetics involves the use of small molecules to screen for a desired phenotype in a biological system under investigation. Once a ligand that induces a phenotype change has been selected it is necessary to identify the protein target of the molecule. Reverse chemical genetics starts with the screening of potential ligands against a known protein target. Once a binding ligand is identified it is used to study the phenotypic consequences of altering the function of this protein in a cellular context. In this manner, forward chemical genetics is from phenotype to protein, in reverse it is from protein to phenotype (Figure 1.3).

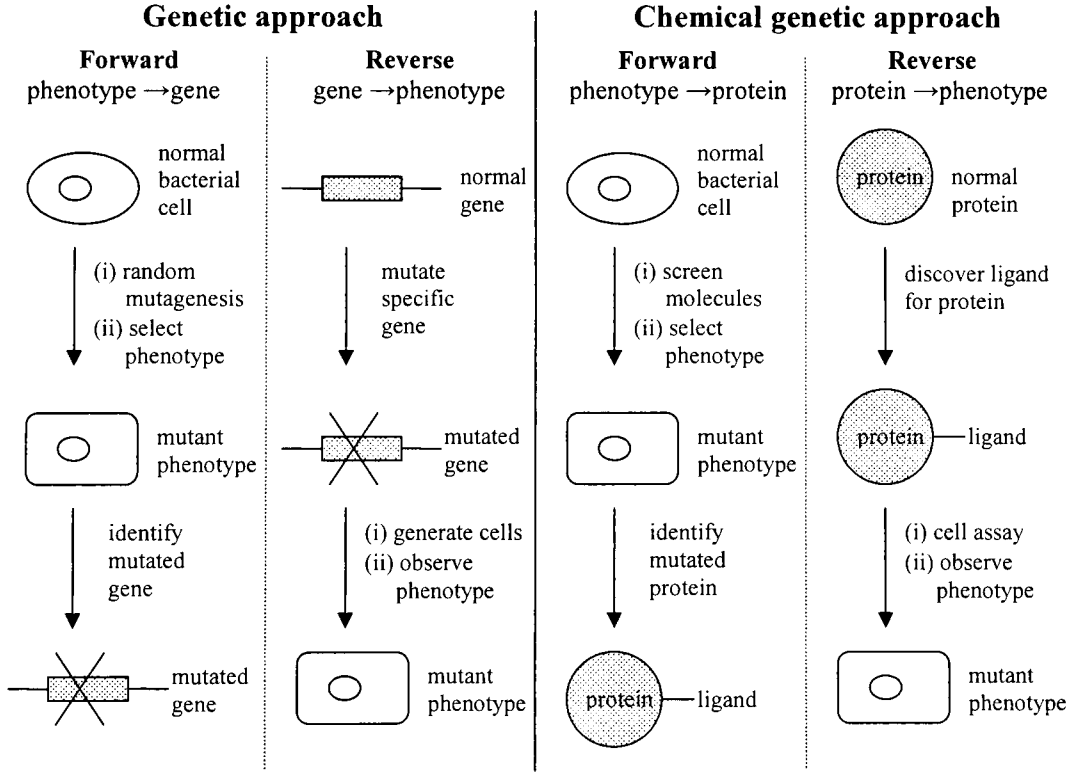

Figure 1.3: Comparison of genetics with chemical genetics.

Traditional genetics has several limitations that are overcome by taking a chemical genetics approach. Most genetic mutations are not conditional; they cannot be reversed post mutagenesis. Conditional mutagens are available, but they are difficult to identify and the effect of modulating the mutant allele can cause environmental stress to the organism masking the original phenotypic consequences; for example a heat shock response from effecting a temperature sensitive mutation. Chemical genetics has the advantage that small molecules most often induce their biological effect reversibly due to *in vivo* metabolism, and temporal control is possible as ligands can be added at any time point in the experiment. Another key advantage of a chemical genetics approach is that the biological effect of small molecules is usually rapid allowing early phenotypic changes to be characterised, genetic studies in mammals are often time consuming due to a slow rate of reproduction. Small molecule ligands can also be introduced into biological systems at varying concentrations allowing for the collection of dose-response data by grading the phenotype change. The disadvantage of chemical genetics is that a ligand selective for a protein of interest is needed, and currently only a tiny fraction of known proteins have such a ligand partner identified.[24]

A chemical genetics study involves three aspects: a selective small molecule ligand, a protein partner and a biological screen capable of assessing the effect of the protein-ligand interaction. The small molecule ligand can either be sourced from a natural product or synthetically derived. For reverse chemical genetics studies structure-based design techniques can be used to guide ligand synthesis when the three-dimensional structure of the protein is known, however this approach is limited as often little is known about the structure of the target protein. Where a ligand for a protein is already known, retrosynthetic analysis of the molecule can be used to design synthetic routes to derivatives. Small libraries of derivatives can then be synthesised using target-orientated synthesis (TOS)[25] and focussed combinatorial chemistry.[26] Forward chemical genetics has benefited from the screening of structurally-diverse small molecules *via* high-throughput protein binding screens.[24] Diversity-orientated synthesis (DOS) can be used to synthesise libraries of small molecules with the aim of broadly populating chemical space with diverse molecular

structures.[27] Unlike TOS, diversity-orientated syntheses are not aimed at one particular target and involve the simultaneous synthesis of structurally complex and diverse compounds; the combinatorial technique of solid-phase split and mix synthesis is readily adaptable to this approach. This method was first introduced by Furka *et al.*, to synthesise peptides,[28] and involves cycles of synthesis, pooling, re-splitting and further chemistry to achieve structurally diverse compounds. Split and mix is also referred to the "one bead-one compound" approach, and in a chemical genetics context it can be seen as being analogous to genetic recombination.[29]

1.1.5 Conclusions

The introduction of structure-based design, combinatorial chemistry, high-throughput screening and the emerging field of chemical genetics have all added to the knowledge of how ligands interact with drug targets, and thus have helped to advance rational drug design. However, it is clear that for all these technological advances made in the late 20th century, organic synthesis remains the cornerstone upon which drug discovery is built.

In the last few years the structure-based design approach has expanded markedly in academia and the pharmaceutical industry, aided by dramatic improvements in computational capabilities and molecular modelling software.[30] Despite this progress, structure-based design still faces a number of limitations. The most important factor is the availability of three-dimensional structures of target proteins. Although there has been a huge increase in the number of published protein structures in recent years, there are still many pharmacologically relevant proteins that have not be resolved. In particular, the number of membrane bound proteins that have been structurally determined lags behind that of soluble proteins.[31] As stated previously, it is still possible to apply structure-based design techniques in the absence of crystallographic data by relying on ligand comparison, but as the level of information on the structural aspects of the protein-ligand system decreases, so does the reliability of any ligand design results.

Medicinal chemistry generally considers ligands and their interactions with the biological target when using a structure-based design approach, but a perfect ligand is not necessarily a good lead for further pharmaceutical development. Considerations such as pharmacokinetics and ADME-Tox (adsorption, distribution, metabolism, excretion and toxicity) are not addressed by structure-based design and are responsible for a high rate of lead drug candidate attrition. The earlier in drug development these issues are considered, the greater the chance of a drug candidate being successfully brought to market. With this in mind, Christopher Lipinski *et al.*, reviewed successful drug candidates and found that 90% of orally active drugs that had achieved phase II clinical status shared four simple physiochemical parameters; a molecular weight of ≤ 500, hydrogen bond donors ≤ 5, hydrogen bond acceptors ≤ 10 and a log P ≤ 5, P being the n-octanol/water partition coefficient.[32] These parameters were called the rule-of-five (RO5) and the goal was to influence drug design from early on in the initial medicinal chemistry discovery phase.[33] Lipinski's RO5 has been largely accepted by the pharmaceutical industry as a guide for new ligand design with a trend towards considering ADME-tox issues early in lead optimisation.

Chemical genetics is proving itself to be a powerful approach, with the possibility of perturbing protein function reversibly and conditionally with temporal and quantitative control in diverse biological systems. The technique has so far been limited by a lack of suitable ligands for protein targets, a consequence of chemical genetics being a relatively new field. The area will no doubt expand, fuelled by a growth in diversity orientated synthesis and related combinatorial chemistry techniques.

Drug discovery has evolved into a multi-disciplined field, whist still keeping synthetic chemistry at its core. Structure-based design will continue to make a positive impact upon medicinal chemistry research for the foreseeable future, enhanced by a combination of emerging new techniques and traditional synthetic methods.

1.2 Peptidyl-prolyl *cis/trans* isomerases (PPIases)

In the 1970s it was thought that protein folding was a spontaneous process, the three-dimensional structure of the protein reflecting the lowest free Gibbs free energy conformation determined by the primary amino acid sequence.[34] Refolding experiments of denatured proteins showed that refolding events of globular single-domain polypeptides occur in the millisecond to second timescale,[35] apart from the *cis/trans* isomerisation of peptidyl-prolyl (Xaa-Pro) amide bonds (Figure 1.4). This conformational change takes longer, and has been demonstrated to be the rate limiting step in refolding experiments.[36]

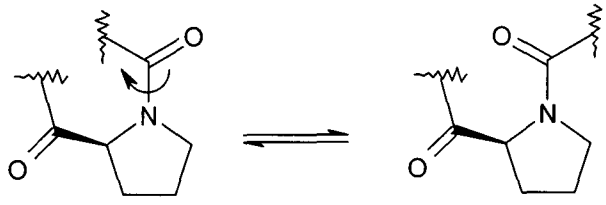

Figure 1.4: Cis-trans isomerisation of a peptidyl-prolyl bond.

In 1984 an enzyme was isolated that was found to catalyse the *cis/trans* isomerisation of peptidyl-prolyl bonds. Fischer *et al.*, extracted the enzyme from porcine kidney cortex and it was classified as a peptidyl-prolyl isomerase (PPIase).[37] In the same year another 18 kDa protein from mammalian thymocytes was found to be the major intracellular receptor for the immunosuppressant drug cyclosporin A (CsA) (**1**, Figure 1.5), and this receptor protein was named cyclophilin A (CypA).[38] Subsequently further cyclophilins were characterised and in 1989 two groups independently demonstrated that cyclophilins were identical to PPIase.[39,40] Another PPIase was discovered in this year during the search for the receptor of the immunosuppressant drug FK506 (**2**, Figure 1.5) and named FK506-binding protein (FKBP).[41,42] FK506 is a polyketide isolated from *Streptomyces tsukubaesis*[43]and is

structurally related to the anti-fungal drug rapamycin (**3**, Figure 1.5), found to also bind to FKBP.[44]

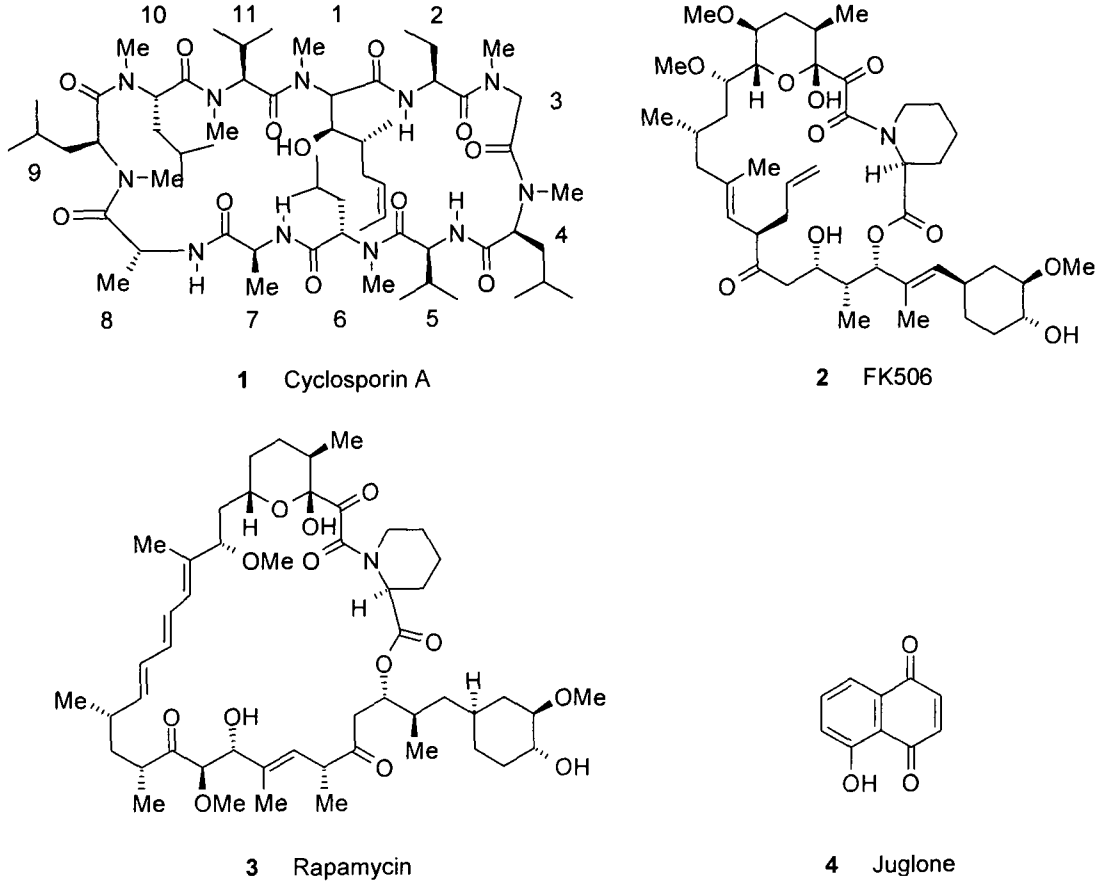

Figure 1.5: Structures of CsA, FK506, rapamycin and juglone.

The amino acid sequence of FKBP was found to be totally different to cyclophilin, and it became obvious that the prolyl isomerases were divided into separate classes; the cyclophilins which selectively bind CsA (**1**), and FKBPs which selectively bind FK506 (**2**) and rapamycin (**3**). CypA and FKBP are also known as immunophilins due to the binding of these immunosuppressants. A third class of PPIase was also discovered, the parvulins, initially isolated from *Escherichia coli*,[45] and it was found that juglone (5-hydroxy-1,4-naphthoquinone) (**4**, Figure 1.5) irreversibly inhibited the PPIase activity of this enzyme.[46]

The cyclophilins family are ubiquitous proteins that have been highly conserved during evolution, found to be widely expressed in many biological tissues in addition to bacteria, fungi and plants. Structural analysis of human cyclophilin A has revealed it to be a cytosolic protein with a molecular mass of 17.7 kDa, consisting of an eight-stranded anti-parallel β-barrel that exists as two perpendicular four-stranded β-sheets. The β-barrel encloses a hydrophobic core and is capped at each end by two short α-helices.[7] Other mammalian isoforms have also been characterised and have been found to share over 50 % sequence homology with CypA, but differ in their subcellular localisation. CypB is a 21 kDa protein found in the endoplasmic reticulum, as is the 23 kDa protein CypC. CypD is a 18 kDa protein found in cellular mitochondria.[35]

1.2.1 PPIase activity

Most amide bonds in peptides adopt the *trans* configuration, however proline containing peptides are unusual in the fact that roughly 10 % of the peptidyl-prolyl bonds are in the energetically unfavourable *cis* conformation. This compares to an estimated occurrence of less than 1.5 % *cis*-amides in other amino acids.[47] This fact may be explained by the free energy difference between the *cis/trans* conformations of Xaa-Pro bonds being less than other non-prolyl amide bonds. It is thought that PPIases catalyse this isomerisation of peptidyl-prolyl amide bonds using the same active site as that used to bind the respective immunosuppressants, this supported by the PPIase activity of the enzyme being abolished upon immunosuppressant binding.

There have been several studies into how the PPIase enzymes catalyse the *cis/trans* interconversion of peptidyl-prolyl bonds, resulting in several mechanisms being proposed. *Cis/trans* isomerisation of amide bonds is restricted by the C-N bond having double bond character. This results from conjugation of the C-N amide bond with the carbonyl group allowing amide/imine resonance. Consequently, *cis/trans* isomerisation of the prolyl amide bond has to overcome this energetic barrier to rotation.

Initial mechanistic studies of cyclophilin led to the suggestion that PPIase catalysis was achieved by the formation of a covalent bond to the carbonyl of the peptidyl-prolyl amide with a cysteine-derived thiol.[48] Loss of sp^2 hybridisation at this carbonyl would eliminate amide resonance and thus lower the energy barrier to rotation about the C-N bond. However, subsequent site-directed mutagenesis of human recombinant cyclophilin allowed the systematic replacement of all four cysteine residues in cyclophilin with alanine. These mutant enzymes were found to be just as active at the *cis/trans* isomerisation of Xaa-Pro bonds, thus ruling out cysteine as a participating residue in catalysis.[49]

A catalysis by distortion mechanism has also been proposed involving a "twisted amide" Xaa-Pro transition-state that is stabilised in the CypA active site (Figure 1.6).[50] In this mechanism the twisted amide transition state has the carbonyl group and the nitrogen lone pair electrons of the Xaa-Pro amide bond in orthogonal orbitals. This lowers the energy barrier to rotation as resonance can no longer occur.

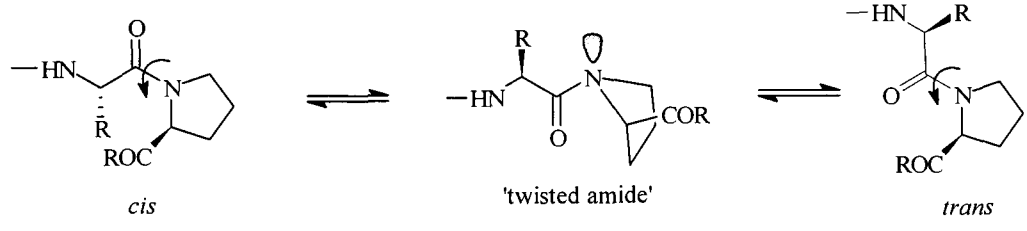

Figure 1.6: Catalysis by distortion mechanism for Xaa-Pro isomerisation.[51]

Another mechanism proposed that the amide nitrogen forms a hydrogen bond with a protonated CypA residue resulting in the prevention of resonance. Molecular orbital calculations supported this hypothesis as protonation of the amide nitrogen lowers the energy barrier to *cis/trans* rotation.[52] The desolvation mechanism proposed that the twisted amide intermediate is stabilised by the hydrophobic character of the PPIase active site as the rate of *cis/trans* isomerisation was found to be significantly accelerated in non-polar solvents.[53] Interestingly, a later study suggested a related but opposing mechanism after determining the crystal structure of CypA complexed with

the substrate Ala-Pro. A solvent-assisted mechanism was put forward in which initially the peptidyl-prolyl bond is desolvated in the ground state by binding to the hydrophobic CypA active site, followed by stabilisation of the intermediate through hydrogen bonding of the amide carbonyl with a water molecule.[54]

1.2.2 Cyclosporin A

Cyclosporin A (**1**) is a non polar cyclic undecapeptide that was first isolated from the fungus *Tolypocladium inflatum* in 1976;[55] its potent immunosuppressive properties first described by Borel *et al.*[56] CsA has subsequently been developed into a major pharmaceutical product, sandimmune, marketed for the prevention of allograft rejection and for the treatment of autoimmune disease.[57]

The conformation of CsA bound to cyclophilin is very different from the dominant conformation of free CsA in chloroform or in single crystals. Free CsA exhibits a *cis* MeLeu9-MeLeu10 amide bond, whereas in the cyclophilin bound form all the peptide bonds are *trans*. Free CsA also has a tightly folded structure with a hydrophobic surface, brought about by four intramolecular hydrogen bonds. In the bound state, the CsA amino acid side chains are flipped over from the inside to the outside. This bound CsA open ring structure has only a single intramolecular hydrogen bond, between the hydroxyl group on the Bmt-1 side chain and the carbonyl group of MeLeu-4.[58]

CsA binds to the PPIase active site of CypA with residues 9, 10, 11, 12, 1, 2, and 3 lying in the CypA active site; the remaining residues protrude out from the CypA surface.[56] This hydrophobic protrusion is termed the "effector loop" and is implicated with specific interactions with the phosphatase calcineurin (CN).[59] X-ray analysis of the CypA-CsA complex revealed that the CsA MeVal-11 residue fits very tightly into a hydrophobic pocket, and there are five direct hydrogen bonds between CypA and CsA, with an additional five water mediated intermolecular interactions.[60]

1.2.3 Mechanism of immunosuppression

Cyclosporin A and FK506 are both powerful suppressors of the immune system, exerting their major therapeutic effect by inhibiting the activation of T-cells, a subset of lymphocytes that are involved in the immune response. Studies have indicated that CsA and FK506 act as prodrugs, only becoming active when complexed to their respective immunophilin partner, with immunosuppression independent of PPIase activity.[61] Although the CypA-CsA and FKBP-FK506 complexes differ in structure, their mechanism of immunosuppression is very similar, with both complexes binding to and inhibiting the calcium and calmodulin dependant phosphatase calcineurin.[62] In this mechanism, the immunosuppressants act like "molecular glue", bringing about the binding of normally non-interacting proteins, namely the immunophilin and calcineurin (Figure 1.7).[63]

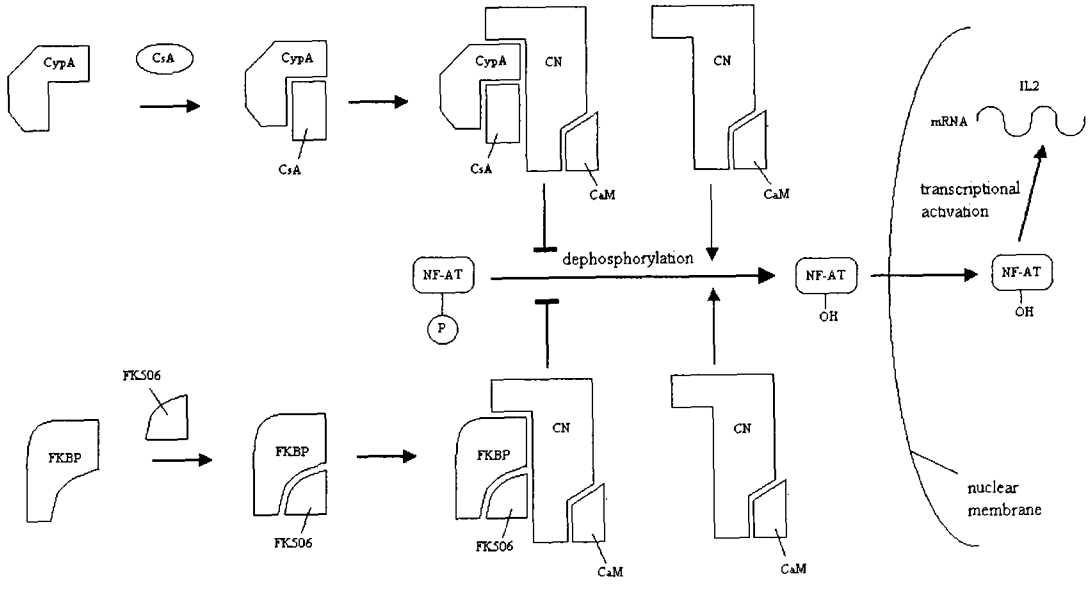

Figure 1.7: Events associated with CypA-CsA and FKBP-FK506 mediated immunosuppression.[35]

During T-cell activation calmodulin (CaM) binds to the phosphatase calcineurin as a result of elevated levels of free intracellular calcium. This complex dephosphorylates the nuclear factor of activated T cells (NF-AT), which in the dephosphorylated form

is able to cross the nuclear membrane. In the nucleus NF-AT acts as a transcriptional activator for interleukin-2 (IL-2) transcription; interleukin-2 is an immune response stimulator involved in the proliferation of T-cells. The CypA-CsA and FKBP-FK506 complexes bind to calcineurin and block the phosphatase activity of the CN/CaM complex. As NF-AT is not dephosphorylated it is unable to cross the nuclear membrane, thus T-cell activation is inhibited.

Calcineurin is not inhibited by either drugs or immunophilins alone, only by the drug-immunophilin complex, indicating that it is the composite surface of the complex that interacts with calcineurin.[64] The crystal structures of the CypA-CsA-CN[65] and FKBP-FK506-CN[66] complexes have both been published and interestingly reveal that CypA-CsA and FKBP-FK506 are both bound to the same surface of calcineurin, with the majority of the CN residues involved in the binding common to both drug-immunophilin complexes.

1.3 Involvement of cyclophilin A in other disease areas

1.3.1 Cyclophilin A as an anti-HIV drug target

It has been reported that the principal structural protein of the human immunodeficiency virus HIV-1, the Gag polyprotein, binds cyclophilins and that CypA is specifically incorporated into HIV-1 virions,[67] comprising up to 10 % of the HIV capsid coat. Late in the infectious cycle, Gag accumulates at the membrane of an infected cell and assembles into immature virions that bud from the cell. As the virion buds and matures, the membrane bound Gag protein is cleaved by viral proteases into three new proteins; matrix, which lines the virion envelope; capsid, which forms the viral core; and nucleocapsid, which coats viral genomic RNA.[68] The virus particle must subsequently disassemble when the virus infects a new cell in order to allow reverse transcription of the RNA genome and transport of the pre-integration complex into the nucleus (Figure 1.8).[69]

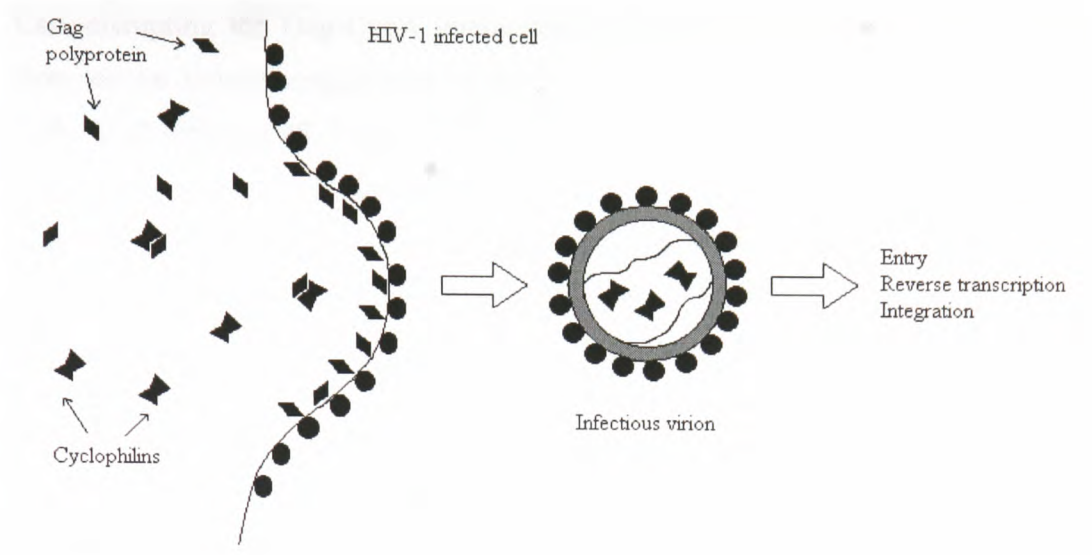

Figure 1.8: Budding of HIV virions from an infected cell.[70]

HIV-1 has been shown to be dependant on Gag-CypA for replication, mutation of a single Gag proline to alanine disrupts Gag-CypA interaction *in vitro*, CypA incorporation into virions and viral replication.[68] The crystal structure of CypA complexed with the *N*-terminus domain of the HIV-1 capsid protein and various fragment lengths have been characterised.[70,71] The capsid protein was found to have a mobile loop of residues that bind in the same CypA active site responsible for peptidyl-prolyl isomerase activity, with Ala88, Gly89 and Pro90 buried in this grove. A 25-mer fragment of HIV-1 capsid was also found to bind to CypA in an equivalent manner, with the same amino acids Ala88 to Ile91 involved in the major binding interactions with CypA. Interestingly, in both of these structures Gly89-Pro90 was found to adopt an unusual *trans* configuration, compared to *cis* configuration seen in other known peptide complexes. Although the precise function of CypA in HIV-1 replication is unknown, due to this interesting *trans* configuration of the binding capsid fragment, it has been hypothesised that CypA is functioning as a chaperone, rather than a *cis/trans* isomerase.[72]

Cyclosporin A has been shown to block the binding of the HIV-1 Gag polyprotein to CypA and prevent its incorporation into the HIV protein coat, resulting in a markedly reduced level of viral proliferation.[72] The mechanism of action is thought to be *via*

CsA disrupting the Gag-CypA interaction by competitive binding to CypA rather than *via* an immunosuppression pathway. A non-immunosuppressive analogue of CsA, SDZ NIM811 (**5**, Figure 1.9), was screened against HIV-1 and was found to selectively inhibit virion replication *in vitro*.[73] SDZ NIM 811 (**5**) is a derivative of CsA which is devoid of immunosuppressive activity but retains full capacity for binding to CypA, thus demonstrating the immunosuppressant function of CsA is not however responsible for the antiviral activity (Figure 1.10).

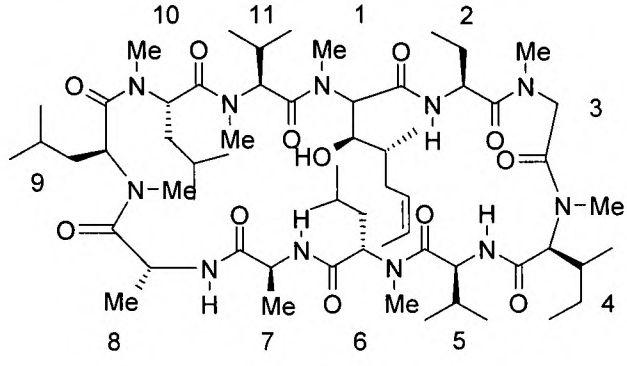

5

Figure 1.9: Structure of SDZ NIM 811 ((Me-Ile-4)cyclosporin) **5**.

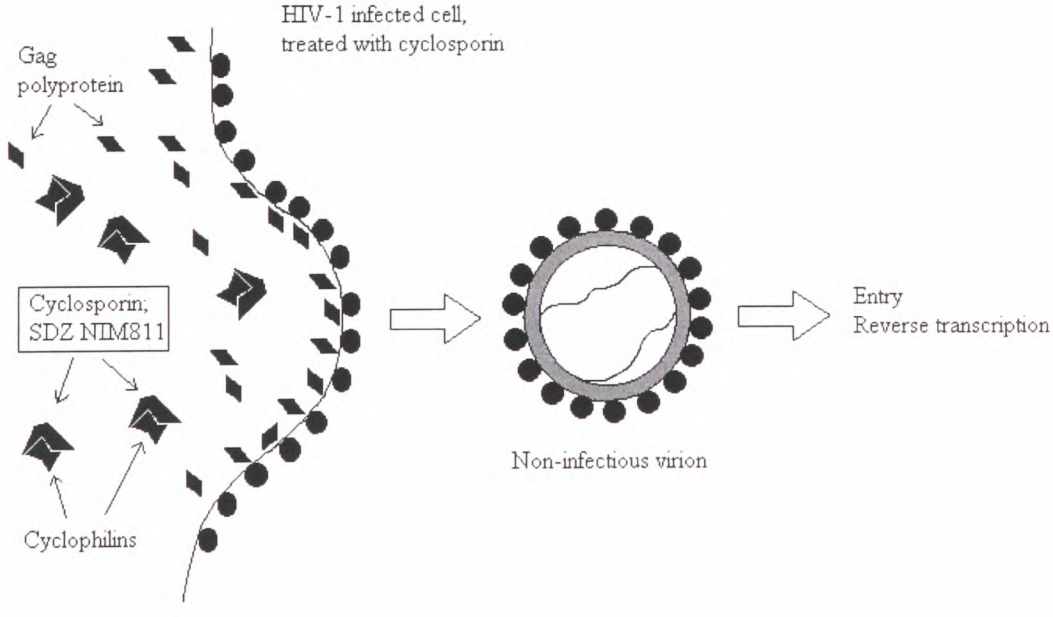

Figure 1.10: Treatment of HIV-1 infected cells with CsA or SDZ NIM811 results in poorly infectious virions.[71]

Whilst CsA and derivatives show potential for the design of novel HIV treatments, especially the non-immunosuppressant analogues, there are some limitations with the approach. The concentration of CsA analogues required to inhibit HIV-1 replication may well be toxic to cellular events *in vivo*, and due to the ubiquitous nature of cyclophilins there may be broad range side-effects involved in such a drug treatment. Administration of sub-optimal doses of a CsA derivative as part of a combination therapy with other HIV pharmaceuticals would probably represent the most viable route to a CsA derived anti-HIV treatment.

1.3.2 Cyclosporin A rheumatoid arthritis therapy

Rheumatoid arthritis is a chronic autoimmune disease characterised by inflammation of the joints, resulting in chronic pain, loss of function and disability. One percent of the world population is affected, with women two to three times more likely than men to suffer symptoms. Initial non-specific complaints of fatigue, malaise and diffuse musculoskeletal pain are followed by stiffness and pain in specific joint areas. The more serious consequences of rheumatoid arthritis involve progressive destruction of joint cartilage, bone and supporting soft tissue. The etiology of the disease is not clear and is thought to involve genetic and environmental factors that lead to an autoimmune response. T-cells have been shown to be involved in the rheumatoid arthritis inflammatory process, with a massive infiltration of T-cells occurring in the affected synovial tissues.[74]

As cyclosporin A is a potent T-cell activation inhibitor through its interaction with cyclophilin A and calcineurin there have been several rheumatoid arthritis clinical trials involving the immunosuppressor.[75] Trials treating patients at a dosage of 6 mg/kg per day for 24 weeks led to a reduction in joint pain and swelling, but were accompanied with impaired renal function in all treated subjects, and hypertension in 70 % of patients. The amount of cyclosporin A given was varied in other trials, and it was found that the drug was apparently effective at doses of $\geq$5 mg/kg day, but limited by nephrotoxicity at this level. Reduction of the dose to 2.5 mg/kg per day diminished the side-effects, but was seldom effective in treating symptoms. The

overall consensus of the clinical trials was that cyclosporin A has too narrow a therapeutic index for effective clinical use in treating rheumatoid arthritis, although patient selection may be a factor in these unfavourable results. The majority of treated subjects were older individuals with advanced, long-standing symptoms and most typically in late and irreversible stages of the disease.[76] Ideally cyclosporin A treatment would be investigated on a younger study population showing early stages of rheumatoid arthritis, however this group of patients generally respond well to treatment with non-steroidal anti-inflammatory drugs and physical therapy.

1.3.3 Anti-parasite activity of cyclosporin A

In the early 1980s parasitology researchers started to investigate the effect of cyclosporin A on various parasitic organisms. Initially, it was hypothesised that CsA treatment would favour the parasite by suppressing the host immune response, thus allowing parasite development and replication to proceed unchallenged. However, early research into schistosome and malaria infections showed that the drug had unexpected anti-parasite activity, with elimination of the parasites and extended host survival.[76] Since this initial discovery, CsA has been shown to adversely affect a wide range of protozoa and helminths both *in vitro* and *in vivo*.[77] The precise mechanism by which CsA exerts its anti-parasitic effects is still subject to debate, but it is thought that CsA binds to parasite cyclophilin; the majority of parasite cyclophilins published in the literature possess a high degree of structural similarity to human CypA.[78] The mode of action may involve inhibition of the PPIase activity of endogenous cyclophilin or inhibition of an essential signal-transduction pathway, perhaps by inhibition of a calcineurin homologue. CsA has been shown to retain anti-parasitic properties at sub-immunosuppressive levels in *in vitro* studies, ruling out the possibility that CsA exerts an indirect effect *via* an interaction with the host's immune system.[77]

1.4 Review of cyclophilin A ligands

1.4.1 Cyclosporin A derivatives

There have been a plethora of cyclosporin derivatives described in the literature since the initial discovery of CsA, all being cyclic undecapeptides that differ from each other by minor differences in the amino acid sequence. A range of naturally occurring cyclosporins, labelled CsB to CsZ, have been insolated from the fungus *Tolypocladium inflatum*, in addition to the main metabolite CsA.[79] Synthetic cyclosporin derivatives have also been produced using solid-phase peptide coupling techniques.[80,81] In an attempt to understand how the small chemical differences between cyclosporin derivatives influence their binding to CypA, Walkinshaw *et al.*, published the analysis of 11 cyclosporin derivatives complexed with CypA (Table 1.1).[58]

Cyclosporin Derivative	R_1	R_2	R_3	R_4	CypA Binding	IL-2
CsA **1**	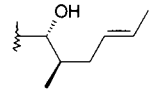				1	1
116450 **6**	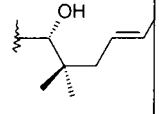	-	-	-	26	4.2
33804 **7**	-		-	-	6	3.1
27402 **8**	-		-	-	1.4	1.0

224698 **9**	-	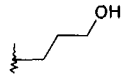	-	-	7.2	7
209313 **10**	-	-	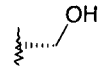	-	0.33	2.4
209650 **11**	-			-	0.69	2.4
209217 **12**	-			-	0.24	1
209825 **13**	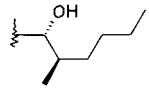			-	0.53	1.8
211810 **14**	-	-	-	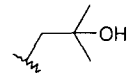	1	110
SDZ NIM 811 **5**	-	-	-	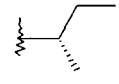	0.6	>1700

Table 1.1: Amino acid side chains for positions 1, 2, 3, and 4 are shown for 11 different CsA derivatives. The CypA binding value in column 6 is relative to CsA, for example derivative **6** binds 26 times weaker than CsA. The IL-2 value in column 7 is a measure of the effect of suppressing the effect of interleukin-2 relative to CsA.

The cyclosporin derivatives outlined in Table 1.1 vary considerably both in their ability to bind to CypA and their immunosuppressant activity. In general, modification of residues 1 and 2 which change the cyclophilin-binding surface of CsA, diminish binding to CypA. This correlates with a slight reduction in immunosuppressive activity. Modification of residue 4 leads to a marked decrease in immunosuppression without substantially affecting CypA binding, this amino acid

forming a sensitive site on the effector loop which protrudes from the CypA active site and binds to calcineurin. Modification at position 3 leads to stronger binding to CypA compared to CsA. The reason for this enhanced binding is not clear as there are no obvious pockets in the protein to accept residue-3 side chains. A possible explanation comes from the observation using NMR spectroscopy that ligand **10** adopts the same conformation in aqueous solution as it does bound to CypA.[82] This pre-organisation into the bound conformation would reduce the entropy loss upon binding to CypA, and may result in an increase in binding affinity.

1.4.2 Sanglifehrins

Screening of microbial broth extracts for metabolites that could block CypA-CsA complex formation led to the discovery of a novel class of macrocylic compounds, the sanglifehrins (SF), produced by *Streptomyces* A92-308110. The structures of sanglifehrins A, B, C and D have been determined by NMR and X-ray crystallography of the CypA-SF complex (Table 1.2).[83] Sanglifehrins A and B are genuine metabolites whereas C and D are formed during the isolation process.[84] The sanglifehrins bind to the same site on CypA as CsA, with sanglifehrins A and B exhibiting approximately 10 to 20 fold higher affinity for CypA than CsA, whereas the affinity of sanglifehrins C and D for CypA is comparable to that of CsA.[85]

The sanglifehrins inhibit the PPIase activity of CypA, but do not form a complex with calcineurin, thus having no effect on its phosphatase activity. However, the compounds are also immunosuppressants, with a mode of action that is unclear but known to be different to CsA. Unlike CsA, sanglifehrins do not inhibit IL-2 transcription, and block T-cell proliferation at a later stage. Interestingly, the immunosuppressive properties of sanglifehrins are independent to binding to CypA; competitive binding of a non-immunosuppressant cyclosporin derivative had no effect on sanglifehrin activity.[86] Sanglifehrins also do not bind to FKBP12, with the effector protein and precise mechanism of immunosuppression currently unknown.

Sanglifehrin derivative	Structure	CypA binding (relative IC_{50})	T-cell inhibition (relative IC_{50})
A **15**	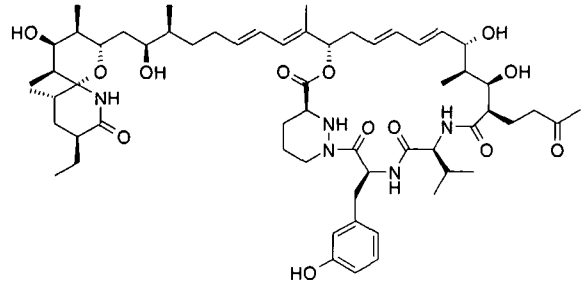	0.05 (20-fold increase)	16 (16-fold decrease)
B **16**	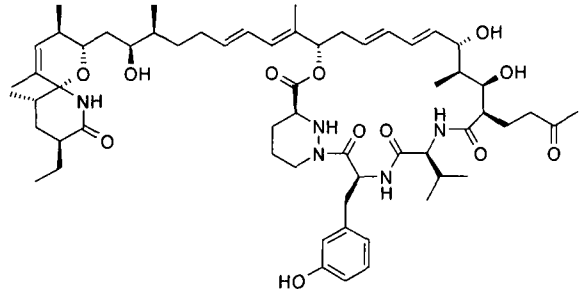	0.05	10
C **17**	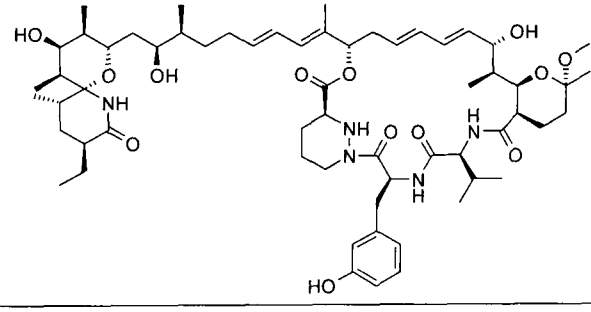	0.61	113
D **18**	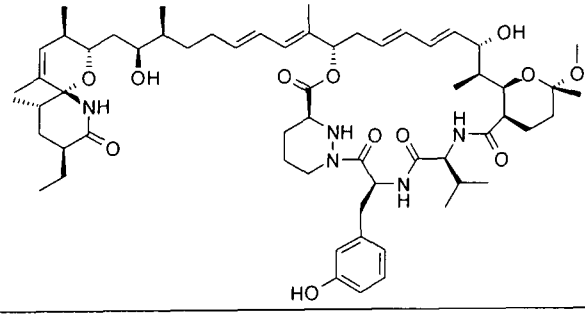	0.71	60

Table 1.2: Structure of Sanglifehrins A – D. CypA. Binding was measured by competitive ELISA format and is described relative to CsA. CsA had a CypA binding IC_{50} of 83 ± 16 nM and T-cell inhibition IC_{50} of 2.7 ± 1.4 nM when measured in the same manner.[86]

1.4.3 Peptide ligands

There have been several X-ray and NMR structures of CypA-peptide complexes published in the literature. The first cyclophilin-peptide structure to be solved was of the tetrapeptide substrate ac-Ala-Ala-Pro-Ala-amc **19** (ac, acetyl; amc, amidomethylcoumarin) (Figure 1.11) bound to the active site of CypA.[87] The proline residue was found to be bound in the *cis* configuration and occupied the CypA hydrophobic pocket defined by the side chains of Phe60, Met61, Phe113, Leu122, and His126. Hydrogen bonding occurred between the backbone amide *NH* and *O* atoms of Asn102 with the corresponding *O* and *NH* atoms of the substrate Ala2 residue, and a third hydrogen bond was detected between Arg55 and the substrate prolyl carbonyl *O* atom.

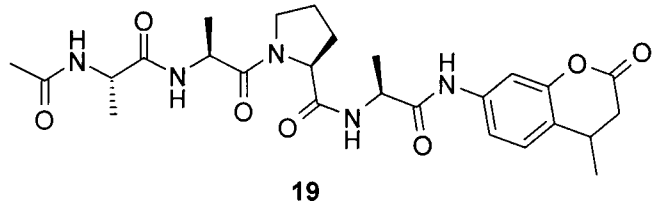

19

Figure 1.11: Structure of ac-Ala-Ala-Pro-Ala-amc.

The structures of CypA complexes with the dipeptides Ala-Pro, Ser-Pro, His-Pro, and Gly-Pro have been determined by X-ray crystallography and refined at high resolution.[88] It was found that a single dipeptide molecule bound to the same CypA hydrophobic binding pocket as CsA, and all dipeptides bound to CypA with similar interactions and in the *cis* conformation. The proline side chains of the dipeptides sit in the CypA hydrophobic pocket, the *C*-terminus of the proline forms two hydrogen bonds with Arg55, and *N*-terminus of the dipeptide hydrogen bonds to the backbone carbonyl oxygen of Asn102 and a water molecule. The side chains of the *N*-terminus amino acids were found to interact weakly with CypA and did not significantly contribute to the binding of the dipeptides; this implies that cyclophilin has a broad catalytic specificity with respect to Xaa in Xaa-Pro.

The crystal structures of succinyl-Ala-Pro-Ala-*p*-nitroanilide[89] **20** and the structurally similar succinyl-Ala-Ala-Pro-Phe-p-nitroanilide[90] **21** (Figure 1.12) bound to CypA have been resolved and show a similar binding pattern to peptide **19** and the dipeptides Ala-Pro, Ser-Pro, His-Pro, and Gly-Pro. Both peptides were revealed to be again binding in the *cis* conformation in the CypA active site, with proline residing in the hydrophobic pocket, and the peptide bonds between Arg55, Asn102 and the peptide substrates were conserved.

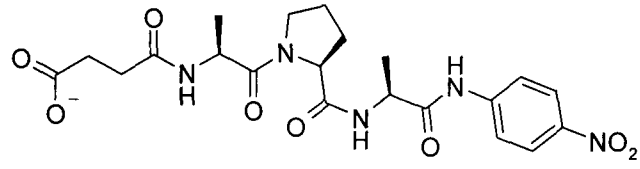

20

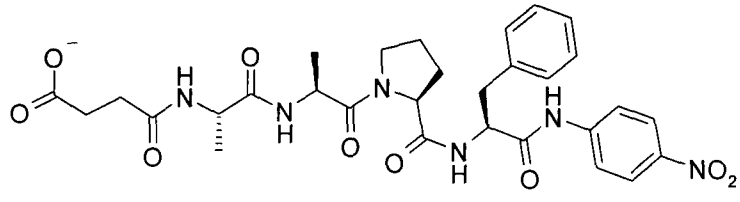

21

Figure 1.12: Structure of suc-APA-na **20** and suc-AAPF-na **21**.

There have been other peptide substrates of varying lengths that have been characterised binding to CypA, and interestingly the conformation of CypA does not significantly alter upon peptide binding.[91] The hydrogen bonding recognition pattern is conserved among different linear peptide substrates, with Asn102 and Arg55 forming key binding interactions with the peptides. Comparison of the CypA-peptide structures with the CypA-CsA complex structure also revealed that the prolyl of the peptides and MeVal-11 of CsA interact with the same hydrophobic pocket in the CypA binding site.[91]

1.4.4 Non-peptide ligands

There are few reported examples of non-peptide synthetic ligands that have been designed to bind to CypA, with CsA derivatives and peptide ligands predominating. The majority of interest in synthetic CypA ligands has arisen from attempts to investigate cyclophilin PPIase mechanisms. Good examples of this type of ligand are the first *de novo* ground-state and transition-state analogue inhibitors reported by Wang *et al.* These ligands were inspired by the structure of *cis* bound Xaa-Pro peptide ligands and the "twisted amide" transition state proposed by the catalysis by distortion mechanism (Figure 1.13).[51]

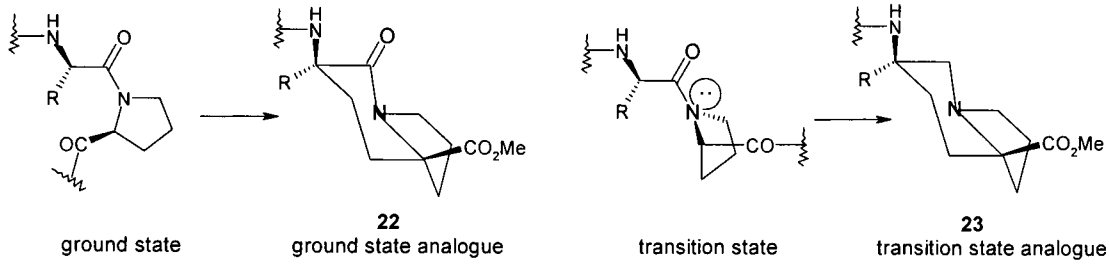

Figure 1.13: Ground- and transition-state analogue structures.[51]

The ground state analogues were based on a bicyclic lactam structure that had previously shown structural similarity to the dipeptide *cis* Gly-Pro upon binding to CypA.[92] A number of derivatives incorporating aryl groups adjacent to the lactam carbonyl were synthesised; it was reasoned that increasing the ligand lipophilicity would result in a tighter binding within the CypA hydrophobic pocket (Figure 1.14).

Inspection of the general bicyclic lactam structure **22** revealed that the lactam nitrogen atom corresponded to the peptide substrate proline nitrogen that undergoes sp^2 to sp^3 rehybridisation in the course of *cis/trans* isomerisation. With this in mind, the transition state analogue **23** was designed around a tertiary amine structure; it was reasoned that the amine would be capable of forming a hydrogen bond with Arg55 in the active site, mimicking the proposed "twisted amide" transition state (Figure 1.15).[51]

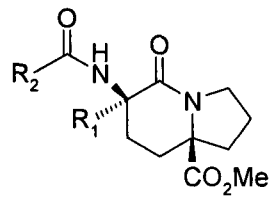

22a: R_1 = 2-$CH_2C_{10}H_7$, R_2 = tert-BuO
22b: R_1 = $CH_2C_6H_5$, R_2 = BnO
22c: R_1 = 2-$CH_2C_{10}H_7$, R_2 = BnO
22d: R_1 = 2-$CH_2C_{10}H_7$, R_2 = Me
22e: R_1 = $CH_2C_6H_5$, R_2 = tert-BuO
22f: R_1 = H, R_2 = BnO

Figure 1.14: Ligands based on a ground state structure.

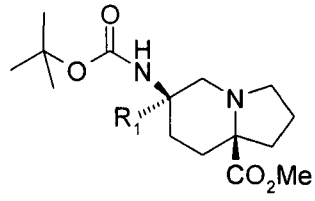

23a: R_1 = H
23b: R_1 = 2-$CH_2C_{10}H_7$

Figure 1.15: Ligands based upon a transition-state structure.

The ground state analogues followed the expected trend upon screening against CypA with binding affinity increasing as the hydrophobic nature of the ligand increased. However, the affinity of ligand **23b** was found to be four times weaker than that of the corresponding lactam **22a**. This conflicted with the expected outcome that the proposed transition-state analogue would bind more strongly to the CypA active site than the ground-state analogue. It was postulated that the carbonyl group of the lactam may be important for the stability of the CypA-ligand complex, or that the position of the nitrogen lone pair in **23b** might not coincide with peptide's proline nitrogen lone pair upon binding to CypA.[51]

1.5 Previous ligand design and lead discovery

The previous research on this project initially focussed upon *de novo* ligand design using *in silico* screening; this was followed by virtual lead compound selection and optimisation. Synthesis and modification of lead compounds was carried out by Elizabeth Moir; this would allow for the screening of ligands to ascertain efficacy against CypA. Reiteration of the process allowed any structure activity relationship (SAR) information to be used in the design of subsequent ligands (Figure 1.16).

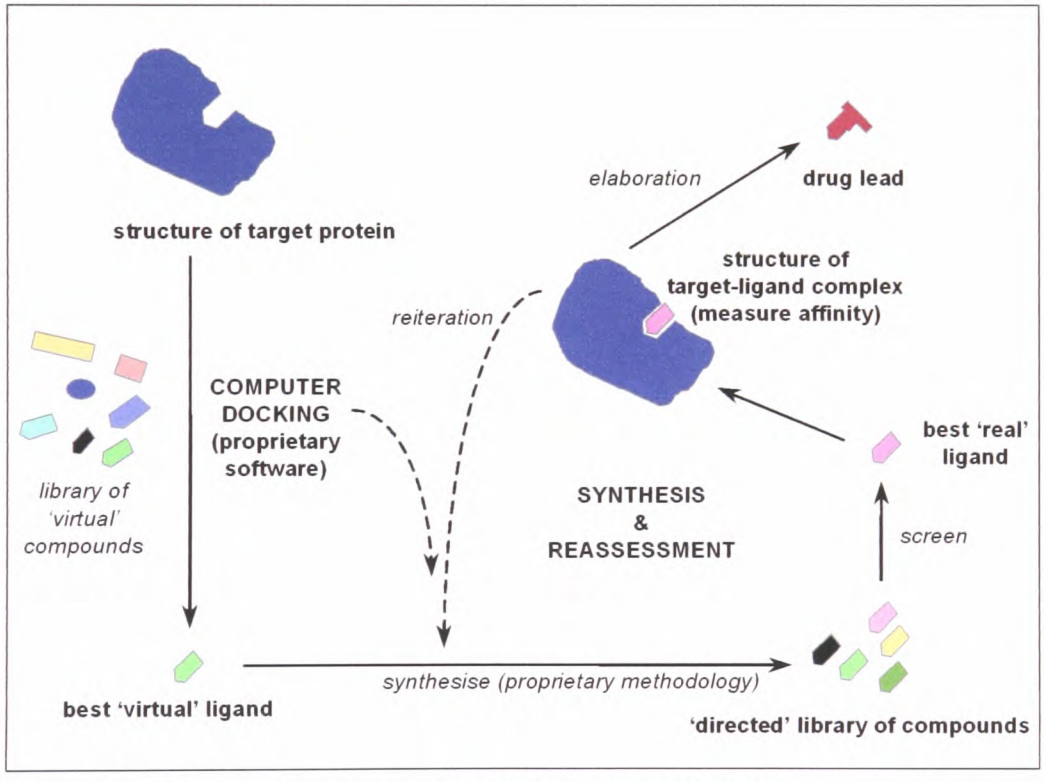

Figure 1.16: Schematic representation of ligand design and synthesis.[93]

The computer docking program used for the *in silico* screening was LIDAEUS (Ligand Design at Edinburgh University) in collaboration with Professor Malcolm Walkinshaw at the Structural Biochemistry Group at the University of Edinburgh. The LIDAEUS screening procedure uses a database of small molecule three-dimensional structures by fitting ligand atoms of each test structure onto site points

representing the physiochemical nature and structure of the protein active site.[94] The strength of protein-ligand binding depends on the complimentary of shape and charge between the ligand and the protein receptor site, as well as entropic factors. The ligand affinity for the protein can be graded using scoring functions that account for van der Waals, hydrogen bonding and hydrophobic interactions. The Maybridge Fine Chemicals database can then be searched to highlight commercially available ligands.

The LIDAEUS programme was used to discover the first non-peptide ligands that were found to bind to CypA.[91] The novel ligands were found to bind to the CsA binding pocket on CypA upon X-ray analysis, and belong to three structural groups: piperidines (3-acetyl-1-methyl piperidine **24** and ethyl piperidine glyoxylate **25**); DMSO and derivatives (dimethyl sulfoxide **26**, tetramethylene sulfoxide **27** and cyclopentanone **28**) and dimedone (5,5-dimethyl-1,3-cyclohexanedione **29**) (Table 1.3).

Piperidines	DMSO derivatives	Dimedone
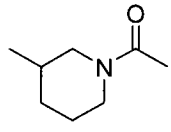 **24**	 **26**	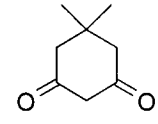 **29**
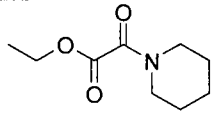 **25**	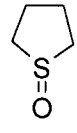 **27**	
	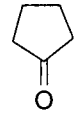 **28**	

Table 1.3: Novel CypA ligands discovered by LIDAEUS programme.

1.5.1 Initial lead compound - dimedone

It was decided at an early stage in the project to focus on dimedone (**29**) as the core pharmacophore for subsequent ligand synthesis. The versatile reactivity of the 1,3-diketone moiety is well known and well suited to chemical derivatisation. Dimedone was tested experimentally for binding to CypA and a K_d of 22 mM was determined using a fluorescence assay, as outlined in Chapter 4. For comparison, CsA has been reported to have a K_d of 36.8 nM using the same assay conditions.[95] It was possible to obtain a crystal structure of the CypA-dimedone complex by soaking a crystal of CypA into a solution of dimedone and then subjecting the crystal to X-ray diffraction.[58] Inspection of the structure revealed that dimedone binds in the same hydrophobic binding pocket as Pro-containing peptides and CsA. Superimposing the dimedone binding co-ordinates onto the crystal structure of CypA-CsA reveals that the dimedone geminal dimethyl groups bind in the same defined hydrophobic cavity as the MeVal11 of CsA. Also, one of the carbonyl groups of dimedone is in hydrogen bonding distance of Arg55, known to be a key hydrogen bonding residue in the CypA binding pocket (Figure 1.16).

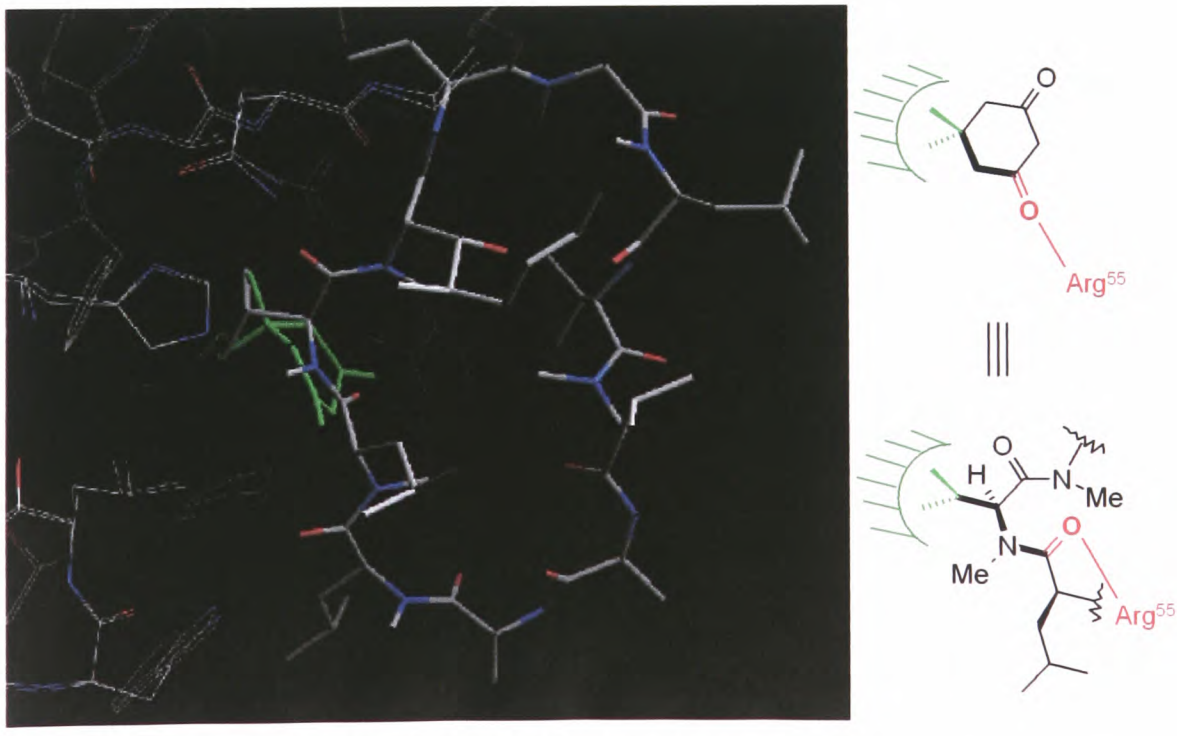

Figure 1.16: Crystal structure of CypA-CsA (white) and -dimdone (green).

1.5.2 Lead optimisation

Comparison of the CypA-dimedone complex with the CypA-CsA structure revealed that although dimedone was binding in the same active site, CsA was able to bind to several more of the CypA residues *via* hydrogen bonding and hydrophobic interactions. As CsA is an undecapeptide it was hypothesised that attachment of amino acids to the dimedone core would result in a greater binding affinity by mimicking some of these CypA-CsA interactions. A variety of ligands based upon an *O*-acylated dimedone enol ester structure were synthesised by Elizabeth Moir, and upon screening against CypA, ligand **30** (Figure 1.17) was found to have a dissociation constant of 22 μM, a ca. 1,000 fold improvement on dimedone.[94]

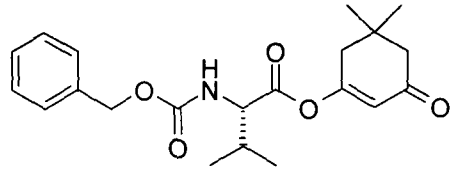

30

Figure 1.17: Structure of ligand **30**.

An X-ray crystal structure of CypA-**30** was obtained (Figure 1.18), and upon inspection of the complex it appeared that attachment of the Cbz-valine moiety to the dimedone core had reproduced several of the CypA-CsA binding interactions (Figure 1.19). The dimedone core was still bound in the CypA hydrophobic pocket, and also the valine dimethyl groups appeared to be mimicking the CypA-CsA Abu2 hydrophobic interaction. The probable hydrogen bond between the dimedone carbonyl group and Arg55 was conserved, with additional potential hydrogen bonding interactions between ligand **30** and Asn102 and Gln111 of CypA.

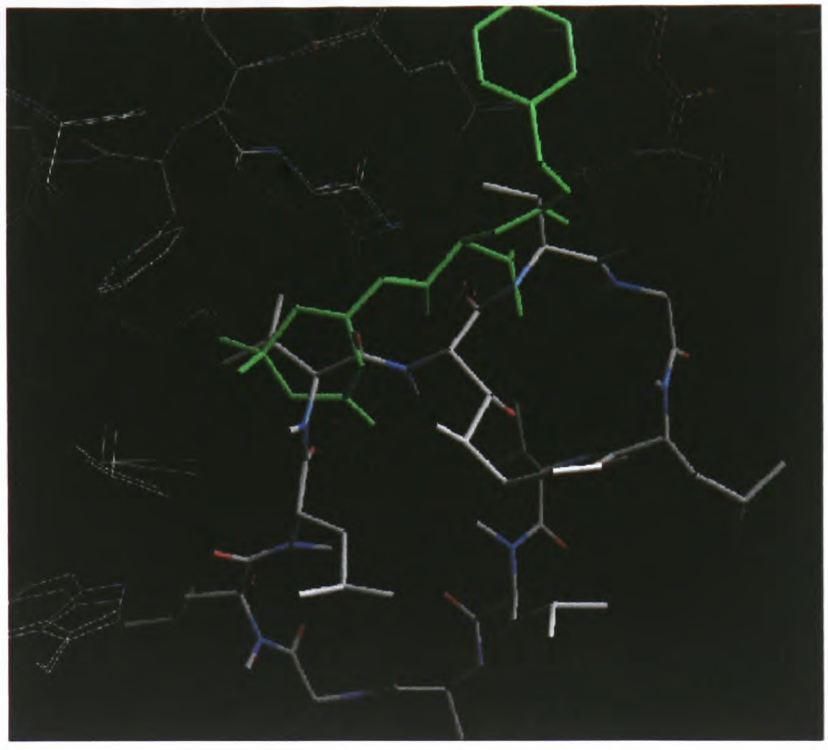

Figure 1.18: Crystal structure of CypA-CsA (white) and **-30** (green).

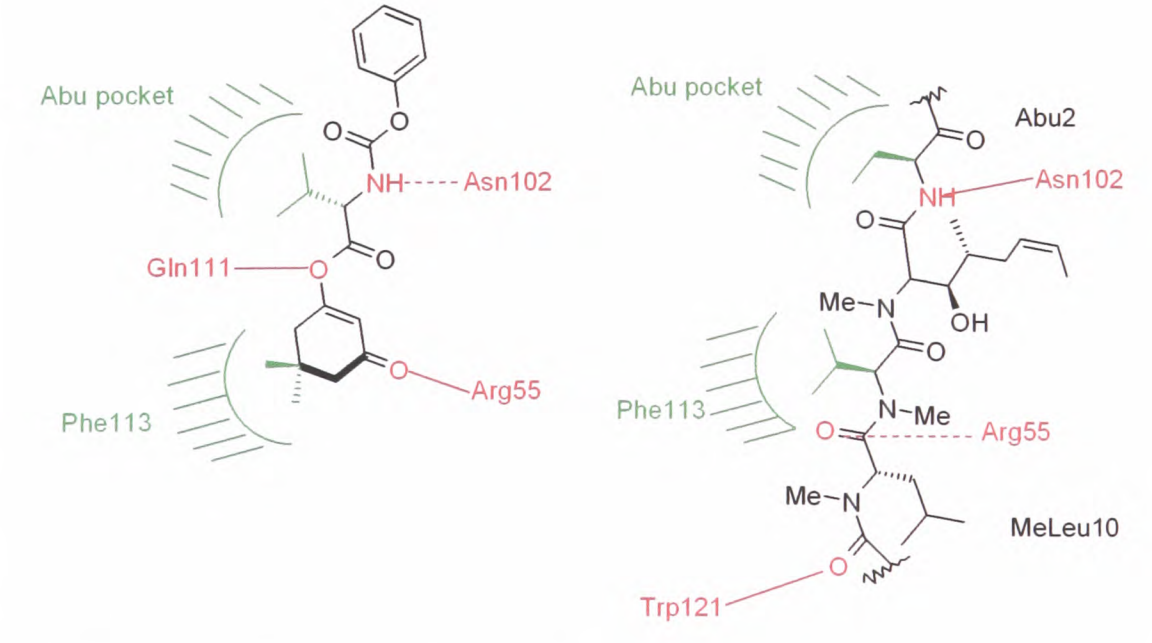

Figure 1.19: Structure of ligand **30** and CsA residues MeLeu10-MeVal11-MeBmt1-Abu2. Hydrophobic interactions with CypA are highlighted in green, H-bonds in red.

References

(1) A. S. Travis, *Technol. Cult.*, **1990**, *31*, 51.

(2) J. Drews, *Science*, **2000**, *287*, 1960.

(3) G. R. Hamilton, T. F. Baskett, *Can. J. Anesth.*, **2000**, *47*, 367.

(4) R. J. Huxtable, S. K. W. Schwarz, *Mol. Interv.*, **2001**, *1*, 189.

(5) A. Fleming, *Br. J. Exp. Pathol.*, **1940**, *10*, 226.

(6) D. M. Armistead, M. W. Harding, *Ann. Rep. Med. Chem.*, **1993**, *28*, 207.

(7) Adapted from M. Lutz, T. Kenakin, *Quantitative Molecular Pharmacology and Informatics in Drug Discovery*, Wiley, Chichester, **1999**.

(8) B. Cudney, S. Patel, K. Weisgraber, Y. Newhouse, A. McPherson, *Acta Cryst. Sect. D*, **1994**, *50*, 414.

(9) S. W. Fesik, *J. Med. Chem.*, **1991**, *34*, 2937.

(10) www.rcsb.org/pdb.

(11) G. Klebe, *J. Mol. Med.*, **2000**, *78*, 269.

(12) R. E. Babine, S. L. Bender, *Chem. Rev.*, **1997**, *97*, 1359.

(13) D. H. Williams, E. Stephens, D. P. O'Brien, M. Zhou, *Angew. Chem. Int. Ed.*, **2004**, *43*, 6596.

(14) H. - J. Böhm, G. Klebe, *Angew. Chem. Int. Ed. Engl.*, **1996**, *35*, 2588.

(15) N. Muller, *Acc. Chem. Res.*, **1990**, *23*, 23.

(16) T. D. P. Stack, Z. Hou, K. N. Raymond, *J. Am. Chem. Soc.*, **1993**, *115*, 6466.

(17) D. J. Cram, *Angew. Chem. Int. Ed. Engl.*, **1988**, *27*, 1009.

(18) A. S. Ripka, D. H. Rich, *Curr. Opin. Chem. Biol.*, **1998**, *2*, 441.

(19) N. R. A. Beeley, *Drug Disc. Today*, **2000**, *5*, 354.

(20) R. Hirshmann, *Angew. Chem. Int. Ed. Engl.*, **1991**, *30*, 1278.

(21) S. L. Schreiber, *Bioorg. Med. Chem.*, **1998**, *6*, 1127.

(22) T. J. Mitchison, *Chem. Biol.*, **1994**, *1*, 3.

(23) B. R. Stockwell, *Nat. Genet.*, **2000**, 116.

(24) D. R. Spring, *Chem. Soc. Rev.*, **2005**, *34*, 472.

(25) S. L. Schreiber, *Chem. Eng. News*, **2003**, *81*, 51.

(26) E. M. Gordon, M. A. Gallop, D. V. Patel, *Acc. Chem. Res.*, **1996**, *29*, 144.

(27) M. D. Burke, S. L. Schreiber, *Angew. Chem. Int. Ed.*, **2004**, *43*, 46.

(28) A. Furka, F. Sebestyen, M. Asgedom, G. Dido, *Int. J. Pept. Protein. Res.*, **1991**, *37*, 487.

(29) S. L. Schreiber, *Science*, **2000**, *287*, 1964.

(30) H. Kubinyi, *EFMC-Yearbook*, **2003**, 14.

(31) S. H. White, *Protein Science*, **2004**, *13*, 1948.

(32) C. A. Lipinski, F. Lombardo, B. W. Dominy, P. J. Feeney, *Adv. Drug. Deliv. Rev.*, **1997**, *23*, 3.

(33) C. A. Lipinski, *Drug Disc. Today*, **2004**, *1*, 337.

(34) C. B. Anfinsen, *Science*, **1973**, *181*, 223.

(35) S. F. Göthel, M. A. Marahiel, *Cell Mol. Life Sci.*, **1999**, *55*, 423.

(36) T. Kiefhaber, R. Quaas, U. Hahn, F. Schmid, *Biochemistry,* 1990, **29**, 3061

(37) G. Fischer, H. Bang, H. Mech, *Biomed. Biochim. Acta*, **1984**, *43*, 1101.

(38) R. E. Handschumacher, M. W. Harding, J. Rice, R. J. Drugge, D. W. Speicher, *Science*, **1984**, *226*, 544.

(39) G. Fischer, B. Wittmann-Liebold, K. Land, T. Kiefhaber, F. X. Schmid, *Nature*, **1989**, *337*, 476.

(40) N. Takahashi, T. Hayano, M. Suzuki, *Nature*, **1989**, *337*, 473.

(41) J. J. Sikierka, S. H. Y. Hung, M. Poe, S. C. Lin, N. H. Singal, *Nature*, **1989**, *341*, 755.

(42) M. W. Harding, A. Galat, S. L. Ueling, S. L. Schreiber, *Nature*, **1989**, *341*, 758.

(43) T. Kino, H. Hatanaka, M. Hashimoto, M. Nishiyama, T. Goto, M. Okuhara, *J. Antibiotics*, **1987**, *40*, 1249.

(44) S. L. Schreiber, *Science*, **1991**, *251*, 283.

(45) J. U. Rahfeld, A. Schierhorn, K. Mann, G. Fischer, *FEBS Letters*, **1994**, *343*, 64.

(46) L. Henning, C. Chistner, M. Kipping, B. Schelbert, K. Rücknagel, S. Grabley, G. Küllertz, G. Fischer, *Biochemistry*, **1998**, *37*, 5953.

(47) D. Stewart, A. Sarkar, J. Wampler, *J. Mol. Biol.*, **1990**, *214*, 253.

(48) G. Fisher, E. Berger, H. Bang, *FEBS Letters*, **1989**, *250*, 276.

(49) J. Liu, M. W. Albers, C. -M. Chen, S. L. Schreiber, C. T. Walsh, *Proc. Nat. Acad. Sci. U.S.A.*, **1990**, *87*, 2304.

(50) R. Harrison, R. Stein, *Biochemistry*, **1990**, *29*, 1684.

(51) H. Wang, K. Kim, R. Bakhtiar, J. Germanas, *J. Med. Chem,* **2001**, *44*, 2593.

(52) J. L. Kofron, P. Kuzmic, V. Kichore, E. Colon-Bonilla, D. H. Rich, *Biochemistry*, **1991**, *30*, 6127.

(53) A. Radzacki, S. A. Acheson, R. Wolfenden, *Bioorg. Chem.*, **1992**, *20*, 382.

(54) H. M. Ke, D. Mayrose, W. Cao, *Proc. Nat. Acad. Sci. U.S.A.*, **1993**, *90*, 3324.

(55) M. Dreyfuss, E. Haerri, H.Hoffman, H. Kobel, H. Tscherter, *Eur. J. Appl. Microbiol*, **1976**, *3*, 125.

(56) J. F. Borel, C. Faurer, H. U. Gubler, H. Stacholin, *Agents Actions*, **1976**, *6*, 458.

(57) F. E. Padova, *Perspect. Drug Discov.*, **1994**, *2*, 49.

(58) J. Kallen, V. Mikol, P. Taylor, M. D. Walkinshaw, *J. Mol. Biol.*, **1998**, *283*, 435.

(59) M. K. Rosen, P. J. Belshaw, David. G. Alberg, S. L. Schreiber, *Bioorg. Med. Chem. Lett.*, **1992**, *2*, 747.

(60) V. Mikol, J. Kallen, G. Pflügl, M. D. Walkinshaw, *J. Mol. Biol.*, **1993**, *234*, 1119.

(61) L. D. Zydowsky, F. A. Etzkorn, H. Y. Chang, S. B. Ferguson, L. A. Stolz, S. I. Ho, C. T. Walsh, *Protein Sci.*, **1992**, *1*, 1092.

(62) J. Liu, J. D. Farmer, W. S. Lane, J. Friedman, I. Weissman, S. L. Schreiber, *Cell*, **1991**, *66*, 807.

(63) S. L. Schreiber, G. R. Crabtree, *Immunol. Today*, **1992**, *13*, 136.

(64) M. T. G. Ivery, *Bioorg. Med. Chem.*, **1999**, *7*, 1389.

(65) Q. Huai, H. -Y. Kim, Y. Liu, Y. Zhoa, A. Mondragon, J. O. Liu, H. Ke, *Proc. Nat. Acad. Sci. U.S.A.*, **2002**, *99*, 12037.

(66) J. P. Griffith, J. L. Kim, E. E. Kim, M. D. Sintchak, J. A. Thompson, M. J. Fitzgibbon, M. A. Fleming, P. R. Caron, K. Hsiao, M. A. Navia, *Cell*, **1995**, *82*, 507.

(67) E. K. Franke, H. E. H. Yuan, J. Luban, *Nature*, **1994**, *372*, 359.

(68) D. Braaten, J. Luban, *EMBO J.*, **2001**, *20*, 1300.

(69) T. R. Gamble, F. F. Vajdos, S. Yoo, D. K. Worthylake, M. Houseweart, W. I. Sundquist, C. P. Hill, *Cell*, **1996**, *87*, 1285.

(70) M. Thali, *Mol. Med. Today*, **1995**, 287.

(71) Y. D. Zhoa, Y. Q. Chen, M. Schutkowski, G, Fischer, H. Ke, *Structure*, **1997**, *5*, 139.

(72) E. K. Franke, J. Luban, *Virology*, **1996**, *222*, 279.

(73) B. Rosenwirth, A. Billich, R. Datema, P. Donatsch, F. Hammerschmid, R. Harrison, P. Hiestand, H. Jaksche, P. Mayer, P. Peichl, *Antimicrob. Agents Chemother.*, **1994**, *38*, 1763.

(74) Y. Kobari, Y. Misaki, K. Setoguchi, W. Zhao, Y. Komagata, K. Kawahata, Y. Iwakura, K. Yamamoto, *Int. Immunol.*, **2004**, *16*, 131.

(75) J. R. Seibold, *Persp. Drug. Discov.*, **1994**, *2*, 25.

(76) A. P. Page, S. Kumar, C. K. S. Carlow, *Parasitology Today*, **1995**, *11*, 385.

(77) L. H. Chappell, J. M. Wastling, *Parasitology*, **1992**, *105*, S25.

(78) D. Ma, L. S. Nelson, K. LeCoz, C. Poole, C. K. S. Carlow, *J. Biol. Chem.*, **2002**, *277*, 14925.

(79) v. R. Traber, H. Hofmann, H. –R. Loosli, M. Ponelle, A. v. Wartburg, *Helv. Chim. Acta*, **1987**, *70*, 13.

(80) S. Y. Ko, R. M. Wenger, *Helv. Chim. Acta*, **1997**, *80*, 695.

(81) P. Li, J. C. Xu, *J. Org. Chem.*, **2000**, *65*, 2951.

(82) R. M. Wenger, J. France, G. Bovermann, L. Wallister, A. Widmer, H. Widmer, *FEBS Letters*, **1994**, *340*, 255.

(83) J. Kallen, R. Sedrani, G. Zenke, J. Wagner, *J. Bio. Chem.*, **2005**, *280*, 21965.

(84) T. Fehr, J. Kallen, L. Oberer, J. –J. Sanglier, W. Schilling, *J. Antibiotics*, **1999**, *52*, 474.

(85) J. –J. Sanglier, V. Quesniaux, T. Fehr, H. Hofmann, M. Mahnke, K. Memmert, W. Schuler, G. Zenke, L. Gschwind, C. Maurer, W. Schilling, *J. Antibiotics*, **1999**, *52*, 466.

(86) G. Zenke, U. Strittmatter, S. Fuchs, V. F. J. Quesniaux,V. Brinkmann, W. Schuler, M. Zurini, A. Enz, A. Billich, J. –J. Sanglier, T. Fehr, *J. Immunol.*, **2001**, *166 (12)*, 7165.

(87) J. Kallen, M. D. Walkinshaw, *FEBS Letters*, **1992**, *300*, 286.

(88) Y. Zhoa, H. Ke, *Biochemistry*, **1996**, *35*, 7362.

(89) M. Konno, M. Ito, T. Hayano, N. Takahashi, *J. Mol. Biol.*, **1996**, *256*, 897.

(90) Y. Zhao, H. Ke, *Biochemistry*, **1996**, *35*, 7356.

(91) P. Taylor, H. Husi, G. Kontopidis, M. D. Walkinshaw, *Prog. Biophys. Molec. Biol.*, **1997**, *67*, 155.

(92) K. Kim, J. –P. Dumas, J. P. Germanas, *J. Org. Chem.*, **1996**, *61*, 3138.

(93) E. M. Moir, *Design and Synthesis of High Affinity Ligands for Human Cyclophilin A*, Ph.D. Thesis, University of Edinburgh, **2001**.

(94) S. Y. Wu, I. McNae, G. Kontopidis, S. J. McClue, C. McInnes, K. J. Stewart, S. Wang, D. I. Zheleva, H. Marriage, D. P. Lane, P. Taylor, P. M. Fischer, M. D. Walkinshaw, *Structure*, **2003**, *11*, 399.

(95) H. Husi, M. Zurini, *Anal. Biochem.*, **1994**, *222*, 251.

2. Results and Discussion I - Ligand Design and Synthesis

2.1 *O*-acylated dimedone enol esters

The initial objective of the project was to re-synthesise several *O*-acylated dimedone enol-ester ligands. The aim was to improve yields, confirm purity and to further develop assay methods. A variety of synthetic routes to the *O*-acylated dimedone enol ester type compounds had been previously utilised,[1] but it was found that reactions between acid fluorides and dimedone were the most facile.

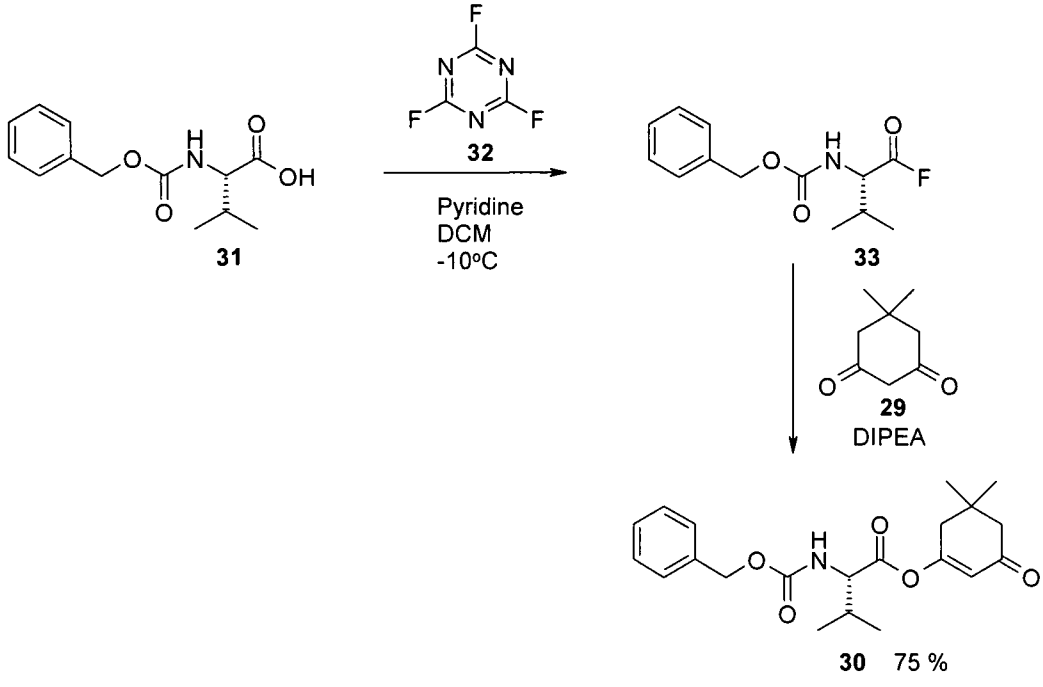

Scheme 2.1: Synthesis of ligand **30**

To re-synthesise the lead compound **30**, dimedone was acylated using the *N*-Cbz-amino acid fluorination strategy described by Carpino *et al.*, (Scheme 2.1).[2] Commercially available *N*-benzyloxycarbonyl-L-valine **31** was firstly reacted with cyanuric fluoride **32** in the presence of pyridine to form the intermediate acid fluoride **33**.[3] Acid fluorides were used in preference to acid chlorides as they are known to be more stable to hydrolysis than the chlorides.[4] Dimedone was then

reacted with the acid fluoride in the presence of *N,N'*-diisopropylethylamine base to give the enol ester product **30**. It was found that the overall yields were improved by proceeding directly to the dimedone addition step after work-up of the acid fluoride reaction mixture, rather than isolation and full characterisation of the acid fluoride itself. Infra-red spectroscopy was used as the principle analytical tool, acid fluorides having a distinctive peak at around ν_{max} 1845 cm^{-1}.

The same acid fluoride strategy was used to make two further enol ester ligands, **37** and **38** (Scheme 2.2). Phenylalanine and 1-amino-1-cyclopentane carboxylic acid were each protected as their alloc derivative by dissolving the amino acid in 4M sodium hydroxide solution and adding aliquots of allyl chloroformate at 0°C. The *N*-protected amino acids were then activated as the acid fluoride and coupled to dimedone using the same procedure outlined above.

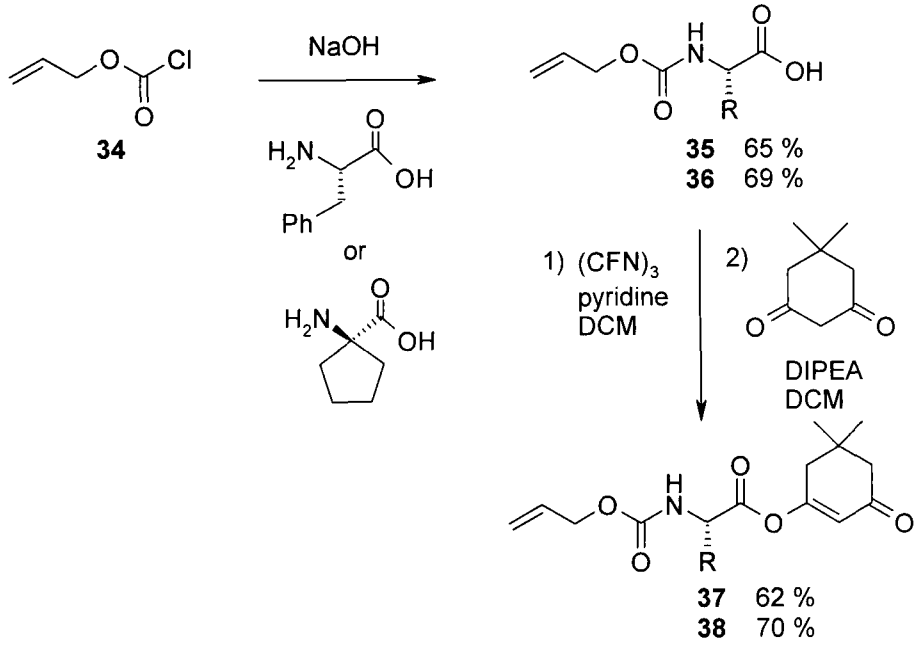

Scheme 2.2: Synthesis of *N*-alloc-amino acid dimedone derivatives. (R = benzyl in structures **35**, **37** or cyclopentyl in structures **36**, **38**)

Whilst the acid fluoride chemistry shown in Schemes 2.1 and 2.2 resulted in the synthesis of the desired products in acceptable yields, there were shortcomings deriving from the use of cyanuric fluoride. Although the fluorination reaction gives

the crude acid fluoride in good yield, the by-product of the reaction is cyanuric acid **39** (Scheme 2.3),[5] which forms a sticky white precipitate that is sparingly soluble in dichloromethane and requires several aqueous wash and filtration steps to fully remove. Although ice-water is used there is still a risk of hydrolysing the acid fluoride, thus reducing the yield of the next coupling step.

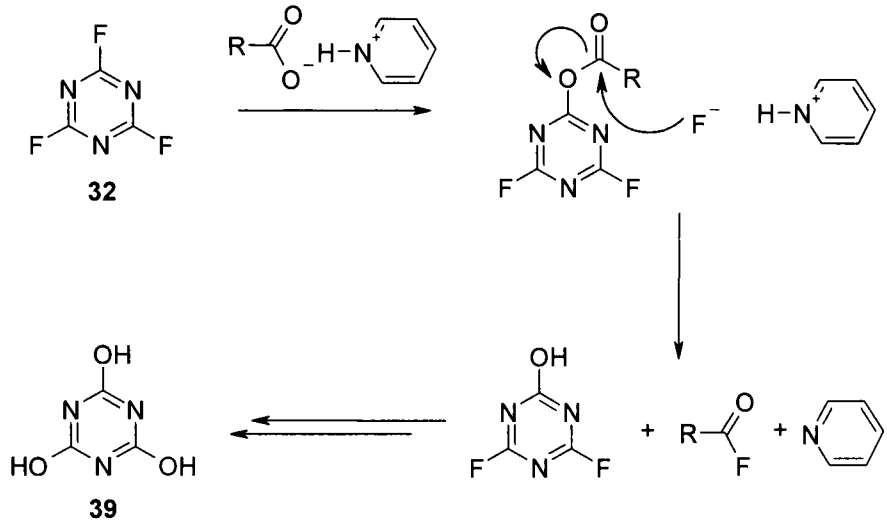

Scheme 2.3: Mechanism of amino acid fluorination by cyanuric fluoride and pyridine.

To overcome the problems posed by the formation of cyanuric acid it was necessary to investigate the use of other fluorinating reagents. Sulfur tetrafluoride,[6] benzoyl fluoride,[7] selenium tetrafluoride[8] and tetramethylfluorformamidinium hexafluorophosphate (TFFH)[9] have all been used to fluorinate carboxylic acids, however diethylaminosulfur trifluoride (DAST) seemed the most promising reagent. Previously used to convert alcohols to fluorides,[10] DAST has also been shown to successfully fluorinate Fmoc-α-amino acids.[11] Using the procedure described by Suresh *et al.*,[12] *N*-benzyloxycarbonyl-L-valine was reacted with DAST at room temperature to give the acid fluoride that was then coupled to dimedone to give the enol-ester product **30** as previously. This method was found to work well, requiring only one wash with ice-water to give the pure acid fluoride in excellent 94 % yield, and unlike in the case of cyanuric fluoride, no base was necessary.

2.2 Alkyl-dimedone derivatives

Previous work on the project by Lizzie Moir revealed that the lead ligand **30** and CsA occupy similar positioning within the CypA active site. In an attempt to further probe the active site, the crystal structure of the CypA-ligand complex was analysed to see if it was possible to extend out from the dimedone core in more than one direction. Examination of the crystal structure indicated space available within the CypA active site outwith the binding site of dimedone (represented in Figure 2.1 by the red arrow). Alkylation at the C-6 position of dimedone would thus allow for preservation of the main interactions of the ligand with the active site, whilst introducing the potential for additional binding interactions.

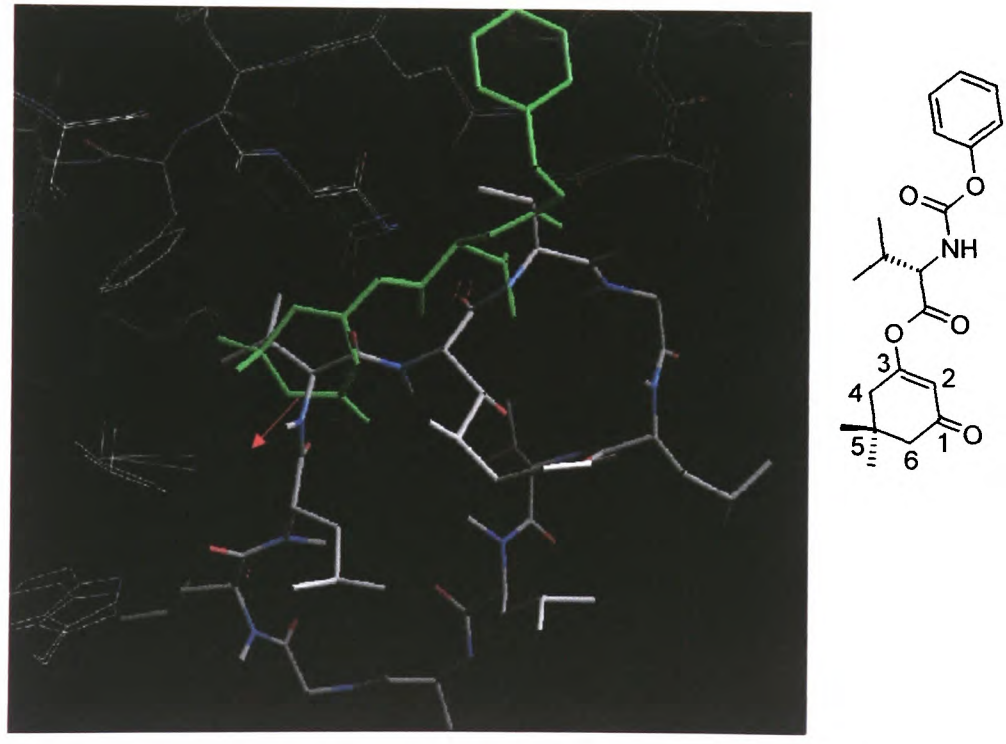

Figure 2.1: Crystal structure of CypA-CsA (white) and -**30** (green). Dimedone ring numbering scheme for *o*-acylated compounds shown on the right.

A review of the literature revealed that Harwood and co-workers, had successfully alkylated 1,3-cyclohexanediones at the C-4 position using various alkyl halides.[13] The method involved the generation of the dimedone dianionic species using lithium diisopropylamide (LDA) and hexamethylphosphoric triamide (HPMA) as a

complexing agent, followed by alkylation (Scheme 2.4). Alkylation at C-4 is accomplished through reaction of the kinetic enolate at low temperature, as opposed to the energetically more stable thermodynamic enolate at the dicarbonyl C-2 position.

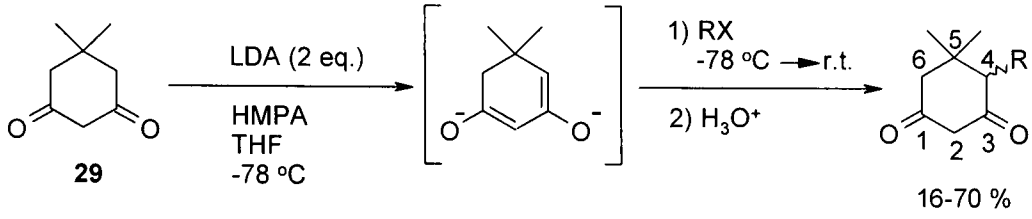

R = CH_3, $CH_2CH_2CH_3$, $CH(CH_3)_2$, cyclohexyl, benzyl

Scheme 2.4: Harwood *et al.*, strategy for alkylation of dimedone at C-4.[13]

However, despite the literature precedence this approach proved to be very problematic. The yields were low, due to the reaction giving a mixture of *O* and *C*-alkylated products, and after column chromatography often only the starting material dimedone (**29**) was isolated.[12] In an attempt to improve the reaction, the procedure was repeated using sodium iodide to effect *in situ* halogen exchange (Scheme 2.5). Hexamethylphosphoric triamide was also replaced by the less toxic *N,N'*-dimethylpropyleneurea, used in excess as a co-solvent as well as complexing agent.

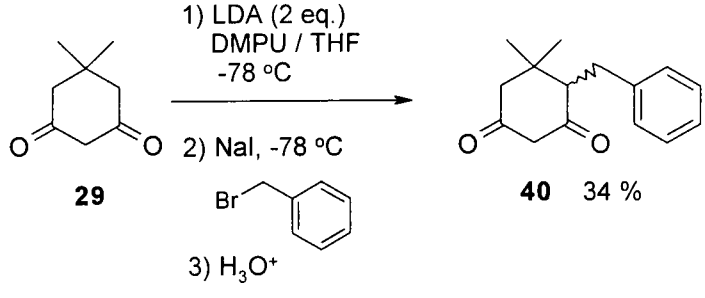

Scheme 2.5: Synthesis of 4-benzyl-5,5-dimethyl-cyclohexane-1,3-dione **40** from dimedone (**29**).

Although the addition of sodium iodide did increase the yield of the reaction, unreacted dimedone and a mixture of products were still present prior to chromatography. A key problem with the reaction was the poor solubility of

dimedone in THF/DMPU at -78°C, thus resulting in incomplete enolate formation. To overcome the solubility problem it was decided to try the reaction using 3-methoxy-5,5-dimethyl-2-cyclohexene-1-one (**41**). This derivative of dimedone is a non-viscous oil at room temperature formed in quantitative yield by reacting dimedone with chlorotrimethylsilane in methanol (Scheme 2.6).

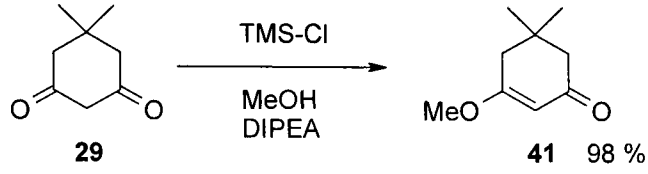

Scheme 2.6: Synthesis of 3-methoxy-5,5-dimethyl-cyclohexe-2-enone **41**.

Enone **41** was reacted with various alkyl bromides using similar methodology as Harwood and co-workers. This approach proved to be a significant improvement with the reaction giving solely the desired products in good yield (Scheme 2.7).

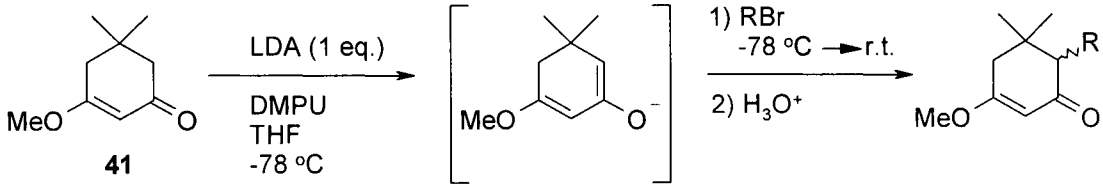

Ligand	R	Yield
42	$-CH_3$	85 %
43	$-CH_2CH{=}CH_2$	87 %
44	$-CH_2Ph$	89 %
45	$-CH_2CH{=}CHPh$	76 %
46	$-CH_2CO_2Bu^t$	86 %

Scheme 2.7: Alkylation of 3-methoxy-5,5-dimethyl-cyclohexe-2-enone (**41**).

The alkyl bromides used were selected to introduce alkyl groups of differing sizes, from a small methyl group to the sterically more demanding cinnamyl moiety. This study would investigate the size limit of groups at this position tolerated by the active

site of CypA. The *tert*-butyl ester moiety was chosen not only due to its steric bulk, but also as a possible site for future derivatisation.

Additional advantages of alkylating enone **41** was that only one equivalent of lithium diisopropylamide was needed to form the required enolate, and it was found that high yields could be attained without the need for sodium iodide. *N,N'*-dimethylpropyleneurea was added purely as a co-solvent, its role as a chelating agent is needed only when generating dianionic species. Harwood *et al.*, found that omission of chelating agent resulted in the absence of dianion formation,[13] and kinetic enolate anions of 3-alkoxy-2-cyclohexen-1-ones have also been generated without the use of chelating agents.[14]

The reactions outlined above gave alkylation exclusively at the desired C-6 position of enone **41**, owing to lithium diisopropylamide being a strong enough base to irreversibly generate the kinetic enolate by deprotonating the α′-proton (C-6) of the α, β-unsaturated ketone. It is known that the abstraction of the γ-proton (C-4) from an α, β-unsaturated ketone results in a dienolate anion that is more stable than its cross-conjugated isomer generated by abstraction of the α′-proton (Figure 2.2).[15] Thus under conditions where equilibration can take place the thermodynamically controlled α-alkyl-β, γ-unsaturated ketone product dominates.

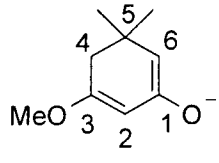

Kinetic enolate: cross-conjugated isomer generated by irreversible abstraction of α′-proton (C-6).

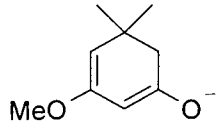

Thermodynamic enolate: conjugated unsaturation leads to greater stability and lower reactivity.

Figure 2.2: Kinetic and thermodynamic anions of 3-methoxy-5,5-dimethyl-cyclohexe-2-enone **41**.

The regioselective alkylation of ligands **23-46** was confirmed by ^{13}C NMR spectroscopy, the distinctive peak of the C-4 CH_2 at δ_C 50 ppm being absent from the

^{13}C spectra of the ligands. This was conclusively proven by x-ray crystallography of ligand **44** (Figure 2.3).

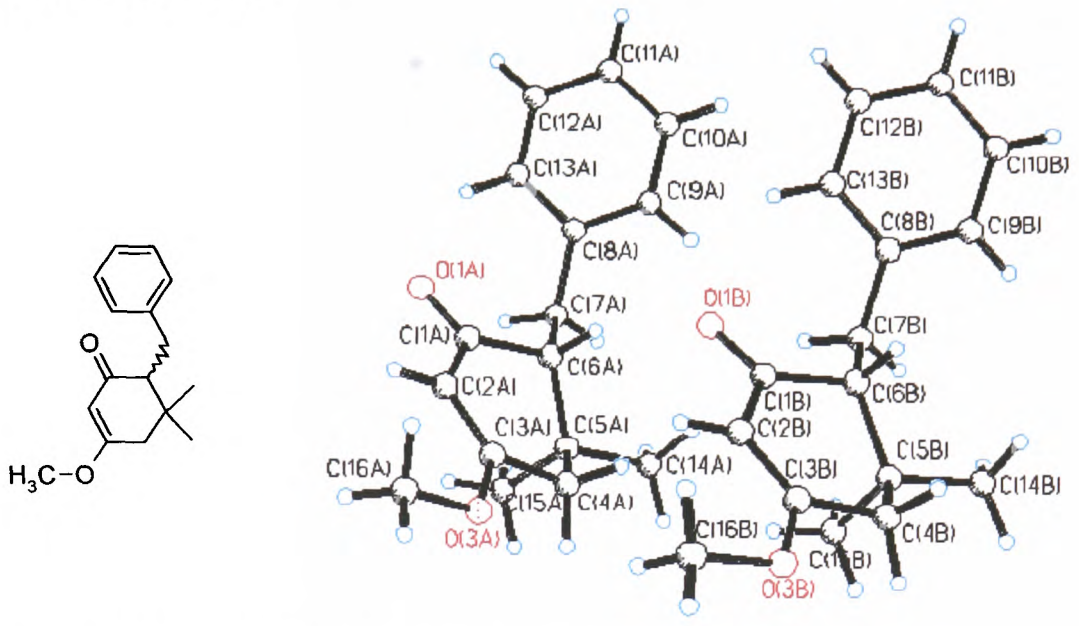

Figure 2.3: X-ray crystal structure of ligand **44**.

The benzylated analogue of lead compound **30** was synthesised by first reacting ligand **44** with hydrochloric acid in THF to give the diketone in excellent 91 % yield. The DAST acid fluoride strategy used previously was employed to make enol ester type ligand **47** (Scheme 2.8).

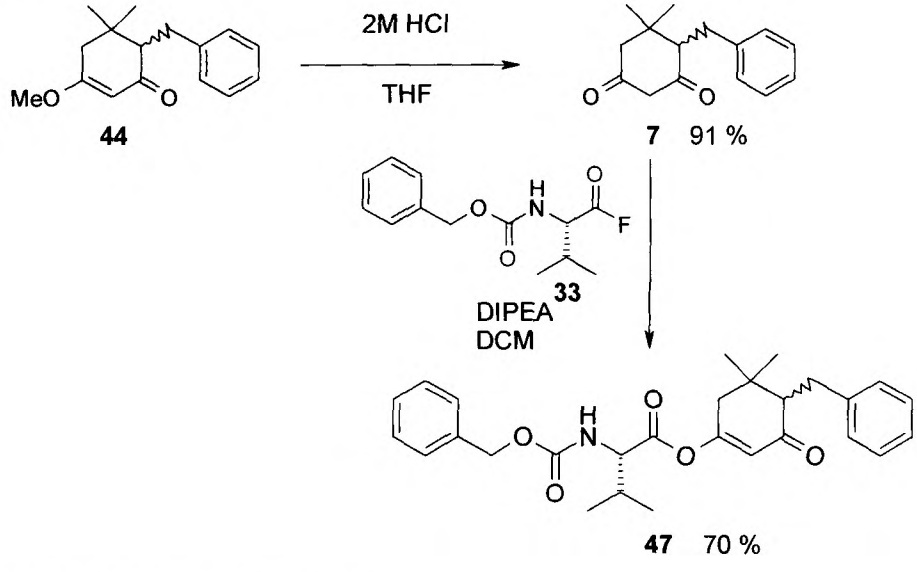

Scheme 2.8: Synthetic route to ligand **47**.

One of the key advantages of this strategy was the total regioselectivity of the chemistry employed. It is interesting to note that none of the alternative enol ester regioisomer **48** was seen during analysis, this being attributed to energetically unfavourable steric crowding of the benzyl and enol ester moieties (Figure 2.4). However, the limitation is that the alkyl dimedone derivatives were generated as a mixture of enantiomers, thus ligand **47** was synthesised as a 1:1 diastereomeric mixture, as confirmed by NMR analysis.

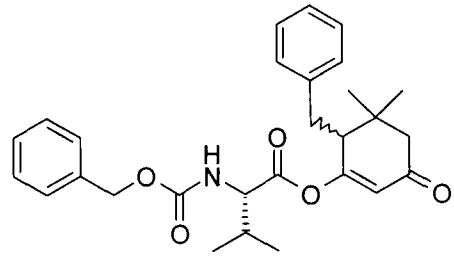

48

Figure 2.4: Sterically hindered regioisomer **48**.

2.3 Amide-linked derivatives

Compounds based around the lead structure ligand **30** do not make particularly suitable drug candidates due to the presence of the enol ester group. This linkage can be readily hydrolysed to reform the amino acid and dimedone starting materials. To overcome this problem another focus of the project was to make complementary ligands based upon the replacement of the ester linkage with the more stable amide group (Scheme 2.9, **49**). Interestingly this modification would also reverse the potential hydrogen bonding interaction at this point of the molecule from acceptor to donor. Retrosynthetic analysis of **49** suggested that analogues could be synthesised by coupling activated amino acids to enaminone **50** (Scheme 2.9).

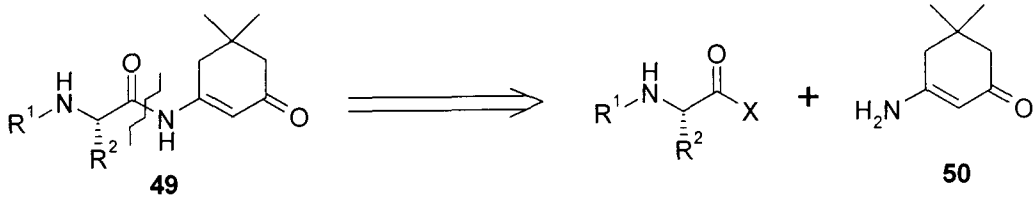

49 **50**

Scheme 2.9: Retrosynthetic analysis of amide-linked ligand **49**.

Enaminone **50** was readily synthesised in good yield by reacting dimedone with ammonium acetate (Scheme 2.10).[16] The reaction is carried out by refluxing the components in the presence of acetic acid in toluene solution with azeotropic removal of water using a Dean-Stark apparatus.

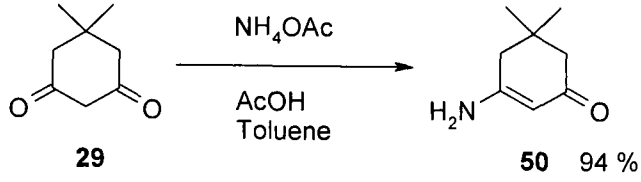

29 **50** 94 %

Scheme 2.10: Synthesis of 3-amino-5,5-dimethyl-2-cyclohexen-1-one **50**.

It was envisioned that the coupling enaminone **50** to *N*-protected amino acids could be carried out using standard peptide coupling reagents and protocols. In a typical coupling reaction, the carboxylic acid moiety of an *N*-protected amino acid is firstly activated by a suitable peptide coupling reagent, and then reacted with the amine moiety of a *C*-protected amino acid (Scheme 2.11).

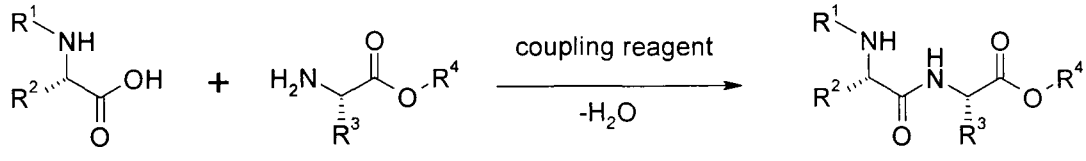

Scheme 2.11: Generalised peptide coupling reaction.

The most commonly used coupling reagents are the carbodiimides, widely used because they show good activity and are reasonably inexpensive. Of these, 1,3-dicyclohexylcarbodiimide (DCC) (**51**) was the first reported and still the most frequently used.[17] Problems associated with carbodiimide couplings include unwanted side reactions such as *N*-acylurea formation and racemisation *via* formation of an oxazalone intermediate. To alleviate these problems coupling additives were developed, of which the most common is 1-hydroxybenzotriazole (HOBt) (**52**).[18] HOBt reduces racemisation by rapidly forming a

hydroxybenzotriazole/carboxylic acid activated species that suppresses oxazalone formation (Scheme 2.12).

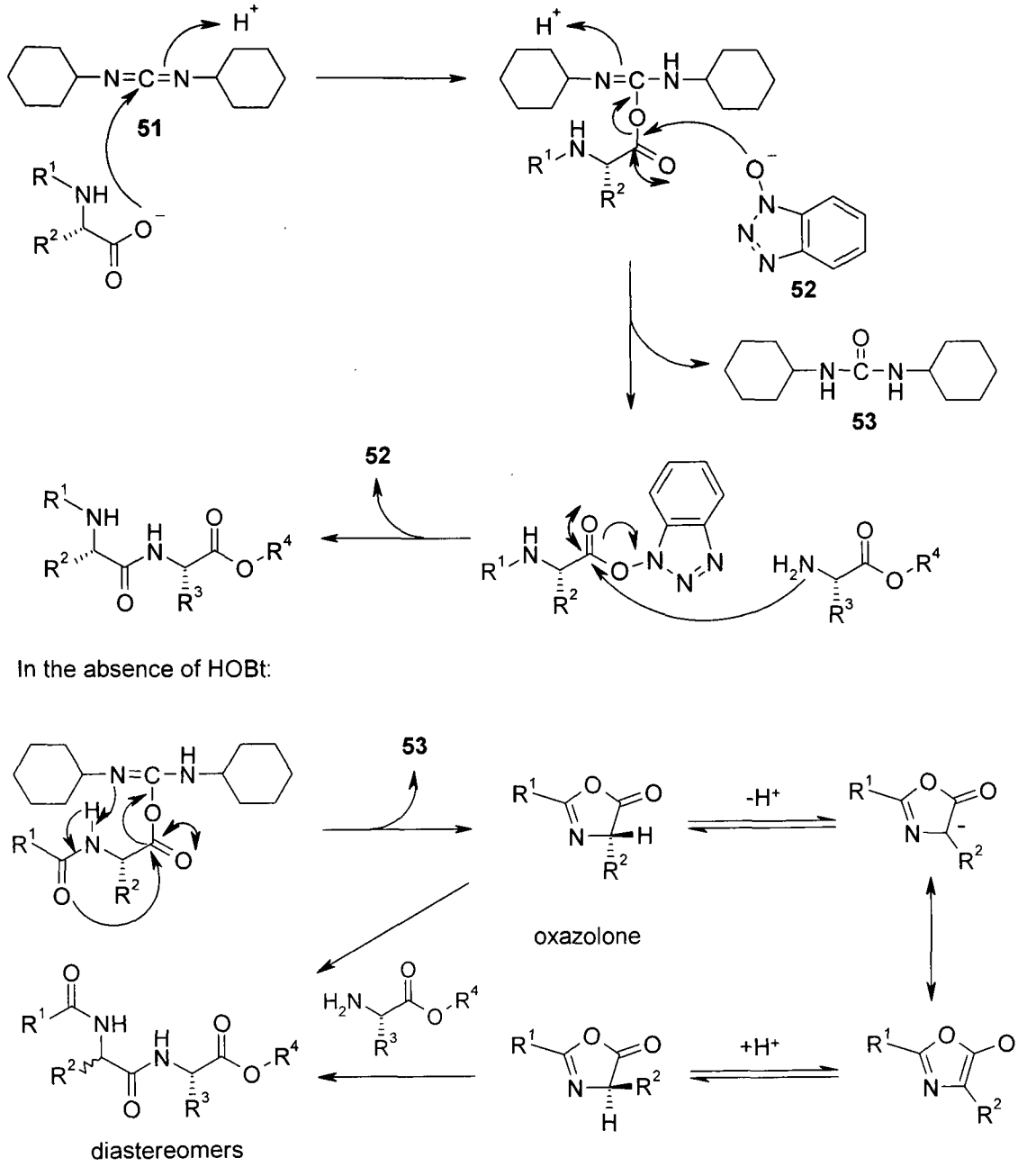

Scheme 2.12: General mechanism of a DCC/HOBt peptide coupling reaction.

Typically, DCC is added to an equimolar solution of carboxylic acid, amine and HOBt in dichloromethane or dimethylformamide, the by-product being dicyclohexylurea (DCU) (**53**) which precipitates out of solution. However, sometimes a quantity of DCU remains in solution, making purification of the product more difficult. Water-soluble derivatives such as 1-(3-dimethylaminopropyl)-3-ethylcarbodiimide (EDCI) (**54**) (Figure 2.5) were developed to obviate this problem,[19] the urea produced being water soluble and easily removed by extraction. Another reagent, 1,3-diisopropylcarbodiimide (DIC) (**55**), has a urea by-product that is soluble in organic solvents. This is used when the insolubility of DCU could cause problems, for example in solid-phase synthesis washing protocols.

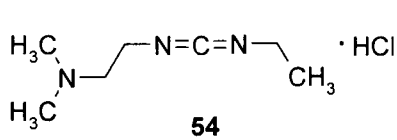

54

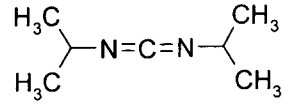

55

Figure 2.5: Structures of EDCI **54** and DIC **55**.

Another type of commonly used coupling reagents are the uronium salts based upon a benzotriazole structure. In general these offer complementary reactivity to the carbodiimides, often being employed to successfully couple peptides when the use of carbodiimides had been ineffective. The first to be introduced was *O*-(benzotriazol-1-yl)-*N,N,N',N'*-tetramethyluronium hexafluorophosphate (HBTU) (**56**),[20] the active structure of which was found to be based upon the *N*-guanidium rather than the *O*-uronium salt.[21] The mechanism of peptide coupling is similar to that of carbodiimides, the carboxylate anion attacking the guanidium/uronium carbon, with the release of benzotriazolyloxy anion (BtO^-). The BtO^- then attacks the acyloxyuronium intermediate *via* two pathways to afford the corresponding benzotriazolyl activated ester and a small amount of N^3-acylbenzotriazole 1-oxide intermediate. The benzotriazolyl ester intermediate can spontaneously rearrange into the corresponding *N*-acylated isomer. The amine component of the reaction mixture can then react with both forms of the active intermediate to give the amide product (Scheme 2.13).[22]

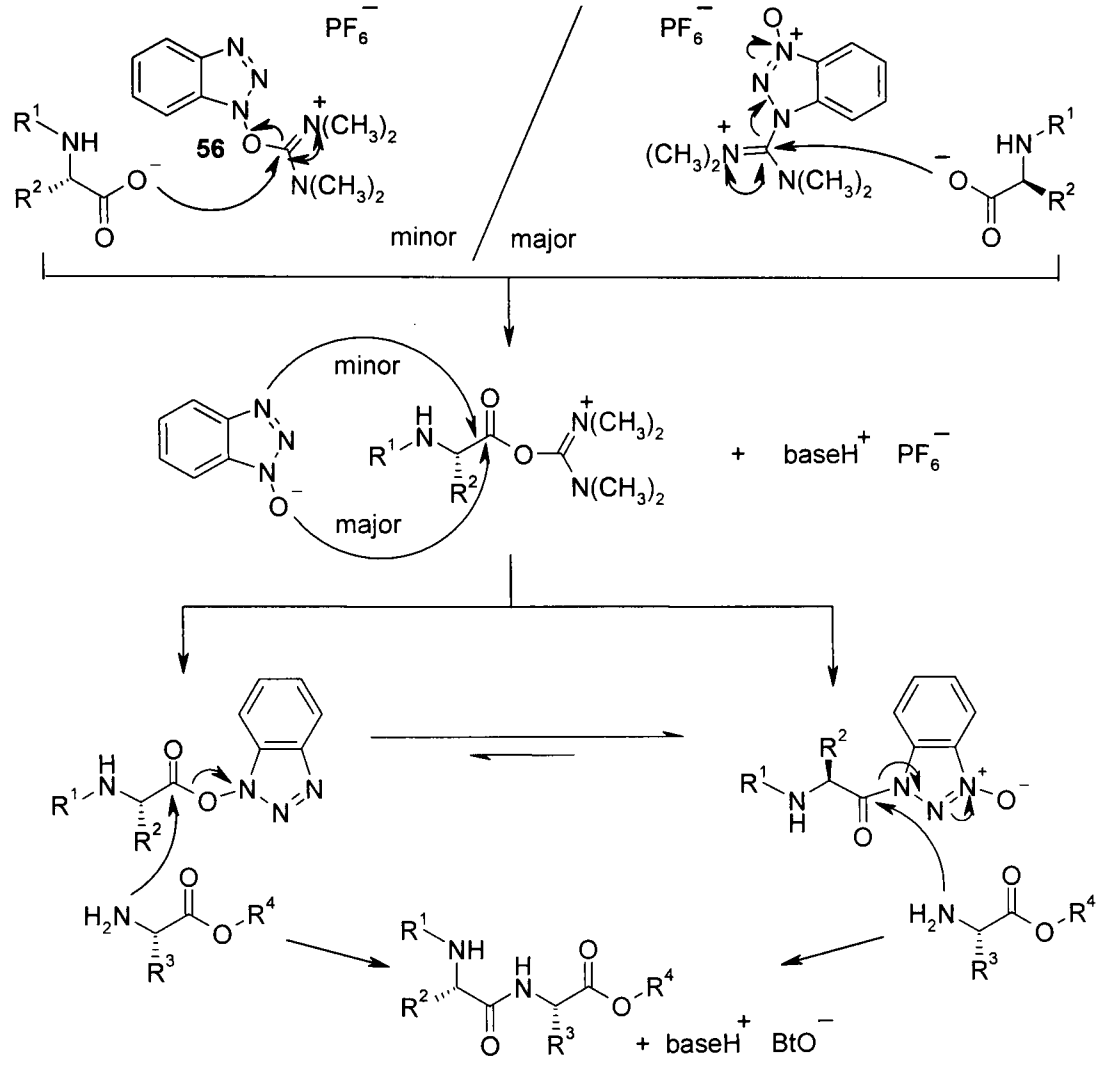

Scheme 2.13: General mechanism of a HBTU peptide coupling reaction.[22]

Normally these reagents are used with an equimolar amount of the acid and amine, in the presence of a non-nucleophilic base such as diisopropylethylamine. The advantage of using this type of reagent is that the racemisation-suppressing HOBt is formed *in situ*, negating the need for its separate addition. Structural modification of HBTU has led to many variants being produced and used in peptide synthesis. Common reagents include TBTU (**57**) where the hexafluorophosphate counter ion is replaced by tetrafluoroborate, and HATU (**58**) where the hydroxybenzotriazole moiety has been replaced by hydroxyazotriazole (Figure 2.6).[23]

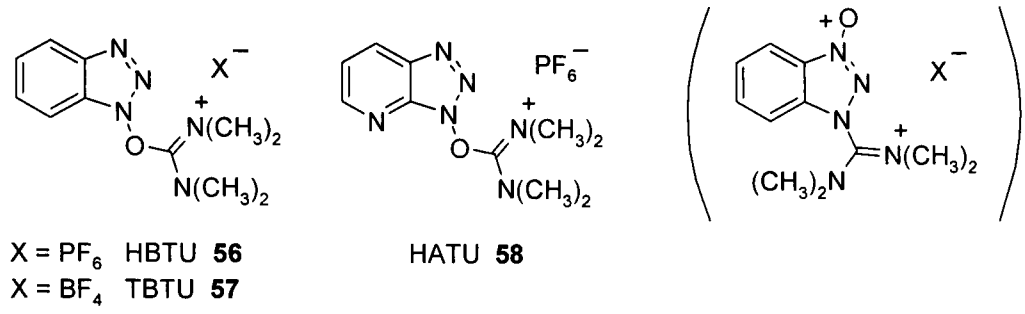

Figure 2.6: Common uronium based coupling reagents (active species in brackets).

The coupling of *N*-benzyloxycarbonyl-L-valine and enaminone **50** to make the amide linked analogue of lead compound **30** was attempted using the standard peptide coupling conditions outlined above. However, the synthesis of this ligand proved to be more problematic than first envisaged. The reaction was tried using the carbodiimide reagents DCC and EDCI in the presence of HOBt, and also the uronium reagent TBTU. Each method failed to give the coupled product in detectable yield, TLC analysis and mass spectrometry indicating starting material only. This was ascribed to enaminones such as **50** having decreased nitrogen nucleophilicity compared to the amines that are usually used in peptide couplings. Enaminones have only ambient nitrogen nucleophilicity due to the interaction between the amino group and the electron-withdrawing carbonyl group *via* the vinyl group, the other common term for this type of functionality being vinylogous amide. This "push-pull" type resonance results in decreased *N*-nucleophilicity (Figure 2.7).[24]

Figure 2.7: Enaminone resonance resulting in lower *N*-nucleophilicity.

Enaminone systems can undergo a range of chemical reactions as there are three nucleophilic sites (a, c and e, Figure 2.8) and two electrophilic sites (b and d). While

this makes the moiety synthetically useful, there is the potential for alternate reactions to occur leading to lower yields and impurity formation.

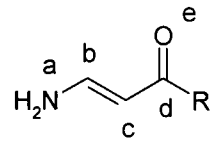

Figure 2.8: Possible enaminone reaction centres.

In an attempt to investigate the regioselectivity of reaction of enaminones, Kascheres *et al.*, reacted benzyldiazoketone with enaminone **50** and acyclic enaminone **59** (Scheme 2.14).[25] It was found that reaction with **59** formed the α-acyl-enaminoketone **60** principally, a product of reaction at α-C of the enaminone. However, the enaminone **50** reacted *via* nucleophilic attack of the amino group to give the *N*-acylated product **61**.

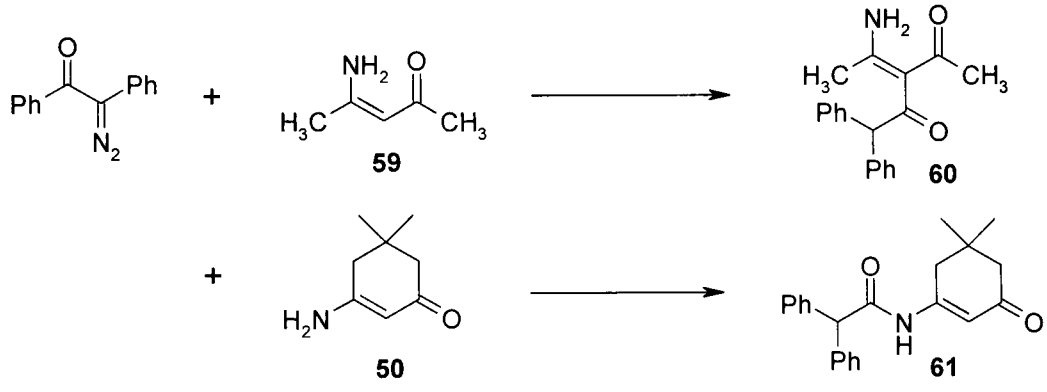

Scheme 2.14: Literature reaction of benzyldiazoketone with enaminones **50** and **59**.[25]

The alternate regioselectivity of the reactions can be rationalised by considering the geometric form of the two enaminones. Acyclic enaminones such as **59** exist predominantly in the *Z,s-Z* form in apolar solvents allowing for intramolecular hydrogen bonding (Figure 2.9). However, cyclic enaminones such as **50** are fixed in a *E,s-E* geometric form. Intramolecular hydrogen bonding is not possible, decreasing

conjugation compared to acyclic *Z,s-Z* enaminones, which would result in increased electron density on nitrogen compared to the *Z,s-Z* systems, and thus favour reaction at this site.[26]

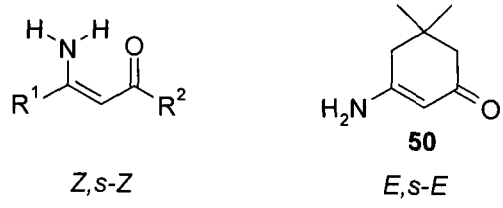

Figure 2.9: The effect of geometric form on intramolecular hydrogen bonding.

Although not as nucleophilic as an amine functional group, it was encouraging to have the precedent of enaminone **50** reacting *via* the nitrogen. A review of the literature revealed that compounds based upon an amide-linked structure had been synthesised by reacting enaminone **50** with acid chlorides, albeit it in low yield (Scheme 2.15).

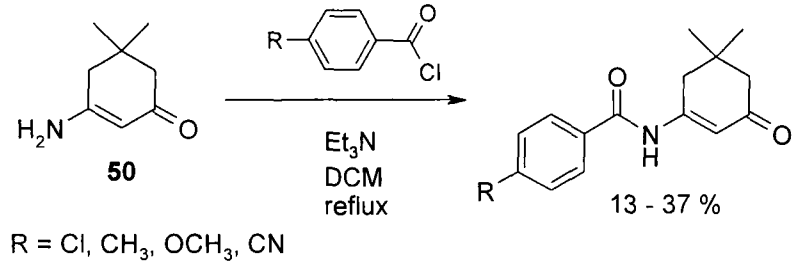

Scheme 2.15: Literature reaction of enaminone **50** with acid chlorides.[27]

Scott and co-workers reacted enaminone **50** with various *p*-substituted benzoyl chlorides in the presence of triethylamine as an acid scavenger under reflux conditions to give amide-linked enaminones.[27] Although of interest, this method was deemed not to be applicable to the synthesis of amide-linked ligands based upon an amino acid structure due to the problems of oxazolone formation with the use of protected acid chlorides during peptide synthesis. Acid fluorides are known to be more resistant to this conversion,[28] therefore it was decided to use the same acid

fluoride strategy previously employed. Amide-linked analogues of the enol ester compounds **30**, **31** and **32** were successfully synthesised by using DAST to generate acid fluorides of the relevant *N*-protected amino acid, followed by reaction with enaminone **50** (Scheme 2.16).

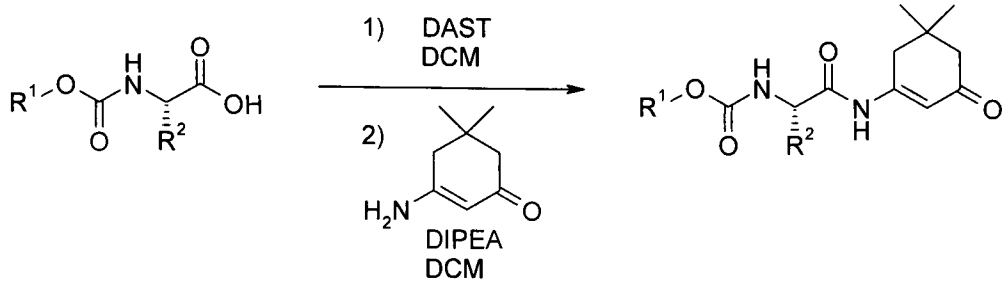

Ligand	Structure	Yield
62	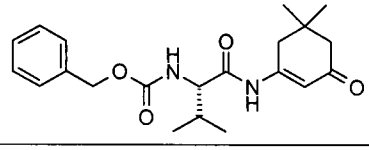	40 %
63	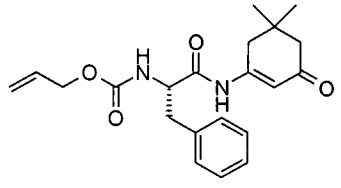	79 %
64	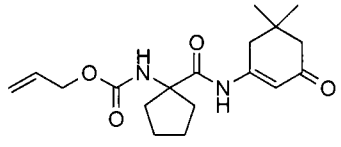	21 %

Scheme 2.16: Synthesis of amide-linked ligands *via* acid-fluorides.

The difference in the isolated yield of the ligands shown in Scheme 2.16 may be due to the nature of the amino acids used. Valine and 1-amino-1-cyclopentane carboxylic acid are sterically hindered compared to phenylalanine, this being reflected in the lower yields. It is postulated that ligand **64** was synthesised in the lowest yield due to the fact it is based on an α,α-dialkyl-amino acid structure, the structurally similar α-aminoisobutyric acid has long been recognised as a difficult amino acid to use in peptide synthesis due to steric hindrance.[29]

In an attempt to increase the yield of the coupling step, it was decided to substitute enaminone **50** with the methylamino derivative **65** (Figure 2.10). It was envisioned that the use of a secondary enaminone would increase electron density on nitrogen due to the positive inductive effect of the methyl group, although the extra methyl group would increase the steric crowding on the nitrogen.

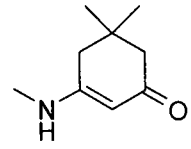

65

Figure 2.10: 3-Methylamino-5,5-dimethyl-cyclohex-2-enone **65**.

Enaminone **65** was readily synthesised by reacting dimedone with methylamine using the same refluxing conditions as previously used (Scheme 2.10). However, as with enaminone **50**, all attempts to react enaminone **65** with *N*-protected amino acids using standard peptide coupling reagents resulted in the recovery of starting material only. When the same acid fluoride approach as Scheme 2.16 was used it was found that enaminone **65** was even less reactive than enaminone **50**, only the *N*-alloc-phenylalanine derivative ligand **66** being successfully isolated, albeit in low yield (Scheme 2.17). The extra steric hindrance of the methyl group appeared to have outweighed any positive electronic inductive effect, this being highlighted by only the least sterically hindered amino acid yielding any coupled product.

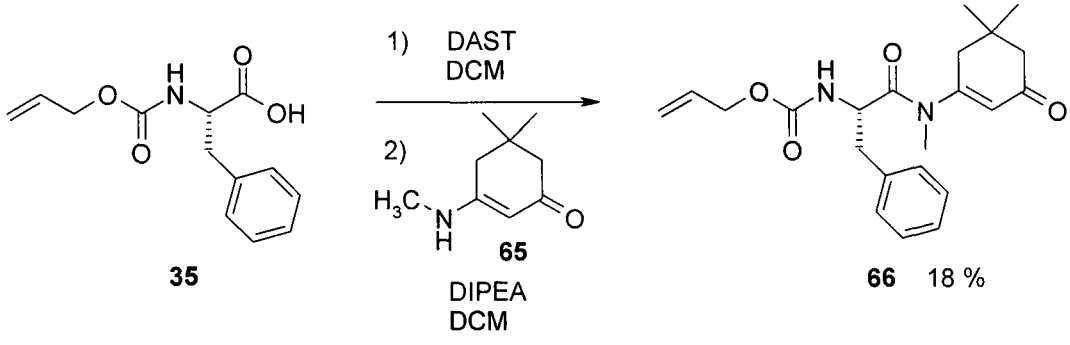

Scheme 2.17: Synthesis of ligand **66**.

An aim of this project was to develop synthetic methodologies that would allow the synthesis of compounds in a library format using combinatorial chemistry techniques. Whilst the acid fluoride strategy outlined above provided a route into the amide linked compounds, the chemistry employed was not ideal for parallel synthesis. The intermediate acid fluoride had to be pre-formed, resulting in an additional reaction step, and the ice-water wash involved risked hydrolysis back to the amino acid starting material with subsequent loss of overall product yield. A route involving a one pot, *in situ* amino acid activation strategy would have obvious synthetic advantages. A class of peptide coupling reagents that remained untried were the phosphonium reagents. An early example was BOP (**67**) (Figure 2.10) introduced by Castro and co-workers.[30] This was found to be an excellent coupling reagent, and has been widely used in peptide chemistry, also involving the synthesis of sterically hindered and longer chain peptides.[31]

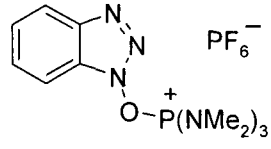

67

Figure 2.10: 1-Benzotriazolyoxytris(dimethylamino)phosphonium hexafluorophosphate (BOP) (**67**).

However, the disadvantage of BOP is that its use involves the generation of carcinogenic hexamethylphosphoric triamide (HMPA). In the search for a non-toxic derivative Castro and co-workers replaced the methyl groups on the phosphorus with pyrrolidino groups. The resulting reagent, nicknamed PyBOP (**68**) (Figure 2.11), yielded coupling rates comparable, or better than, those observed with BOP.[32]

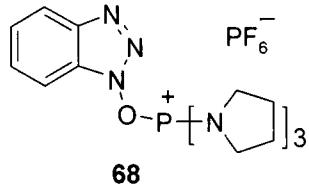

68

Figure 2.11: 1-Benzotriazolyoxytris(pyrrolidino)phosphonium hexafluorophosphate (PyBOP) (**68**).

The synthesis of ligand **62** was attempted using PyBOP in order to investigate the suitability of phosphonium reagents for synthesising amide-linked derivatives. A solution of *N*-benzyloxycarbonyl-L-valine and enaminone **50** was reacted with PyBOP in the presence of diisopropylethylamine at room temperature for two hours (Scheme 2.18). After work-up and purification *via* column chromatography, ligand **62** was isolated in modest yield. The result was encouraging as for the first time *in situ* amino acid activation had resulted in the synthesis of a desired amide-linked ligand, although the yield was only comparable to the previous acid fluoride strategy.

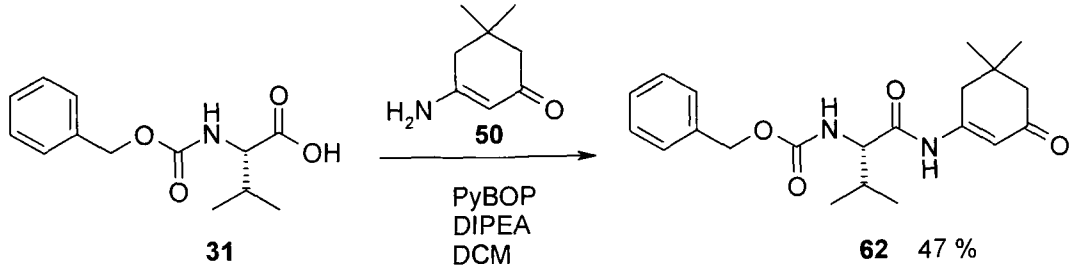

Scheme 2.18: Synthesis of ligand **62** using PyBOP.

Whilst being an excellent general peptide coupling reagent, Coste *et al.*, found PyBOP to have low efficacy in coupling hindered or *N*-methylated amino acids. However, the related halogenated reagent PyBroP (**69**) (Figure 2.12) was found to give excellent yields.[33, 34]

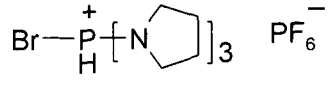

69

Figure 2.12: 1-Bromotris(pyrrolidino)phosphonium hexafluorophosphate (PyBroP).

Coste *et al.*, also showed that dimethylaminopyridine (DMAP) could be used to catalyse PyBroP couplings of highly hindered amino acids. The synthesis of Boc-Aib-Aib-OMe was achieved in 61 % yield with PyBroP/DMAP, this coupling having failed with PyBOP. Interestingly for the possible synthesis of the enaminone amide-linked compounds, it was also shown that PyBroP/DMAP could couple Cbz-Aib **70** to the very weakly nucleophilic amine benzocaine (**71**) (Scheme 2.19).[35]

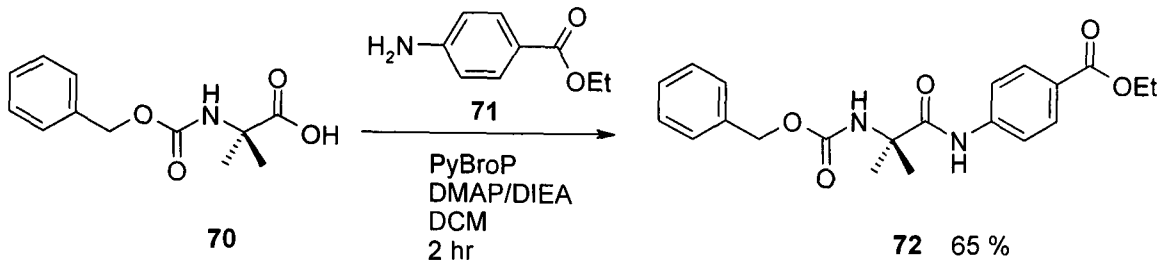

Scheme 2.19: Literature coupling of Cbz-Aib **70** with benzocaine **71** using PyBroP/DMAP.[35]

Coste and co-workers proposed three mechanistic pathways involved in phoshonium reagent peptide couplings (Scheme 2.20).[35] In a general case with BOP or PyBOP an acyloxyphosphonium salt is first formed, which is aminolysed to give the *C*-protected amino acid (Scheme 2.20, Pathway a). If coupling involved two hindered Aib residues or a weakly nucleophilic amine then the oxybenzotriazole anion firstly reacts with acyloxyphosphonium salt to produce an oxybenzotriazole ester, this then reacts slowly with the amine to give the product (Pathway b). In couplings involving PyBroP a mechanistic route *via* the symmetric anhydride was proposed (Pathway c). The PyBroP reactions were found to be accelerated by the addition of DMAP, a reagent known to catalyse the aminolysis of anhydrides.

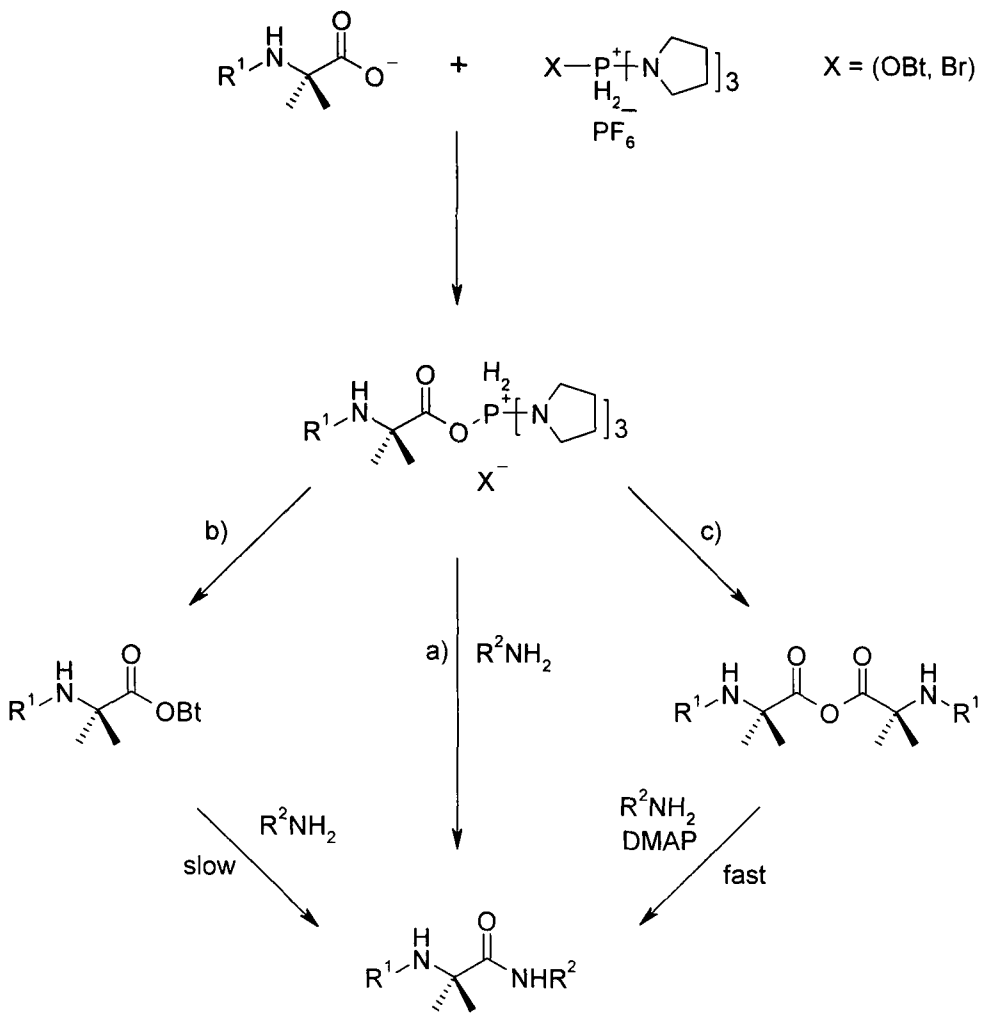

Scheme 2.20: Proposed mechanistic routes of phosponium reagent mediated peptide couplings.[35]

The mechanistic proposals in Scheme 2.20 might explain the modest yield of ligand **62** when the coupling was attempted with PyBOP. As enaminones have only ambient nucleophilicity a reaction route similar to pathway b could be envisioned. With the above mechanisms in mind, the coupling of *N*-benzyloxycarbonyl-L-valine **31** and enaminone **50** was attempted using PyBroP/DMAP (Scheme 2.21). After some refinement, it was found that the reaction proceeded in excellent yield when one equivalent of enaminone **50** was reacted with one and a half equivalents of Cbz-valine (**31**) and PyBroP, with DMAP being used in excess as catalyst and base.

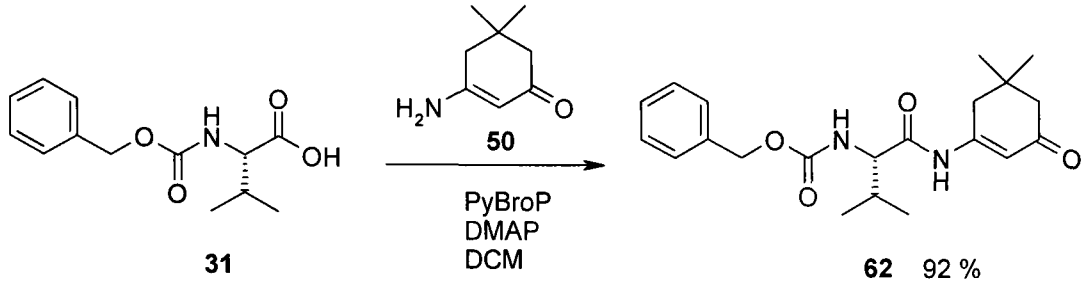

Scheme 2.21: Synthesis of ligand **62** using PyBroP/DMAP.

The result shown in Scheme 2.21 represented a significant synthetic breakthrough as for the first time an amide-linked ligand was synthesised in high yield. The additional benefit was the use of a one pot, *in situ* amino acid activation strategy that would be readily amenable to future ligand synthesis.

2.4 C-6 alkylated amide-linked derivatives

It was deemed that ligands based upon an alkylated enaminone **50** core were of interest as they would combine the greater stability of the amide group with the potential to probe the active site in more than one direction. A combination of strategies that were found to be successful previously were employed in the synthesis of such ligands. The alkylated enone derivatives **42 - 46** were first hydrolysed to the 1,3-diketone, followed by reaction with ammonium acetate with azeotropic removal of water using a Dean-Stark apparatus (Scheme 2.22).

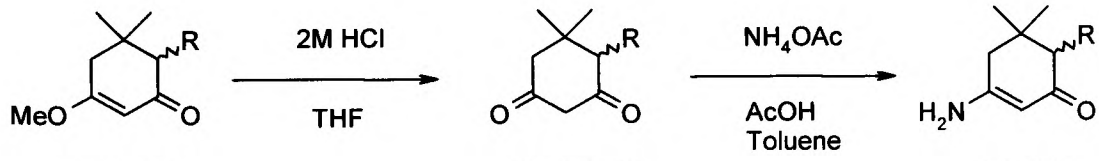

42 - 46 **40, 73 - 76** **77 - 81**

R	Ligand	Yield	Ligand	Yield
$-CH_3$	**73**	86 %	**77**	83 %
$-CH_2CH{=}CH_2$	**74**	88 %	**78**	88 %
$-CH_2Ph$	**40**	91 %	**79**	86 %
$-CH_2\ (CH)_2Ph$	**75**	95 %	**80**	85 %
$-CH_2CO_2Bu^t$	**76**	94 %	**81**	80 %

Scheme 2.22: Synthesis of ligands **77 - 81**.

Ligands **77 - 81** were purified *via* a simple recrystallisation from ethyl acetate, and the reactions were found to be completely regioselective; comparison of the ^{13}C NMR data with that of ligands **42 - 46** showed that the ligands were structurally similar. Regioselectivity was conclusively proven by X-ray crystallography of ligand **78** (Figure 2.13).

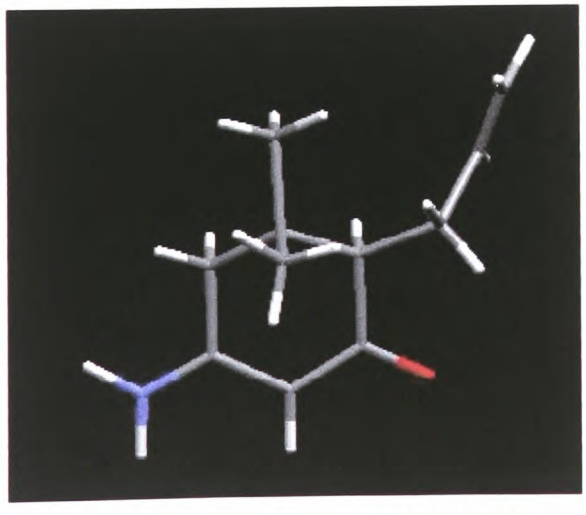

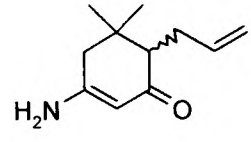

Figure 2.13: X-ray crystal structure of ligand **78**.

It is interesting that none of the other regioisomers (Figure 2.14) were synthesised *via* the enamination reaction. It is postulated that the alkyl group sterically shields the adjacent carbonyl group from the nucleophilic attack of ammonia, thus directing the substitution to the opposite side of the dimedone ring.

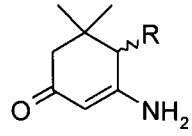

Figure 2.14: Regioisomers not synthesised *via* Scheme 2.22.

In order to see if alkylated amide-linked compounds could be synthesised using the previous PyBroP/DMAP strategy, two trial reactions were attempted. The coupling of 4-amino-6-allyl-5,5-dimethylcyclohex-2-enone (**78**) and 4-amino-6-((*E*)-3-phenyl-allyl)-5,5-dimethylcyclohex-2-enone (**80**) with *N*-benzyloxycarbonyl-L-valine (**31**) using PyBroP/DMAP was found to proceed satisfactorily, the products being obtained in excellent yield (Scheme 2.23).

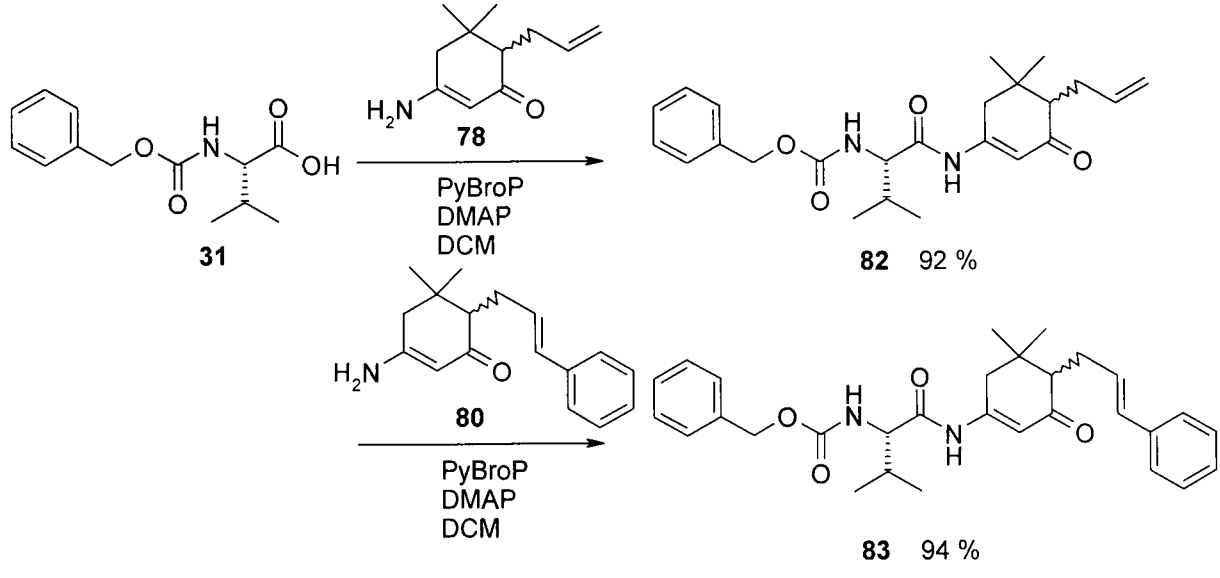

Scheme 2.23: Synthesis of ligands **82** and **83** using PyBroP/DMAP.

The coupling of 3-amino-6-benzyl-5,5-dimethylcyclohex-2-enone (**79**) with *N*-benzyloxycarbonyl-L-valine (**31**) was also attempted using the previously used acid fluoride chemistry as a comparison (Scheme 2.24). As expected, the yield of the desired product was substantially lower than those shown in Scheme 2.23.

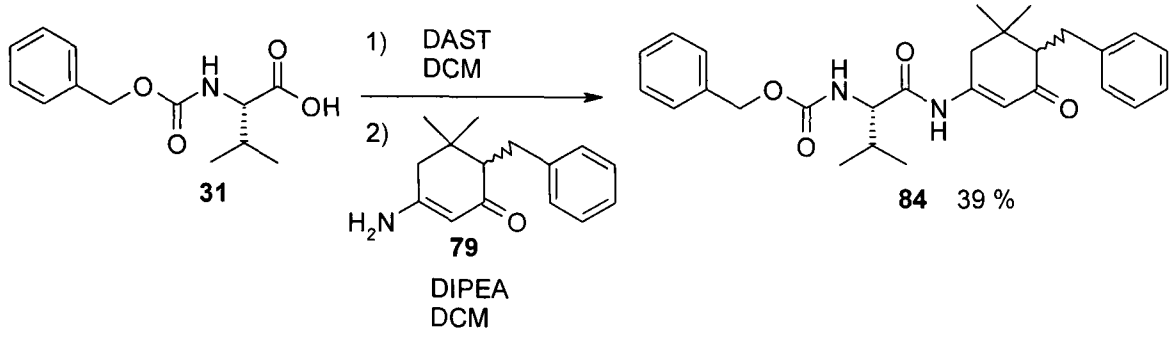

Scheme 2.24: Synthesis of ligands **84** using DAST.

The aim of having a synthetic route robust enough to allow the parallel synthesis of ligands was achieved by using the reagents PyBroP and DMAP in combination. With amenable chemistry in place, a library of ligands based upon a valine template was synthesised. The five alkylated enaminone building blocks, **77-81**, prepared in Scheme 2.22 and enaminone **50** were reacted with valines with varying *N*-protection (Scheme 2.25). The library was designed to investigate the effect of different *N*-protecting groups upon ligand binding, whilst exploring the active site steric limits tolerated at the C-6 position of the dimedone ring.

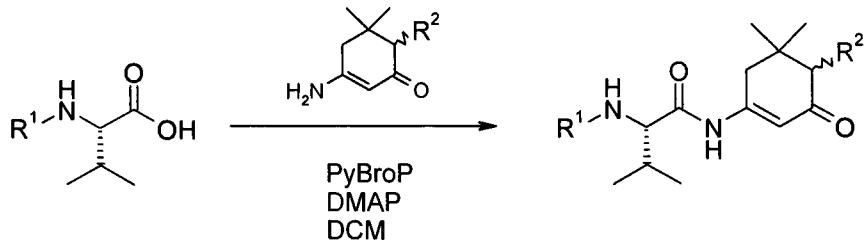

	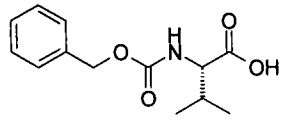	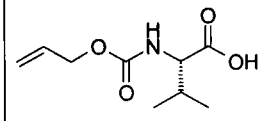	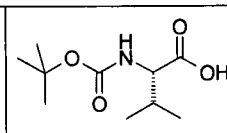
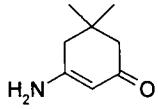	**62** 80 %	**85** 67 %	**86** 62 %
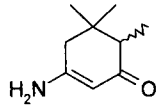	**87** 82 %	**88** 65 %	**89** 74 %
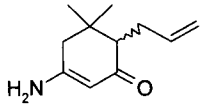	**82** 70 %	**90** 79 %	**91** 66 %
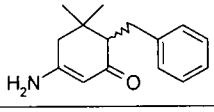	**84** 75 %	**92** 72 %	**93** 80 %
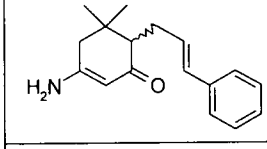	**83** 72 %	**94** 68 %	**95** 83 %
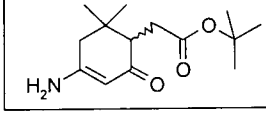	**96** 78 %	**97** 61 %	**98** 58 %

Scheme 2.25: Parallel synthesis of alkylated amide-linked ligands.

The parallel synthesis carried out in Scheme 2.25 was accomplished using the Bohdan MiniBlock™ apparatus.[36] This consists of a multi-well reaction vessel, the MiniBlock, and an accompanying Shaker Station (Figure.2.15). The MiniBlock™ is a compact parallel synthesiser that is compatible with solution or solid phase synthesis. Chemistry is carried out in individual vessels that at a turn of a key can drain through a frit into a standard 48 well microtitre plate. Agitation of the reaction vessels is accomplished *via* vortex mixing on the shaker station.

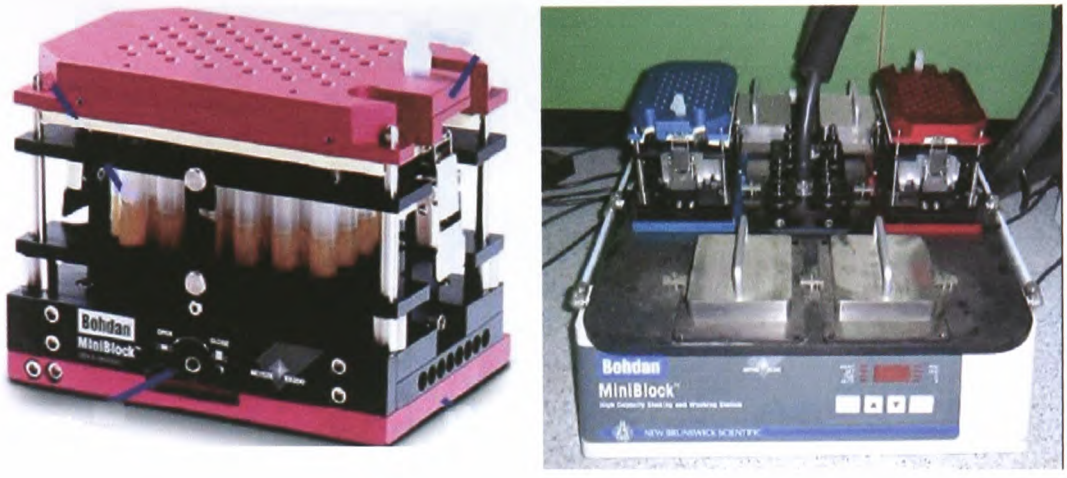

Figure 2.15: Bohdan MiniBlock™ reaction vessel and shaker station.

The ligands shown in Scheme 2.25 were synthesised by firstly making up stock solutions of the starting materials and coupling reagents in dichloromethane. Equal aliquots of the PyBroP and DMAP solutions were then manually dispensed into each of the 18 MiniBlock vessels that were used in the array. Aliquots of the valine derivatives were then manually dispensed into a vertical line of 6 reaction vessels, followed by separate addition of the enaminone **50** and derivatives **77-81** into the horizontal line of 3 tubes. After overnight agitation, purification was carried out by draining the MiniBlock into a 48 well plate followed by manual transfer of the DCM solution onto pre-packed silica columns. Column chromatography was then carried out using the Biotage Quad 3™ system (Figure 2.16). This is an automated flash chromatography system that runs up to 12 pre-packed silica cartridges in parallel. Fractions are collected by an automated fraction collector, allowing unattended operation.

Figure 2.16: Biotage Quad 3 automated flash column chromatography apparatus.

The parallel synthesis of the array was a success, each ligand being isolated in good yield. However, the yields were not as high as those seen in the previous individual PyBroP/DMAP couplings. This was largely as a result of utilising the Quad 3 system for purification. Although the apparatus is an excellent way of accomplishing moderately high-throughput column chromatography, it uses a common solvent stock for the elutions. Thus solvent gradients cannot be individually tailored towards the optimum purification of each compound. However, this was not an issue for the purposes of this project as the amount of ligand synthesised was sufficient for biological assay applications.

2.5 Alternate dimedone-based ligands

All the ligands that contain an amino acid moiety synthesised so far have involved the coupling of an *N*-protected amino acid with dimedone or an enaminone. Ligands based upon the attachment of amino acids to the dimedone core *via* the *N*-terminus would make a complementary family of ligands to the type previously described (Scheme 2.26). To investigate ligands of this type, *O*-protected phenylalanine, valine and tyrosine were reacted with dimedone using the same Dean-Stark conditions employed in the synthesis of the previous amino-dimedone derivatives (Scheme 2.22).

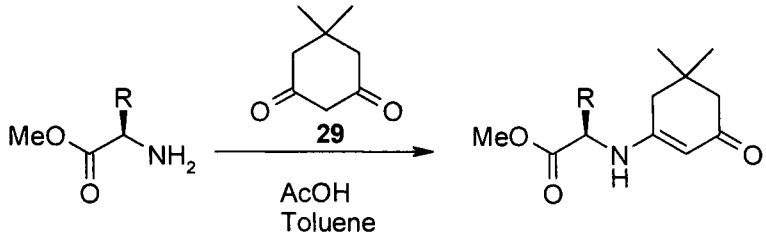

Ligand	R	Yield
99	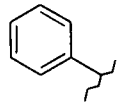	97 %
100	$(H_3C)_2$-	92 %
101	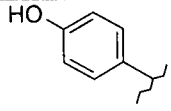	74 %

Scheme 2.26: Condensation of *O*-protected amino acids with dimedone under Dean-Stark conditions.

The condensation of the *O*-protected amino acids with dimedone was found to proceed in good yield, the previous Dean-Stark conditions providing a robust general route into such enaminone-type ligands. It is worth noting though that these ligands lack the amide carbonyl group present in the previous amide-linked ligands, which would possibly have a detrimental effect on the binding affinity to CypA due to the loss of a potential hydrogen bonding acceptor site.

An alternate point for derivatisation of the dimedone core structure was provided through the modification of ligand **46**. The *tert*-butyl ester group was hydrolysed to the carboxylic acid in good yield using trifluoroacetic acid and triethylsilane as a cation scavenger.[37] The resulting acid moiety gave a versatile handle onto which the peptide couplings of amines and amino acids could be carried out (Scheme 2.27).

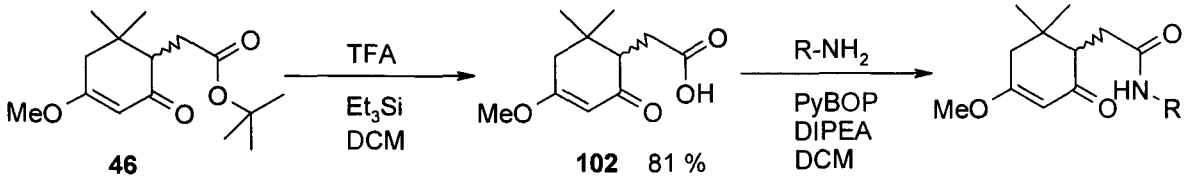

46 **102** 81 %

Ligand	R-NH_2	Yield
103	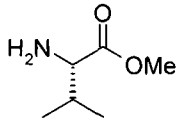	74 %
104	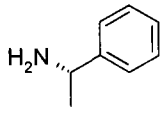	82 %
105	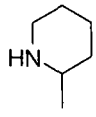	79 %

Scheme 2.27: Hydrolysis of ligand **46** and subsequent peptide couplings.

Ligand **102** was coupled to *L*-valine methyl ester, (*S*)-α methylbenzylamine and 2-methylpiperidine in good yield using PyBoP as the coupling reagent. The amines were chosen to introduce amino acid and sterically demanding primary and secondary amine moieties.

2.6 Ligand Optimisation

2.6.1 Lead compound selection

A key aim of this project was to establish electrospray ionisation mass spectrometry (ESI-MS) as a primary screening tool through the analysis of CypA-ligand complexes. Any ligands found to bind to CypA could then be fast-tracked into biological testing and used as a base for subsequent ligand design. The results are reported in Chapter 3, and initial findings from the ESI-MS screen highlighted C-6 allyl ligand **82** as an early lead compound. Interestingly, it was found that the structurally similar C-6 cinammyl ligand **83** did not give a protein-ligand complex under ESI-MS conditions. In an attempt to rationalise this finding the ligand

structures were modelled into the CypA active site using the modelling package Insight II®.[38] The X-ray crystal structure of ligand **30** bound to CypA was used as a template over which the structures of ligands **82** and **83** were manually docked (Figure 2.17). The *S*-diastereomer of each ligand was used for the modelling as the C-6 alkyl chain of the *R*-diastereomers was found to sterically clash with the CypA active site when overlaid upon the ligand **30** scaffold.

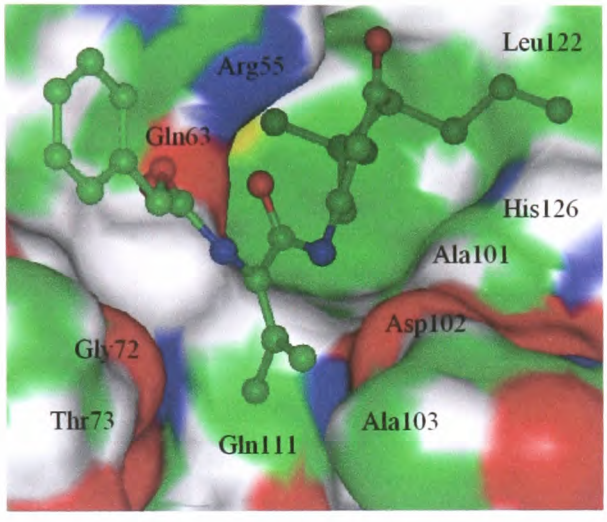

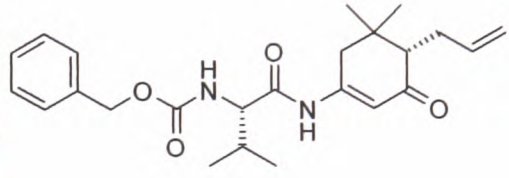

82

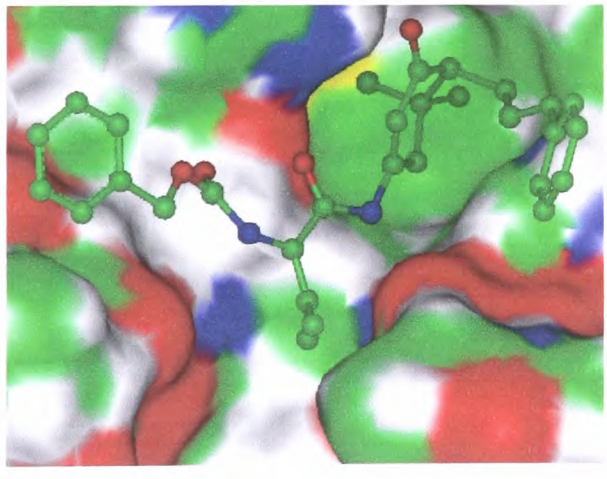

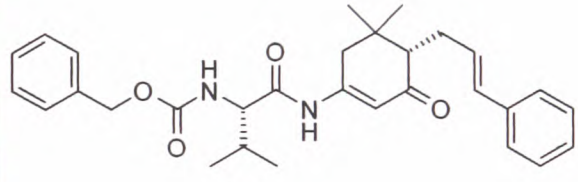

83

Figure 2.17: Manual docking of ligands **82** and **83** using Insight II®.

Upon inspection of the modelling data for ligand **83** it appears that the cinnamyl moiety is too large to fit into the defined hydrophobic cavity occupied by the dimedone core, sterically clashing with the His126 and Ala101 residues. The allyl

group of ligand **82** is sterically less demanding, and is thus tolerated at that position in the active site. The modelling suggests that the binding of ligand **82** to CypA preserves the same interactions as ligand **30**; the dimedone dimethyl moiety resides in the hydrophobic binding pocket, the enaminone carbonyl can hydrogen bond to Arg55 and the amide NH can hydrogen bond to Gln63. Ligand **82** may also benefit from a hydrogen bonding interaction between the enaminone NH and Asp102, and the allyl group may have a positive effect on binding affinity through a possible hydrophobic interaction with Leu122.

While the images shown in Figure 2.17 helped to rationalise the initial ligand binding data, their limitations should be acknowledged. The modelling of ligands **82** and **83** was based upon the crystal data for ligand **30**, this structure having an enol ester link between the dimedone and Cbz-valine moieties. Ligands **82** and **83** have the alternate amide link, resulting in the amide and the enaminone moieties being in the same geometrical plane through resonance. Thus the amide-linked ligands would be expected to be structurally more rigid than their enol ester analogues and potentially have a different binding mode in the CypA active site. However, in the absence of X-ray crystallographic data showing ligand **82** binding to CypA the molecular modelling was used as the primary tool to visualise ligand binding.

It was decided to use the new lead compound ligand **82** as a template for subsequent ligand synthesis as the initial mass spectrometry screening hit was supported by the modelling outlined above. Subsequent ligands could be structurally varied at three points whilst preserving the enaminone/dimedone core structure of **82** (Figure 2.18).

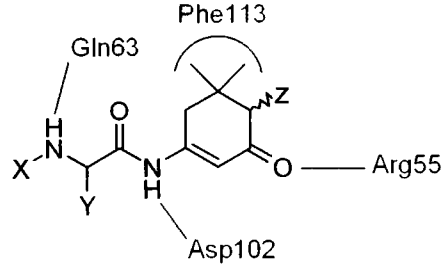

X - Cbz or functionalised aryl groups
Y - valine or different amino acids
Z - allyl or alternate hydrophilic groups

Figure 2.18: Potential sites of derivatisation using a template based upon ligand **82**.

group of ligand **82** is sterically less demanding, and is thus tolerated at that position in the active site. The modelling suggests that the binding of ligand **82** to CypA preserves the same interactions as ligand **30**; the dimedone dimethyl moiety resides in the hydrophobic binding pocket, the enaminone carbonyl can hydrogen bond to Arg55 and the amide NH can hydrogen bond to Gln63. Ligand **82** may also benefit from a hydrogen bonding interaction between the enaminone NH and Asp102, and the allyl group may have a positive effect on binding affinity through a possible hydrophobic interaction with Leu122.

While the images shown in Figure 2.17 helped to rationalise the initial ligand binding data, their limitations should be acknowledged. The modelling of ligands **82** and **83** was based upon the crystal data for ligand **30**, this structure having an enol ester link between the dimedone and Cbz-valine moieties. Ligands **82** and **83** have the alternate amide link, resulting in the amide and the enaminone moieties being in the same geometrical plane through resonance. Thus the amide-linked ligands would be expected to be structurally more rigid than their enol ester analogues and potentially have a different binding mode in the CypA active site. However, in the absence of X-ray crystallographic data showing ligand **82** binding to CypA the molecular modelling was used as the primary tool to visualise ligand binding.

It was decided to use the new lead compound ligand **82** as a template for subsequent ligand synthesis as the initial mass spectrometry screening hit was supported by the modelling outlined above. Subsequent ligands could be structurally varied at three points whilst preserving the enaminone/dimedone core structure of **82** (Figure 2.18).

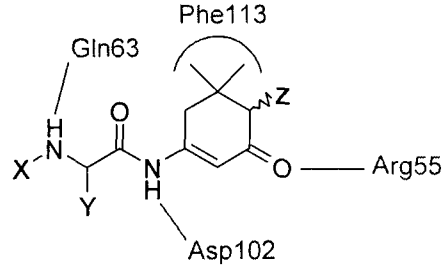

X - Cbz or functionalised aryl groups
Y - valine or different amino acids
Z - allyl or alternate hydrophilic groups

Figure 2.18: Potential sites of derivatisation using a template based upon ligand **82**.

Preservation of the backbone structure should enable the key interactions between ligand and the CypA binding site to be conserved, as shown in red in Figure 2.18. In order to assess the effect of derivatisation at a particular site of the ligand it was decided to modify the ligand structure one site at a time, as outlined below.

2.6.2 Alternate amino acids

Ligands based upon substitution of the valine moiety with alternate amino-acids were prepared in good yield by utilising the same PyBroP/DMAP chemistry successfully employed earlier (Scheme 2.28).

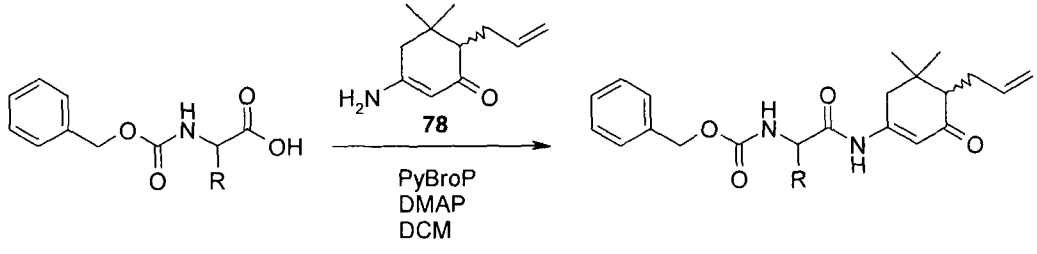

Ligand	R	Yield
106		89 %
107	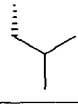	87 %
108		83 %
109	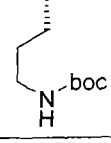	88 %
110	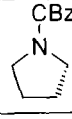	85 %

Scheme 2.28: Synthesis of alternate amino-acid ligands

The Cbz-protected amino acids D-valine, leucine, isoleucine and Cbz-(boc)-lysine were chosen in order to introduce a slight structural change to the ligand **82** core structure. Cbz-proline was chosen to provide a second ring to the ligand structure to investigate the effect upon binding of this extra structural rigidity. In each case the Cbz-group and the allyl moiety were retained to focus just on the effect of changing the amino acid.

2.6.3 Hydrophilic ligands

An alternate synthetic strategy focussed on the retention of the Cbz-valine moiety and replacement of the C-6 allyl group. The majority of the previously synthesised ligands had hydrophobic groups at this position, replacement with hydrophilic moieties would afford an interesting subset of contrasting ligands. The *tert*-butyl ester functionalised ligand **96** provided a route into one such hydrophilic ligand. Hydrolysis of the *tert*-butyl ester moiety was achieved in good yield using trifluoroacetic acid and triethylsilane to give the free carboxylic acid containing ligand **111** (Scheme 2.29).

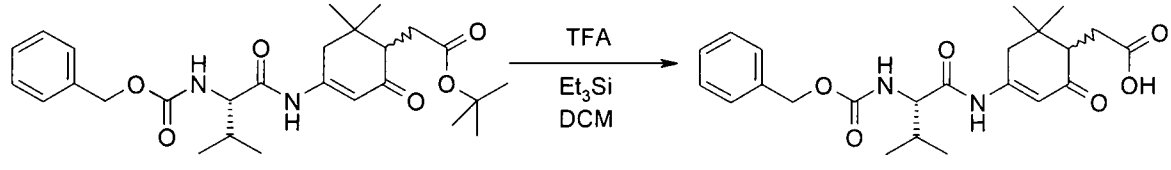

96 **111** 83 %

Scheme 2.29: Removal of the *tert*-butyl ester group to give ligand **111**.

Ligand **82** was also used as the starting material for the synthesis of two hydrophilic ligands (Scheme 2.30). The allyl group was firstly converted to the *cis*-1,2-diol *via* an osmium-catalysed dihydroxylation using the procedure of Kolb *et al.*[39] Here *N*-methyl morpholine *N*-oxide was used as an oxidant to regenerate the active osmium (VIII) species required for the dihydroxylation. A sample of the resulting ligand **112** was then treated with a combination of sodium periodate and wet silica gel resulting in the cleavage of the 1,2-diol moiety to give the aldehyde ligand **113**.[40]

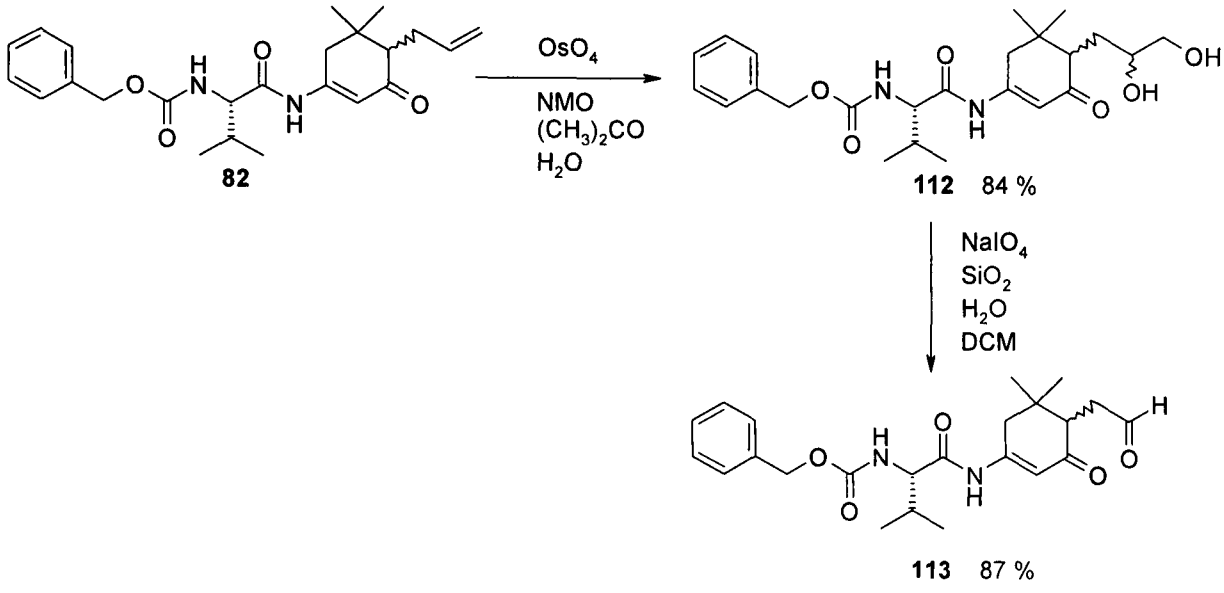

Scheme 2.30: Synthesis of hydrophilic ligands **112** and **113**.

The hydrophilic ligands shown above should retain the same hydrogen bonding interactions with the CypA binding site as ligand **82** and could potentially benefit from an additional hydrogen bond with the imidazole ring of His126.

2.6.4 Cbz group replacement

Ligands designed to retain the valine and C-6 allyl scaffold, whilst introducing functionality at the amino acid *N*-terminus, were synthesised using ligand **82** as the starting point. The Cbz carbamate group was firstly cleaved using iodotrimethylsilane to give the deprotected amine containing ligand **114** (Scheme 2.31). The first step of this reaction is proposed to be a fast complexation of the trimethylsilyl group with the carbamate oxygen, followed by cleavage of the benzyl group *via* attack of the iodide to give benzyl iodide. Treatment with acidic methanol cleaves the oxygen–silicon bond of the silyl carbamate formed to give a carbamic acid, which spontaneously decarboxylates to give the free amine.[41] With a free amino group in place it was decided to introduce differing aryl groups at this position *via* the reductive amination of various aldehydes. Reductive amination reactions are thought to proceed through an imine or iminium intermediate, followed by an *in situ* reduction to an amine of higher order by a reducing agent.[42] A variety of

borohydride-based reducing agents have been used for this transformation, with sodium cyanoborohydride widely used. Under neutral conditions in methanol there is negligible reduction of aldehydes using this reagent, thus it is possible to selectively reduce the intermediate imine.[43] It was decided to use a commercially available polymer-supported cyanoborohydride (PS-CBH) reagent to synthesise a small library of ligands from the starting point of ligand **114** (Scheme 2.31). The use of resin-bound cyanoborohydride is advantageous as the polymer retains the toxic residues,[44] the beads then separated from the reaction mixture through filtration. The reactions were carried out using a Bohdan MiniBlock, as used previously in Scheme 2.25.

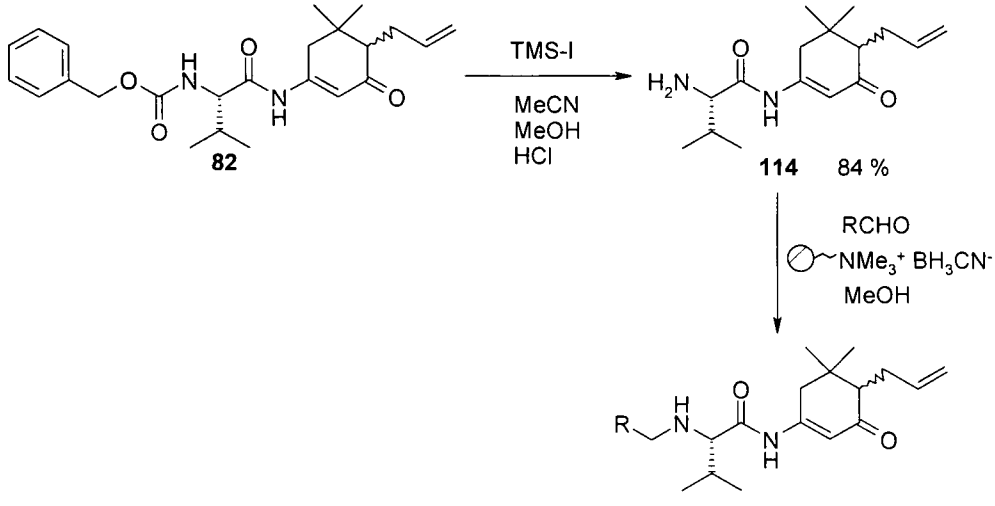

Ligand	R	Yield	Ligand	R	Yield
115	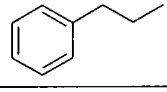	54 %	**120**	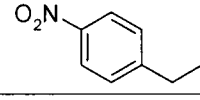	62 %
116	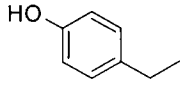	52 %	**121**	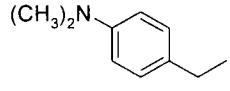	53 %
117	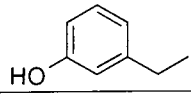	53 %	**122**	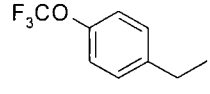	59 %
118	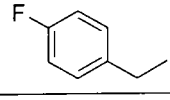	60 %	**123**	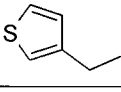	46 %
119	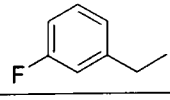	54 %			

Scheme 2.31: Replacement of the Cbz group *via* reductive amination reactions.

The amine starting material ligand **114** was dissolved in methanol and equal aliquots were manually dispensed into nine reaction vessels of the MiniBlock. The aldehydes were then individually added to each reaction vessel, along with 4Å molecular sieves, added to promote dehydration and imine formation. A slight excess of **114** was used to restrict tertiary amine formation, the aldehyde being the limiting reagent. The MiniBlock was agitated for an hour, then PS-CBH was added and the MiniBlock returned to the shaker station overnight. Purification was attempted by firstly adding 4-benzyloxybenzaldehyde polystyrene resin to the reaction vessels and agitating overnight. This electrophilic scavenger resin has been shown to selectively sequester primary amines in the presence of secondary amines,[45] and was intended to remove the excess primary amine starting material **114**. In principle, filtration through the MiniBlock reaction vessel frits would then allow the collection of pure ligand solutions in a microtitre plate. However, analysis of the filtrate solutions by thin layer chromatography indicated that the ligand solutions contained impurities, necessitating additional purification. This was achieved by using the Biotage Parallex Flex preparative HPLC system.[46] The apparatus consists of an automated sample injection module, up to four reverse phase HPLC columns, and an automated UV-triggered fraction collection module. The relevant fractions were collected into deep-well sample plates; this was followed by evaporation of solvent to afford ligands **115-123**. A limitation of using the Flex system is that generally the isolated yields are lower than might be expected, as found in Scheme 2.31. Product yields are dependent on the threshold set for the UV-triggered collection of fractions; a lower threshold results in more product being collected, but increases the potential for contamination from any neighbouring impurity peaks.

2.6.5 Fluorescently labelled ligands

At this point in the project it became desirable to synthesise a ligand containing a fluorescent marker that could be used in *in vivo* screening studies. Amine **114** provided a useful scaffold for this purpose as there are many commercially available amine-reactive fluorescent probes that are widely used to modify proteins, peptides, ligands and other biomolecules. One of the most commonly used amine-reactive

dyes is fluorescein isothiocyanate (FITC) which forms a stable thiourea upon reactions with amines. However, when this reaction was attempted with amine **114** no product was detected. Analysis by thin layer chromatography and mass spectrometry indicated that FITC starting material was present, along with a compound that had a mass of the desired product minus enaminone **78**. It was proposed that during the reaction of amine **114** with FITC a spontaneous cyclisation occurred that resulted in the fragmentation of ligand **114** (Scheme 2.32).

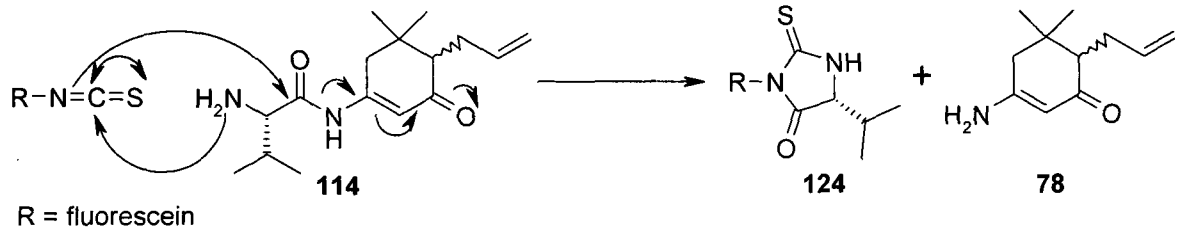

Scheme 2.32: Proposed reaction of FITC with ligand **114**.

The *in situ* cyclisation outlined in Scheme 2.32 is possible as ligand **78** could act as a good leaving group due to electron resonance through the enaminone conjugated structure. To avoid this problem, it was decided to react the commercially available dansyl-L-valine (**125**) with enaminone **78** using the same PyBroP/DMAP chemistry successfully employed earlier to synthesise the amide linked ligands (Scheme 2.33).

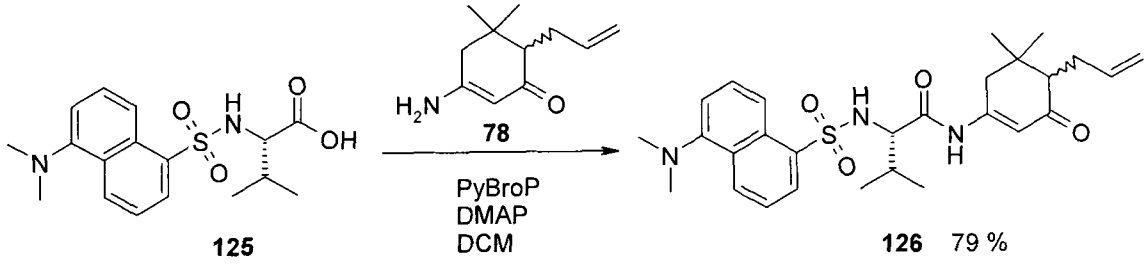

Scheme 2.33: Reaction of dansyl-L-valine **125** with enaminone **78**.

Dansyl groups are also commonly used fluorescent probes, dansyl chloride being widely used for the end-group analysis of proteins, amino acid analysis and HPLC

fluorescence detection. As expected, the reaction of dansyl-L-valine with ligand **78** was successful, the dansyl labelled ligand **126** being synthesised in good yield.

The next stage of the project was to screen the ligands prepared against CypA to determine any biological activity. This was achieved by using electrospray mass spectrometry as a primary screen, with any ligands displaying binding to CypA then being subject to further biological assay. These results are outlined in Chapters 3 and 4 respectively.

References

(1) PhD Thesis: E. Moir, *Design and Synthesis of High Affinity for CypA*, Edinburgh University, **2001.**

(2) L. A. Carpino, E. M. E. Mansour, D. Sadat-Aalace, *J. Org. Chem.*, **1991**, *56*, 8, 2611.

(3) J. N. Bertho, A. Loffet, C. Pinel, F. Reuther, G. Sennyey, *Tetrahedron Lett.*, **1991**, *32*, 1303.

(4) G. A. Olah, *J. Org. Chem.*, **1961**, *26*, 225.

(5) G. A. Olah, M. Nojima, I. Kerekes, *Synthesis*, **1973**, 487.

(6) W. R. Hasek, W. C. Smith, V. Engelhardt, *J. Am. Chem. Soc.*, **1960**, *82*, 543.

(7) G. A. Olah, S. J. Kuhn, *Org. Synth.*, **1965**, *45*, 3.

(8) G. A. Olah, M. Nojima, I. Kerekes, *J. Am. Chem. Soc.*, **1974**, *96(3)*, 925.

(9) L. A. Carpino, A. El-Faham, *J. Am. Chem. Soc.*, **1995**, *117*, 5401.

(10) W. J. Middleton, *J. Org. Chem.*, **1975**, *40*, 574.

(11) C. Kaduk, H. Wenschuh, M. Beyermann, K.Former, L. A. Carpino, *Lett. in Pept. Sci.*, **1970**, *103*, 594.

(12) V. V. Suresh Babu, H. N. Gopi, K. Ananda, *Indian J. Chem.*, **2000**, *39B*, 384.

(13) N. Berry, M. Davey, L. Harwood, *Synthesis*, **1986**, 476.

(14) S. Toru, T. Inokucki, H. Ogawa, *Bull. Chem. Soc. Jap.*, **1979**, *52*, 1233.

(15) R. A. Lee, M.C. McAndrews, K. M. Patel, *Tetrahedron Lett.*, **1973**, *14*, 965.

(16) P.G.Baraldi, D. Simoni, S. Manfredini, *Synthesis*, **1983**, 903.

(17) J. C. Sheehan, G. P. Hess, *J. Am. Chem. Soc.*, **1955**, *77*, 1067.

(18) W. König, R. Geiger, *Chem. Ber.*, **1970**, *103*, 788.

(19) J. C. Sheehan, P. A. Cruickshank, G. L. Boshart, *J. Org. Chem.*, **1961**, *26*, 2525.

(20) V. Dourtoglou, J. -C. Ziegler, B. Gross, *Tetrahedron Lett.*, **1978**, *15*, 1269.

(21) L. A. Carpino, H. Imazumi, A. El-Faham, F. J. Ferrer, C. Zhang, Y. Lee, B. M. Foxman, P. Henklein, C. Hanay, C. Mügge, H. Wenschuh, J. Klose, M. Beyermann, M. Bienert, *Angew. Chem. Int. Ed.*, **2002**, 41, 441.

(22) P. Li, J. C. Xu, *J. Chem. Soc., Perkin Trans. 2*, **2001**, 113.

(23) L. A. Carpino, *J. Am. Chem. Soc.*, **1993**, *115*, 4397.

(24) J. P. Michael, C. B. deKoning, D. Gravestock, G. D. Hosken, A. S. Howard, C. M. Jungmann, R. W. M. Krause, A. S. Parsons, S. C. Pelly, T. V. Stanbury, *Pure Appl. Chem.*, **1999**, *71*, 979.

(25) M. N. Eberlin, Y. Takahata, C. M. Kacheres, *J. Org. Chem.*, **1993**, *55*, 5150.

(26) C. M. Kascheres, *J. Braz. Chem. Soc.*, **2003**, *6*, 945.

(27) J. E. Foster, J. M. Nicholson, R. Butcher, J. P. Stables, I. O. Edafiogho, A. M. Goodwin, M. C. Henson, K. R. Scott, *Bioorg. Med. Chem.*, **1999**, *7*, 2415.

(28) L. A. Carpino, D. Ionescu, A. El-Faham, *Tetrahedron Lett.*, **1998**, *39*, 241.

(29) M. T. Leplawy, D. S. Jones, G. W. Kenner, R. C. Sheppard, *Tetrahedron*, **1960**, *11*, 39.

(30) B. Castro, J. R. Dormoy, G. Evin, C.Selve, *Tetrahedron Lett.*, **1975**, *14*, 1219.

(31) D. Le-Nguyen, R. Seyer, A. Heitz, B. Castro, *J. Chem. Soc. Perkin Trans. I* **1985**, 1025.

(32) J. Coste, D. Le-Nguyen, B. Castro, *Tetrahedron Lett.*, **1990**, *31*, 205.

(33) J. Coste, E. Frérot, P. Jouin, *Tetrahedron Lett.*, **1991**, *17*, 1967.

(34) J. Coste, E. Frérot, P. Jouin, *J. Org. Chem.*, **1994**, *59*, 2437.

(35) E. Frérot, J. Coste, A. Pantaloni, M-N. Dufour, P. Jouin, *Tetrahedron*, **1991**, *47*, 259.

(36) Mettler-Toledo Ltd., 64 Boston Road, Beaumont Leys, Leicester, LE4 1AW

(37) A. Mehta, R. Jaouhari, T. J. Benson, K. T. Douglas, *Tetrahedron Lett.*, **1992**, *37*, 5441.

(38) Accelrys Ltd, 334 Cambridge Science Park, Cambridge, CB4 0WN.

(39) H. C. Kolb, M. S. VanNieuwenhze, K. B. Sharpless, *Chem. Rev.*, **1994**, *94*, 2483.

(40) M.Daumas, Y. Vo-Quang, L. Vo-Quang, F. Le Goffic, *Synthesis*, **1989**, 64.

(41) M. E. Jung, M. A. Lyster, *J. Chem. Soc. Chem. Commun.*, **1978**, 315.

(42) S. Bhattacharyya, S. Rana, O. W. Gooding, J. Labadie, *Tetrahedron Lett.*, **2003**, *44*, 4957.

(43) C. F. Lane, *Synthesis*, **1975**, 135.

(44) R. O. Hutchins, N. R. Natale, I. M. Taffer, *J.Chem. Soc. Chem. Commum*, **1978**, 1088.

(45) R. J. Booth, J. C. Hodges, *Acc. Chem. Res.*, **1999**, *32*, 18.

(46) Biotage, 15 Harforde Court, Foxholes Business Park, John Tate Road, Hertford, SG13 7NW.

3. Results and Discussion II – Mass Spectrometry Screening

3.1 Introduction

One aim of this project was to develop electrospray ionisation mass spectrometry (ESI-MS)[1] as a primary screening technique to detect protein:ligand binding, in collaboration with the Barran research group at the University of Edinburgh.[2] The plan was to use mass spectrometry to highlight any ligands that bound to CypA; these ligands could then be subject to further biological testing. Mass spectrometry is adept at this role as it is versatile, fast and low on sample consumption. In this chapter the general principles of mass spectrometry are outlined, followed by a discussion of the ligand screening techniques and results.

3.2 Mass spectrometry

Mass spectrometry relies on a method of ionising the sample; once the compound is ionised the ions are then separated by their mass to charge ratio and then counted by an ion detector. To achieve this, mass spectrometers are generally comprised of the following component parts:

i) Sample introduction – either direct injection or capillary infusion, for example post HPLC;
ii) an ionisation source for the generation of ions in the gas phase;
iii) mass analyser;
iv) detector;
v) processing unit.

3.2.1 Ionisation

The earliest ionisation method used was electron impact (EI). The sample is firstly heated to facilitate evaporation; the gaseous sample is then ionised in an electron

ionisation region. This is achieved by striking the analyte with an electron beam, causing ionisation through electron ejection. However, the usefulness of EI decreases for compounds with a molecular weight of greater than about 400 Da. This is largely due to the involatility of larger molecules leading to thermal decomposition of the sample prior to vaporisation, and fragmentation of the molecules during the electron ionisation process.

Alternate ionisation techniques have been developed to overcome the limitations of electron impact. Fast atom bombardment (FAB)[3] generates ions by bombarding a matrix/analyte mix with a fast particle beam of an inert gas such as argon or xenon. When the particle beam strikes the surface of the matrix energy is transferred to the surroundings, setting up momentary collisions and disruptions. This results in the ejection of some species off the surface as positive and negative ions, a process known as sputtering. The polarity of the source extraction can be switched depending on what species are to be analysed. Matrix assisted laser desorption ionisation (MALDI) is a similar matrix based technique but uses a laser to ionise the analyte sample.[4] The matrix used is typically an aromatic acid with a chromophore that strongly absorbs at the laser wavelength resulting in desorption of bulk portions of the analyte sample. Both FAB and MALDI are comparatively soft ionisation techniques that tend to limit fragmentation upon ionisation, typically producing large peaks for the pseudo-molecular ion species $[M+H]^+$ and $[M-H]^-$.

The ionisation technique used in this project was electrospray ionisation (ESI). This is an exceptionally versatile method of ionisation enabling the study of a wide range of molecules including large biomolecules. The sample is dissolved in a volatile solvent at low concentration which is then pumped through a fine capillary at a rate of 0.1-0.3 ml/hr. A high potential is applied to the tip of the capillary, either positive or negative depending on the mode chosen, resulting in the creation of a fine electrostatic spray of charged droplets. This is sprayed through a warm nitrogen stream to promote evaporation and to reduce the droplets in size. The actual mechanism of ionisation is subject to two theories, the charge residue mechanism (CRM)[5] and the ion evaporation mechanism (IEM).[6] In both theories the droplets

decrease in size due to evaporation, increasing the charge density on the droplet until the coulombic repulsion between the species eventually equals that of the surface tension resulting in droplet fission (Figure 3.1).

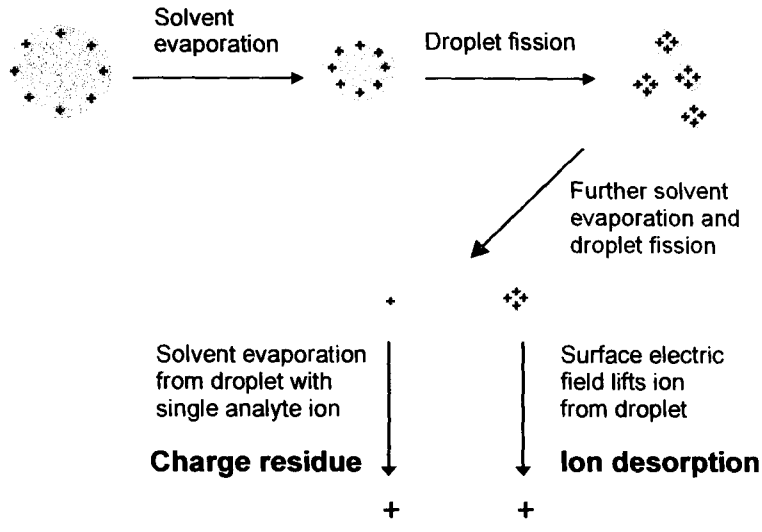

Figure 3.1: Electrospray ionisation process in positive ion mode.[7]

The charge residue mechanism depicts a series of fission events that ultimately leads to the production of final small droplets that bear one or more excess charges, but only a single analyte molecule. As the last few solvent molecules evaporate the analyte molecule retains this droplet charge, forming a free gas-phase ion. The alternate ion evaporation mechanism contends that gas phase ions are emitted directly from charged droplets after the radii of the droplets decrease to a suitable size (radius <10 nm).[8] Some of the droplet's charge is carried by the molecule as it desorbs from the droplet, thereby relieving coulombic repulsion. The exact mechanism of desorption of small molecules is still subject to debate between proponents of the two theories, but for very large molecules such as proteins a consensus has emerged which favours the charge residue model.[9,9]

A distinctive feature of ESI is that multiply charged ions can be produced. As all mass analysers differentiate on the basis of mass to charge ratio (m/z) the effective mass range can be extended by detecting these multiply charged ions. For example, a

decrease in size due to evaporation, increasing the charge density on the droplet until the coulombic repulsion between the species eventually equals that of the surface tension resulting in droplet fission (Figure 3.1).

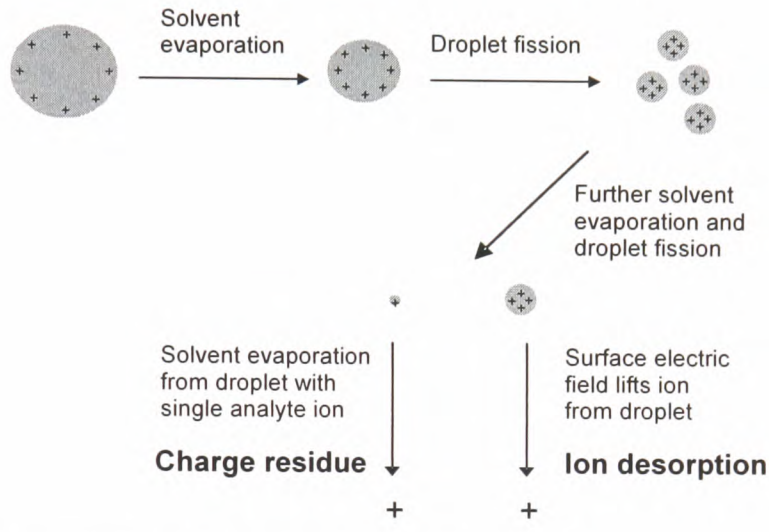

Figure 3.1: Electrospray ionisation process in positive ion mode.[7]

The charge residue mechanism depicts a series of fission events that ultimately leads to the production of final small droplets that bear one or more excess charges, but only a single analyte molecule. As the last few solvent molecules evaporate the analyte molecule retains this droplet charge, forming a free gas-phase ion. The alternate ion evaporation mechanism contends that gas phase ions are emitted directly from charged droplets after the radii of the droplets decrease to a suitable size (radius <10 nm).[8] Some of the droplet's charge is carried by the molecule as it desorbs from the droplet, thereby relieving coulombic repulsion. The exact mechanism of desorption of small molecules is still subject to debate between proponents of the two theories, but for very large molecules such as proteins a consensus has emerged which favours the charge residue model.[9,9]

A distinctive feature of ESI is that multiply charged ions can be produced. As all mass analysers differentiate on the basis of mass to charge ratio (m/z) the effective mass range can be extended by detecting these multiply charged ions. For example, a

protein with a molecular weight of 10,000 Da would be detected at several different m/z peaks depending on the number of charges being carried (Figure 3.2).

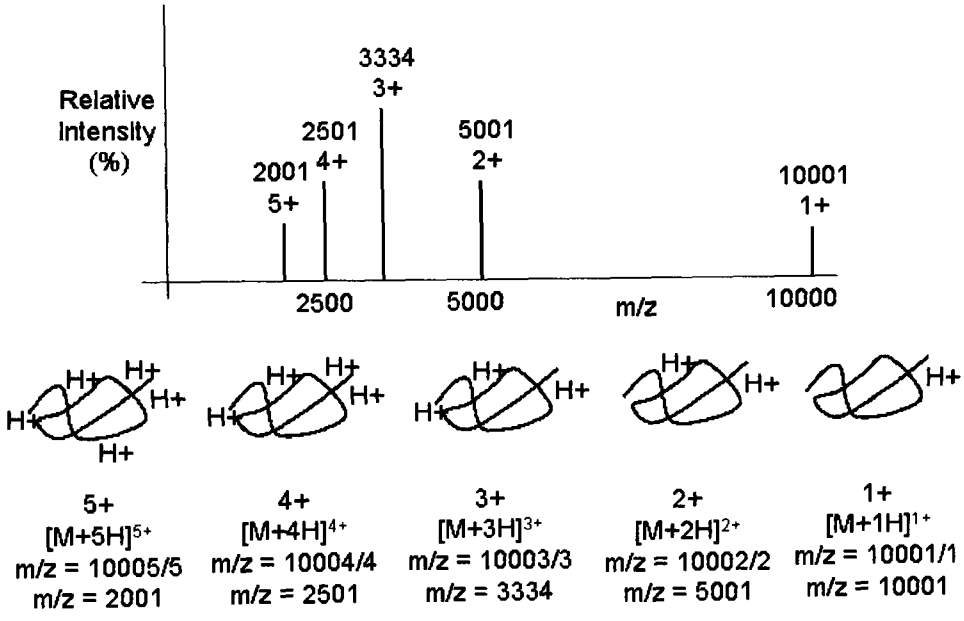

Figure 3.2: Schematic spectra of a multiple charged ion series.[10]

The ion sources described above produce ions either by ionising a neutral molecule though protonation, cationisation, or deprotonation for ESI, FAB and MALDI; or through electron capture or ejection when EI is used. Protonation involves the addition of a proton to an analyte molecule to give a net positive charge of +1 for every proton added. The charge tends to reside on the more basic residues, but because of the covalent nature of proton binding the charge can be delocalised from the proton onto the molecule, potentially destabilising the molecular ion resulting in fragmentation. Cationisation is similar to protonation but involves the non-covalent addition of a positively charged ion to a neutral molecule, for example Na^+. This ionisation method is useful for molecules that are not stable to protonation as the charge remains localised on the cation. Deprotonation involves the ejection of a proton from a molecule, resulting in a net negative charge of -1 for each proton ejected. This method is typically used for ionising acidic species, for example carboxylic acids. Electron ejection is usually performed on relatively non-polar, low molecular weight molecules and involves the ejection of an electron to produce a net

positive charge of +1. The related electron capture involves the absorption of an electron to produce a net negative charge of -1, and is primarily observed in molecules with a high electron affinity.

3.2.2 Analysers

The analyser is the component of the mass spectrometer that separates ions according to their mass to charge ratio, thus influences the sensitivity, range and accuracy of the equipment. There are several different types of analyser available, the type used in this project were quadrupole and time of flight analysers.

Quadrupoles are widely used analysers that can scan over a fairly wide mass to charge range (typically 10 to 4000 Da) with good accuracy (0.1 to 0.2 Da).[11] The apparatus consists of four parallel rods to which a direct current voltage is applied and a radio frequency (RF) potential is imposed. Ions entering the field region will oscillate depending upon their mass to charge ratio. At a specific RF and voltage, only ions at a given m/z will pass through the quadrupole to the detector, other ions will be destabilised and will impact on the side of the apparatus (Figure 3.3). By changing the RF potential the field on the quadrupole can be changed enabling the complete mass range for a sample to be scanned.

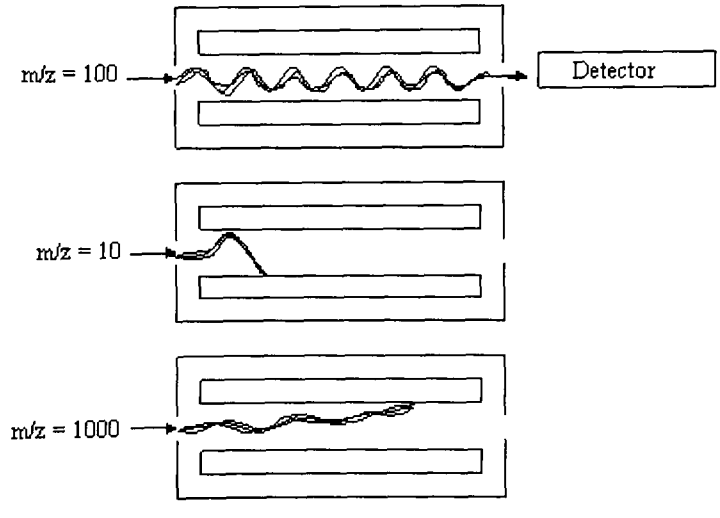

Figure 3.3: Quadrupole analyser at a fixed RF.[11]

Time of flight (TOF) analysis is based upon the principle of accelerating ions *via* a set voltage through a field free region.[12] The time taken for the ions to travel from the source to the detector can be related to their m/z. The TOF apparatus consists of a drift tube through which the ions are accelerated, the distance between the ion source and the detector being fixed (Figure 3.4). As the accelerating voltage is also fixed, the time taken for the ion to pass through the analyser is dependant on the square root of the mass to charge ratio. The resolution of a TOF analyser is dependant on the size of the drift tube, this can be increased by extending the tube length or through fitting a reflectron. This acts as an electronic mirror and consists of a series of charged plates that deflect ions back on a different trajectory towards the detector, thus artificially lengthening the drift tube.

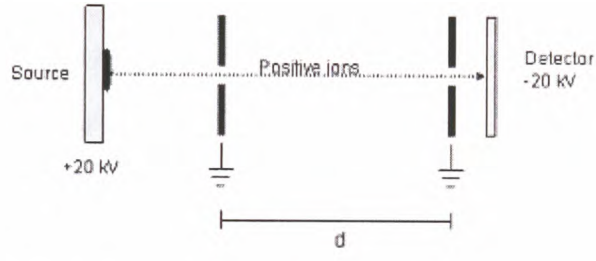

Figure 3.4: Schematic of a time of flight analyser.[13]

3.2.3 Tandem mass spectrometry

Ionisation techniques such as ESI, FAB and MALDI are relatively gentle and do not produce a significant amount of fragment ions, in contrast with EI. Tandem mass spectrometry (MS/MS) has been developed to induce fragmentation and then mass analyse the fragments, this potentially revealing useful structural information. Fragmentation is achieved by inducing ion-molecule collisions by a process called collision induced dissociation (CID). CID is accomplished by selecting an ion of interest with the first mass analyser, and introducing the ion to a collision cell. The cell is filled with an inert gas, typically argon, and the selected ion collides with the gas atoms, resulting in fragmentation. The fragment ions are then analysed in a second mass analyser.

A commonly used tandem mass spectrometer is the triple quadrupole mass spectrometer, which uses the first and third quadrupoles as mass analysers and the second quadrupole as a collisions cell to generate fragment ions. Another common instrument is the quadrupole-time of flight (Q-TOF) mass spectrometer. This is similar to the triple quadrupole, however replaces the third quadrupole with a TOF mass analyser. Both of these instruments are extensively used in peptide and carbohydrate sequencing.

3.2.4 Detectors

Detectors operate by converting kinetic energy from incident ions into secondary electrons, which are further amplified to produce a signal. There are three common types of detectors used in commercial mass spectrometers; electron multipliers, photomultipiers and microchannel plates. Electron multipliers use a series of dynodes maintained at increasing potentials. Ions strike the surface, generating an emission of electrons. These secondary electrons are attracted towards the next dynode, generating more electrons, ultimately resulting in a cascade sequence that typically amplifies the current by 10^6. Photomultiplier detectors operate in a similar manner to electron multipliers; ions initially strike a dynode resulting in electron emission. These secondary electrons then strike a phosphorus screen, this generates photons which are in turn detected by a photomultiplier. This type of detector has the advantage of being sealed in a vacuum, unexposed to the environment inside the mass spectrometer and thus resistant to contamination. Both photomultipliers and electron multipliers are commonly used with quadrupole analysers.

Time of flight analysers are often coupled to microchannel plate (MCP) detectors. These consist of a glass plate with many individual channels. Each channel is comparable to a single electron multiplier, and an incident ion hitting a channel on one side of the plate produces a charge pulse of about 1000 electrons from the other side. MCPs have a large planar detection area with only a few channels out of thousands being affected by the detection of a single ion. It is therefore possible to

detect many ions at the same time, ideal for laser ionisation where hundreds of ions can be created within a few nanoseconds.

3.3 Detection of protein complexes by ESI-MS

The first reported detection and analysis of a receptor:ligand complex by mass spectrometry was by Ganem *et al.*, in the early 1990s. The group utilised ion-spray mass spectrometry to investigate the binding of the immunosuppressants FK506 and rapomycin with the cytoplasmic receptor FK binding protein.[14] Ion-spray is also known as pneumatically assisted electrospray, but in contrast to electrospray can be performed in water without co-solvent.[15] It was found that multiple charging produced a family of molecular ions and dramatically reduced the mass to charge ratio enabling a quadrupole mass spectrometer to analyse the high molecular weight complexes, as outlined earlier in Figure 3.2. When FKBP was mixed with a slight excess of FK506 at pH 7.5 a signal was detected at m/z 1803.1, corresponding to a FKBP:FK506 complex in the 7+ charge state. A much weaker signal for the same complex in the 6+ charge state was also evident at m/z 2103.5. As a control, a sample of FK506 combined with denatured FKBP was analysed. This did not give a signal for the complex, implying that the FKBP:FK506 complex seen in previous experiments resulted from genuine binding and not merely non-specific adduct formation.

The subject of whether the protein:ligand complexes observed under ESI-MS conditions represent specific binding or non-specific adduct formation has been debated since the initial work of Ganem *et al.* One limitation of the technique is that simple observation of ions indicative of a complex by ESI-MS is insufficient evidence for a structurally specific protein:ligand interaction. An early 1990s paper by Smith *et al.*, attempted to review the initial literature on the analysis of protein:ligand complexes by ESI-MS to see if specific and non-specific non-covalent associations could be distinguished.[16] An opinion of the authors was that while it may be impossible to prove beyond doubt that a specific protein:ligand association

exists solely on the basis of ESI-MS, several kinds of evidence could be employed to support such a conclusion:

i) *Complex relative intensity and preferred stoichiometry* - complexes should be observed with preferred or reasonable stoichiometry, i.e. without random aggregation.

ii) *Gas-phase lability* - complexes due to weak non-specific intermolecular interactions should be labile and readily dissociated under more severe ESI-MS or tandem mass spectrometry conditions.

iii) *Complex dissociation due to modification of solution conditions* - changes in solution temperature, pH, the addition of organic solvents etc., can destroy specific protein:ligand associations and should produce a corresponding change in the ESI mass spectra.

iv) *Sensitivity to modification of complex components* - a substantial change in the relative intensity of the complex in the mass spectrum following alteration of either the protein (i.e. though denaturing) or ligand provides good evidence of a specific protein:ligand interaction.

The use of mass spectrometry to observe and analyse protein complexes has expanded rapidly since the initial reports of Ganem *et al.*, and the early perspective of Smith *et al.* This is largely due to the advantages of the technique such as sensitivity, specificity and speed, and due to the widespread availability of mass spectrometry equipment. Compared to other techniques such as NMR and X-ray crystallography, mass spectrometry is very fast and can be performed on a very small amount of sample. Of direct relevance to this project, mass spectrometry has found use in the screening of libraries of potential ligands. An example of this research was carried out by Smith and co-workers who screened a combinatorial library of benzenesulfonamide based compounds for binding with the protein carbonic anhydrase II (CAII, molecular weight 28,996 Da).[17] It was found that the relative abundance of the ligand:CAII complex ions observed were consistent with the binding constants of the ligands in solution. A control experiment using denatured

protein resulted in no complexes being observed, again showing that the complexes observed with mass spectrometry were the result of active site binding.

Swayze *et al.*, extended the principle of ESI-MS ligand screening to investigate structural activity relationships by mass spectrometry, and successfully incorporated this approach in drug design. This "SAR by MS" process was a development of previous high-throughput ESI-MS screening methods used by the group for the study of non-covalently bound drug candidates to model RNA sequences.[18, 19] The process began by screening a set of compounds to identify hits against a RNA target of interest The structural activity relationships between the ligands and RNA targets were then explored through synthesising ligand derivatives and/or additional MS experiments; the SAR data being used as a guide to the synthesis of more elaborate higher affinity ligands (Figure 3.5).[20]

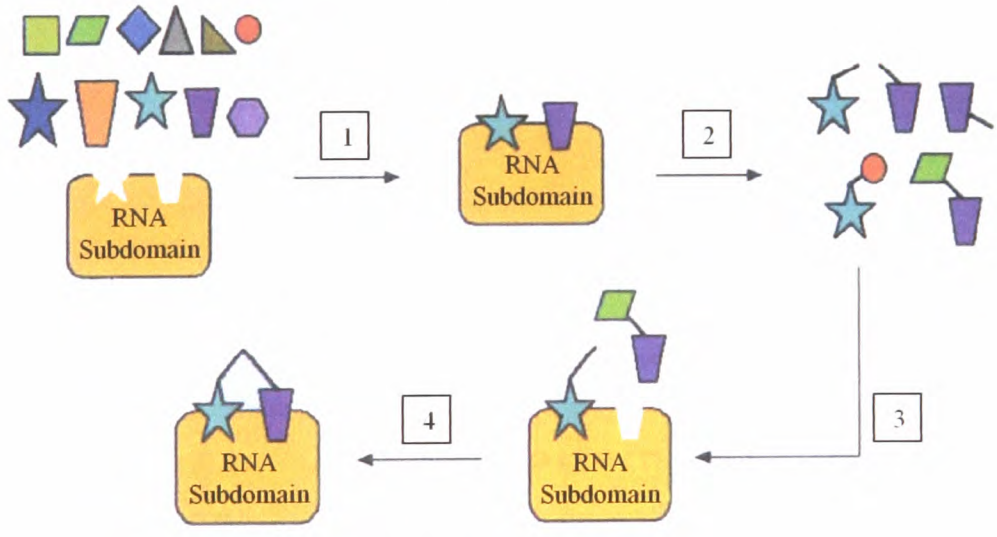

Figure 3.5: SAR by MS ligand-based lead discovery strategy as outlined by Swayze *et al.* 1 - Ligands are screened against a RNA subdomain, ligands that bind are highlighted by MS. 2 - Simple derivatives of the most interesting ligands are prepared. 3 - The compounds are re-screened using the MS assay, and any observed SAR data provides information about the binding site. 4 - The SAR data is used to guide the synthesis of higher affinity compounds via the linking of individual ligands.[20]

Through the initial screening of combinatorial libraries, Swayze *et al.*, discovered two classes of compounds that displayed an interesting SAR towards the RNA target; a D-amino acid and a quinoxalin-2,3-dione class. Following the strategy outlined in Figure 3.5, Swayze *et al.*, discovered that some members of the two ligand classes seem to bind co-operatively. To test this hypothesis, several fused compounds were prepared, and all were found to bind markedly tighter to the target RNA than the parent ligands, thus supporting the process summarised in Figure 3.5.[20] The "SAR by MS" method has also been used by Ockey *et al.*, to discover a novel class of non-peptide inhibitors of the matrix metalloproteinase stromelysin (MMP-3). Here a similar approach to *Swayze et al.*, was used and competition studies between ligand fragments using ESI-MS were carried out; novel inhibitors of the target protein were then constructed by chemically linking promising ligand fragments.[21]

A key factor in detecting non-covalent protein complexes is the preservation of the protein tertiary structure. The native structure of proteins may be lost while in solution prior to analysis or during the ESI process, and optimum mass spectrometry conditions may not correspond with the optimum conditions for protein folding, for example the pH range. To maintain native protein structure and thus hopefully detect genuine ligand binding it is often necessary to use volatile organic buffers. Ammonium acetate and ammonium bicarbonate are generally the most popular choices for ESI-MS experiments because they do not often form extensive gas phase adducts with the analyte macromolecules, unlike phosphate- and sulfate- based buffers.[22] Typically buffer concentration is in the range of 2 - 50 mM, although higher concentrations are sometimes used.

3.4 Analysis of cyclophilin A by ESI-MS

Initial mass spectrometry research in this project focussed upon the analysis of CypA alone. This was necessary in order to optimise experimental conditions, enabling the native tertiary structure of CypA to be retained during ESI-MS analysis. The mass

spectrometer used for the analysis of CypA and the screening of ligands was the Waters ZMD system,[23] and the experimental conditions are outlined in Table 3.1.

Solvent flow rate	200-300 μL/hr
Injection volume	35 μL
Buffer	Ammonium acetate, pH 6.8
Desolvation temperature	90 °C
Source block temperature	65 °C
Cone voltage	50 V (+/- 2 V)
Capillary voltage	3.5 kV

Table 3.1: Experimental conditions used for mass spectrum analysis.[8]

CypA was analysed by ESI-MS at various pHs to investigate if the tertiary structure was retained in the gas phase after ionisation. Acidic conditions would denature the protein by interrupting the intermolecular forces that govern the tertiary structure, allowing greater accessibility of charging to inner residues. This would result in higher charge states observed in the mass spectra. The pH was altered by adding 1% v/v formic acid to CypA buffered in an aqueous ammonium acetate solution. Upon analysis, it was found that the mass spectra varied according to the pH (Figure 3.6).

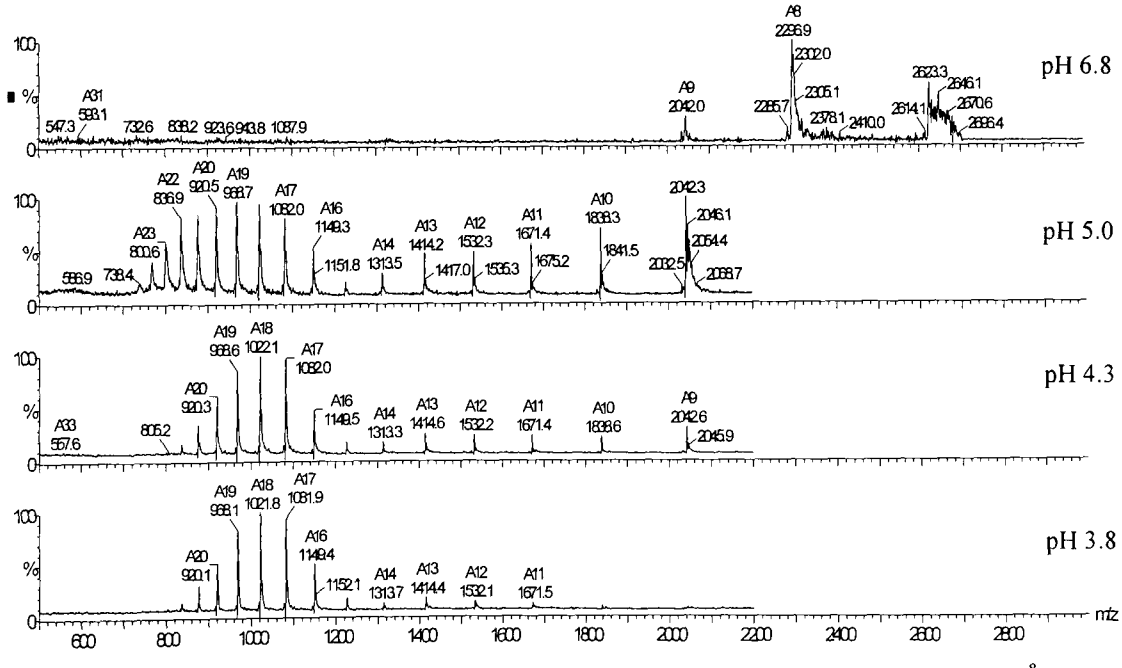

Figure 3.6: Mass spectra of CypA at various pHs. The values labelled A denote the +ve charge.[8]

The mass spectrum of CypA at the near physiological pH 6.8 shows a compact charged ion series of +7 to +9 indicating conservation of the CypA tertiary structure. As the pH is lowered CypA unfolds exposing more amino acid residues to protonation. This results in the higher charge states of +16 to +20 dominating the spectra.

3.5 Analysis of cyclophilin A complexes by ESI-MS

3.5.1 Cyclophilin A:cyclosporin A

The first complex to be investigated by ESI-MS in this project was CypA:CsA. With the mass spectrometry conditions for cyclophilin A optimised, the CypA:CsA complex would be used as a positive control to show that ligand binding could be seen by mass spectrometry. CypA (20 μM) was incubated with CsA (20μM) at a 1:1 ratio at room temperature for 30 minutes in a mix of aqueous ammonium acetate buffer (pH 6.8), and 10 % methanol to aid CsA dissolution. Identical mass spectrometry conditions to those used previously for CypA were used, as outlined in Table 3.1. Upon analysis by ESI-MS it was found that the CypA:CsA complex gave clear m/z signal peaks (figure 3.7).

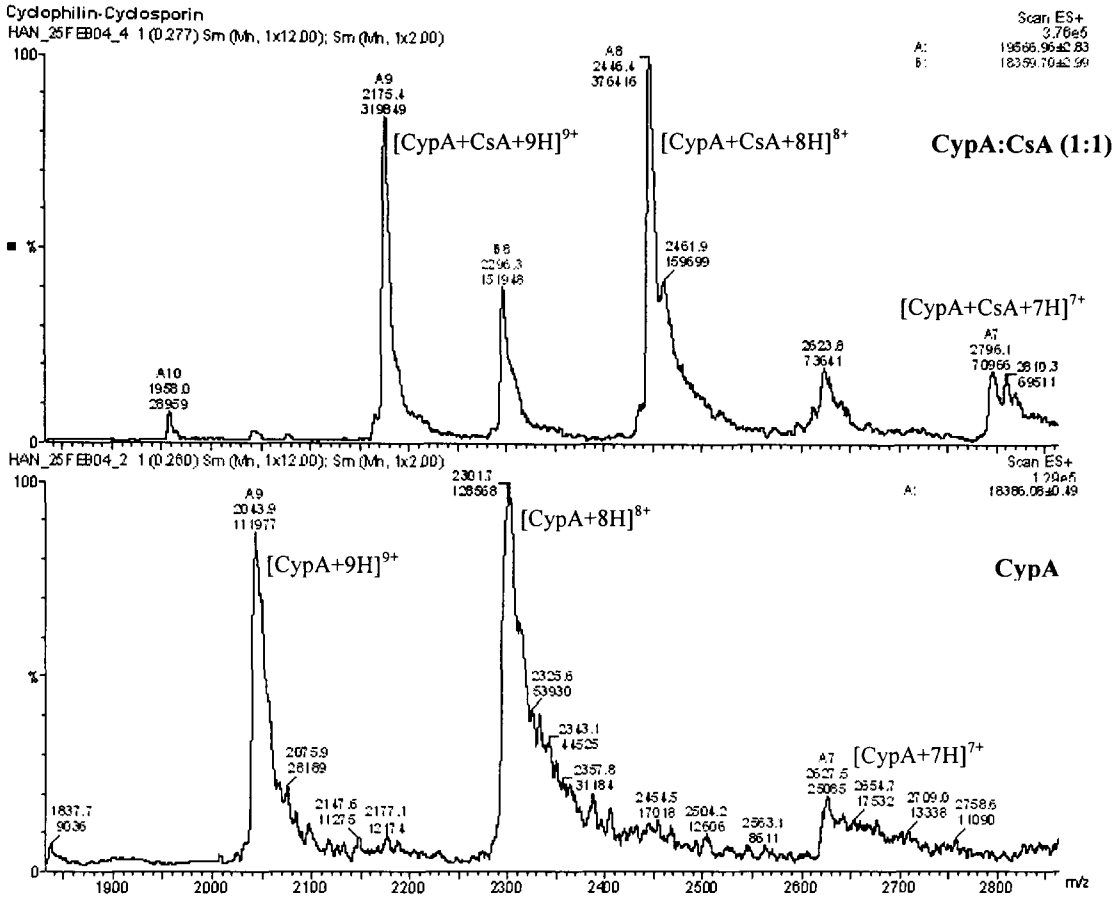

Figure 3.7: Mass spectra of CypA:CsA complex and CypA under identical conditions.

Figure 3.7 shows the mass spectra of CypA and the CypA:CsA complex at pH 6.8. As seen in Figure 3.6, CypA is preferentially detected as the +7 to +9 charge states. The CypA:CsA complex produced a very similar spectrum under ESI-MS conditions, with the +8 and +9 charged complex dominating, although at the 1:1 ratio uncomplexed CypA peaks remained in the spectra. In order to investigate the effect of ligand concentration upon binding the experiment was repeated with an increased concentration of CsA (200 μM), a ratio of 1:10 (Figure 3.8).

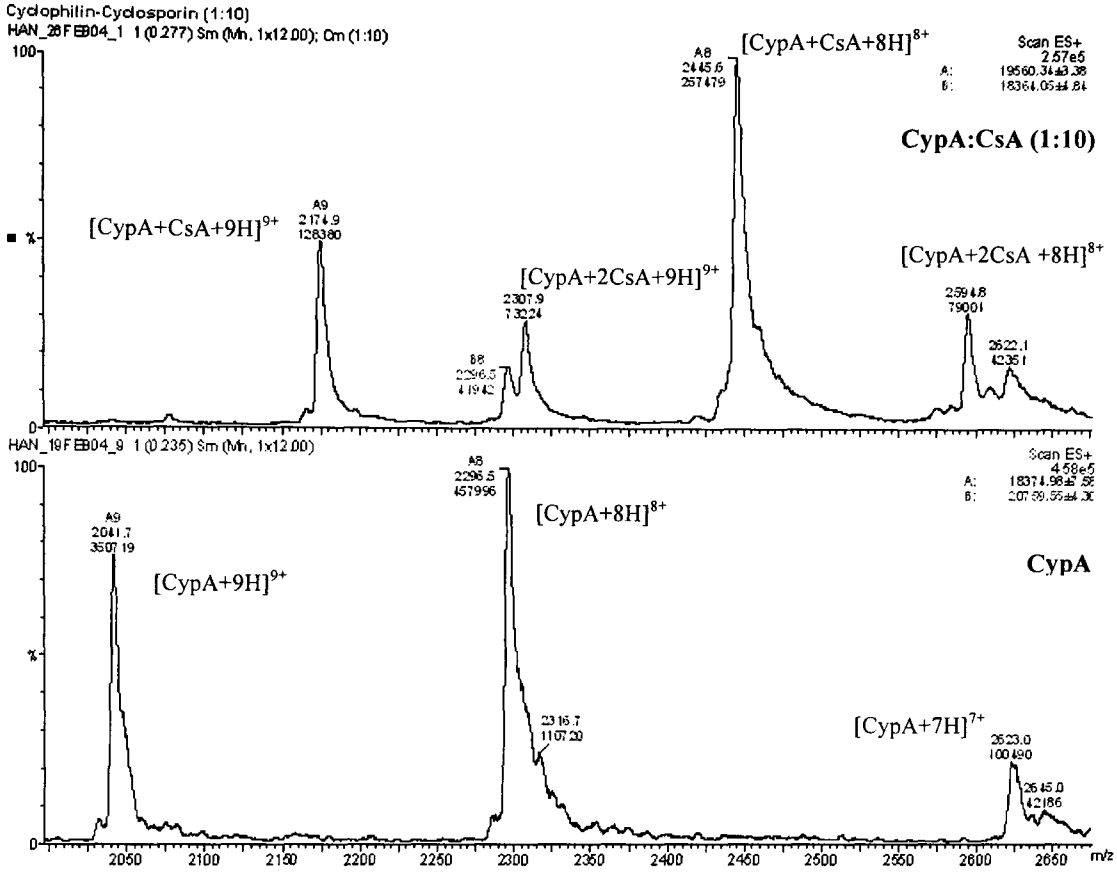

Figure 3.8: Mass spectra of CypA:CsA at increased concentration of CsA (1:10).

When the concentration of CsA was increased the amount of uncomplexed CypA was reduced, resulting in a smaller peak area, as shown in the top spectrum of figure 3.8. Interestingly, peaks corresponding to a two ligand:CypA complex were also detected. It was thought that these peaks could due to ligand aggregation at the higher concentration, with one ligand residing in the active site and another ligand aggregating to the residues lying outside the site, or alternatively due to non-specific binding of one ligand to the CypA surface.

In an attempt to gain an understanding of the mechanisms of binding involved in the two ligand complex, tandem mass spectrometry was utilised. The MS/MS analysis was carried out using a tandem quadrupole–time of flight (Q-TOF) analyser. The complex peak at approximately m/z 2308 was selected using the quadrupole, this corresponding to $[Cyp+2CsA+9H]^{9+}$. The ligands were then dissociated from the

protein by accelerating the complex into a cell filled with pressurised argon gas positioned between the quadrapole and TOF detectors. The acceleration voltage was stepped up to increase the impact energy in the dissociation cell, the collision induced dissociation data could then be used as a guide to assess the strength of CypA:CsA binding (Figure 3.9).

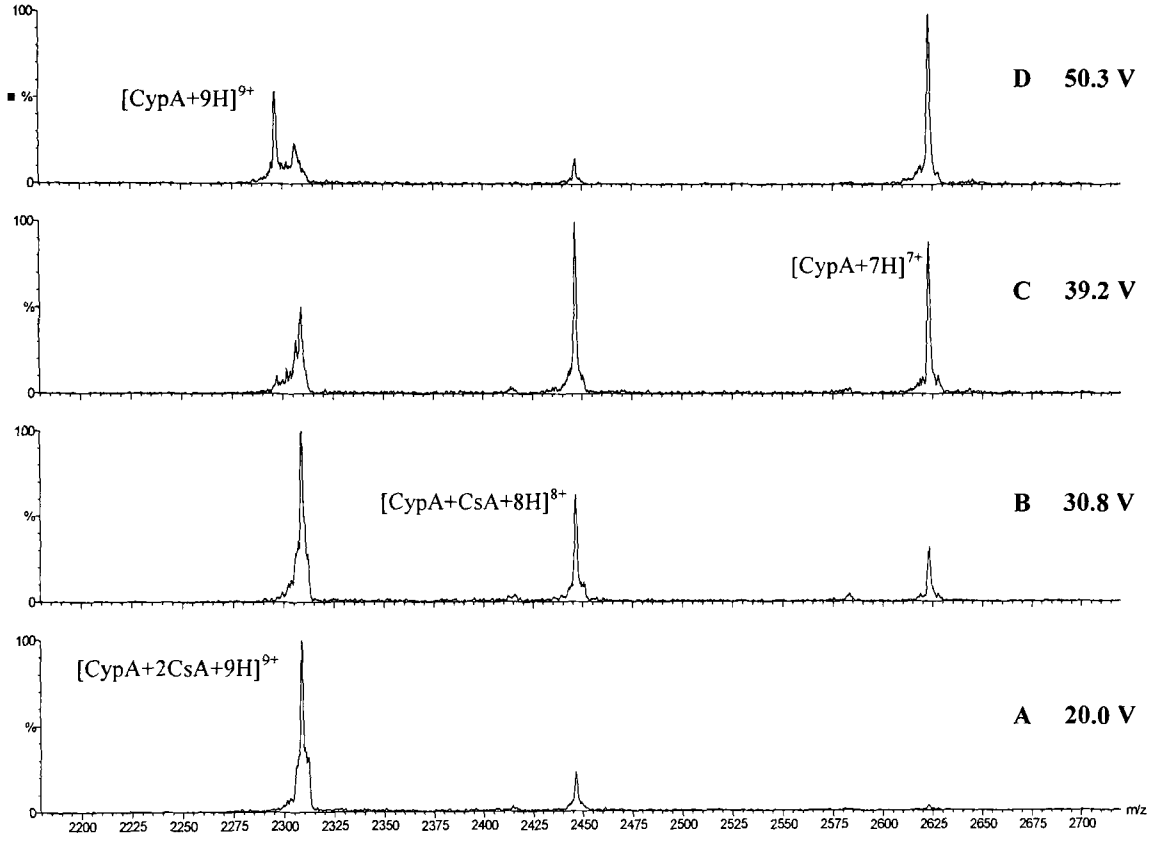

Figure 3.9: MS/MS data showing the fragmentation pattern of the removal of the two CsA ligands as the collision voltage is increased.

Figure 3.9 shows that at an acceleration voltage of 20.0 V the two-ligand complex in the +9 charge state is predominant, but with a peak corresponding to $[CypA+CsA+8H]^{8+}$ also present (Figure 3.9, A). This shows at a relatively low acceleration energy there is some dissociation of one ligand. When the voltage is increased to 30.8 V the one ligand:CypA complex increases in size showing a greater degree of one ligand dissociation, and there is a small peak corresponding to $[CypA+7H]^{7+}$ due to both ligands dissociating (Figure 3.9, B). As would be

expected, further increases in the acceleration voltage results in almost complete dissociation of firstly the two ligand complex (Figure 3.9, C), then the one ligand complex (Figure 3.9, D). It can be seen from this data that low acceleration energies result in the facile loss of one ligand, this ligand thus being held by weak intermolecular forces. The second ligand requires higher collisional energy to dissociate, and it is hypothesised that this ligand is tightly bound in the active site of CypA. Whilst it is not possible to draw definite conclusions as to whether the first dissociated ligand is binding to CypA non-specifically or forming ligand aggregates, it is clear that two ligands are not binding in the same manner, and only one is relevant to active site binding.

3.5.2 Cyclophilin A:synthetic ligands

Having observed CypA:CsA complexes by ESI-MS, the next step was to take the optimised mass spectrometry conditions and apply them to the screening of the synthetic ligands. Ligands **30** and **62** were initially used at a concentration of 20 μM, a ratio of 1:1 with CypA, using the same conditions as the previous CsA screening; however it was found that no binding was seen at these concentrations. When the experiment was repeated at an increased concentration of 100 μM, a ligand:CypA complex was seen for ligand **62**, but ligand **30** seemed to fragment under the ESI conditions to give a complex spectrum (Figure 3.10).

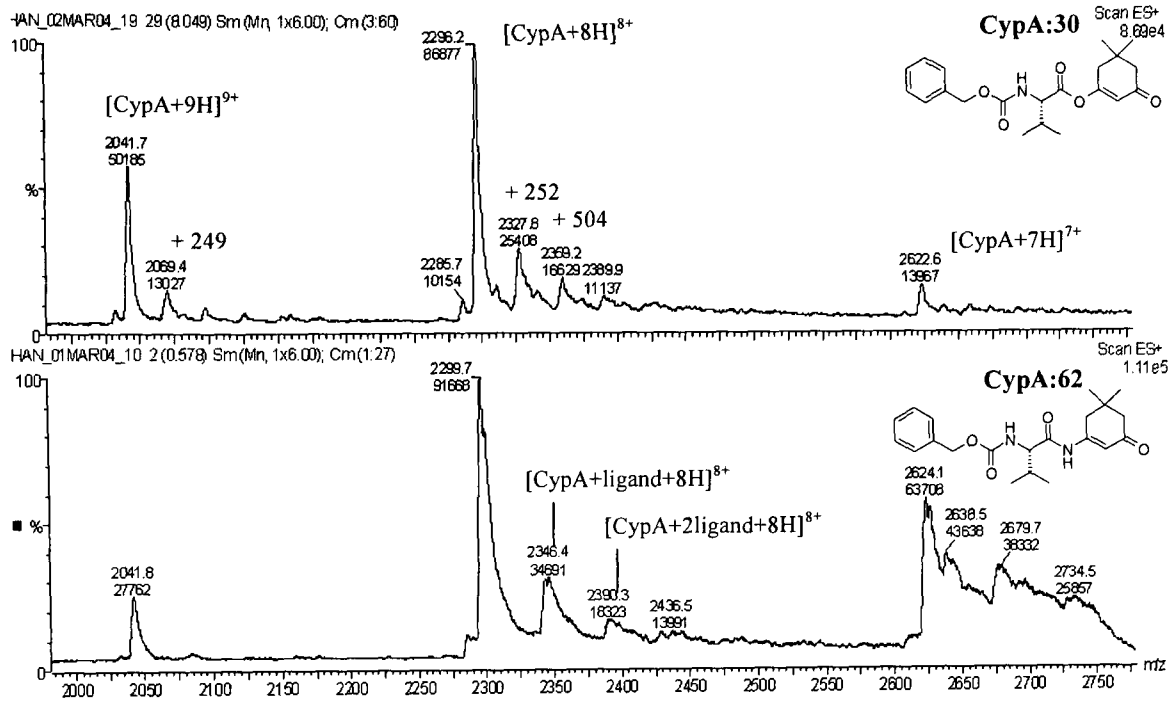

Figure 3.10: Mass spectra for CypA:ligand complexes for ligands **30** and **62**, 1:5 ratio, 30 min incubation.

The enol-ester linked ligand **30** gave a m/z peak at 2327 Da which corresponded to $[CypA+252Da+8H]^{8+}$. This mass increase corresponds to that of Cbz-valine, it would appear that ligand **30** fragmented under the electrospray conditions to yield the amino acid starting material. Encouragingly, when the experiment was repeated with ligand **62**, peaks corresponding to 1 and 2 ligand:cyclophilin complexes were detected, with the ligands binding to the protein in the +8 charge state. It was presumed that the two ligand complexes were a result of the increased ligand concentration, the same phenomenon as seen in the previous CsA screening. Interestingly, no protein:ligand complexes were seen for the other CypA charge states, the peaks associated with the +7 charge state did not correspond to the mass of ligand **62** and were hard to differentiate against the background noise.

Further ESI-MS experiments were carried out using in an attempt to optimise the ligand screening conditions. The concentration of ligand **62** was initially varied from 20 μM to 150 μM to give ratios of 1:1 to 1:7.5 CypA:**62** (Figure 3.11).

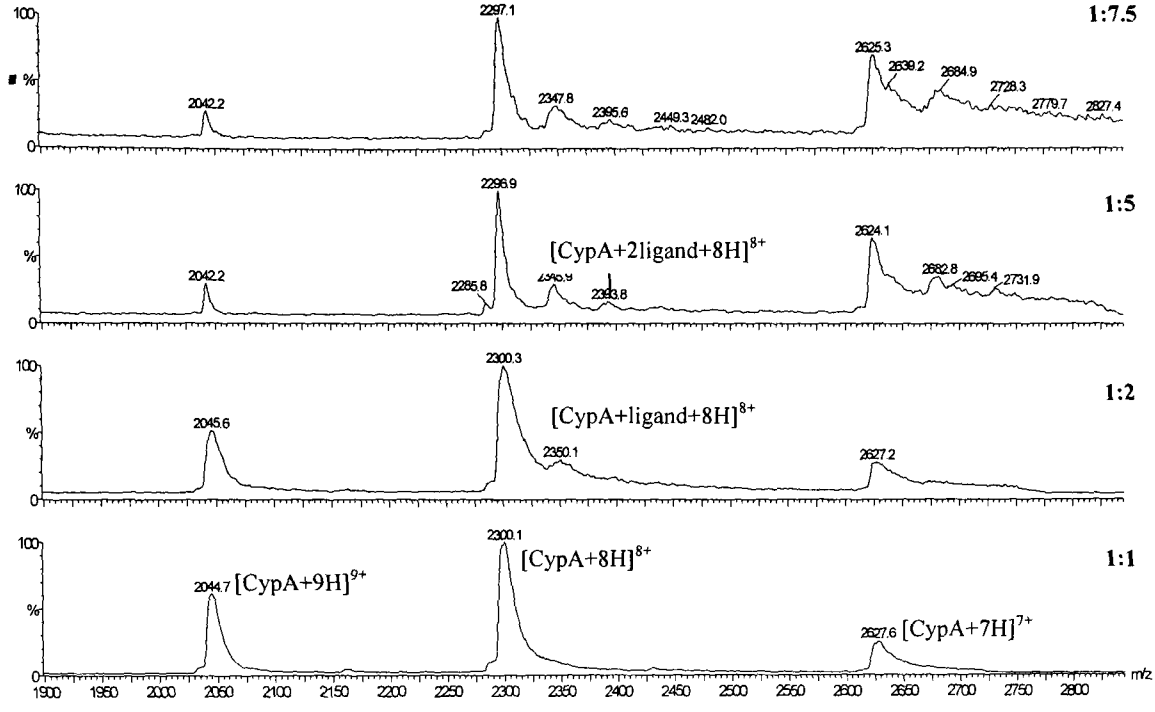

Figure 3.11: Mass spectra of CypA:**62** at varying concentrations, 30 min incubation.

Inspection of the spectra in figure 3.11 shows that the CypA:ligand complex is initially detected in the presence of excess ligand at a ratio of 1:2. This contrasts with the CypA:CsA complex which gave a strong complex peak at a ratio of 1:1, reflecting the stronger binding affinity of CsA compared to the synthetic ligand **62**. Increasing the concentration to a 1:5 protein:ligand ratio resulted in an increased peak intensity at the m/z corresponding to $[CypA+ligand+8H]^{8+}$ and also gave a small peak for the two ligand complex. Further increasing the concentration to 150 μM to give a 1:7.5 ratio did not lead to an increased peak size for the complex. Indeed, it was found that the signal to noise ratio was reduced at the higher ligand concentration, and ligand solubility in the 10 % methanol/ammonium acetate buffer solution became problematic at this concentration. As the best results were seen at the 1:5 CypA:ligand ratio it was decided to use this concentration as the standard for future ligand screening.

With a standard ligand concentration set, it was then necessary to investigate the effect of incubation time upon ligand binding. Ligand **62** was incubated with CypA

in a 10 % methanol/ammonium acetate buffer at pH 6.8 and left standing at room temperature for 30 minutes, 3 hours and overnight followed by analysis by ESI-MS using the standard MS conditions used previously (Figure 3.12).

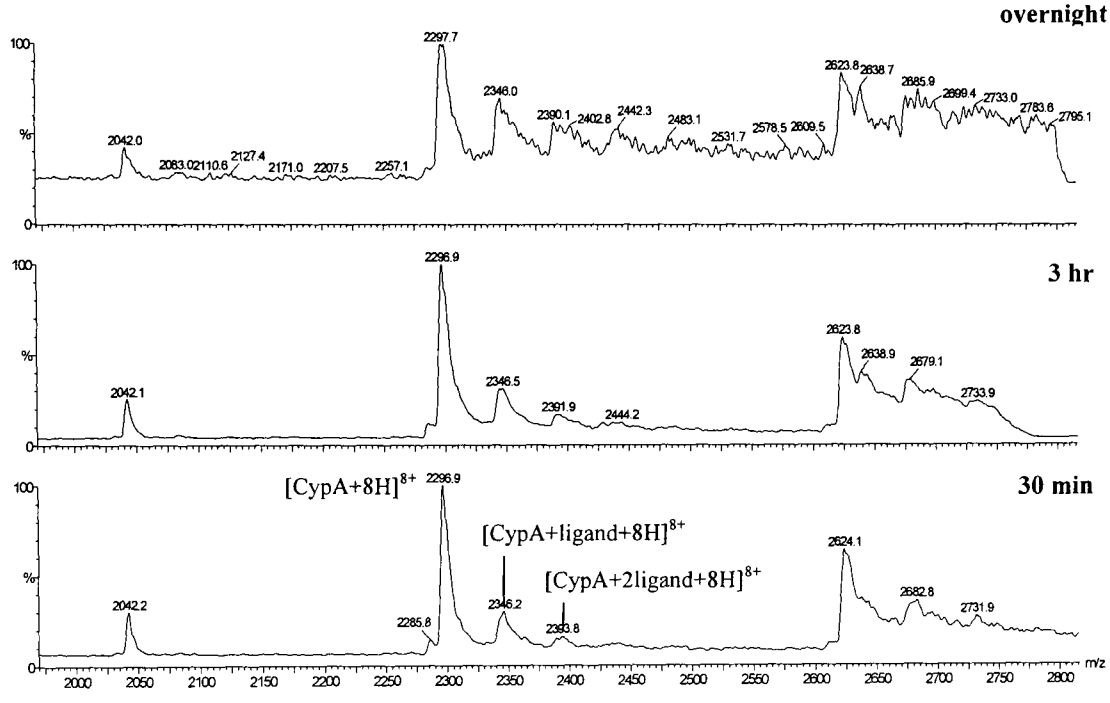

Figure 3.12: Effect of incubation time upon ligand binding for CypA:**62** at a 1:5 ratio.

Analysis by ESI-MS showed that there was no significant difference in the spectra between the sample incubated for 30 minutes or 3 hours, both showed clear peaks at the m/z corresponding to one and two ligand:CypA complexes. This finding was seen as beneficial to the prospect of screening multiple ligands as the incubation time would vary according to the ligand screening order. An overnight incubation period resulted in degradation of the protein:ligand peak and led to an increase in the background noise of the spectrum.

The mass spectrometry experiments outlined above were used to define a set of standard experimental conditions that would be used for the screening of other synthetic ligands. It was decided to screen the ligands at a ratio of 1:5 CypA:ligand, with an incubation time between 30 minutes and 3 hours. Although the use of standard conditions would not allow for the optimisation of the experiment

parameters for every ligand, it would allow for a higher throughput of ligands and suited the needs of an initial screen. To investigate the suitability of the standard conditions to the testing of other synthetic ligands, ligands **82** and **83** were screened (Figure 3.13).

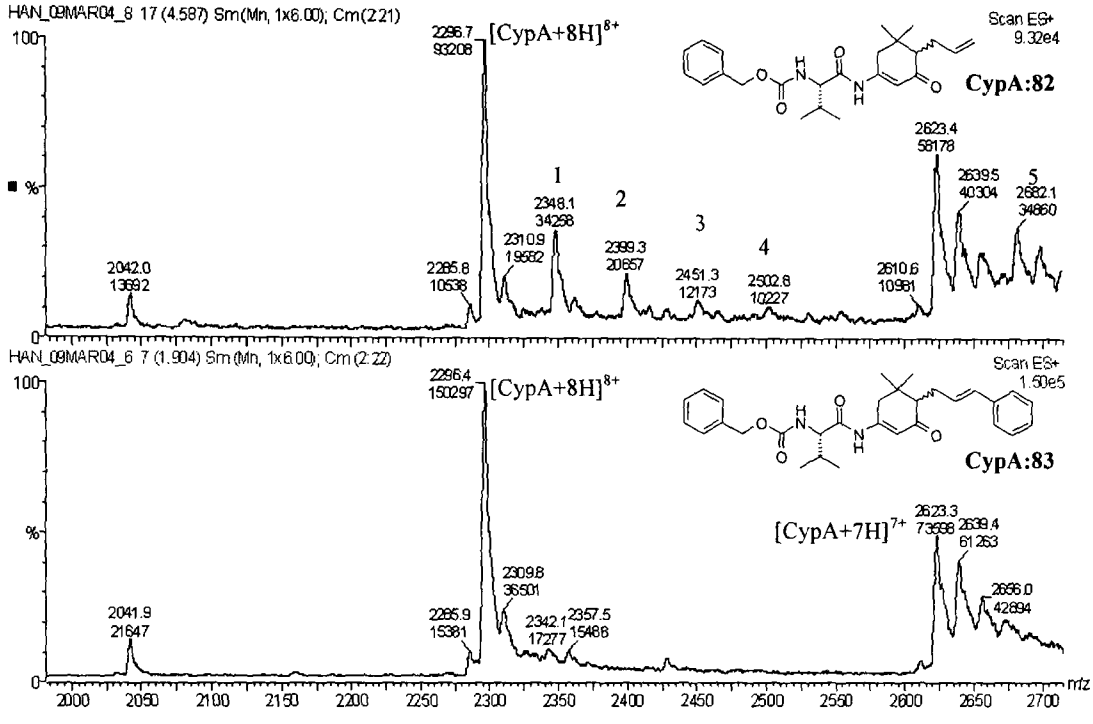

Figure 3.13: Mass spectra for CypA-ligand complexes for ligands **82** and **83**, 30 min incubation. Peaks 1, 2, 3 & 4 correspond to [CypA+ x ligand+8H]$^{8+}$, peak 5 corresponds to [CypA+ligand+7H]$^{7+}$.

Ligand **82** gave the most positive synthetic ligand result so far when screened against CypA under the standard ESI-MS conditions. It was found that the ligand produced a strong ligand:CypA complex peak at the +8 charge state, and interestingly peaks corresponding to two, three and four ligand:CypA^{8+} complexes were also observed. Ligand **82** is more lipophilic compared to ligand **62** due to the extra allyl group, possibly resulting in decreased solubility in the methanol/ammonium acetate buffer solution with subsequent micelle formation and ligand aggregation. As with the previous two CsA:CypA complex, it is not clear whether a ligand aggregate is binding to the active site, or just one ligand binds and the other complex peaks are due to non-specific binding. A peak was also detected for a [CypA+ligand+7H]$^{7+}$ complex. Ligand **83** did not give a signal for any protein:ligand complexes. As

outlined in Chapter 2.6.1, molecular modelling suggested that the cinnamyl moiety does not fit into the hydrophobic cavity occupied by the dimedone core, resulting in the ligand being too sterically demanding to bind in the CypA active site.

It is worth noting that both ligand **82** and **83** were screened against CypA as a 1:1 mixture of both diastereomers. The molecular modelling in Chapter 2.6.1 predicted that the *S*-diastereomer of ligand **82** would preferentially bind to CypA due to possible steric clashing of the *R*-diasteromer C-6 allyl moiety with the active site. Although both ligand **82** diastereomers were separated by using a HPLC fitted with a chiral column, unfortunately the control experiment of screening both diastereomers independently against CypA was not carried out due to time constraints.

3.5.3 Measuring dissociation constants by mass spectrometry

The binding affinity between a protein and a ligand can be measured in terms of the association constant, K_a, or the dissociation constant K_d. The association constant is the measure of the extent of the reversible association between a protein (P) and a ligand (L) at equilibrium (Equation 3.1).[24]

$$P + L \underset{}{\overset{K_a}{\rightleftharpoons}} PL \qquad \text{therefore} \qquad K_a = \frac{[PL]}{[P]\,[L]}$$

Equation 3.1: Association constant.

The association constant is measured in the units of concentration^{-1}, therefore the reciprocal dissociation constant is more often used, the units being quoted in terms of concentration (equation 3.2).

$$PL \underset{}{\overset{K_d}{\rightleftharpoons}} P + L \qquad \text{therefore} \qquad K_d = \frac{[P]\,[L]}{[PL]}$$

Equation 3.2: Dissociation constant.

The dissociation constant is a useful way of describing the affinity of a ligand for a protein, for when the concentration of ligand equals that of the K_d then half of the ligand receptors will be occupied at equilibrium. Thus if the ligand has a high affinity for the protein the K_d will be low, as it will take a low concentration of ligand to bind half the receptors.

The dissociation constants for the one and two ligand:CypA complexes were calculated separately from the mass spectra peak intensities using Equation 3.3:

$$K_d = \frac{[P]\,[L]}{[PL]} = \frac{[P]\,([L_i] - [PL])}{[PL]}$$

[P] represents the peak area for the +8 charge state of free CypA
[L] represents the peak area of the free ligand
[PL] represents the peak area for the +8 charge state of the CypA:ligand complex
$[L_i]$ is the initial concentration of ligand

Equation 3.3: Equation used to calculate mass spectrometry derived K_d values.[25]

It was possible to substitute the mass spectrometry peak areas for concentrations in Equation 3.3 based on the fact that the total protein concentration used, $[P_{total}]$, is known. For a protein with one binding site, such as CypA, $[P_{total}]$ is equal to the sum of both [P] and [PL] peak areas.[25] Thus, the peak areas can be converted to concentration units using Equations 3.4:

$$[P] = \frac{P}{P_{total}\,[P_{init}]}$$

$$[PL] = \frac{PL}{P_{total}\,[P_{init}]}$$

P is the free CypA peak area

PL is the CypA:ligand peak area

P_{total} is the free and complexed CypA peak areas

$[P_{init}]$ is the initial CypA concentration

Equations 3.4: Equations relating mass spectrometry peak areas to concentrations.[7]

Equations 3.3 and 3.4 were used to calculate the K_d values for ligands **62** and **82** and CsA (Table 3.2). The ratio of CypA to ligand was varied in order to calculate K_d values at differing concentrations, and the experiments using the synthetic ligands were repeated at least twice to investigate the reproducibility of the results.

Ligand	CypA:Ligand	K_{d1} μM	K_{d2} μM
62	1:1	94 75	- -
	1:2	31 101	- -
	1:5	39 46	69 79
	1:7.5	40 35	178 110
82	1:1	291 222	- -
	1:5	74 34 39	55 85 46
	1:10	27 36	22 10
CsA	1:1	11	37
	1:2	1	7

Table 3.2: K_d values calculated for **62**, **82** and CsA at various ratios against 20 μM CypA. K_{d1} refers to the one ligand:CypA complex, K_{d2} refers to the two ligand complex.[26]

It is clear from looking at the data in Table 3.2 that the measurement of K_d values by ESI-MS is not without its limitations. There was a certain amount of variability between repeated experiments, albeit with exceptions. Also, the calculated K_d values for CsA are significantly higher than the reported K_d value of 46 nM.[27] It was found that an increase in the concentration of ligand led to a decreased K_{d1} value, implying a greater degree of binding. This was to be expected as an increased ratio of ligand to protein would improve the binding probability, thus decrease the binding constant. This trend was also mirrored in the K_{d2} values, with the exception of ligand **62**, where the increased concentration gave higher K_{d2} values.

3.5.4 High throughput ligand screening

The ultimate aim of the mass spectrometry research in this project was to develop a high throughput system that could be used as the primary ligand screen. Ideally, this would involve a minimum of manual intervention, and would be capable of screening ligands multiple times to ensure the results are statistically reproducible. To fulfil these requirements a Waters 2700 auto-sampler was coupled *via* a Waters 600 HPLC pump to the ZMD mass spectrometer.[18] However, this particular apparatus is primarily a preparative mass directed HPLC purification system, designed for larger injection volumes and flow rates than those used for the previous mass spectrometry screening. At smaller volumes the aspiration of sample by the injection needle was found to be inaccurate, so all injection volumes were regulated by using a 50 μl sample loop.

As the previous experimental conditions had been optimised and had already produced CypA:ligand complex peaks, the conditions in Table 3.1 were maintained. With any high throughput system it is important to limit any residual sample carry over between runs as this could led to contamination of subsequent ligand screening results. To avoid this, a solvent gradient was used that incorporated an organic solvent flush to remove any residual sample (Table 3.3). The solvent dead volume in the interface tubing accounted for 2 minutes of the solvent run; at this point the

solvent flow was switched to the organic mobile phase for a period, then conditions were re-equilibrated back to the aqueous phase ready for the next sample.

Time (minutes)	10mM ammonium acetate / 10% methanol (%)	95% methanol / 5% water (%)
0	100	0
2.0	100	0
2.5	0	100
4.0	0	100
5.0	100	0
6.0	100	0

Table 3.3: Solvent gradient conditions for high throughput analysis.

The ligand dissociation values were calculated in a slightly different manner to the previous values in Table 3.2. It was decided to use deconvoluted mass spectrometry data in which the spectrum is converted from the multiply-charged spectra into the overall masses of protein and ligand. The purpose of the high throughput screen was to give a relative binding affinity for the ligands tested; therefore it was decided to sum the CypA:ligand peak areas and to calculate the K_d values using Equation 3.5:

$$K_d = \frac{[P]\,([L_i] - [PL_1+PL_2+PL_3....])}{[PL_1+PL_2+PL_3....]}$$

PL_n represents the peak area for the CypA:(ligand x n) complex

Equation 3.5: Equation used to calculate the Kd values for the high throughput screen.

The high throughput system was used to successfully screen a selection of ligands, with a throughput of around 9 ligands an hour. The ligands were then ranked according to their calculated relative dissociation constants (Table 3.4).

Ranking	Ligand	Structure	K_d μM
1	**82**	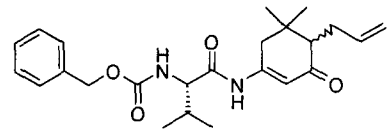	102
2	**62**	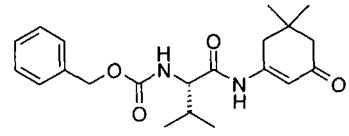	127
3	**111**	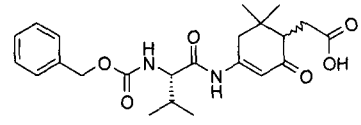	137
4	**89**	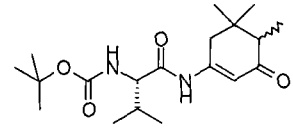	159
5	**97**	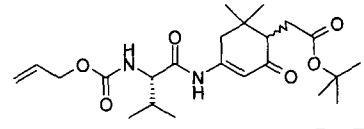	196
6	**112**	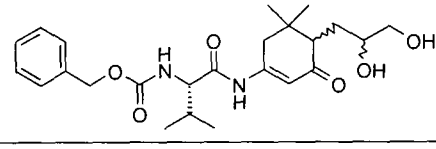	243
7	**96**	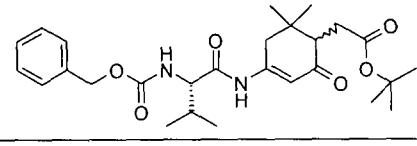	244
8	**30**	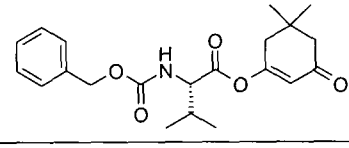	260*
9	**87**	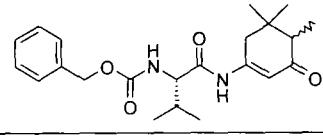	341
10	**84**	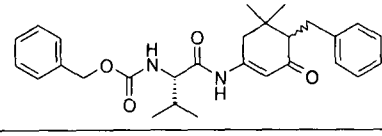	389
11	**64**	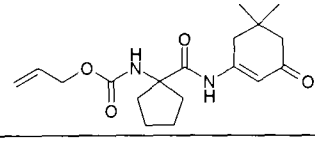	403

12	**117**	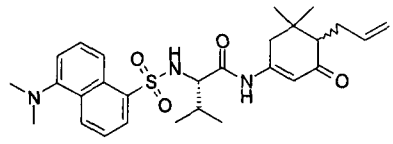	434
13	**116**	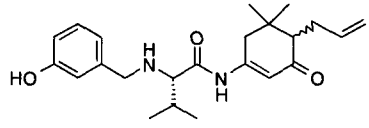	452
14	**91**	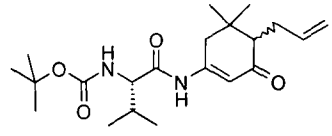	520
15	**98**	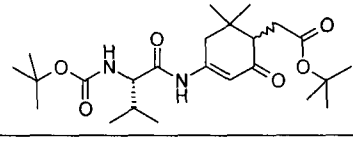	545

Table 3.4: Calculated K_d values for various ligands using data collected by high throughput analysis using the Waters ZMD system. All incubations were between 30 – 90 minutes, using a 1:5 ratio of CypA (20μM):Ligand (100μM). * Ligand fragmentation was observed in the mass spectrum.

Ranking the ligands in order of dissociation constants revealed that ligand **82** had the highest binding affinity, with a K_d value slightly larger than the values previously calculated and shown in Table 3.2. The structurally similar ligand **62** and the hydrophilic ligand **111** also ranked highly, both with dissociation constants below 150 μM. It is difficult to determine any relationships between ligand structure and the corresponding K_d value for the remaining ligands, for example ligand **87** varies from ligand **62** by just an extra methyl group at C-6 on the dimedone ring, yet was found to have a Kd value almost three times higher. However, it is worth noting that the technique was not intended to elucidate trends in activity but to function as a primary ligand screen, and was found to be well suited to this role.

3.6 Conclusions

The initial mass spectrometry research outlined in this chapter focussed upon the analysis of CypA alone, followed by the successful characterisation of CypA:CsA complexes by ESI-MS. Although this data may appear unconnected to the screening

of small molecule ligands, it was necessary in order to optimise experimental conditions and acted as a proof of principle introduction to the detection of CypA:ligand complexes in the gas phase. Tandem MS/MS analysis of the CypA:CsA complex revealed that although two CsA:CypA complexes were observed under screening conditions, the ligand affinity for the protein is different, with one of the ligands more weakly bound than the other.

It has also been demonstrated that electrospray mass spectrometry is able to identify CypA:synthetic ligands complexes using a standard set of experimental conditions. The successful detection of CypA complexes with ligands **62** and **82** led to the mass spectrometry derived dissociation constant being determined, giving a method of quantifying the observed interactions with the protein. Once the binding of a ligand to CypA could be quantified, it allowed different ligands to be directly compared to each other, thus forming the basis of a screen. The goal of a functional high throughput screen using ESI-MS was achieved through the use of HPLC auto-sampler, and by using Equation 3.5 the dissociation constants of the screened ligands could be determined.

After ranking the ligands in terms of their calculated dissociation constants, it was decided to focus primarily on further biological screening of the top three ligands, ligands **82**, **62** and **111**. These results are outlined in Chapter 4.

References

(1) C. M. Whitehouse, R. N. Dreyer, M. Yamashita, J. B. Fenn, *Anal. Chem.*, **1985**, *57*, 675.

(2) Barran research group members involved were Hannah Florance, Dr. Sally Shirran and Dr. Perdita Barran, School of Chemistry, University of Edinburgh.

(3) M. Barber, R. S. Bordoli, R. D. Sedgewick, A. N. Tyler, *J. Chem. Soc. Chem. Commum.*, **1981**, 325.

(4) M. Karas, D. Bachmann, U. Bahr, F. Hillenkamp, *Int. J. Mass Spectrom. Ion. Process.*, **1987**, *78*, 53.

(5) M. Dole, L. L. Mack, R. L. Hines, R. C. Mobley, L. D. Ferguson, M. B. Alice, *J. Chem. Phys.*, **1968**, *49*, 2240.

(6) J. V. Iribarne, B.A. Thomson, *J. Chem. Phys.*, **1976**, *64*, 2287.

(7) H. Florance, *The Analysis of Protein – Ligand Complexes by High Throughput Mass Spectrometry*, 1st Year PhD report, University of Edinburgh, **2004**.

(8) R. B. Cole, *J. Mass Spectrom.*, **2000**, *35*, 763.

(9) J. Fernandez de la Mora, *Anal. Chim. Acta*, **2000**, *406*, 93.

(10) G. Suizdak, *Mass Spectrometry for Biotechnology*, Academic Press, New York, **1996**.

(11) W. Paul, *Angew. Chem. Int. Ed. Engl.*, **1990**, *29*, 739.

(12) W. C. Wiley, I. H. McLaren, *Rev. Sci. Instr.*, **1955**, *26*, 1150.

(13) S. L. Shirran, *Maintaining and Analysing Protein Complexes in the Gas Phase by Electrospray Ionisation Mass Spectrometry*, PhD Thesis, University of Edinburgh, 2005.

(14) B. Ganem, Y-T Li, J. D. Henion, *J. Am. Chem. Soc.*, **1991**, *113*, 6294.

(15) J. B. Fenn, M. Mann, C. K. Meng, S.F. Wong, C. M. Whitehouse, *Science*, **1989**, *246*, 64.

(16) R. D. Smith, K. J. Light-Wahl, *Biol. Mass Spectrom.*, **1993**, *22*, 493.

(17) X. Cheng, R. Chen, J. E. Bruce, B. L. Schwartz, G. A. Anderson, S. A. Hofstadler, D. C. Gale, R. D. Smith, *J. Am. Chem. Soc.*, **1995**, *117*, 8859.

(18) R. H. Griffey, K. A. Sannes-Lowery, J. J. Drader, V. Mohan, E. E. Swayze, S. A. Hofstadler, *J. Am. Chem. Soc.*, **2000**, *122*, 9933.

(19) S. A. Hofstadler, K. A. Sannes-Lowery, S. T. Crooke, D. J. Ecker, H. Sasmor, S. Manalili, R. H. Griffey, *Anal. Chem.*, **1999**, *71*, 3436.

(20) E. E. Swayze, E. A. Jefferson, K. A. Sannes-Lowery, L. B. Blyn, L. M. Risen, S. Arakawa, S. A. Osgood, S. A. Hofstadler, R. H. Griffey, *J. Med. Chem.*, **2002**, *45*, 3816.

(21) D. A. Ockey, J. L. Dotson, M. E. Struble, J. T. Stults, J. H. Bourell, K. R. Clark, T. R. Gadek, *Bioorg. Med. Chem.*, **2004**, *12*, 37.

(22) J. A. Loo, *Int. J. Mass Spectrom.*, **2000**, *200*, 175.

(23) Waters UK Ltd, 730-740 Centennial Court, Centennial Park, Elstree, Hertofordshire, WD6 3SZ.

(24) T. E. Greighton, , *Proteins: Structures and Molecular Properties*, W. H. Freeman, 1992.

(25) S. Zhang, C. K. Van Pelt, D. B. Wilson, *Anal. Chem.*, **2003**, *75*, 3010.

(26) H. Florance, P. Barran, *unpublished results.*

(27) J. Liu, M. W. Albers, C. M. Chen, S. L. Schreiber, C. T. Walsh, *Proc. Natl. Acad. Sci. U.S.A.*, **1990**, *87*, 2304.

4. Results and Discussion III– Biological Assays

4.1 Introduction

The mass spectrometry screening technique outlined in Chapter 3 provided a useful method of measuring the relative ligand binding affinities. Through ranking the ligands in terms of their calculated dissociation constants an order of binding could be determined, promising ligands were then subject to further testing. *In vitro* fluorescence and PPIase assays were carried out in collaboration with the Walkinshaw research group at the University of Edinburgh,[1] and *in vivo* testing against the nematode worm *Caenorhabditis elegans* was carried out by Dr. Tony Page at the University of Glasgow.[2]

4.2 Intrinsic fluorescence binding assay

All proteins are fluorescent in the ultraviolet region due to the presence of three aromatic amino acids in their structures: phenylalanine, tyrosine and tryptophan.[3] Of these, tryptophan dominates the fluorescence with a higher quantum yield than the other amino acids. Fluorescence spectroscopy can be used to detect interactions between proteins and ligands, provided that the optical properties of the protein-ligand complex differ from those of free ligand and free protein.

CypA has a single tryptophan residue (Trp121) located about 8 Å from the centre of the substrate proline binding pocket of the active site. The structure of CypA-CsA complex shows a strong H-bonded interaction between Trp121 and the carbonyl oxygen of MeLeu9 in CsA.[4] In addition to this interaction contributing to the binding affinity and specificity of CsA for CypA, it accounts for the spectra changes in the fluorescence of Trp121 observed upon complex formation.[5] Binding of CsA produces an enhancement and roughly an 8 nm blue shift in the emission maxima, from 350 to 342 nm. This perturbation of the fluorescence spectra upon immunophilin binding has been used to estimate the dissociation constant between

various CsA derivatives and CypA,[6] and was used to calculate the dissociation constant of synthetic ligands highlighted by the mass spectrometry binding screen. The assay depends on ligands binding close enough to Trp121 (within 5 – 6 Å) to alter the polar environment around the residue and cause specific and saturable changes in the intrinsic tryptophan fluorescence, either through enhancement or quenching.

4.2.1 Experimental methods

Fluorescence emission spectra for CypA were obtained on a PTI Quantmaster™ spectrofluorometer,[7] using a 160 µl cuvette at 25°C. Tryptophan fluorescence was excited at 295 nm (5 nm band pass), and emission was scanned from 310 to 430 nm (5 nm band pass). CypA (0.3 µM) was incubated in the absence or presence of increasing amounts of either CsA or synthetic ligand in 25 mM tris (hydroxymethyl) aminomethane buffer, pH 7.5; 100 mM NaCl; 1 % ethanol; 1 mM NaN_3, for 60 minutes at 25°C, and the emission spectra measured. Each spectrum was obtained from a separate incubation mixture, not sequential additions of ligand to the same sample of CypA. Any change in the fluorescence signal was assumed to be proportional to the concentration of CypA-ligand complex. The observed fluorescence was buffer background subtracted, and corrected for dilution and inner filter effects by Equation 4.1.[8]

Equation 4.1:
$$f_{corr} = \{(vol_0+vol_{add}/vol_0) \times f_{obs}\} / e^{(-2.303 \times \varepsilon 295nm \times L \times [Lig])}$$

Where f_{corr} is the corrected fluorescence signal, f_{obs} is the observed fluorescence signal, ε_{295nm} is the ligand extinction co-efficient at 295 nm, L is the path length (0.5 cm) and [Lig] is the molar ligand concentration. The corrected fluorescence signal, f_{corr} (in arbitrary units), upon complex formation can be defined by Equation 4.2.

Equation 4.2:
$$f_{corr} = f_f + (f_b - f_f)$$

Where f_f is the fluorescence of free uncomplexed CypA and f_b is the fluorescence of the CypA-ligand complex at infinite concentration of ligand.

The f_{corr} data was plotted *versus* the total concentration of ligand. At any total concentration of CypA [CypA], f depends on the total ligand concentration [Lig] and the dissociation equilibrium constant (K_d) for the complex according to Equation 4.3. The dissociation constants for the CypA-ligand complexes were determined by fitting the data to Equation 4.3 using Kaleidagraph v3.6 software.[9]

Equation 4.3:

$$f_{corr} = f_f + (f_b - f_f) \times \{(K_d + [CypA] + [Lig]) - \sqrt{((K_d + [CypA] + [Lig])^2 - (4 \times [CypA] \times [Lig]))} / 2 \times [Lig])\}$$

A representative graph of the fluorescence binding assay is shown in Figure 4.1.

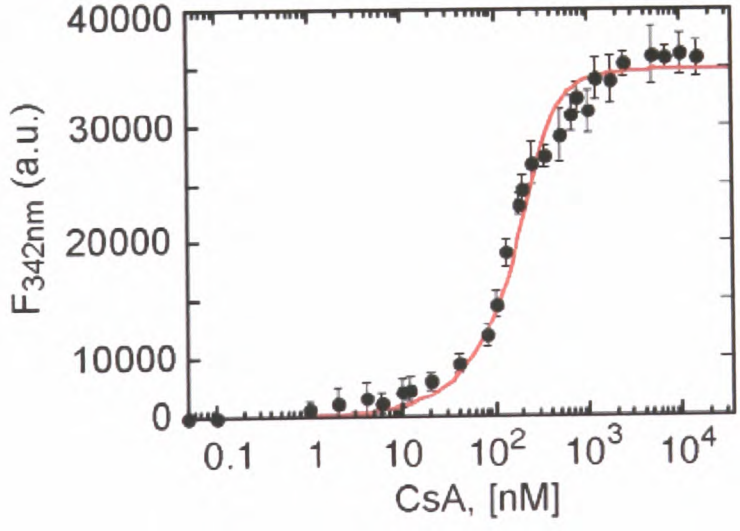

Figure 4.1: The fluorescent enhancement at 342 nm of 0.25 CypA (0.3 μM) plotted against concentration of CsA. Each point is the mean of three separate measurements ± standard error. The points were least squares fit to Equation 4.3, shown by the red line.[8]

4.2.2 Results and discussion

Table 4.1 shows the dissociation constants calculated by the fluorescent assay for the three top-ranking ligands as determined by the MS screen, ligands **62**, **82** and **111**. The K_d values of the enol-ester ligand **30** and fluorescent ligand **126** were also determined, with the K_d of CsA calculated in the same manner as a comparison.

Ligand	Structure	K_d – CypA (μM)	Remarks
1	Cyclosporin A	0.03 ± 0.01	Enhancement at λ_{em} max of 340 nm
30	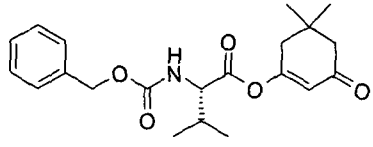	21.2 ± 10.0	Quenching at λ_{em} max of 346 nm
62	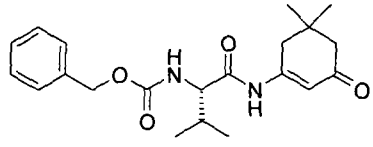	15.1 ± 8.8	Quenching at λ_{em} max of 346 nm
82	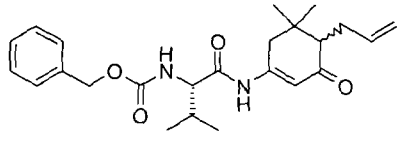	12.2 ± 9.2	Enhancement at λ_{em} max of 346 nm
111	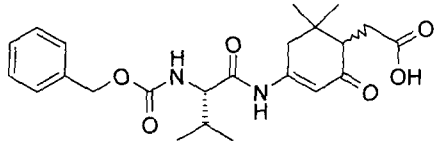	29.0 ± 21.3	Quenching at λ_{em} max of 346 nm
126	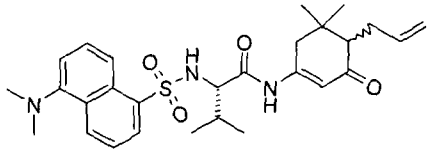	22*	Quenching at λ_{em} max of 348 nm

Table 4.1: Apparent K_d values of CsA and synthetic ligands for CypA *in vitro*. Each K_d value is the mean of three measurements ± standard error. * Assay complicated due to ligand fluorescence.

The intrinsic fluorescence binding assay revealed that whilst none of the synthetic ligands could compare to the binding affinity of CsA, ligands **62**, **82** and **111** were found to retain the same relative dissociation constant ranking as observed in the mass spectrometry screen. Ligand **62** had a lower K_d value than the original enol-

ester lead ligand **30**, a comparison of the two ligands using the mass spectrometry screen was limited by the fragmentation of enol-ester **30** under the ESI-MS conditions. The amide moiety in ligand **62** may exert an effect upon binding through reversal of the hydrogen bonding potential at this point on the ligand from acceptor to donor, and the increase in the planar rigidity of the ligand *via* resonance may also contribute to the lower K_d.

Ligand **82** was found to have the lowest K_d out of the ligands tested, suggesting that the extra allyl moiety has a positive effect upon ligand binding. This finding is not only consistent with the MS screening results, it also supports the molecular modelling outlined in Chapter 2.6.1; analysis of the modelling suggested that the allyl group may have a positive effect on binding affinity through a possible hydrophobic interaction with Leu122. Interestingly, ligand **82** gave an enhancement of fluorescence upon screening, whereas the other small molecule ligands quenched the fluorescence. The allyl group of ligand **82** may potentially displace a water molecule from the vicinity of the Trp121 upon ligand binding. Tryptophan fluorescence is known to be susceptible to quenching by water,[10] thus fluorescent enhancement may be a result of the increased hydrophobic environment upon ligand binding. Although both diastereomers of ligand **82** were also screened separately, the results were inconclusive due to problems with the solubility of the batch of CypA used for the assays. Unfortunately these assays were not repeated due to time constraints. The hydrophilic ligand **111** was found to have a larger K_d than ligand **82**, again suggesting that the allyl moiety of ligand **82** is involved in a positive hydrophobic interaction with the CypA active site.

Upon screening ligand **126** it was found that the assay was complicated by ligand auto-fluorescence. The dansyl fluorophore has an emission wavelength of ca. 340 nm, the same region as the CypA fluorescence emission. Although an attempt was made to correct the dissociation constant value for ligand **126** due to this auto-fluorescence, it was decided to use the fluorescence assay as an indication of ligand **126** binding, rather than a quantitative figure.

The main limitation with the intrinsic fluorescence assay results was the large amount of variation between the calculated K_d values upon repetition of each ligand, reflected in the large error margins shown in Table 4.1. The variation was largely related to slight differences in the solubility of ligand and the particular batch of CypA used for each repeat. As a consequence of this variation it is difficult to ascertain any conclusive structure activity relationships for the ligands, but nonetheless the assay served as a useful guide to the binding of ligands to CypA and helped to corroborate the finding of the mass spectrometry screen.

4.3 Peptidyl-prolyl *cis-trans* isomerase (PPIase) assay

The peptidyl-prolyl isomerase activity of CypA can be monitored *in vitro* through the measurement of an α-chymotrypsin-coupled cleavage of a synthetic peptide substrate.[11] The substrate used was Suc-Ala-Ala-Pro-Phe-pNa, which exists in equilibrium between the *cis* and *trans* forms. α-Chymotrypsin selectively cleaves the *C*-terminal 4-nitroaniline group only if the Ala-Pro bond is in the *trans* form (Figure 4.2). This isomer-specific cleavage can be monitored by measuring the absorbance of the released 4-nitroaniline chromophore at 400 nm as a function of time. CypA catalyses the *cis-trans* isomerisation of the peptide substrate resulting in the release of 4-nitroaniline, the pre-existing *trans* peptide is cleaved within the assay deadtime, so this cleavage does not contribute to the assay results. Any inhibition of the PPIase activity of CypA through competitive ligand binding would retard the rate of 4-nitroanilide cleavage and thus be detected by the assay.

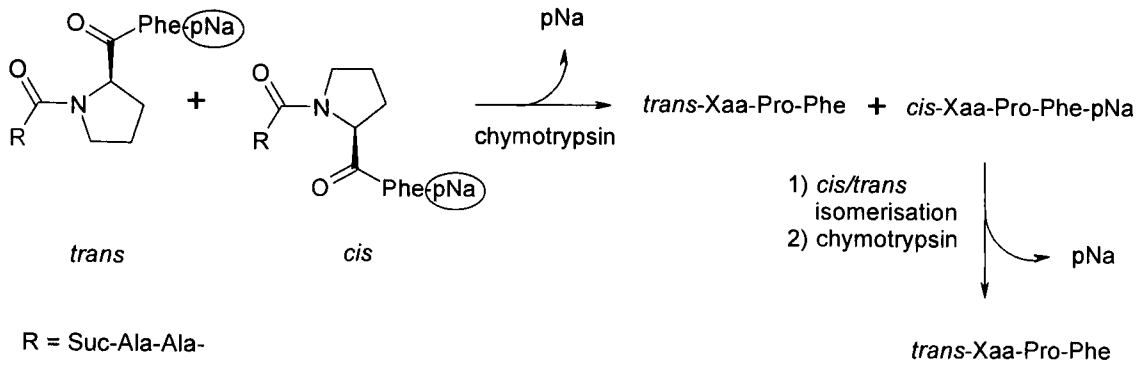

Figure 4.2: Mechanism of the assay to monitor peptidyl-prolyl *cis-trans* isomerisation based upon isomer-specific proteolysis.[12]

One limitation of this assay is that only one direction of the reversible isomerisation, from *cis* to *trans*, can be followed. In standard aqueous conditions only 10 % of the peptidyl-prolyl bonds are in the energetically unfavourable *cis* conformation, resulting in a poor assay signal-to-noise ratio. Kofron *et al.*, found that the use of lithium chloride in trifluoroethanol (TFE) as a co-solvent perturbed the *cis/trans* equilibria in favour of *cis* from 10 % up to 70 %.[13] This significantly improved the signal-to-noise ratio and thus the sensitivity of the PPIase assay.

4.3.1 Experimental methods

The synthetic peptide substrate was initially suspended in a solution of LiCl/TFE (0.02 mg/ml). CypA (10 nM) was incubated with varying concentrations of inhibitor (typically a range of 10 to 100 μM of synthetic ligands, nM range for Cyclosporin A) in a HEPES/NaCl buffer and organic solvent solution. The mix was transferred to a plastic cuvette, and the reaction initiated by addition of chymotrypsin (23 nM), followed by 120 μM peptide substrate to make a final reaction volume of 1 ml. The reaction was rapidly mixed, and the change in absorbance at 400 nm was measured over a 2 minute period after addition of chymotrypsin and substrate. Measurements were taken every 0.1 seconds using a Perkin Elmer Lambda 20 spectrophotometer fitted with a thermostatted Peltier cell holder,[14] which cools the reaction to 4 °C to limit thermal isomerisation of the peptide substrate. The initial rate for each condition at a set concentration of substrate was then calculated. A plot of the rate of

enzymatic isomerisation against ligand concentration was used to determine the total concentration of ligand at which 50 % inhibition occurred, the IC_{50} value (Figure 4.2). The calculation assumes that the rate of *cis* to *trans* isomerisation is directly comparable to the rate of 4-nitroaniline release.

4.3.2 Results and discussion

Table 4.2 shows the IC_{50} values calculated by the PPIase assay for ligands **62**, **82**, and **111**, with comparisons made to the CsA (**1**), dimedone (**29**) and ligand **30** IC_{50} values calculated in the same manner.

Ligand	Structure	IC50 (μM)	Solubility	Solvent
1	Cyclosporin A	0.009	Good	EtOH
29	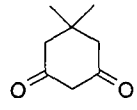	22,000	Fair	MeOH
30	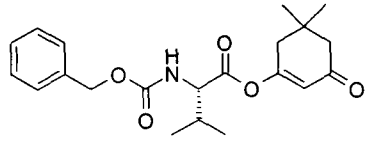	26	Fair	MeOH
62	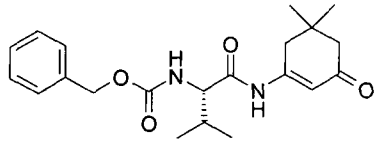	-	Poor	MeOH/DMSO
82	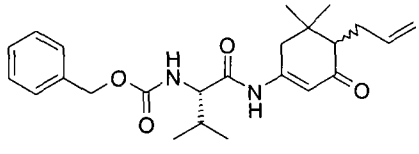	22	Fair	DMSO
111	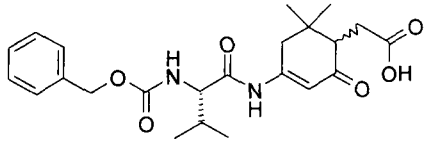	21	Fair	DMSO

Table 4.2: IC_{50} values of CsA and synthetic ligands for CypA *in vitro*.

Unlike the previous ESI-MS screen and intrinsic fluorescence assay, the PPIase

assay results outlined in Table 4.2 show that ligands **30**, **82** and **111** all have similar activity towards CypA; all three ligands have IC_{50} values in the low- to mid- 20s μM range. These figures represent a marked improvement over the original lead compound dimedone that had an IC_{50} of 22mM, but again the activity of the synthetic ligands trails behind that of CsA; the calculated IC_{50} of 9 nM closely matches the published figure of 6 nM.[15]

The main restriction in the use of the PPIase assay was the limited solubility of the synthetic ligands in the solvent conditions required for the assay. Ligand insolubility often resulted in an increase in absorbance at ca. 400 nm due to the ligand precipitating out of solution during the assay, this was a particular problem when methanol was used as solvent, and ligand **62** was unable to be assayed due to poor solubility. DMSO was used to dissolve ligand **82** and **111** successfully, but its use resulted in other complications. Previous work within the group has shown that DMSO actually binds to CypA, the X-ray crystal structure showing one molecule located in the proline binding pocket.[16] The use of DMSO as solvent may have resulted in competitive binding between solvent and ligand, thus affecting the assay results.

4.4 *In vivo* activity assay

Five of the diseases currently in the Tropical Diseases Research Programme (TDR) of the World Health Organisation (WHO) portfolio are caused by parasites. Malaria, leishmaniasis, trypanosomiasis, schistosomiasis and filariasis, along with other human diseases caused by protozoans and helminths, present intractable problems of control,[17] disproportionally affecting poor and marginalised populations. Many anti-parasitic drugs currently in use suffer from serious deficiencies, especially those of toxicity and resistance, so the development of new approaches for treating and controlling such infectious diseases remains an important medicinal area. The unexpected finding that cyclosporin A showed promising anti-parasitic activity has prompted the drug to be used in seminal research into parasitic infections.[17] Whilst it

is unlikely that CsA could ever be used clinically to control parasites due to its immunosuppressive properties and toxicity, non-immunosuppressive CsA analogues or synthetic small molecule mimics may potentially lead to novel anti-parasitic therapies.

Caenorhabditis elegans, a free-living nematode worm, has been used extensively as a model for studying nematode parasites as well as higher eukaryotes. It is multi-tissue organism that is not only genetically tractable, but is easily and quickly cultured in liquid media and has a relatively rapid reproductive life cycle, of the order of 24 hours. *C. elegans* expresses 18 cyclophilin isoforms, the greatest number of isoforms described in a single species.[18] These multiple isoforms of cyclophilin appear to play important roles in reproduction and larval development, body-wall muscle formation and in the proper folding and processing of proteins, for example the collagens involved in the formation of the extra cellular matrix and cuticle.[19] Whilst the precise mechanism of the CsA anti-parasitic activity is yet to be elucidated, its interaction with parasite cyclophilin is suspected to be a key factor, thus making *C. elegans* an interesting *in vivo* model to investigate the anti-parasitic effects of CsA and synthetic ligands.

An *in vivo* screen was developed to examine the biological effects of CsA and the lead compound, ligand **82**, on *C. elegans*. The biological effects were assessed by several parameters. These included morphological and developmental abnormalities such as cuticle shedding defects and gut malformation, loss of motility, and loss of reproductive efficiency judged by counting larval numbers. Affected worms were then further analysed under light microscopy to allow a more detailed assessment of the observed defects.

Sexually mature worms were cultured at 25°C in liquid media, with OP50 *E. coli* as a food source, and exposed to varying doses of CsA and ligand **82**. Analyse took place over the course of five days to allow for several reproductive cycles. Compared to control conditions (Figure 4.3 A), worms exposed to ligand **82** had growth defects, the worms were shorter and "dumpier" in general (Figure 4.3 B), and showed

reduced motility. The worms treated with ligand **82** also had cuticle shedding defects similar to those observed in organisms treated with CsA (red arrows in Figure 4.3B & 4.3C, respectively). Furthermore, exposure to ligand **82** or CsA markedly affected the reproductive abilities of the worms, reflected in a reduction of larvae numbers, with an apparent IC_{50} of 190 μM for ligand **82** and 28 μM for CsA (Figure 4.3 D).

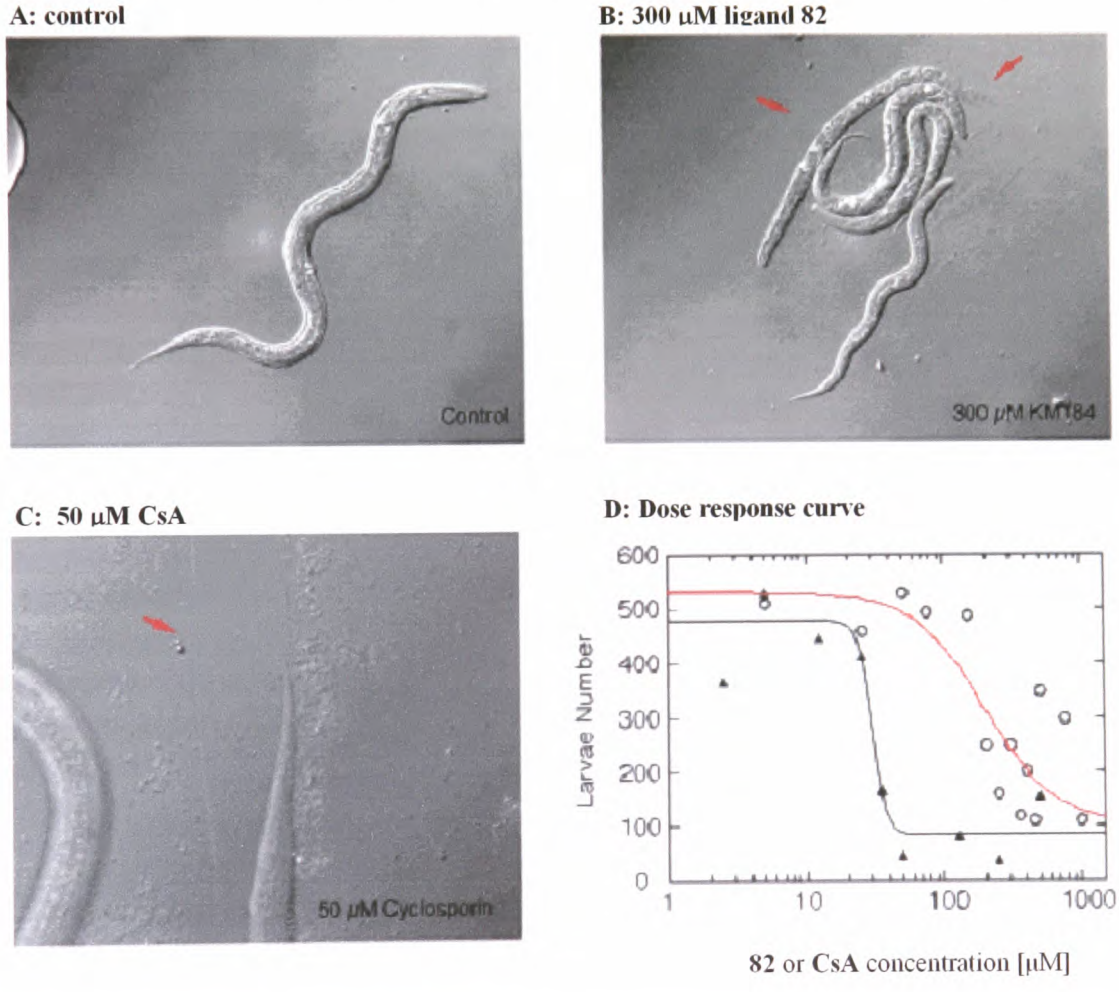

Figure 4.3: Representative light-micrographs of worms grown in the absence or presence of either **82** (300 μM) or CsA (50 μM) are shown in panels **(A)**, **(B)** and **(C)**, respectively. In **(B)** and **(C)**, the cuticle shedding defect, absent in **(A)**, is highlighted by red arrows. **(D)** Dose response curves for **82** (open circles) and CsA (closed triangles) after 48 hrs exposure. Each data point is the mean from three separate measurements. The IC_{50} values for **82** and CsA are 190±60 μM and 28±13 μM, respectively. Larvae numbers are plotted against the concentration of **82** or CsA in μM. The apparent IC_{50} values were derived by non-linear fitting of a standard four-parameter logistic model where the IC_{50} corresponds to a response halfway between the upper and lower asymptotes.

C. elegans were also exposed to the fluorescently labelled ligand **126** using the same *in vivo* screening conditions as previously. The worms were observed under light microscopy using a DAPI (4',6-diamidino-2-phenylindole) filter set. DAPI is a fluorescent marker normally used to visualise DNA and had a relatively broad emission spectra, allowing the filter sets to be used to visualise dansyl fluorescence (Figure 4.4).

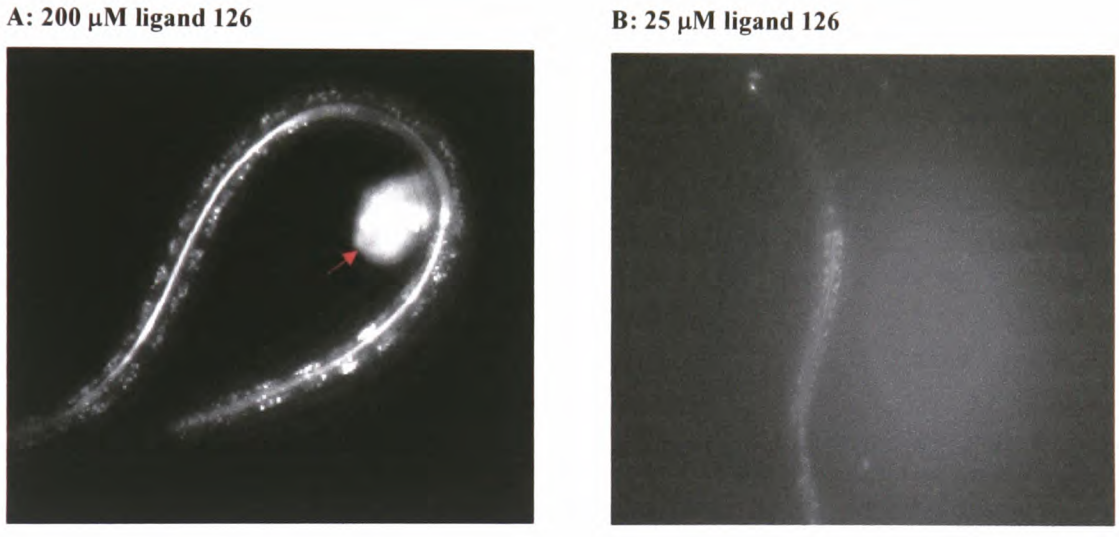

Figure 4.4: Representative light-micrographs of *C. elegans* nematodes grown in the presence of ligand **126** and observed through a fluorescence microscope using a DAPI filter set. At concentrations of ligand **126** between 50 - 200 μM (**A**) a very strong green fluorescence in pharyngeal gut lining was observed, with deep blue vesicles in the gut tissues. Exposure to UV caused these vesicles to lyse and turn the entire gut purple. Higher concentrations resulted in some ligand precipitating out of solution (red arrow, **A**). Lower concentrations of ligand **126** resulted in the ligand still being taken up but with less intense staining in the gut (**B**).

Visualisation of the fluorescent ligand **126** upon ingestion by the *C. elegans* worms revealed strong fluorescent staining of the gut lumen and surrounding tissues, as shown by the representative light-micrographs in Figure 4.4. Exposure to ligand **126** also resulted in the worms displaying the same phenotypic changes as seen with CsA and ligand **82**, namely stunted growth, loss of mobility, cuticle shedding defects and a reduction in fecundity. Unfortunately, it was not possible to visualise the exact localisation of ligand **126** in terms of organelle specificity as a higher magnification

microscope would be required. However, as the worms displayed the same phenotype upon exposure to CsA and both synthetic ligands, it is felt that ligand **126** did not merely stain the gut lumen of *C. elegans* as the ligand was ingested and excreted, but was being taken up into the same tissues and organelles as CsA and ligand **82**.

Whilst it is clear that ligands **82** and **126** display anti-nematode activity towards *C. elegans* due to the phenotypic changes outlined above, it can only be inferred that they act by inhibiting the function of nematode cyclophilins through circumstantial evidence. For instance, the cuticle shedding defect observed in ligand treated *C. elegans* may be due to the inhibition of cyclophilin and/or a related protein disulfide isomerase (PDI) enzyme.[20] Both enzymes are important catalysis of collagen folding and are expressed in the cuticle synthesising tissue, the hypodermis, and have peaks of expression corresponding to the moulting cycle.[21] As the enzymes play a key role in the folding of the structural proteins that form the nematode cuticle, the observed cuticle shedding defects strongly suggest an interaction of these proteins with the ligands. The staining of the gut lumen of *C. elegans* upon exposure to fluorescent ligand **126** also suggests an interaction with cyclophilin; the gut cell cytoplasm is known to be rich in cyclophilin-5, the structure of which closely resembles human cyclophilin B.[18]

4.5 Conclusions

The incorporation of an initial mass spectrometry screen, two different *in vitro* assays and *in vivo* testing into this project was found to be a success, and the process is represented schematically in Figure 4.5. After a period of optimisation and analysis of CypA and CypA:ligand complexes, electrospray ionisation mass spectrometry was developed into a moderately high throughput screening technique. Through calculation of the K_d values for the ligands a relative rank order of ligands could be compiled, allowing the most promising ligands to pass through the screen and into *in vitro* assays. The intrinsic fluorescence assay was found to concur with the ligand

ranking order from the mass spectrometry screen and although it was not as constructive as the fluorescent assay, the PPIase assay was still useful as it showed that the synthetic ligands tested had IC_{50} values 10^{-3} times that of the original lead compound, dimedone (**29**).

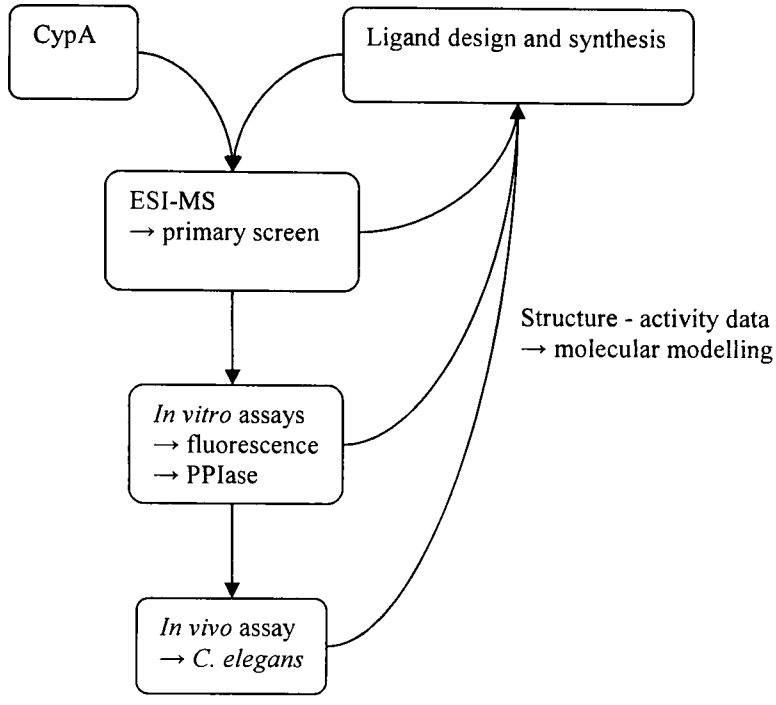

Figure 4.5: Schematic representation of the ligand synthesis and biological assay process.

The positive *in vivo* assay results were especially encouraging and added credence to the overall project approach. The fluorescent studies using ligand **126** demonstrated it was possible to synthesise fluorescent ligand derivatives that are taken up by the nematodes, and cause phenotypic changes concurrent with anti-nematode effects. Further development of this method, perhaps involving higher power microscopy and/or the use of an alternate fluorescent group, may allow the identification of specific cyclophilin-rich *C. elegans* organelles. Such an approach may be useful in identifying the location and function of the *C. elegans* multiple cyclophilin isoforms, and thus potentially assist in elucidating the role of cyclophilins in nematode development.

References

(1) Walkinshaw research group members involved were Alan Paterson, Dr. Martin Wear, Dr. Brian McHew and Prof. Malcolm Walkinshaw, Institute of Structural and Molecular Biology, University of Edinburgh.

(2) Dr. Tony Page, The Page Laboratory, The Anderson College, University of Glasgow.

(3) J. Galbán, Y. Andreu, J. F. Sierra, S. de Marcos, J. R. Castillo, *Luminescence*, **2001**, *16*, 199.

(4) J. Kallen, C. Spitzfaden, M. G. M. Zurini, G. Wilder, H. Widmer, K. Wüthrich, M. D. Walkinshaw, *Nature*, **1991**, *353*, 276.

(5) M. Gastmans, G. Volckaert, Y. Engelborghs, *Proteins*, **1999**, *35*, 464.

(6) H. Husi, M. G. M. Zurini, *Anal. Biochem.*, **1994**, *222*, 251.

(7) Photon Technology International, Unit M1 Rudford Industrial Estate, Ford Road, Ford, West Sussex, BN18 0BF.

(8) M. A. Wear, A. Patterson, K. Malone, C. Dunsmore, N. J. Turner, M. D. Walkinshaw, *Anal. Biochem.*, **2005**, *in press*

(9) Synergy Software, 2457 Perkiomen Avenue, Reading, PA 19606, USA.

(10) A. S. Ladokhin, *Encyclopedia of Analytical Chemistry*, John Wiley & Sons Ltd, Chichester, **2000**, 5762.

(11) J. L. Kofron, P. Kuzmic, V. Kishore, E. Bonilla-Kolon, D. H. Rich, *Biochemistry*, **1991**, *30*, 6127.

(12) S. F. Göthel, M. A. Marahiel, *Cell Mol. Life Sci.*, **1999**, *55*, 423.

(13) J. L. Kofron, P. Kuzmic, V. Kishore, G. Gemmecker, S. W. Fesik, D. H. Rich, *J. Am. Chem. Soc.*, **1992**, *114*, 2670.

(14) PerkinElmer UK, Chalfont Road, Seer Green, Beaconsfield, HP9 2FX.

(15) J. Liu, C.-M. Chen, C. T. Walsh, *Biochemistry*, **1991**, *30*, 2306.

(16) P. Taylor, G. Kontopidis, M. D. Walkinshaw, *unpublished results*.

(17) A. Bell, H. C. Roberts, L. H. Chappell, *Gen. Pharmac.*, **1996**, *27*, 963.

(18) N. C. Picken, S. Eschenlauer, P. Taylor, A. P. Page, M. D. Walkinshaw, *J. Mol. Biol.*, **2002**, *322*, 15.

(19) A. P. Page, K. MacNiven, M. O. Hengartner, *Biochem. J.*, **1996**, *317*, 179.

(20) A. P. Page, *DNA Cell Biol.*, **1997**, *16*, 1335.

(21) A. P. Page, A. D. Winters, *Mol. Biochem. Parasit.*, **1998**, *95*, 215.

5. Experimental

5.1 General techniques

TLC was performed using plastic backed plates coated with 0.2 mm thick silica gel $60F_{254}$ (Mackerey-Nagel). Plates were visualised using UV light (254nm) or permanganate dip. Chemicals were purchased from Sigma-Aldrich, Acros or Novabiochem unless otherwise stated. All reagents were standard laboratory grade and solvents anhydrous, and used as supplied unless otherwise stated. IR absorption spectra were recorded on a Jasco-FT/IR-410 Spectrophotometer using standard techniques and ν_{max} values are quoted in cm^{-1}. ^{1}H-NMR and ^{13}C-NMR were recorded on a Bruker AC250, AC360 or AC600 spectrometer. The following abbreviations are used: δ, chemical shift; d, doublet; dd, doublet of doublets; dt, doublet of triplets; *J*, coupling constant; m, multiplet; q, quartet; s, singlet; t, triplet; br, broad. Chemical shifts (δ) are reported in parts per million (ppm) and coupling constants (*J*) in Hz. Residual protic solvent, $CHCl_3$ (δ_H 7.26, s) was used as the internal standard in ^{1}H NMR spectra, and ^{13}C NMR shifts were referenced using $CDCl_3$ (δ_C 77.0, t) with broad band decoupling. Nominal mass spectra were recorded on a Micromass Platform-2 instrument under positive and negative ion electrospray conditions. Fast Atom Bombardment (FAB) high resolution mass spectra were recorded on a Kratos MS50TC instrument. Flash chromatography was carried out using silica gel 60H (Merck 9385, 0.04-0.063 mm, 230-400 mesh) or in parallel using pre-packed silica columns in a Biotage QUAD 3 purification system. High performance liquid chromatography (HPLC) was carried out using a Waters 486 tunable absorbance detector and Waters 600E controller and pump. A Chiralcel OD-H column with dimensions 25 x 0.46 cm was used. Samples were injected *via* a 20 µl loop and a flow rate of 1 ml/min was employed for elution using an isocratic system of hexane/ethanol (95:5) detecting at a wavelength of 254nm. Preparative HPLC was performed on a Biotage Parallex FLEX system using a Supercosil ABZ plus reverse-phase column of dimension 25 cm x 2.12 cm, particle size 12 µM. Samples were eluted using 10 - 90 % water (0.05 % TFA)/acetonitrile gradient over 30 minutes

using a flow rate of 20 ml/min. Melting points were obtained on Gallenkamp melting point apparatus and are uncorrected. Optical rotations were performed on an Optical Activity Ltd AA1000 polarimeter and concentrations are given in g/100 ml.

5.2 Experimental procedures

5.2.1 N-benzyloxycarbonyl-L-valinyl fluoride (33)[1]

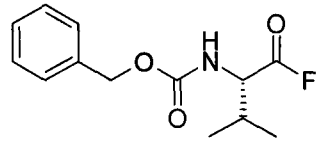

Method A

To a stirred solution of *N*-benzyloxycarbonyl-L-valine (0.5 g, 2.0 mmol) and pyridine (0.16 ml, 2.0 mmol) in anhydrous DCM (5 ml) under N_2 atmosphere was added cyanuric fluoride (0.84 ml, 10.0 mmol) at -15°C. A white precipitate formed after 5 minutes. The reaction mixture was allowed to warm to room temperature and stirred for 2 hours. Ice-cold water (5 ml) was added along with DCM (10 ml), and the white precipitate was removed by filtration. The organic layer was separated and the aqueous layer extracted with DCM (5 ml). The combined DCM layers were washed twice with ice-cold water (5 ml), dried ($MgSO_4$) and the solvent removed *in vacuo* to afford a colourless oil (0.45 g, 89 %) which was used in subsequent reactions without further purification; R_f 0.75 (10 % MeOH in DCM), ν_{max} (thin film) 3323 (N-H), 1845(acid fluoride), 1738 (urethane, C=O), 1522 (amide II); δ_H (250 MHz, $CDCl_3$) 1.03 (3H, d, J = 7.0, $CH(C^AH_3C^BH_3)$), 1.06 (3H, d, J = 7.0, $CH(C^AH_3C^BH_3)$), 2.17-2.26 (1H, m, $CH(CH_3)_2$), 4.44-4.49 (1H, m, NHC*H*), 5.12-5.14 (3H, m, OCH_2Ph & N*H*), 7.36 (5H, s, Ar-*H*); MS ES (+ve) m/z 253.0 $(M+H)^+$.

Method B

To a stirred room temperature solution of *N*-benzyloxycarbonyl-L-valine (0.5 g, 2.0 mmol) in anhydrous DCM (5 ml) under N_2 atmosphere was added

dimethylaminosulfur trifluoride (0.31 ml, 2.4 mmol). After stirring for 2 hours ice-cold water (5 ml) was added. The organic layer was separated and the aqueous layer extracted with DCM (5 ml). The combined DCM layers were washed twice with ice-cold water (5 ml), dried ($MgSO_4$) and the solvent removed *in vacuo* to afford a colourless oil (0.47 g, 94 %) which was used in subsequent reactions without further purification; analysis identical to *Method A*.

5.2.2 3-(N-benzyloxycarbonyl-L-valinyl-oxy)-5,5-dimethyl-cyclohex2-enone (30)

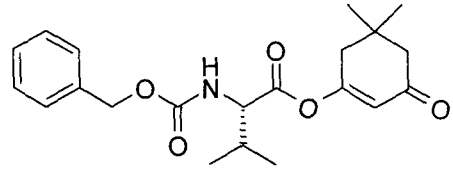

To a stirred room temperature solution of *N*-benzyloxycarbonyl-L-valinylfluoride (0.45 g, 1.79 mmol) in anhydrous DCM (20 ml) was added dimedone (0.25 g, 1.79 mmol) and DIPEA (0.62 ml, 3.58 mmol). The solution went from yellow to blue/purple after 5 minutes. After stirring for 30 minutes, the solution was washed with 1N HCl (2 x 5 ml), saturated $NaHCO_3$ solution (2 x 5 ml), water (2 x 5 ml), dried ($MgSO_4$) and the solvent removed *in vacuo* to give a yellow oil (0.64 g). Flash column chromatography on silica gel using 30 % ethyl acetate in petroleum ether 40-60 as eluent afforded a pale yellow oil (0.50 g, 75 %); R_f 0.60 (30 % EtOAc in petroleum ether 40-60); ν_{max}(NaCl) 3326br (N-H), 1769 (vinyl ester), 1715 (urethane C=O), 1668 (α,β-unsaturated ketone), 1532 (amide II); δ_H (250 MHz, $CDCl_3$) 0.95 (3H, d, J = 7.0, CH($C^AH_3C^BH_3$)), 1.02 (3H, d, J = 7.0, CH($C^AH_3C^BH_3$)), 1.09 (6H, s, C(CH_3)$_2$), 2.26-2.28 (3H, m, C*H*(CH_3)$_2$ & CH_2C(CH_3)$_2$), 2.39 (2H, s, C(CH_3)$_2$CH_2), 4.36 (1H, dd, J = 5.0, 7.5, NHC*H*), 5.12 (2H, s, OCH_2Ph), 5.24 (1H, d, J = 7.5, N*H*), 5.89 (1H, s, CO=C*H*CO), 7.35 (5H, s, Ar-*H*); δ_C (63 MHz, DEPT, $CDCl_3$) 17.5 (CH($C^AH_3C^BH_3$)), 19.0 (CH($C^AH_3C^BH_3$)), 28.0 (C($C^AH_3C^BH_3$)), 28.1 (C($C^AH_3C^BH_3$)), 30.0 (*C*H(CH_3)$_2$), 33.1 (*C*(CH_3)$_2$), 41.9 (COCH_2C(CH_3)$_2$), 50.7 (C(CH_3)$_2$CH_2C=O), 60.0 (NH*C*H), 67.3 (O*C*H_2Ph), 116.9 (CO=*C*HCO), 128.0 (CH), 128.2 (CH), 128.5 [(CH), 5C, *Ar*-H], 135.9 (OCH$_2$*Ph*), 156.1 (*C*ONH), 167.7

(COOC=CH), 169.1 (NHCHCO), 199.0 (COOC=CHCO); HRMS FAB (+ve) m/z 374.1962 $(M+H)^+$, $C_{21}H_{28}NO_5$ requires 374.1967.

5.2.3 N-allyloxycarbonyl-L-phenylalanine (35)[2]

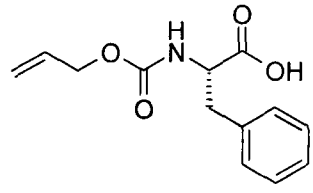

Method A

To a stirred solution of *L*-phenylalanine (1.0 g, 6.0 mmol) in sodium bicarbonate solution (25ml, 0.5M) was added a solution of allyl chloroformate (0.64 ml, 6.0 mmol) in acetonitrile (25 ml). The resulting solution was stirred at room temperature overnight. The acetonitrile was the removed *in vacuo* and the remaining solution acidified to pH 2 with 2M HCl, then extracted with EtOAc (3 x 30 ml). The combined organic phases were washed with water (10 ml) and dried ($MgSO_4$) and the solvent removed *in vacuo* to give a yellow oil (0.62g). Flash column chromatography on silica gel using 5 % methanol in dichloromethane as eluent afforded a pale yellow oil (0.53 g, 35 %); δ_H (250 MHz, DMSO) 2.68 (1H, dd, J = 4.4, 14.0, C*H*^{A}H^{B}Ph), 2.90 (1H, dd, J = 4.4, 14.0, CH^A*H*^{B}Ph), 3.95-3.97 (1H, m, C*H*CH_2Ph), 4.22-4.26 (2H, m, CH_2=CHC*H*$_2$), 4.94-5.09 (2H, m, C*H*$_2$=CHCH_2), 5.63-5.74 (1H, m, CH_2=C*H*CH_2), 7.06-7.12 (5H, m, Ar-*H*), 7.36 (1H, d, J = 8.4, N*H*); δ_C (63 MHz, DEPT, DMSO); 37.4 (*C*H_2Ph), 56.5 (*C*HCH_2Ph), 65.2 (CH_2=CH*C*H_2), 117.7 (*C*H_2=CHCH_2), [127.2 (CH), 129.0 (CH), 129.9 (CH), 5C, *Ar*-H], 134.4 (CH_2=*C*HCH_2), 139.0 (OCH_2*Ph*), 156.6 (*C*ONH), 174.5 (*C*OOH); HRMS FAB (+ve) m/z 250.1079 $(M+H)^+$, $C_{13}H_{16}NO_4$ requires 250.1079.

Method B

Phenylalanine (1.0 g, 6.0 mmol) was dissolved in sodium hydroxide (10 ml, 4.0 M) and cooled to 0°C. Allyl chloroformate (0.64 ml, 6.0 mmol) was added over 5 minutes, the resulting solution allowed to warm to room temperature and stirred for a further 30 minutes. The solution was washed with diethyl ether (20 ml) to remove

excess unreacted allyl chloroformate, the aqueous phase then acidified to pH 2 with 2M HCl. The aqueous phase was then extracted with diethyl ether (2 x 50 ml). The combined organic phases were washed with water (5 ml) and dried ($MgSO_4$) and the solvent removed *in vacuo* to give a pale yellow oil (0.97 g, 65 %); analysis identical to *Method A.*

5.2.4 N-allyloxycarbonyl-L-phenylalaninyl fluoride

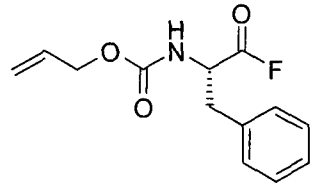

Experimental procedure 5.2.1.A was followed using *N*-allyloxycarbonyl-L-phenylalanine (0.97 g, 3.89 mmol) and cyanuric fluoride (1.64 ml, 19.4 mmol) to yield a pale white oil (0.78 g, 80 %); ν_{max} (nujol) 3321 (N-H), 1846 (acid fluoride), 1703 (urethane, C=O), 1525 (amide II).

5.2.5 3-(N-allyloxycarbonyl-L-phenylalaninyloxy)-5,5-dimethyl-cyclohex-2-enone (37)

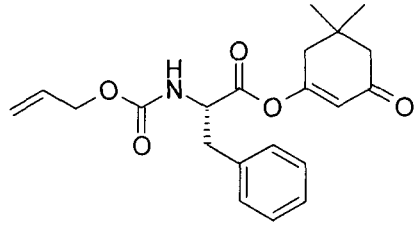

Experimental procedure 5.2.2 was followed using *N*-allyloxycarbonyl-L-phenylalaninyl fluoride (0.26 g, 1.03 mmol), dimedone (0.14 g, 1.03 mmol) and DIPEA (0.36 ml, 2.06 mmol) in DCM (10 ml) to yield a pale yellow oil (0.24 g, 62 %); R_f 0.57 (50 % EtOAc in Hexane); δ_H (250 MHz, $CDCl_3$) 0.93 (6H, s, $C(CH_3)_2$), 2.10 (2H, s, $CH_2C(CH_3)_2$), 2.16 (2H, s, $C(CH_3)_2CH_2$), 3.00 (2H, d, J = 6.3, CH_2Ph), 4.42 (2H, d, J = 5.6, CH_2=CHCH_2), 4.57 (1H, dd, J = 6.3, 14.1, $CHCH_2Ph$), 5.05-5.18 (3H, m, CH_2=$CHCH_2$ & CO=CHCO), 5.67-5.85 (2H, m, CH_2=$CH$$CH_2$ & N*H*),

7.00-7.04 (2H, m, Ar-*H*), 7.11-7.22 (3H, m, Ar-*H*); δ_C (63 MHz, DEPT, $CDCl_3$) 28.3 ($C(CH_3)_2$), 33.3 ($C(CH_3)_2$), 38.2 (CH_2Ph), 41.9 ($COCH_2C(CH_3)_2$), 50.9 ($C(CH_3)_2CH_2C=O$), 55.2 (NH*C*H), 66.2 ($CH_2=CHCH_2$), 116.8 (CO=*C*HCO), 118.3 ($CH_2=CHCH_2$), [127.7 (CH), 129.0 (CH), 129.4 (CH), 5C, *Ar*-H], 132.5 ($CH_2=CHCH_2$), 135.1 (OCH_2Ph), 155.6 (*C*ONH), 167.7 (COO*C*=CH), 168.9 (NHCHCO), 199.0 (COOC=CHCO); HRMS FAB (+ve) m/z 372.179 $(M+H)^+$, $C_{21}H_{26}NO_5$ requires 372.181.

5.2.6 N-allyloxycarbonyl-1-amino-1-cyclopentanecarboxylic acid (36)

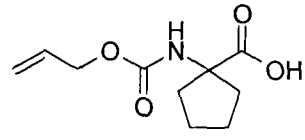

Experimental procedure 5.2.3 was followed using 1-amino-1-cyclopentanecarboxylic acid (1.00 g, 7.74 mmol) and allyl chloroformate (0.82 ml, 7.74 mmol) to yield a white solid (0.6 g, 36 % [method A], 1.15 g, 69 % [method B]); δ_H (250 MHz, DMSO) 1.71-1.77 (4H, m, $CCH_2(CH_2)_2CH_2$), 1.90-1.95 (2H, m, $CCH^AH^B(CH_2)_2CH^AH^B$), 2.14-2.25 (2H, m, $CCH^AH^B(CH_2)_2CH^AH^B$), 4.50 (2H, d, J = 5.0, $CH_2=CHCH_2$), 5.12-5.27 (2H, m, $CH_2=CHCH_2$), 5.16 (1H, s, N*H*), 5.78-5.91 (1H, m, $CH_2=CHCH_2$); δ_C (63 MHz, DEPT, DMSO) 25.1 ($CCH_2(CH_2)_2CH_2$), 38.0 ($CCH_2(CH_2)_2CH_2$), 66.1 ($CCH_2(CH_2)_2CH_2$), 66.2 ($CH_2=CHCH_2$), 118.3 ($CH_2=CHCH_2$), 132.9 ($CH_2=CHCH_2$), 156.0 (*C*ONH), 176.7 (*C*OOH); HRMS FAB (+ve) m/z 214.1073 $(M+H)^+$, $C_{10}H_{15}NO_4$ requires 214.1079; mp 74-77°C.

5.2.7 N-allyloxycarbonyl-1-amino-1-cyclopentyl fluoride

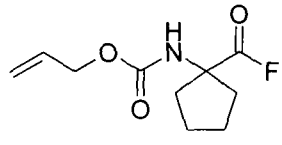

Experimental procedure 5.2.1.A was followed using *N*-allyloxycarbonyl-1-amino-1-cyclopentanecarboxylic acid (0.75 g, 3.5 mmol) and cyanuric fluoride (1.47 ml, 17.5 mmol) to yield a pale yellow oil (0.60 g, 80 %); ν_{max} (nujol) 3333 (N-H), 1838 (acid fluoride), 1699 (urethane, C=O), 1524 (amide II).

5.2.8 *3-(N-allyloxycarbonyl-1-amino-1-cyclopentanecarboxyl-oxy)-5,5-dimethyl-cyclohex-2-enone (38)*

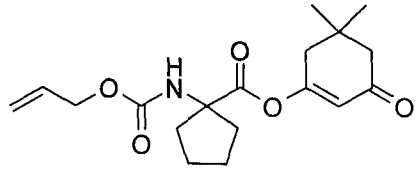

Experimental procedure 5.2.2 was followed using *N*-(allyloxycarbonyl)-1-amino-1-cyclopentyl fluoride (0.23 g, 1.1 mmol) and dimedone (0.15 g, 1.1 mmol) to yield a yellow oil. Flash column chromatography on silica gel using 20 % ethyl acetate in hexane as eluent afforded a pale yellow oil (0.25 g, 70 %); R_f 0.13 (20 % EtOAc in hexane); δ_H (250 MHz, $CDCl_3$) 1.03 (6H, s, $C(CH_3)_2$), 1.73-1.77 (4H, m, $CCH_2(CH_2)_2CH_2$), 1.88-1.94 (2H, m, $CCH^AH^B(CH_2)_2CH^AH^B$), 2.20 (2H, s, $CH_2C(CH_3)_2$), 2.22-2.26 (2H, m, $CCH^AH^B(CH_2)_2CH^AH^B$), 2.37 (2H, s, $C(CH_3)_2CH_2$), 4.50 (2H, d, J = 5.0, CH_2=CHCH_2), 5.12-5.28 (2H, m, CH_2=CHCH_2), 5.17 (1H, s, N*H*), 5.77 (1H, s, CO=C*H*CO), 5.76-5.89 (1H, m, CH_2=C*H*CH_2); δ_C (63 MHz, DEPT, $CDCl_3$) 24.7 ($CCH_2(CH_2)_2CH_2$), 28.5 ($C(CH_3)_2$), 33.7 ($C(CH_3)_2$), 38.0 ($CCH_2(CH_2)_2CH_2$), 42.1 ($COCH_2C(CH_3)_2$), 51.3 ($C(CH_3)_2CH_2C$=O), 66.2 ($CCH_2(CH_2)_2CH_2$), 66.7 (CH_2=CHCH_2), 117.1 (CO=C*H*CO), 118.4 (CH_2=CHCH_2), 132.9 (CH_2=C*H*CH_2), 155.8 (*C*ONH), 167.7 (COO*C*=CH), 171.8 (NHCH*C*O), 199.8 (COOC=CH*C*O); HRMS FAB (+ve) m/z 336.180 $(M+H)^+$, $C_{18}H_{26}NO_5$ requires 336.180.

5.2.9 *4-benzyl-5,5-dimethyl-cyclohexane-1,3-dione (40)*[3]

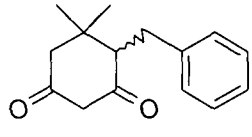

Method A

N-Butyllithium (39.24 ml, 0.062 mol, 1.6 M solution in hexanes) was added dropwise to a dry stirred solution of diisopropylamine (8.80 ml, 0.062 mol) in THF (40 ml) at 0°C. After 40 min the reaction was cooled to -78°C and a solution of

dimedone (4.00 g, 0.028 mol) in DMPU (15 ml) and THF (15 ml) was added over 5 min. After stirring for 1 hour at -78°C a solution of benzyl bromide (3.73 ml, 0.031 mol) and sodium iodide (4.70 g, 0.031 mol) in THF (5 ml) was added over 5 min and the solution allowed to reach room temperature overnight. The reaction was quenched by water (10 ml), diluted with ether (150 ml) and washed with 2M $KHSO_4$ solution (2 x 20 ml). The combined aqueous phases were extracted with ether (3 x 50 ml), and the total organic phase washed with water (15 ml), saturated $NaHCO_3$ solution (2 x 20 ml), brine (20 ml), dried ($MgSO_4$) and the solvent removed *in vacuo* to give a dark yellow oil. Flash column chromatography on silica gel using 30 % ethyl acetate in hexane as eluent yielded a yellow oil (2.21 g, 34 %); R_f 0.35 (50 % EtOAc in hexane); δ_H (250 MHz, $CDCl_3$) 0.79 (3H, s, $C(C^AH_3C^BH_3)$), 1.18 (3H, s, $C(C^AH_3C^BH_3)$), 2.47 (1H, dd, J = 1.8, 14.9, $CH^AH^BC(CH_3)_2$), 2.59 (1H, d, J = 14.9, $CH^AH^BC(CH_3)_2$), 2.68-2.75 (2H, m, $CHCH^AH^BPh$), 3.07 (1H, dd, J = 10.0, 14.9, $CHCH^AH^BPh$), 3.25 (1H, dd, J = 1.8, 16.0, $COCH^AH^BCO$), 3.34 (1H, d, J = 16.0, $COCH^AH^BCO$), 7.08-7.24 (5H, m, Ar-*H*); δ_C (63 MHz, DEPT, $CDCl_3$) 22.9 ($C(C^AH_3C^BH_3)$), 29.7 ($C(C^AH_3C^BH_3)$), 30.4 (CH_2Ph), 34.9 ($C(CH_3)_2$), 55.9 ($COCH_2C(CH_3)_2$), 59.3 ($COCH_2CO$), 63.1 ($CHCH_2Ph$), [126.8 (CH), 129.1 (CH), 129.6 (CH), 5C, *Ar*-H], 141.3 (CH_2Ph), 203.5 ($COCH_2CO$), 203.7 ($COCH_2CO$); HRMS FAB (+ve) m/z 231.1386 ($M+H^+$), $C_{15}H_{19}O_2$ requires 231.1385.

Method B

A solution of **44** (0.37 g, 1.5 mmol) in 2M HCl (10 ml) and THF (10 ml) was stirred overnight at room temperature. The solution was then extracted with ethyl acetate (3 x 25 ml), the combined organic phases then washed with water (10 ml), saturated $NaHCO_3$ solution (2 x 5 ml), brine (5 ml) and dried ($MgSO_4$). The solvent was removed *in vacuo* to yield a viscous yellow oil (0.315 g, 91 %); analysis identical to *Method A*.

5.2.10 5,5-dimethyl-3-methoxy-cyclohexe-2-enone (41)[4]

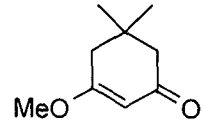

Chlorotrimethylsilane (1.9 ml, 0.015 mol) was added to a solution of dimedone (2.0 g, 0.014 mol) in methanol (20 ml). Diisopropylethylamine (5.19 ml, 0.03 mol) was added dropwise to the solution with white HCl fumes evolved. The solution was stirred at room temperature for 2 hours, the solvent then removed *in vacuo*. The residue was re-dissolved in ethyl acetate then washed with water (10 ml), saturated $NaHCO_3$ solution (2 x 10 ml), brine (10 ml), dried ($MgSO_4$) and the solvent removed *in vacuo* to give a non-viscous yellow oil (2.16 g, 98 %); R_f 0.5 (50 % EtOAc in DCM); δ_H (250 MHz, $CDCl_3$) 1.25 (6H, s, $C(CH_3)_2$), 2.39 (2H, s, $CH_2C(CH_3)_2$), 2.45 (2H, s, $CH_2C(CH_3)_2$), 3.87 (3H, s, OCH_3), 5.54 (1H, s, CO=CHCO); δ_C (63 MHz, DEPT, $CDCl_3$) 27.8 ($C(CH_3)_2$), 32.1 ($C(CH_3)_2$), 42.2 ($COCH_2C(CH_3)_2$), 50.3 ($C(CH_3)_2CH_2C=O$), 55.2 (OCH_3), 100.7 (CO=CHCO), 176.5 ($CH_3OC=CH$), 199.8 ($CH_3OC=CHCO$); HRMS FAB (+ve) m/z 155.1072 $(M+H)^+$, $C_9H_{14}O_2$ requires 155.1074.

5.2.11 3-methoxy-5,5,6-trimethyl-cyclohex-2-enone (42)

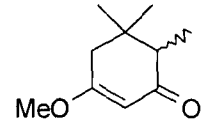

N-Butyllithium (27.5 ml, 0.036 mol, 1.6 M solution in hexanes) was added dropwise to a dry stirred solution of diisopropylamine (5.1 ml, 0.036 mol) in THF (10 ml) at 0°C. After 40 min the reaction was cooled to -78°C and a solution of **41** (5.0 g, 0.032 mol) in DMPU (15 ml) and THF (5 ml) was added over 5 min. After stirring for 1 hour at -78°C a solution of methyl iodide (6.0 ml, 0.096 mol) in THF (35 ml) and DMPU (25 ml) was added over 5 min and the solution allowed to reach room temperature overnight. The reaction was quenched by water (10ml), diluted with ether (150 ml) and washed with 2M $KHSO_4$ solution (2 x 20 ml). The combined

aqueous phases were extracted with ether (2 x 100 ml) then ethyl acetate (3 x 50 ml), and the total organic phase washed with water (15 ml), saturated $NaHCO_3$ solution (2 x 20 ml), brine (20 ml), dried ($MgSO_4$) and the solvent removed *in vacuo* to give a yellow oil. Flash column chromatography on silica gel using 30 % ethyl acetate in petroleum ether 40-60 as eluent afforded a yellow oil (4.57 g, 85 %); R_f 0.40 (50 % ethyl acetate in petroleum ether 40-60); δ_H (250 MHz, $CDCl_3$) 0.88 (3H, s, $C(C^AH_3C^BH_3)$), 1.03 (3H, d, J = 7.04, $CHCH_3$), 1.04 (3H, s, $C(C^AH_3C^BH_3)$), 2.11 (1H, q, J = 7.0, $CHCH_3$), 2.20 (1H, d, J = 17.4, $COCH^AH^BC(CH_3)_2$), 2.29 (1H, d, J = 17.4, $COCH^AH^BC(CH_3)_2$), 3.64 (3H, s, CH_3O), 5.28 (1H, s, $CH_3OC{=}CHCO$); δ_C (63 MHz, DEPT, $CDCl_3$) 10.1 ($CHCH_3$), 22.4 ($C(C^AH_3C^BH_3)$, 28.7 ($C(C^AH_3C^BH_3)$), 35.1 ($C(CH_3)_2$), 42.3 ($CH_3OCCH_2C(CH_3)_2$), 51.0 ($CHCH_3$), 55.5 (CH_3O), 100.4 ($CH_3OC{=}CHCO$), 175.3 ($CH_3OC{=}CH$), 202.2 ($CH_3OC{=}CHCO$); HRMS EI (+ve) m/z 488.2669, $C_{30}H_{36}N_2O_4$ requires 488.2675.

5.2.12 6-allyl-5,5-dimethyl-3-methoxy-cyclohex-2-enone (43)

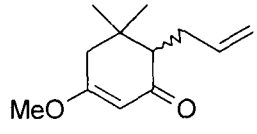

Experimental procedure 5.2.11 was followed using *N*-butyllithium (27.5 ml, 0.036 mol, 1.6 M solution in hexanes), diisopropylamine (5.1 ml, 0.036 mol), **41** (5.0 g, 0.032 mol) and allyl bromide (16.9 ml, 0.16 mol) in THF (35 ml) and DMPU (25 ml). Flash column chromatography on silica gel using 30 % ethyl acetate in petroleum ether 40-60 as eluent afforded a yellow oil (5.41 g, 87 %); R_f 0.44 (30 % ethyl acetate in hexane); δ_H (250 MHz, $CDCl_3$) 1.17 (3H, s, $C(C^AH_3C^BH_3)$), 1.26 (3H, s, $C(C^AH_3C^BH_3)$), 2.24-2.29 (1H, m, $CHCH^AH^BCH{=}CH_2$), 2.42-2.54 (4H, m, $CHCH_2CH{=}CH_2$, $COCH_2C(CH_3)_2$, $CHCH^AH^BCH{=}CH_2$), 3.85 (3H, s, OCH_3), 5.11-5.23 (2H, m, $CHCH_2CH{=}CH_2$), 5.47 (1H, s, $CO{=}CHCO$), 5.97-6.10 (1H, m, $CHCH_2CH{=}CH_2$); δ_C (63 MHz, DEPT, $CDCl_3$) 24.3 ($C(C^AH_3C^BH_3)$), 28.7 ($C(C^AH_3C^BH_3)$), 30.8 ($CH_2CH{=}CH_2$), 35.2 ($C(CH_3)_2$), 41.7 ($CH_3OCCH_2C(CH_3)_2$), 55.5 (CH_3O), 57.0 ($C(CH_3)_2CH$), 100.4 ($CH_3OC{=}CHCO$), 115.3 ($CH_2CH{=}CH_2$),

137.6 ($CH_2CH=CH_2$), 175.1 ($CH_3OC=CH$), 201.3 ($CH_3OC=CHCO$); HRMS EI (+ve) m/z 194.1307 $(M)^+$, $C_{12}H_{18}O_2$ requires 194.1307.

5.2.13 6-benzyl-5,5-dimethyl-3-methoxy-cyclohex-2-enone (44)

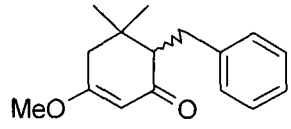

Experimental procedure 5.2.11 was followed using *N*-butyllithium (27.5 ml, 0.036 mol, 1.6 M solution in hexanes), diisopropylamine (5.1 ml, 0.036 mol), **41** (5.0 g, 0.032 mol) and benzyl bromide (4.18 ml, 0.036 mol) in DMPU (10 ml) and THF (10 ml). Flash column chromatography on silica gel using 30 % ethyl acetate in petroleum ether 40-60 as eluent afforded a white solid (6.91 g, 89 %); R_f 0.55 (50 % EtOAc in hexane); δ_H (250 MHz, $CDCl_3$) 0.85 (3H, s, $C(C^AH_3C^BH_3)$), 0.94 (3H, s, $C(C^AH_3C^BH_3)$), 2.14 (2H, s, $CH_2C(CH_3)_2$), 2.21 (1H, dd, J = 4.0, 14.0, $CHCH_2Ph$), 2.53 (1H, dd, J = 8.1, 14.0, $CHCH^AH^BPh$) 2.58 (1H, dd, J = 8.1, 14.0, $CHCH^AH^BPh$), 3.48 (3H, s, OCH_3), 5.15 (1H, s, $CO=CHCO$), 6.94-7.11 (5H, m, Ar-*H*); δ_C (63 MHz, DEPT, $CDCl_3$) 23.6 ($C(CH_3)_2$), 29.1 ($C(CH_3)_2$), 31.8 (CH_2Ph), 36.0 ($C(CH_3)_2$), 42.6 ($COCH_2C(CH_3)_2$), 55.7 (OCH_3), 59.2 ($CHCH_2Ph$), 100.7 ($CO=CHCO$), [125.9 (CH), 128.3 (CH), 129.0 (CH), 5C, *Ar*-H], 141.8 (CH_2Ph), 174.9 ($CH_3OC=CH$), 200.7 ($CH_3OC=CHCO$); HRMS FAB (+ve) m/z 245.1542 $(M+H)^+$, $C_{16}H_{21}O_2$ requires 245.1542; CHN analysis expected C 78.65 %, H 8.25 %, N 0 %, found C 78.40 %, H 8.22 %, N 0.16 %.

5.2.14 5,5-dimethyl-3-methoxy-6-((E)-3-phenyl-allyl)-cyclohex-2-enone (45)

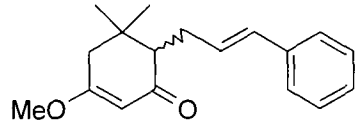

N-Butyllithium (27.5 ml, 0.036 mol, 1.6 M solution in hexanes) was added dropwise to a dry stirred solution of diisopropylamine (5.1 ml, 0.036 mol) in THF (10 ml) at 0°C. After 40 min the reaction was cooled to -78°C and a solution of **41** (5.0 g, 0.032

mol) in DMPU (15 ml) and THF (5 ml) was added over 5 min. After stirring for 1 hour at -78°C a solution of cinnamyl bromide (12.61 g, 0.064 mol) in DMPU (10 ml) and THF (10 ml) was added dropwise. Addition of the cinnamyl bromide solution resulted in precipitate crashing out in the reaction mixture which redissolved upon addition of further DMPU (15 ml) and THF (15 ml). The solution was allowed to reach room temperature overnight. The reaction was quenched by water (10ml), diluted with ethyl acetate (150 ml) and washed with 2M $KHSO_4$ solution (2 x 20 ml). The combined aqueous phases were extracted ethyl acetate (3 x 100 ml), and the total organic phase washed with water (15 ml), saturated $NaHCO_3$ solution (2 x 20 ml), brine (20 ml), dried ($MgSO_4$) and the solvent removed *in vacuo* to give a yellow oil. Flash column chromatography on silica gel using 30 % ethyl acetate in hexane as eluent afforded a white solid (6.54 g, 76 %); R_f 0.50 (50 % EtOAc in petroleum ether 40-60); δ_H (250 MHz, $CDCl_3$) 1.25 (3H, s, $C(C^AH_3C^BH_3)$), 1.36 (3H, s, $C(C^AH_3C^BH_3)$), 2.41 (1H, dd, J = 4.0, 8.4, $CHCH_2CH$=CHPh), 2.53 (2H, d, J = 2.0, $CH_2C(CH_3)_2$), 2.61-2.77 (2H, m $CHCH_2CH$=CHPh), 3.91 (3H, s, OCH_3), 5.56 (1H, s, OC=C*H*CO), 6.49-6.58 (1H, m, $CHCH_2CH$=CHPh), 6.62 (1H, d, J = 16.0, $CHCH_2CH$=C*H*Ph), 7.40-7.58 (5H, m, Ar-*H*); δ_C (63 MHz, DEPT, $CDCl_3$) 23.9 ($C(C^AH_3C^BH_3)$), 28.9 ($C(C^AH_3C^BH_3)$), 29.8 ($CHCH_2CH$=CH_2), 35.4 ($C(CH_3)_2$), 42.2 ($CH_2C(CH_3)_2$), 55.6 (OCH_3), 57.2 ($CHCH_2CH$=CH_2), 100.5 (OC=CHCO), [126.0 (CH), 126.7 (CH), 128.4 (CH), 5C, *Ar*-H], 129.8 ($CHCH_2CH$=CHPh), 130.4 ($CHCH_2CH$=CHPh), 137.6 (CH_2Ph), 175.1 (H_3COC) 201.0 (*C*O); HRMS FAB (+ve) m/z 257.1541 ($M+H^+$), $C_{17}H_{21}O_2$ requires 257.1542.

5.2.15 (6,6-dimethyl-4-methoxy-2-oxo-cyclohex-3-enyl)-acetic acid tert-butyl ester (46)

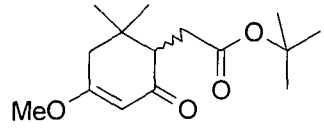

Experimental procedure 5.2.11 was followed using *N*-butyllithium (27.5 ml, 0.036 mol, 1.6 M solution in hexanes), diisopropylamine (5.1 ml, 0.036 mol), **41** (5.0 g, 0.032 mol) and *tert*-butyl bromoacetate (9.45 ml, 0.064 mol) in THF (35 ml) and

DMPU (30 ml). Flash column chromatography on silica gel using 20 % ethyl acetate in hexane as eluent afforded a pale yellow oil that solidified on standing to give a white solid (7.39 g, 86 %); R_f 0.45 (50 % ethyl acetate in hexane); δ_H (250 MHz, CDCl3) 0.86 (3H, s, $C(C^AH_3C^BH_3)$), 1.09 (3H, s, $C(C^AH_3C^BH_3)$), 1.46 (3H, s, $CO_2C(CH_3)_3$), 2.13 (1H, d, J = 17.4, $CH^AH^BC(CH_3)_2$), 2.17 (1H, dd, J = 4.5, 16.0, $CHCH_2$), 2.53 (1H, dd, J = 1.6, 17.4, $CH^AH^BC(CH_3)_2$), 2.63 (1H, dd, J = 8.2, 16.0 $CHCH^AH^BCO_2C(CH_3)_3$), 2.80 (1H, dd, J = 4.5, 8.2, $CHCH^AH^BCO_2C(CH_3)_3$), 3.67 (3H, s, CH_3O), 5.35 (1H, d, J = 1.6, $CH_3OC=CHCO$); δ_C (63 MHz, DEPT, $CDCl_3$) 21.1 ($C(C^AH_3C^BH_3)$), 27.8 ($OC(CH_3)_3$), 28.7 ($C(C^AH_3C^BH_3)$), 30.5 ($CHCH_2$), 35.4 ($C(CH_3)_2$), 52.8 ($C(CH_3)_2CH$), 55.4 (CH_3O), 80.1 ($OC(CH_3)_3$), 100.6 ($CH_3OC=CHCO$), 172.6 ($CO_2C(CH_3)_3$), 175.1 ($CH_3OC=CH$), 198.8 ($CH_3OC=CHCO$); HRMS EI (+ve) m/z 268.1755 $(M+H)^+$, $C_{15}H_{25}O_4$ requires 268.1753.

5.2.16 6-benzyl-3-(N-benzyloxycarbonyl-L-valinyl-oxy)-5,5-dimethyl-cyclohex-2-enone (47)

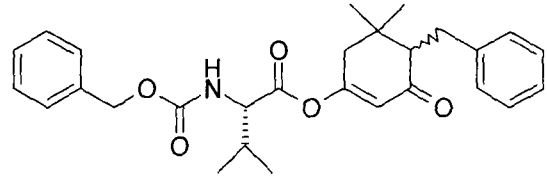

(diastereomers **A** & **B**)

Experimental procedure 5.2.2 was followed using *N*-benzyloxycarbonyl-L-valinylfluoride (0.20 g, 0.79 mmol) and **40** (0.18 g, 0.79 mmol) to yield a yellow oil. Flash column chromatography on silica gel using 20 % ethyl acetate in hexane as eluent afforded a pale yellow oil (0.26 g, 70 %); R_f 0.53 (30 % EtOAc in hexane); δ_H (360 MHz, $CDCl_3$) 0.92-0.97 (3H, m, $CH(C^AH_3C^BH_3$, **A** & **B**), 1.02-1.09 (6H, m, $CH(C^AH_3C^BH_3)$ & $C(C^AH_3C^BH_3)$, **A** & **B**), 1.14 (3H, s, $C(C^AH_3C^BH_3)$, **A** & **B**), 1.97-2.24 (1H, m, $CH(CH_3)_2$, **A** & **B**), 2.40-2.45 (3H, m, $CH_2C(CH_3)_2$ & $CHCH_2Ph$, **A** & **B**), 2.77-2.80 (1H, m, $CHCH^AH^BPh$, **A** & **B**), 2.99-3.06 (1H, m, $CHCH^AH^BPh$, **A** & **B**), 4.39 (1H, dd, J = 4.7, 8.7 NHC*H*, **A** & **B**), 5.12 (2H, s, OCH_2Ph, **A** & **B**), 5.24

(1H, d, J = 8.7, N*H*, **A & B**), 5.83 (1H, s, CO=C*H*CO, **A**), 5.85 (1H, s, CO=C*H*CO, **B**), 7.13-7.34 (10H, m, Ar-*H*, **A & B**); δ_C (63 MHz, DEPT, $CDCl_3$) 17.0 (CH($C^AH_3C^BH_3$), **A & B**), 17.4 (CH($C^AH_3C^BH_3$), **A & B**), 23.3(C($C^AH_3C^BH_3$), **A & B**), 28.6 (C($C^AH_3C^BH_3$), **A & B**), 30.4 (CH_2Ph, **A**), 31.0 ($CH(CH_3)_2$, **A & B**), 31.1 (CH_2Ph, **B**), 36.2 ($C(CH_3)_2$, **A**), 36.3 ($C(CH_3)_2$, **B**), 41.6 (NHC$CH_2C(CH_3)_2$, **A & B**), 59.1 (C*H*CH_2Ph, **A**), 59.3 (C*H*CH_2Ph, **B**), 60.3 (NH*C*H, **A & B**), 67.2 (OCH_2Ph, **A & B**), 116.3 (CO=*C*HCO, **A**), 116.4 (CO=*C*HCO, **B**), [125.9 (CH), 128.0 (CH), 128.2 (CH), 128.3 (CH), 128.5 (CH), 128.8 (CH), 10C, *Ar*-H, **A & B**], 135.8 (OCH_2*Ph*, **A & B**), 140.7 (CH_2*Ph*, **A & B**), 156.1 (*C*ONH, **A & B**), 165.5 (COOC=CH, **A & B**), 169.1 (NHCH*C*O, **A & B**), 200.2 (COOC=CH*C*O, **A & B**); MS ES (+ve) 486.3 $(M+Na)^+$.

5.2.17 3-amino-5,5-dimethyl-cyclohex-2-enone (50)[5]

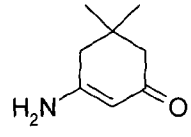

Ammonium acetate (9.25 g, 0.28 mol) was added to a stirring suspension of dimedone (8.3 g, 0.06 mol) in glacial acetic acid (3 ml) and toluene (150 ml). The reaction mixture was heated to reflux for 2 hours and water removed azeotropically using Dean-Stark apparatus. After cooling to room temperature the solution was washed with saturated $NaHCO_3$ solution (2 x 20 ml), a precipitate formed upon washing that was collected by filtration each time and combined to give a yellow solid. The solid was recrystallised from EtOAc (50ml), collected by filtration then washed with Et_2O (2 x 10 ml) and dried under reduced pressure to yield a pale yellow powder (7.83 g, 94 %); R_f 0.1 (10 % MeOH in DCM); δ_H (250 MHz, $CDCl_3$) 0.97 (6H, s, $C(CH_3)_2$), 1.92 (2H, s, $CH_2C(CH_3)_2$), 2.13 (2H, s, $C(CH_3)_2CH_2$), 4.92 (1H, s, NH_2C=C*H*CO), 6.7-7.2 (2H, s, br, NH_2); δ_C (63 MHz, DEPT, $CDCl_3$); 28.9 ($C(CH_3)_2$), 33.1 ($C(CH_3)_2$), 42.4 ($H_2NCCH_2C(CH_3)_2$), 50.7 ($C(CH_3)_2CH_2C$=O), 96.7 (H_2NC=*C*HCO), 176.5 (NH_2C=CH), 195.0 (NH_2C=CH*C*O); HRMS FAB (+ve) m/z 140.1075 $(M+H)^+$, $C_8H_{14}NO$ requires 140.1075; CHN analysis expected C 69.03 %,

H 9.41 %, N 10.06 %, found C 69.31 %, H 9.59 %, N 10.05 %; mp 166-168°C (lit 164-165°C).

5.2.18 Attempted preparation of 3-(N-benzyloxycarbonyl-L-valinyl-amino)-5,5-dimethyl-cyclohex-2-enone (62)

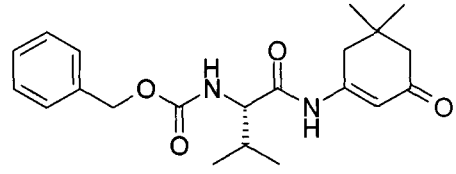

Method A

To a stirred solution of *N*-benzyloxycarbonyl-L-valine (0.9 g, 3.6 mmol) and 1-hydroxybenzotriazole (0.54 g, 4.0 mmol) in DMF was added *N,N'*-dicyclohexylcarbodiimide (0.82 g, 4.0 mmol) and **50** (0.5 g, 3.6 mmol). The solution was stirred overnight at room temperature. TLC analysis (50 % EtOAc in petroleum ether 40-60) indicated starting materials only. MS ES (+ve) 140.2 (**50**+H)$^+$.

Method B

N-benzyloxycarbonyl-L-valine (0.5 g, 2.0 mmol) and 1-hydroxybenzotriazole ((0.27 g, 2.0 mmol) were dissolved in DMF and EDCI (0.38 g, 2.0 mmol) and **50** (0.3 g, 2.1 mmol) were added. The solution was stirred overnight at room temperature. TLC analysis (50 % EtOAc in petroleum ether 40-60) indicated starting materials only. MS ES (+ve) 140.2 (**50**+H)$^+$.

Method C

To a stirred solution of *N*-carboxybenzyloxy-L-valine (0.9 g, 3.6 mmol), 1-hydroxybenzotriazole (0.54 g, 4.0 mmol) and DIPEA (0.93 ml, 5.4 mmol) in DMF was added TBTU (1.27 g, 4.0 mmol) and **50** (0.5 g, 3.6 mmol). The resulting solution was stirred overnight at room temperature. TLC analysis (50 % EtOAc in petroleum ether 40-60) indicated starting material only.

5.2.19 3-(N-benzyloxycarbonyl-L-valinyl-amino)-5,5-dimethyl-cyclohex-2-enone (62)

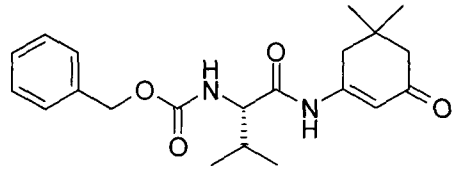

Method A

Experimental procedure 5.2.2 was followed using *N*-benzyloxycarbonyl-L-valinyl fluoride (0.48 g, 1.9 mmol), **50** (0.26 g, 1.9 mmol) and DIPEA (0.65 ml, 3.8 mmol) in DCM (20 ml). Flash column chromatography on silica gel using 20 % ethyl acetate in petroleum ether 40-60 as eluent afforded a pale yellow oil that solidified upon standing (0.28 g, 40 %); R_f 0.22 (50 % EtOAc in petroleum ether 40-60); δ_H (250 MHz, $CDCl_3$) 0.98 (3H, d, *J* = 6.8, $CH(C^AH_3C^BH_3)$), 1.01 (3H, d, *J* = 6.8, $CH(C^AH_3C^BH_3)$), 1.08 (6H, s, $C(CH_3)_2$), 2.15-2.19 (1H, m, $CH(CH_3)_2$), 2.25 (2H, s, $CH_2C(CH_3)_2$), 2.37 (2H, s, $C(CH_3)_2CH_2$), 4.14 (1H, dd, *J* = 5.0, 7.5, NHC*H*), 5.19 (2H, s, OCH_2Ph), 5.67 (1H, d, br, *J* = 7.5, N*H*), 6.69 (1H, s, NHC=C*H*CO), 7.42 (5H, s, Ar-*H*), 5.67 (1H, s, br, N*H*); δ_C (63 MHz, DEPT, DMSO) 18.8 ($CH(C^AH_3C^BH_3)$), 21.6 ($CH(C^AH_3C^BH_3)$), 28.5 ($C(C^AH_3C^BH_3)$), 28.8 ($C(C^AH_3C^BH_3)$), 31.0 ($CH(CH_3)_2$), 33.1 ($C(CH_3)_2$), 42.0 ($NHCCH_2C(CH_3)_2$), 50.9 ($C(CH_3)_2CH_2C=O$), 61.8 (NHCH), 66.4 (OCH_2Ph), 110.4 (HNC=CHCO), [128.5 (CH), 128.7 (CH), 129.2(CH), 5C, *Ar*-H], 137.8 (OCH_2Ph), 154.65 (NHC=CH), 157.2 (CONH), 173.4 (NHCHCO), 199.0 (NHC=CHCO); HRMS EI (+ve) m/z 372.2044 $(M)^+$, $C_{21}H_{28}N_2O_4$ requires 372.2049.

Method B

To a stirred solution of *N*-benzyloxycarbonyl-L-valine (0.82 g, 3.3 mmol), **50** (0.5 g, 3.6 mmol) and DIPEA (1.14 ml, 6.6 mmol) was added PyBOP (1.7 g, 3.3 mmol). After stirring for 2 h at room temperature the solution was washed with 1M $KHSO_4$ solution (2 x 5 ml), saturated $NaHCO_3$ solution (2 x 5 ml), water (2 x 5 ml), dried ($MgSO_4$) and the solvent removed *in vacuo* to give a dark yellow oil (2.13 g). Flash

column chromatography on silica gel using 30 % ethyl acetate in hexane as eluent afforded a pale yellow solid (0.57 g, 47 %). Analysis identical to *Method A*.

Method C

N-Benzyloxycarbonyl-L-valine (0.151 g, 0.6 mmol), PyBroP (0.279 g, 0.6 mmol) and DMAP (0.146 mg, 1.2 mmol) were dissolved in DCM (5ml) and stirred at room temperature. After 5 minutes, **50** (0.055 g, 0.4 mmol) was added and the solution stirred at room temperature. After 2 hours the DCM was evaporated *in vacuo* and EtOAc (5 ml) was added to the residue. A white precipitate formed which dissolved upon addition of water (2 ml). The organic layer was separated and washed with 1M $KHSO_4$ solution (2 ml), water (2 ml), saturated $NaHCO_3$ solution (2 ml), water (2 ml), dried ($MgSO_4$) and the solvent removed *in vacuo* to give a yellow oil. Flash column chromatography on silica gel using 40 % ethyl acetate in hexane as eluent afforded a white solid (0.137 g, 92 %). Analysis identical to *Method A*. $[\alpha]_D^{22}$ -40.4 (*c* 1.0, $CHCl_3$).

5.2.20 3-(N-allyloxycarbonyl-L-phenylalaninyl-amino)-5,5-dimethyl-cyclohex-2-enone (63)

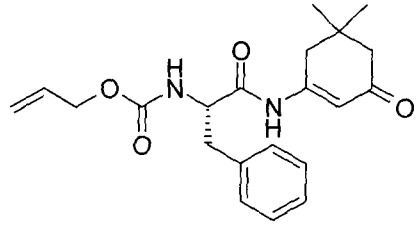

Experimental procedure 5.2.2 was followed using *N*-(allyloxycarbonyl)-L-phenylalaninyl fluoride (0.26 g, 1.03 mmol), **50** (0.14 g, 1.03 mmol) and DIPEA (0.36 ml, 2.06 mmol) in DCM (10 ml) to yield a pale yellow solid. Flash column chromatography on silica gel using 50 % ethyl acetate in hexane as eluent afforded a white solid (0.30 g, 79 %); R_f = 0.22 (50 % EtOAc in Hexane); δ_H (250 MHz, $CDCl_3$) 1.03 (6H, s, $C(CH_3)_2$), 1.98 (2H, s, $CH_2C(CH_3)_2$), 2.20 (2H, s, $C(CH_3)_2CH_2$), 3.09 (2H, d, *J* = 7.3, $CHCH_2Ph$), 4.48 (1H, dd, *J* = 7.3, 7.5, $CHCH_2Ph$), 4.55 (2H,

ddd, J = 1.3, 1.4, 5.6, CH_2=CHCH_2), 5.24 (1H, ddd, J = 1.3, 1.4, 10.4, CH^AH^B=CHCH$_2$), 5.29 (1H, ddd, J = 1.3, 1.4, 14.8, CH$^AH^B$=CHCH$_2$), 5.64 (1H, d, J = 7.5, NH), 5.88 (1H, ddd, J = 5.6, 10.4, 14.8, CH_2=CHCH$_2$), 6.67 (1H, s, NHC=CHCO), 7.17-7.21 (2H, m, Ar-H), 7.26-7.32 (3H, m, Ar-H), 8.03 (1H, s, br, NH); δ_C (63 MHz, DEPT, $CDCl_3$) 27.6 (C($C^AH_3C^BH_3$)), 28.0 (C($C^AH_3C^BH_3$)), 32.3 (C(CH$_3$)$_2$), 37.9 (CH$_2$Ph), 41.7 (NHCCH$_2$C(CH$_3$)$_2$), 50.0 (C(CH$_3$)$_2$$CH_2$C=O), 56.8 (C$HCH_2$Ph), 65.8 ($CH_2$=CHC$H_2$), 111.2 (CO=$C$HCO), 117.81 ($CH_2$=CHCH$_2$), [126.9 (CH), 128.5 (CH), 128.8 (CH), 5C, Ar-H], 135.4 (CH_2=CHCH$_2$), 135.4 (OCH$_2$$Ph$), 152.2 (NH$C$=CH), 155.6 ($C$ONH), 170.21 (NHCH$C$O), 199.6 (COOC=CH$C$O); HRMS FAB (+ve) m/z 371.1970 $(M+H)^+$, $C_{21}H_{27}N_2O_4$ requires 371.1971.

5.2.21 3-(N-allyloxycarbonyl)-1-amino-1-cyclopentyl-amino)-5,5-dimethyl-cyclohex-2-enone (64)

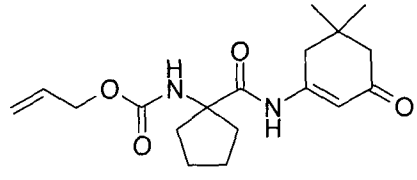

Experimental procedure 5.2.2 was followed using *N*-(allyloxycarbonyl)-1-amino-1-cyclopentyl fluoride (0.6 g, 2.8 mmol), **50** (0.39 g, 2.8 mmol) and DIPEA (0.97 ml, 5.6 mmol) in DCM (20 ml). Flash column chromatography on silica gel using 20 % ethyl acetate in hexane as eluent afforded a white solid (0.20 g, 21 %); R_f 0.18 (50% EtOAc in hexane); δ_H (250 MHz, $CDCl_3$) 1.01(6H, s, C(CH_3)$_2$), 1.70-1.78 (4H, m, CCH$_2$(CH_2)$_2$CH$_2$), 1.91-1.98 (2H, m, CCH^AH^B(CH$_2$)$_2$CH^AH^B), 2.16 (2H, s, CH_2C(CH$_3$)$_2$), 2.19-2.27 (2H, m, CCH$^AH^B$(CH$_2$)$_2$CH$^AH^B$), 2.32 (2H, s, CH_2C(CH$_3$)$_2$), 4.52 (2H, d, J = 5.6, CH_2=CHCH_2), 5.15-5.21 (2H, m, CH_2=CHCH$_2$), 5.28 (1H, s, NHC=CHCO), 5.78-5.91 (1H, m, CH_2=CHCH$_2$), 6.55 (1H, s, NH), 8.98 (1H, s, NH); δ_C (63 MHz, DEPT, $CDCl_3$) 23.7 (CCH$_2$(CH$_2$)$_2$CH$_2$), 28.4 (C(CH$_3$)$_2$), 32.8 (C(CH$_3$)$_2$), 36.5 (CCH$_2$(CH$_2$)$_2$CH$_2$), 42.6 (COCH$_2$C(CH$_3$)$_2$), 50.7 (C(CH$_3$)$_2$$CH_2$C=O), 66.4 ($CH_2$=CH$CH_2$), 68.5 ($CCH_2$(CH$_2$)$_2CH_2$), 111.1 (NHC=C$H$CO), 118.51 ($CH_2$=CHCH$_2$), 132.2 ($CH_2$=$CHCH_2$), 153.7 (NH$C$=CHCO),

156.6 (*C*ONH), 172.7 (NH*C*OO), 199.8 (NHC=CH*C*O); HRMS FAB (+ve) m/z 335.1972 $(M+H)^+$, $C_{18}H_{27}N_2O_4$ requires 335.1971.

5.2.22 5,5-dimethyl-3-(methylamino)-cyclohex-2-enone (65)[6]

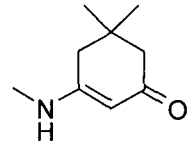

Experimental procedure 5.2.17 was followed using methylamine (1.2 ml, 14 mmol, 40 % solution in water) and dimedone (1.0 g, 7 mmol) in glacial acetic acid (2 ml) and toluene (30 ml) to yield a yellow solid. Recrystallisation from ethyl acetate gave a pale yellow powder (0.69 g, 65 %); δ_H (250 MHz, DMSO) 1.25 (6H, s, $C(CH_3)_2$), 2.13 (2H, s, $CH_2C(CH_3)_2$), 2.32 (2H, s, $C(CH_3)_2CH_2$), 2.77 (3H, d, J = 4, CH_3NH), 4.91 (1H, s, CO=C*H*CO), 7.18 (1H, d, J = 4, CH_3NH); δ_C (63 MHz, DEPT, DMSO) 28.8 ($C(CH_3)_2$), 29.7 (CH_3NH), 33.15 ($C(CH_3)_2$), 42.8 ($COCH_2C(CH_3)_2$), 51.2 ($C(CH_3)_2CH_2C=O$), 93.9 (CO=C*H*CO), 164.5 ($NH_2C=CH$), 194.5 ($CH_3OC=CHCO$); HRMS FAB (+ve) m/z 154.1229 $(M+H)^+$, $C_9H_{16}NO$ requires 154.1232; CHN analysis expected C 70.55 %, H 9.87 %, N 9.14 %, found C 70.26 %, H 9.73 %, N 9.28 %; mp 154-156°C (lit 153-154°C).

5.2.23 3-(N-allyloxycarbonyl-L-phenylalaninyl-methylamino)-5,5-dimethyl-cyclohex-2-enone (66)

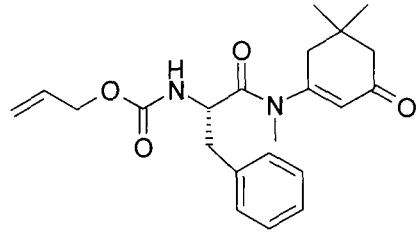

Experimental procedure 5.2.2 was followed using *N*-allyloxycarbonyl-L-phenylalaninyl fluoride (0.26 g, 1.0 mmol) and **65** (0.16 g, 1.0 mmol) and DIPEA (0.36 ml, 2.0 mmol) in DCM (10 ml). Flash column chromatography on silica gel

using 50 % ethyl acetate in hexane as eluent afforded a yellow oil (0.07 g, 18 %); R_f 0.47 (50 % EtOAc in Hexane); δ_H (250 MHz, $CDCl_3$) 0.94 (3H, s, $C(C^AH_3C^BH_3)$), 0.98 (3H, s, $C(C^AH_3C^BH_3)$), 2.30 (2H, d, J = 18.1, $CH^AH^BC(CH_3)_2$), 2.15 (2H, d, J = 3.6, $CH_2C(CH_3)_2$), 2.30 (2H, d, J = 18.1, $CH^AH^BC(CH_3)_2$), 2.89 (3H, s, NCH_3), 2.93 (2H, d, J = 8.2, $CHCH_2Ph$), 4.47 (2H, dd, J = 1.3, 5.5, CH_2=$CHCH_2$), 4.70-4.76 (1H, dd, J = 8.2, 8.5, $CHCH_2Ph$), 5.14 (2H, ddd, J = 1.3, 1.4, 10.4, CH^AH^B=$CHCH_2$), 5.22 (2H, dd, J = 1.4, 16.0, CH^AH^B=$CHCH_2$), 5.36 (1H, s, NC=$CHCO$), 5.42 (1H, d, J = 8.5, NH), 5.82 (1H, ddd, J = 5.5, 10.4, 16.0, CH_2=$CHCH_2$), 7.06-7.10 (2H, m, Ar-H), 7.19-7.25 (3H, m, Ar-H); δ_C (63 MHz, DEPT, $CDCl_3$) 27.7 ($C(C^AH_3C^BH_3)$), 28.3 ($C(C^AH_3C^BH_3)$), 32.2 ($C(CH_3)_2$), 35.1 (NCH_3), 40.6 (CH_2Ph), 42.6 ($NCCH_2C(CH_3)_2$), 50.8 ($C(CH_3)_2CH_2C$=O), 60.5 ($CHCH_2Ph$), 65.9 (CH_2=$CHCH_2$), 112.0 (CH_2=$CHCH_2$), 123.6 (NC=$CHCO$), [127.5 (CH), 128.9 (CH), 129.5 (CH), 5C, Ar-H], 132.6 (CH_2=$CHCH_2$), 136.0 (OCH_2Ph), 155.4 (NC=CH), 159.8 ($CONH$), 171.5 (NHCHCO), 199.2 (NC=CHCO); MS ES (+ve) 407.3 $(M+Na)^+$.

5.2.24 4,5,5-trimethyl-cyclohexane-1,3-dione (73)[3]

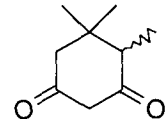

A solution of **42** (4.57 g, 0.027 mol) in 2M HCl (30 ml) and THF (30 ml) was stirred overnight at room temperature. TLC analysis showed some starting material remaining so further 2M HCl (20 ml) was added and the solution stirred for 1 hour. The solution was then extracted with ethyl acetate (3 x 50 ml), the combined organic phases then washed with water (20 ml), saturated $NaHCO_3$ solution (2 x 20 ml), brine (20 ml) and dried ($MgSO_4$). The solvent was removed *in vacuo* to yield a white solid (3.59 g, 86 %); R_f 0.20 (50 % ethyl acetate in petroleum ether 40-60); δ_H (250 MHz, $CDCl_3$) 0.75 (3H, s, $C(C^AH_3C^BH_3)$), 1.11 (3H, s, $C(C^AH_3C^BH_3)$), 1.12 (3H, d, J = 7.2, $CHCH_3$), 2.20 (1H, q, J = 7.2, $CHCH_3$), 2.51 (1H, dd, J = 14.7, 2.0, $COCH^AH^BC(CH_3)_2$), 2.61 (1H, d, J = 14.7, $COCH^AH^BC(CH_3)_2$), 3.30 (1H, dd, J = 16.8, 2.0, $COCH^ACH^BCO$), 3.40 (1H, d, J = 16.8, $COCH^ACH^BCO$); δ_C (63 MHz,

DEPT, $CDCl_3$) 8.8 ($CHCH_3$), 21.4 ($C(C^AH_3C^BH_3)$), 28.5 ($C(C^AH_3C^BH_3)$), 33.7 ($C(CH_3)_2$), 54.0 ($CHCH_3$), 55.3 ($COCH_2C(CH_3)_2$), 57.5 ($COCH_2CO$), 203.5 (*C*O), 205.3 (*C*O); HRMS FAB (+ve) found m/z 155.1071, $C_9H_{15}O_2$ requires 155.1072.

5.2.25 4-allyl-5,5-dimethyl-cyclohexane-1,3-dione (74)[3]

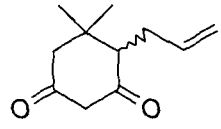

A solution of **43** (5.14 g, 0.028 mol) in 2M HCl (30 ml) and THF (30 ml) was stirred at room temperature for 2 hours. TLC analysis showed some starting material remaining so further 2M HCl (20 ml) was added and the solution stirred overnight. The solution was extracted with ethyl acetate (3 x 50 ml), the combined organic phases then washed with water (20 ml), saturated $NaHCO_3$ solution (2 x 20 ml), brine (20 ml) and dried ($MgSO_4$). The solvent was removed *in vacuo* to yield a pale yellow oil (4.44 g, 88 %); R_f 0.20 (50 % ethyl acetate in petroleum ether 40-60); δ_H (250 MHz, $CDCl_3$) 0.83 (3H, s, $C(C^AH_3C^BH_3)$), 1.11 (3H, s, $C(C^AH_3C^BH_3)$), 2.24-2.35 (1H, m, $CHCH^AH^BCH{=}CH_2$), 2.43-2.55 (4H, m, $CHCH_2CH{=}CH_2$, $COCH_2C(CH_3)_2$, $CHCH^AH^BCH{=}CH_2$), 3.32 (1H, dd, *J* 16.5, 1.5, $COCH^AH^BCO$), 3.41 (1H, d, *J* 16.5, $COCH^AH^BCO$), 4.98-5.12 (2H, m, $CHCH_2CH{=}CH_2$), 5.76-5.87 (1H, m, $CHCH_2CH{=}CH_2$); δ_C (63 MHz, DEPT, $CDCl_3$) 22.8 ($C(C^AH_3C^BH_3)$), 28.8 ($C(C^AH_3C^BH_3)$), 28.9 ($CHCH_2CH{=}CH_2$), 33.6 ($C(CH_3)_2$), 54.4 ($COCH_2C(CH_3)_2$), 57.9 ($COCH_2CO$), 60.0 ($CHCH_2CH{=}CH_2$), 116.3 ($CHCH_2CH{=}CH_2$), 136.3 ($CHCH_2CH{=}CH_2$), 203.0 (*C*O), 203.9 (*C*O); HRMS FAB (+ve) m/z 181.1228 (MH^+), $C_{11}H_{17}O_2$ requires 181.1228.

5.2.26 5,5-dimethyl-4-((E)-3-phenyl-allyl)-cyclohexane-1,3-dione (75)

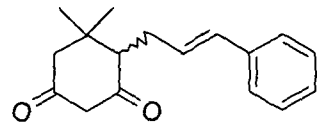

2M HCl (30 ml) was added to a stirred solution of **45** (5.5 g, 0.02 mol) in THF (30 ml) at room temperature. Addition of the HCl resulted in some white precipitate formation which redissolved after stirring for 10 minutes. After 1 hour TLC analysis showed some starting material remaining so further 2M HCl (20 ml) was added and the solution stirred overnight. The solution was extracted with ethyl acetate (3 x 50 ml), the combined organic phases then washed with water (20 ml), saturated $NaHCO_3$ solution (2 x 20 ml), brine (20 ml) and dried ($MgSO_4$). The solvent was removed *in vacuo* to yield a yellow oil (4.87 g, 95 %); R_f 0.36 (50 % ethyl acetate in hexane); δ_H (250 MHz, $CDCl_3$) 0.82 (3H, s, $C(C^A\mathit{H}_3C^BH_3)$), 1.15 (3H, s, $C(C^AH_3C^B\mathit{H}_3)$), 2.15-2.74 (5H, m, $COC\mathit{H}_2C(CH_3)_2$, $C\mathit{H}CH_2CH{=}CHPh$, $CHC\mathit{H}_2CH{=}CHPh$), 3.33 (1H, dd, J = 1.5, 16.3, $COC\mathit{H}^AH^BCO$), 3.44 (1H, d, J = 16.3, $COCH^A\mathit{H}^BCO$), 6.15-6.23 (1H, m, $CHCH_2C\mathit{H}{=}CHPh$), 6.40 (1H, d, J = 16.0, $CHCH_2CH{=}C\mathit{H}Ph$) 7.14-7.29 (5H, m, Ar-*H*); δ_C (63 MHz, DEPT, $CDCl_3$) 22.6 ($C(\mathit{C}^AH_3C^BH_3)$), 27.9 ($C(C^AH_3\mathit{C}^BH_3)$), 28.8 ($CH\mathit{C}H_2CH{=}CH_2$), 33.8 ($\mathit{C}(CH_3)_2$), 54.9 ($COCH_2\mathit{C}(CH_3)_2$), 58.2 ($COCH_2CO$), 60.1 ($\mathit{C}HCH_2CH{=}CH_2$), [126.8 (CH), 129.1 (CH), 129.6 (CH), 5C, *Ar*-H], 128.1 ($CHCH_2\mathit{C}H{=}CHPh$), 131.6 ($CHCH_2CH{=}\mathit{C}HPh$), 137.0 ($CH_2\mathit{Ph}$), 203.0 (*C*O), 203.8 (*C*O); HRMS FAB (+ve) m/z 257.1541 ($M+H^+$), $C_{17}H_{21}O_2$ requires 257.1541.

5.2.27 (6,6-dimethyl-2,4-dioxo-cyclohexyl)-acetic acid tert-butyl ester (76)

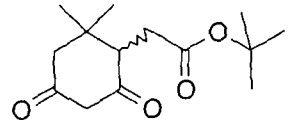

2M HCl (30 ml) was added to a stirred solution of **46** (5.9 g, 0.022 mol) in THF (30 ml) at room temperature. After 1 hour TLC analysis showed some starting material remaining so further 2M HCl (20 ml) and THF (20 ml) was added and the solution

stirred overnight. The solution was extracted with ethyl acetate (3 x 50 ml), the combined organic phases then washed with water (20 ml), saturated $NaHCO_3$ solution (2 x 20 ml), brine (20 ml) and dried ($MgSO_4$). The solvent was removed *in vacuo* to yield a yellow oil (5.26g, 94 %); R_f 0.43 (50 % ethyl acetate in hexane); δ_H (250 MHz, CDCl3) 0.69 (3H, s, $C(C^AH_3C^BH_3)$), 1.15 (3H, s, $C(C^AH_3C^BH_3)$), 1.47 (9H, s, $CO_2C(CH_3)_3$), 2.31 (1H, dd, J = 3.8, 16.7, $C(CH_3)_2CH$), 2.46 (1H, dd, J = 2.5, 14.7, $COCH^AH^BC(CH_3)_2$), 2.68 (1H, dd, J = 9.4, 16.7, $C(CH_3)_2CHCH^ACH^B$), 2.75 (1H, d, J = 14.7, $COCH^AH^BC(CH_3)_2$), 3.14 (1H, dd, J = 3.8, 9.4, $C(CH_3)_2CHCH^AH^B$), 3.27 (1H, dd, J = 2.5, 16.5, $COCH^AH^BCO$), 3.51 (1H, d, J = 16.5, $COCH^AH^BCO$); δ_C (63 MHz, DEPT, $CDCl_3$) 21.0 ($C(C^AH_3C^BH_3)$), 27.9 ($OC(CH_3)_3$), 28.2 ($C(C^AH_3C^BH_3)$), 29.9 ($CHCH_2$), 33.4 ($C(CH_3)_2$), 55.6 ($C(CH_3)_2CH$), 55.9 ($OCCH_2CCH_3$), 58.1 ($OCCH_2CO$) 80.9 ($OC(CH_3)_3$), 171.9 ($CO_2C(CH_3)_3$), 202.8 (*C*O), 202.9 (*C*O); MS ES (+ve) 255.0 $(M+H)^+$, (-ve) 253.0 $(M-H)^-$.

5.2.28 3-amino-4,5,5-trimethyl-cyclohex-2-enone (77)

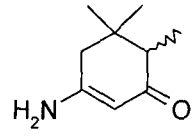

Experimental procedure 5.2.17 was followed using **73** (3.50 g, 0.023 mol) and ammonium acetate (3.50 g, 0.046 mmol) in glacial acetic acid (2 ml) and toluene (100 ml) to give a viscous yellow oil. Recrystallisation from ethyl acetate afforded a pale yellow powder (2.92 g, 83 %); R_f 0.42 (10 % MeOH in DCM); δ_H (250 MHz, $CDCl_3$) 0.89 (3H, s, $C(C^AH_3C^BH_3)$), 1.02 (3H, d, J = 7.1, $CHCH_3$), 1.03 (3H, s, $C(C^AH_3C^BH_3)$), 2.01 (1H, q, J = 7.1, $CHCH_3$), 2.14 (1H, d, J = 16.8, $H_2NCH^AH^BC(CH_3)_2$), 2.22 (1H, d, J = 16.8, $H_2NCH^AH^BC(CH_3)_2$), 5.12 (1H, s, $H_2NC{=}CHCO$), 5.22 (1H, s, br, NH_2); δ_C (63 MHz, DEPT, $CDCl_3$) 10.2 ($CHCH_3$), 23.2 ($C(C^AH_3C^BH_3)$), 28.6 ($C(C^AH_3C^BH_3)$), 35.1 ($C(CH_3)_2$), 41.4 ($H_2NCCH_2C(CH_3)_2$), 50.0 ($CHCH_3$), 97.6 ($H_2NC{=}CHCO$), 163.5 ($H_2NC{=}CH$), 200.6 ($H_2NC{=}CHCO$); HRMS FAB (+ve) 153.1152, $C_9H_{15}NO$ requires 153.1153; CHN analysis expected C

70.55 %, H 9.87 %, N 9.14 %, found C 69.21 %, H 9.79 %, N 8.92 %; mp 122-124°C.

5.2.29 6-allyl-3-amino-5,5-dimethyl-cyclohex-2-enone (78)

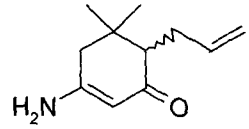

Experimental procedure 5.2.17 was followed using **74** (4.20 g, 0.023 mol) and ammonium acetate (3.50 g, 0.046 mol) in glacial acetic acid (2 ml) and toluene (100 ml) to give a viscous dark yellow oil. Recrystalisation from ethyl acetate afforded a white powder (3.63 g, 88 %); δ_H (360 MHz, CDCl3) 0.97 (3H, s, C($C^AH_3C^BH_3$)), 1.05 (3H, s, C($C^AH_3C^BH_3$)), 1.96 (1H, t, J = 6.7, C*H*$CH_2CH{=}CH_2$), 2.07 (1H, d, J = 17.0, $H_2NCCH^AH^BC(CH_3)_2$), 2.25-2.34 (2H, t, J = 6.7 $CHCH_2CH{=}CH_2$), 2.31 (1H, d, J = 17.0, $H_2NCCH^AH^BC(CH_3)_2$), 4.87-5.02 (2H, m, $CHCH_2CH{=}CH_2$), 5.12 (1H, s, $H_2NC{=}CHCO$), 5.17 (2H, s, br, NH_2), 5.82-5.93 (1H, m, $CHCH_2CH{=}CH_2$); δ_C (63 MHz, DEPT, $CDCl_3$) 24.9 (C($C^AH_3C^BH_3$), 28.9 (C($C^AH_3C^BH_3$), 31.8 ($CH_2CH{=}CH_2$), 35.4 ($C(CH_3)_2$), 41.1 ($NH_2CCH_2C(CH_3)_2$), 55.9 ($C(CH_3)_2CH$), 98.0 ($H_2NC{=}CHCO$), 114.9 ($CH_2CH{=}CH_2$), 138.1 ($CH_2CH{=}CH_2$), 162.8 ($H_2NC{=}CH$), 199.7 ($H_2NC{=}CHCO$); HRMS EI (+ve) m/z 179.1306, $C_{11}H_{19}NO$ requires 179.1310; CHN analysis expected C 73.70 %, H 9.56 %, N 7.81 %, found C 73.37 %, H 9.43 %, N 8.08 %; mp 108-110°C.

5.2.30 3-amino-6-benzyl-5,5-dimethyl-cyclohex-2-enone (79)

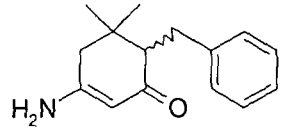

Experimental procedure 5.2.17 was followed using **40** (0.28 g, 1.2 mmol) and ammonium acetate (0.18 g, 2.4 mmol) in glacial acetic acid (0.25 ml) and toluene (15 ml) to give a viscous yellow oil. Recrystalisation from ethyl acetate afforded a pale

yellow powder (0.24 g, 86 %); R_f 0.48 (10 % MeOH in DCM); δ_H (250 MHz, $CDCl_3$) 0.94 (3H, s, $C(C^AH_3C^BH_3)$), 1.01 (3H, s, $C(C^AH_3C^BH_3)$), 2.11 (2H, s, $CH_2C(CH_3)_2$), 2.22 (1H, dd, J = 4.4, 7.7, $CHCH_2Ph$), 2.64 (1H, dd, J = 4.4, 14.0, $CHCH^AH^BPh$), 2.94 (1H, dd, J = 7.7, 14.0, $CHCH^AH^BPh$), 4.64 (2H, s, NH_2), 5.08 (1H, s, $NH_2C=CHCO$), 7.06-7.19 (5H, m, Ar-*H*); δ_C (63 MHz, DEPT, $CDCl_3$) 23.8 ($C(C^AH_3C^BH_3)$), 28.9 ($C(C^AH_3C^BH_3)$), 32.4 (CH_2Ph), 36.0 ($C(CH_3)_2$), 41.7 ($NH_2CCH_2C(CH_3)_2$), 57.9 ($CHCH_2Ph$), 98.0 ($NH_2C=CHCO$), [125.4 (CH), 127.9(CH), 128.9 (CH), 5C, *Ar*-H], 142.1 (CH_2Ph), 162.0 ($NH_2C=CHCO$), 198.9 ($NH_2C=CHCO$); HRMS ES (+ve) m/z 229.1463 M^+, $C_{15}H_{19}NO$ requires 229.1466; mp 127-130°C.

5.2.31 4-amino-6-((E)-3-phenyl-allyl)-5,5-dimethyl-cyclohex-2-enone (80)

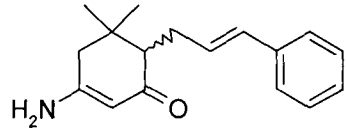

Experimental procedure 5.2.17 was followed using **75** (5.04 g, 0.020 mol) and ammonium acetate (3.03 g, 0.040 mol) in glacial acetic acid (2 ml) and toluene (150 ml) to give a yellow solid. Recrystalisation from ethyl acetate afforded a white powder (4.34 g, 85 %); δ_H (250 MHz, $CDCl_3$) 1.27 (3H, s, $C(C^AH_3C^BH_3)$), 1.35 (3H, s, $C(C^AH_3C^BH_3)$), 2.33 (1H, d, J = 7.9, $CHCH^AH^BC(CH_3)_2$), 2.34 (1H, dd, J = 5.0, 7.8, $C(CH_3)_2CH$), 2.51 (1H, d, J = 7.9, $CH^AH^BC(CH_3)_2$), 2.70-2.83 (2H, m, $CHCH_2CH=CHPh$), 5.09 (2H, s, NH_2), 5.43 (1H, s, $H_2NC=CHCO$), 6.47-6.65 (2H, m, $CHCH_2CH=CHPh$), 7.40-7.58 (5H, m, Ar-*H*); δ_C (63 MHz, DEPT, $CDCl_3$) 24.6 ($C(C^AH_3C^BH_3)$), 30.0 ($C(C^AH_3C^BH_3)$), 30.9 ($CHCH_2CH=CH_2$), 35.5 ($C(CH_3)_2$), 41.4 ($H_2NCCH_2C(CH_3)_2$), 56.1 ($CHCH_2CH=CH_2$), 98.3 ($H_2NC=CHCO$), [126.0 (CH), 126.7 (CH), 128.4 (CH), 5C, *Ar*-H], 130.0 ($CHCH_2CH=CHPh$), 130.2 ($CHCH_2CH=CHPh$), 137.7 (CH_2Ph), 162.5 (H_2NC), 200.0 (*CO*); HRMS EI (+ve) m/z 255.1621, $C_{17}H_{21}NO$ requires 255.1623; CHN analysis expected C 79.96 %, H 8.29 %, N 5.49 %, found C 79.77 %, H 8.27 %, N 5.51 %; mp 145-148°C.

5.2.32 *(4-amino-6,6-dimethyl-2-oxo-cyclohex-3enyl)-acetic acid tert-butyl ester (81)*

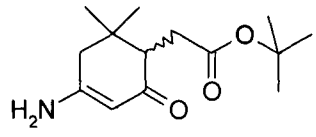

Experimental procedure 5.2.17 was followed using **76** (3.0 g, 0.012 mol) and ammonium acetate (1.8 g, 0.024 mol) in glacial acetic acid (2 ml) and toluene (100 ml) to give a dark yellow solid. Recrystallisation from ethyl acetate afforded a white powder (2.43 g, 80 %); δ_H (250 MHz, $CDCl_3$) 0.86 (3H, s, $C(C^AH_3C^BH_3)$), 1.06 (3H, s, $C(C^AH_3C^BH_3)$), 1.45 (9H, s, $CO_2C(CH_3)_3$), 2.00 (1H, d, J = 16.6, $NH_2CCH^AH^BC(CH_3)_2$), 2.13 (1H, dd, J = 4.5, 15.6, $CHCH^AH^BCO_2C(CH_3)_3$), 2.48 (1H, d, J = 16.6, $NH_2CCH^AH^BC(CH_3)_2$), 2.59 (1H, dd, J = 8.0, 15.6, $CHCH^AH^BCO_2C(CH_3)_3$), 2.70 (1H, dd, J = 4.5, 8.0, $CHCH_2$), 4.99 (2H, s, br, NH_2), 5.12 (1H, d, J = 1.0, $NH_2C{=}CHCO$); δ_C (63 MHz, DEPT, $CDCl_3$) 21.4 ($C(C^AH_3C^BH_3)$), 27.9 ($OC(CH_3)_3$), 28.9 ($C(C^AH_3C^BH_3)$), 31.2 ($CHCH_2$), 35.6 ($C(CH_3)_2$), 43.9 ($CH_2C(CH_3)_2$), 51.9 ($C(CH_3)_2CH$), 79.9 ($OC(CH_3)_3$), 98.0 ($NH_2C{=}CHCO$), 162.7 ($NH_2C{=}CHCO$), 173.2 ($CO_2C(CH_3)_3$), 196.9 ($NH_2C{=}CHCO$); HRMS EI (+ve) m/z 253.1679, $C_{14}H_{23}NO_3$ requires 253.1677; mp 142-145°C.

5.2.33 *6-allyl-3-(N-benzyloxycarbonyl-L-valinyl-amino)-5,5-dimethyl-cyclohex-2-enone (82)*

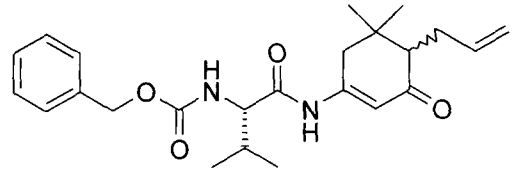

(diastereomers **A** & **B**)

N-benzyloxycarbonyl-L-valine (0.146 g, 0.58 mmol), PyBroP (0.270 g, 0.58 mmol) and DMAP (0.143 mg, 1.17 mmol) were dissolved in DCM (5ml) and stirred at room temperature. After 5 minutes, **78** (0.069 g, 0.39 mmol) was added and the solution

stirred at room temperature. After 2 hours the DCM was evaporated *in vacuo* and EtOAc (5 ml) was added to the residue. A white precipitate formed which dissolved upon addition of water (2 ml). The organic layer was separated and washed with 1M $KHSO_4$ solution (2 ml), water (2 ml), saturated $NaHCO_3$ solution (2 ml), water (2 ml), dried ($MgSO_4$) and the solvent removed *in vacuo* to give a yellow oil. Flash column chromatography on silica gel using 30 % ethyl acetate in petroleum ether 40-60 as eluent afforded a white solid (0.148 g, 92 %). δ_C (63 MHz, DEPT, DMSO) 17.7 (CH($C^AH_3C^BH_3$), **A & B**), 19.3 (CH($C^AH_3C^BH_3$), **A & B**), 24.1 (C($C^AH_3C^BH_3$), **A & B**), 28.6 (C($C^AH_3C^BH_3$), **A & B**), 30.4 ($CH_2CH{=}CH_2$, **A & B**), 30.7 ($CH(CH_3)_2$, **A & B**), 35.5 ($C(CH_3)_2$, **A & B**), 41.3 ($NHCCH_2C(CH_3)_2$, **A & B**), 56.7 ($C(CH_3)_2CH$, **A & B**), 61.1 (NHCH, **A & B**), 67.4 ($PhCH_2O$, **A & B**), 111.0 (HNC=CHCO, **A & B**), 115.5 ($CH_2CH{=}CH_2$, **A & B**), [127.9 (CH), 128.4 (CH), 128.6 (CH), 5C, *Ar*-H, **A & B**], 135.7 ($PhCH_2O$, **A & B**), 137.4 ($CH_2CH{=}CH_2$, **A & B**), 151.2 (NHC=CH, **A & B**), 156.8 (CONH, **A & B**), 170.9 (NHCHCO, **A & B**), 201.7 (NHC=CHCO, **A & B**); HRMS EI (+ve) m/z 412.2363 (M^+), $C_{24}H_{32}N_2O_4$ requires 412.2362.

The diasteromers were separated by using a HPLC fitted with a Chiralcel OD-H column preparatively using an isocratic system of hexane/ethanol (95:5) as eluent.

Diasteromer	**Retention time (min)**	**Peak area**	**δ_H (600 MHz, $CDCl_3$)**
A	31.85	6938054 (49.98 %)	0.96 (3H, d, *J* = 6.8, CH($C^AH_3C^BH_3$)), 0.99 (3H, d, *J* = 6.8, CH($C^AH_3C^BH_3$)), 1.00 (3H, s, C($C^AH_3C^BH_3$)), 1.09 (3H, s, C($C^AH_3C^BH_3$)), 2.11 (1H, dd, *J* = 4.2, 9.0, $CHCH_2CH{=}CH_2$), 2.17-2.36 (5H, m, $CH(CH_3)_2$, $CH_2C(CH_3)_2$, $CHCH_2CH{=}CH_2$), 3.97 (1H, dd, *J* = 7.0 7.1, NHCH), 4.95-5.03 (2H, m, $CHCH_2CH{=}CH_2$), 5.13 (2H, s, $PhCH_2O$), 5.28 (1H, d, *J* = 7.1, br, NH), 5.83-5.87 (1H, m, $CHCH_2CH{=}CH_2$), 6.52 (1H, s, NHC=CHCO), 7.32-7.38 (5H, m, Ar-H), 7.76 (1H, s, br, NH)

B	40.49	6944140 (50.02 %)	0.95 (3H, d, J = 6.8, CH($C^AH_3C^BH_3$)), 0.99 (3H, d, J = 6.8, CH($C^AH_3C^BH_3$)), 1.00 (3H, s, C($C^AH_3C^BH_3$)), 1.08 (3H, s, C($C^AH_3C^BH_3$)), 2.12 (1H, dd, J = 4.2, 8.9, CHCH$_2$CH=CH$_2$), 2.17-2.24 (1H, m, CH(CH^ACH^B)CH=CH$_2$), 2.25-2.43 (4H, m, CH_2C(CH$_3$)$_2$ CH(CH$_3$)$_2$, CH(CH^{A}CH^B)CH=CH$_2$), 3.96 (1H, dd, J = 6.8, 8.4, NHCH), 4.96-5.03 (2H, m, CHCH$_2$CH=CH_2), 5.13 (2H, s, PhCH_2O), 5.29 (1H, d, J = 8.4, NH), 5.82-5.86 (1H, m, CHCH$_2$CH=CH$_2$), 6.52 (1H, s, NHC=CHCO), 7.33-7.38 (5H, m, Ar-H), 7.77 (1H, s, br, NH)

5.2.34 3-(N-benzyloxycarbonyl-L-valinyl-amino)-5,5-dimethyl-6-((E)-3-phenyl-allyl)-cyclohex-2-enone (83)

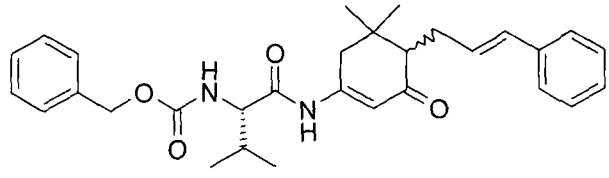

(diastereomers **A** & **B**)

N-Benzyloxycarbonyl-L-valine (0.146 g, 0.58 mmol), PyBroP (0.270 g, 0.58 mmol) and DMAP (0.143 mg, 1.17 mmol) were dissolved in DCM (5ml) and stirred at room temperature. After 5 minutes, **80** (0.100 g, 0.39 mmol) was added and the solution stirred at room temperature. After 2 hours the DCM was evaporated *in vacuo* and EtOAc (5 ml) was added to the residue. A white precipitate formed which dissolved upon addition of water (2 ml). The organic layer was separated and washed with 1M $KHSO_4$ solution (2 ml), water (2 ml), saturated $NaHCO_3$ solution (2 ml), water (2 ml), dried ($MgSO_4$) and the solvent removed *in vacuo* to give a yellow oil. Flash column chromatography on silica gel using 30 % ethyl acetate in petroleum ether 40-60 as eluent afforded a white solid (0.179 g, 94 %); δ_H (360 MHz, $CDCl_3$) 0.91 (3H, d, J = 6.8, CH($C^AH_3C^BH_3$), **A**), 0.92 (3H, d, J = 6.8, CH($C^AH_3C^BH_3$), **B**), 0.95 (3H, d, J = 6.8, CH($C^AH_3C^BH_3$), **A**), 0.96 (3H, d, J = 6.8, CH($C^AH_3C^BH_3$), **B**), 0.98 (3H, s, C($C^AH_3C^BH_3$), **A**), 0.99 (3H, s, C($C^AH_3C^BH_3$), **B**), 1.08 (3H, s, C($C^AH_3C^BH_3$), **A**),

1.09 (3H, s, C($C^AH_3C^BH_3$), **B**), 2.11-2.52 (6H, m, C*H*CH_2CH=CH, C*H*$(CH_3)_2$, CHC*H*$_2$CH=CH, C*H*$_2$C$(CH_3)_2$, **A & B**), 4.09-4.12 (1H, m, NHC*H*, **A & B**), 5.10 (2H, s, PhC*H*$_2$O, **A & B**), 5.56 (1H, d, *J* = 7.5, N*H*, **A**), 5.58 (1H, d, *J* = 7.5, N*H*, **B**) 6.23-6.38 (2H, m, CH_2C*H*=C*H*Ph, **A & B**), 6.59 (1H, s, NHC=C*H*CO, **A & B**), 7.15-7.34 (10H, m, Ar-*H*, **A & B**), 8.25 (1H, s, br, N*H*, **A**), 8.28 (1H, s, br, N*H*, **B**); δ_C (63 MHz, DEPT, DMSO) 17.6 (CH($C^AH_3C^BH_3$), **A & B**), 19.1 (CH($C^AH_3C^BH_3$), **A & B**), 23.7 (C($C^AH_3C^BH_3$), **A**), 23.8 (C($C^AH_3C^BH_3$), **B**), 28.6 (C($C^AH_3C^BH_3$), **A & B**), 29.4 (*C*H_2CH=CH_2, **A**), 29.5 (*C*H_2CH=CH_2, **B**), 30.9 (*C*H$(CH_3)_2$, **A & B**), 35.5 (*C*$(CH_3)_2$, **A**), 35.6 (*C*$(CH_3)_2$, **B**), 41.5 (NHC*C*H_2C$(CH_3)_2$, **A & B**), 56.7 (C$(CH_3)_2$*C*H, **A**), 56.8 (C$(CH_3)_2$*C*H, **B**), 60.9 (NH*C*H, **A & B**), 67.1 (O*C*H_2Ph, **A & B**), 110.9 (HNC=*C*HCO, **A & B**, [125.8 (CH), 126.7 (CH), 127.7 (CH), 128.1 (CH), 128.2 (CH), 128.4 (CH) 10C, *Ar*-H, **A & B**], 129.4 (CHCH_2*C*H=CHPh, **A & B**), 130.5 (CHCH_2CH=*C*HPh, **A & B**), 135.7 (CH*Ph*, **A & B**), 137.7 (CH_2*Ph*, **A & B**), 151.6 (NH*C*=CH, **A & B**), 156.7 (*C*ONH, **A & B**), 171.2 (NHCH*C*O, **A & B**), 201.7 (NHC=CH*C*O, **A & B**); HRMS EI (+ve) m/z 488.2669, $C_{30}H_{36}N_2O_4$ requires 488.2675.

5.2.35 6-benzyl-3-(N-benzyloxycarbonyl-L-valinyl-amino)-5,5-dimethyl-cyclohex-2-enone (84)

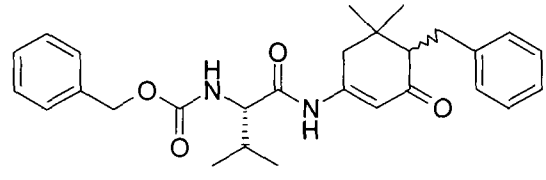

(diastereomers **A & B**)

Experimental procedure 5.2.2 was followed using *N*-benzyloxycarbonyl-L-valinylfluoride (0.13 g, 0.5 mmol) and **79** (0.13 g, 0.55 mmol) and DIPEA (0.19 ml, 1.1 mmol) in DCM (20 ml). Flash column chromatography on silica gel using 30 % ethyl acetate in hexane as eluent afforded a yellow oil (0.09 g, 39 %); R_f 0.6 (50 % EtOAc in hexane); δ_H (360 MHz, $CDCl_3$) 0.87 (3H, d, *J* = 6.9, CH($C^AH_3C^BH_3$), **A & B**), 0.91 (3H, d, *J* = 6.9, CH($C^AH_3C^BH_3$), **A & B**), 0.93 (3H, s, C($C^AH_3C^BH_3$), **A & B**), 1.02 (3H, s, C($C^AH_3C^BH_3$), **A & B**), 2.11-2.15 (1H, m, C*H*$(CH_3)_2$, **A & B**), 2.36-

2.41 (3H, m, $CH_2C(CH_3)_2$ & $CHCH_2Ph$, **A** & **B**), 2.69 (1H, dt, J = 3.6, 3.6, 14.1, $CHCH^AH^BPh$, **A** & **B**), 3.00 (1H, dd, J = 8.1, 14.1, $CHCH^AH^BPh$, **A** & **B**), 4.01-4.06 (1H, m, NHC*H*, **A** & **B**), 5.09 (2H, s, OCH_2Ph, **A** & **B**), 5.52 (1H, d, J = 8.4, N*H*, **A** & **B**), 6.54 (1H, s, NHC=C*H*CO, **A**), 6.56 (1H, s, NHC=C*H*CO, **B**), 7.11-7.36 (10H, m, Ar-*H*, **A** & **B**), 8.25 (1H, s, N*H*, **A** & **B**); δ_C (63 MHz, DEPT, $CDCl_3$) 18.0 ($CH(C^AH_3C^BH_3)$, **A** & **B**), 19.5 ($CH(C^AH_3C^BH_3)$, **A** & **B**), 23.5 ($C(C^AH_3C^BH_3)$, **A** & **B**), 29.1 ($C(C^AH_3C^BH_3)$, **A** & **B**), 29.8 (CH_2Ph, **A**), 30.5 ($CH(CH_3)_2$, **A** & **B**), 31.5 (CH_2Ph, **B**), 36.3 ($C(CH_3)_2$, **A** & **B**), 42.3 ($NHCCH_2C(CH_3)_2$, **A** & **B**), 59.0 ($CHCH_2Ph$, **A**), 59.1 ($CHCH_2Ph$, **B**), 61.6 (NHCH, **A** & **B**), 67.7 (OCH_2Ph, **A** & **B**), 111.4 (NHC=C*H*CO, **A** & **B**), [125.9 (CH), 128.2 (CH), 128.4 (CH), 128.6 (CH), 128.8 (CH), 129.1 (CH), 10C, *Ar*-H, **A** & **B**], 135.9 (OCH_2Ph, **A** & **B**), 141.6 (CH_2Ph, **A** & **B**), 150.8 (NH*C*=CH, **A** & **B**), 157.1 (*C*ONH, **A** & **B**), 170.9 (NHCH*C*O, **A** & **B**), 201.2 (NHC=CH*C*O, **A** & **B**); HRMS FAB (+ve) m/z 463.2596, $C_{28}H_{35}N_2O_4$ requires 463.2596.

5.2.36 N-allyloxycarbonyl-1-amino-1-cyclopentanecarboxylic acid [7]

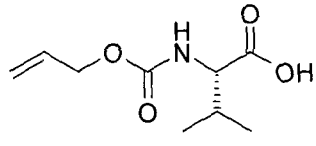

Experimental procedure 5.2.3.B was followed using L-valine (3.00 g, 25.7 mmol) and allyl chloroformate (3.9 ml, 37.5 mmol) dissolved in sodium hydroxide (25 ml, 4.0 M) to yield a colourless oil (3.86 g, 77 %); δ_H (250 MHz, $CDCl_3$) 0.92 (3H, d, J = 6.8, $CH(C^AH_3C^BH_3)$), 0.99 (3H, d, J = 6.8, $CH(C^AH_3C^BH_3)$), 2.18-2.21 (1H, m, $CH(CH_3)_2$), 4.30 (1H, dd, J = 4.4, 6.9, NHC*H*), 5.00 (2H, d, J = 5.4, $CH_2=CHCH_2$), 5.20-5.32 (1H, m, $CH_2=CHCH_2$), 5.84-5.99 (1H, m, $CH_2=CHCH_2$), 5.92 (1H, d, J = 6.9, NH); δ_C (63 MHz, DEPT, $CDCl_3$) 17.2 ($CH(C^AH_3C^BH_3)$), 18.9 ($CH(C^AH_3C^BH_3)$), 30.9 ($CH(CH_3)_2$), 58.6 (NHCH), 65.9 ($CH_2=CHCH_2$), 117.8 ($CH_2=CHCH_2$), 132.3 ($CH_2=CHCH_2$), 156.2 (CONH), 176.5 (CO_2H); MS ES m/z 202.2 $(M+H)^+$, 200.2 $(M-H)^-$.

5.2.37 Valine template library (3x6) synthesis

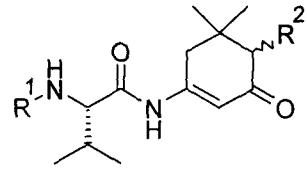

R^1 = Ph-, Alloc-, Boc-

R^2 = -H, $-CH_3$, $-CH_2CHCH_2$, $-CH_2Ph$, $-CH_2CO_2C(CH_3)_3$, $-CH_2(CH_2)_2Ph$

Table 5.1 Reagents

Reagent	No. Moles in stock solution (mmol)	DCM stock sol. volume (ml)	No. Moles Dispensed (mmol)	DCM Volume Dispensed (ml)
Amino acid	2.7	6.0	0.45	1.0
Enaminone	0.9	3.0	0.3	1.0
PyBroP	8.1	9.0	0.45	0.5
DMAP	16.2	9.0	0.9	0.5

Stock solutions of the reagents were prepared as in table 5.1. The PyBroP (0.5 ml) and DMAP (0.5 ml) solutions were dispensed into each of the 18 tubes being used in a MiniBlock^{TM}. Each valine derivative solution (1 ml) was manually dispensed into a vertical line of 6 tubes in the MiniBlock, the MiniBlock was then shaken on the Shaking and Washing Station for 5 minutes. The Miniblock was removed from the shaker and each amino-dimedone derivative solution (1 ml) was manually dispensed into a horizontal line of 3 tubes, the MiniBlock was then shaken overnight. The MiniBlock was drained into a 48 well plate and the DCM solutions transferred manually onto pre-packed silica columns. These were then subject to flash column chromatography in parallel on a Biotage QUAD 3 purification system using 30 % ethyl acetate in petroleum ether 40-60 as eluent.

Table 5.2 Array products

Ligand	Structure	Yield and Analysis
62	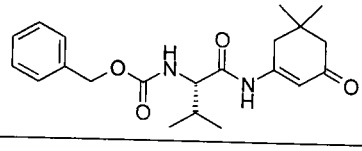	0.088 g, 80 %. Analysis same as **5.2.19**.
85	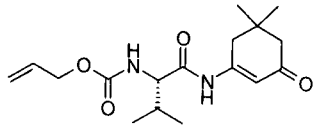	0.065 g, 67 %; δ_H (360 MHz, MeOD) 0.93 (3H, d, J = 6.8, CH($C^AH_3C^BH_3$)), 1.00 (3H, d, J = 6.8, CH($C^AH_3C^BH_3$)), 1.07 (6H, s, C(CH_3)$_2$), 2.19-2.26 (1H, m, CH(CH$_3$)$_2$), 2.27 (2H, s, CH_2C(CH$_3$)$_2$), 2.38 (2H, s, CH_2C(CH$_3$)$_2$), 4.30 (1H, dd, J = 5.5, 71, NHCH), 4.49-4.52 (2H, m, CH$_2$=CHCH_2), 5.13-5.30 (2H, m, CH_2=CHCH$_2$), 5.86-5.91 (1H, m, CH$_2$=CHCH$_2$), 6.78 (1H, s, NHC=CHCO); MS ES (+ve) m/z 323.1 $(M+H)^+$, 321.0 $(M-H)^-$.
86	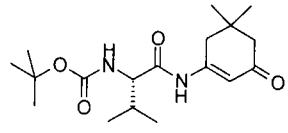	0.062 g, 62 %; δ_H (250 MHz, MeOD) 0.94 (3H, d, J = 6.8, CH($C^AH_3C^BH_3$)), 0.98 (3H, d, J = 6.8, CH($C^AH_3C^BH_3$),), 1.03 (6H, s, C(CH_3)$_2$), 1.41 (9H, s, C(CH_3)$_3$,), 2.13-2.16 (1H, m, CH(CH$_3$)$_2$), 2.22 (2H, s, CH_2C(CH$_3$)$_2$), 2.34 (2H, s, C(CH$_3$)$_2$CH_2), 4.20 (1H, dd, J = 4.0, 7.0, NHCH), 5.12 (1H, d, J = 7.0, NH), 6.62 (1H, s, NHC=CHCO), 8.05 (1H, s, br, NH); MS ES (+ve) m/z 339.2 $(M+H)^+$, 337.3 $(M-H)^-$.
87	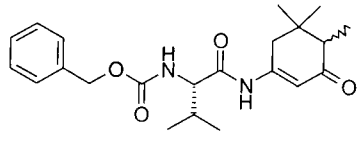 (diastereomers **A** & **B**)	0.095 g, 82 %; δ_H (250 MHz, $CDCl_3$) 0.93 (3H, d, J = 7.8, CH($C^AH_3C^BH_3$), **A** & **B**), 0.94 (3H, s, C($C^AH_3C^BH_3$), **A** & **B**), 0.95 (3H, d, J = 7.8, CH($C^AH_3C^BH_3$), **A** & **B**), 0.99 (3H, d, J = 6.9, CHCH_3, **A** & **B**), 1.02 (3H, s, C($C^AH_3C^BH_3$), **A** & **B**), 2.05-2.09 (1H, m, CH(CH$_3$)$_2$), 2.14-2.27 (3H, m, CH_2C(CH$_3$)$_2$, C(CH$_3$)$_2$CH, **A** & **B**), 3.98 (1H, dd, J = 7.2, 8.1, NHCH, **A** & **B**), 5.12 (2H, s, PhCH_2O, **A** & **B**), 5.54 (1H, d, J = 8.1, NH, **A** & **B**), 6.70 (1H, s, NHC=CHCO, **A**) , 6.71 (1H, s, NHC=CHCO, **B**), 7.25-7.35 (5H, m, Ar-H, **A** & **B**); MS ES (+ve) m/z 387.2 $(M+H)^+$, 385.2 $(M-H)^-$.
88	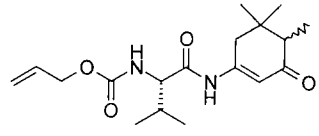 (diastereomers **A** & **B**)	0.066 g, 65 %; δ_H (250 MHz, $CDCl_3$) 0.85 (3H, d, J = 7.9, CH($C^AH_3C^BH_3$), **A** & **B**), 0.92 (3H, s, C($C^AH_3C^BH_3$), **A** & **B**), 0.94 (3H, d, J = 7.9, CH($C^AH_3C^BH_3$), **A** & **B**), 1.00 (3H, d, J = 7.1, CHCH_3, **A** & **B**), 1.02 (3H, s, C($C^AH_3C^BH_3$), **A** & **B**), 2.05-2.38 (4H, m, CHCH$_3$, CH(CH$_3$)$_2$, CH_2C(CH$_3$)$_2$, **A** & **B**), 4.06 (1H, dd, J = 7.4, 7.9, NHCH, **A** & **B**), 4.52 (2H, d, J = 5.5, CH$_2$CH=CH_2O, **A** & **B**), 5.18 (1H, dd, J = 1.3, 10.4, (CH^AH^B)CH=CH$_2$O, **A** & **B**), 5.19 (1H, dd, J

		= 1.3, 17.2, (CH^AH^B)CH=CH_2O, **A** & **B**), 5.54 (1H, d, *J* = 7.9, N*H*, **A** & **B**), 5.84 (1H, ddd, *J* = 5.5, 10.4, 17.2, CH_2CH=CH_2O, **A** & **B**), 6.57 (1H, s, NHC=C*H*CO, **A** & **B**), 8.36 (1H, s, br, N*H*, **A** & **B**); MS ES (+ve) m/z 337.1 $(M+H)^+$, 335.1 $(M-H)^-$.
89	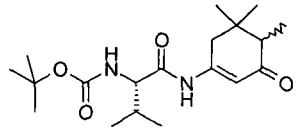 (diastereomers **A** & **B**)	0.078 g, 74 %; δ_H (250 MHz, $CDCl_3$) 0.91 (3H, d, *J* = 6.9, CH($C^AH_3C^BH_3$), **A** & **B**), 0.95 (3H, s, C($C^AH_3C^BH_3$), **A** & **B**), 0.98 (3H, d, *J* = 6.9, CH($C^AH_3C^BH_3$), **A** & **B**), 1.04 (3H, d, *J* = 7.0, $CHCH_3$, **A** & **B**), 1.05 (3H, s, C($C^AH_3C^BH_3$), **A** & **B**), 1.73 (9H, s, $C(CH_3)_3$, **A** & **B**), 2.11-2.39 (4H, m, $CHCH_3$, $CH(CH_3)_2$, $CH_2C(CH_3)_2$, **A** & **B**), 4.20 (1H, dd, *J* = 4.3, 8.4, NHC*H*, **A** & **B**), 5.12 (1H, d, *J* = 8.4, N*H*, **A** & **B**), 6.62 (1H, s, NHC=C*H*CO, **A**), 6.64 (1H, s, NHC=C*H*CO, **B**), 8.05 (1H, s, br, N*H*, **A** & **B**); MS ES (+ve) m/z 353.2 $(M+H)^+$, 351.2 $(M-H)^-$.
82	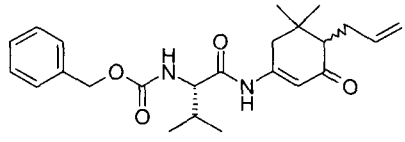 (diastereomers **A** & **B**)	0.086 g, 70 %. Analysis same as **5.2.33**.
90	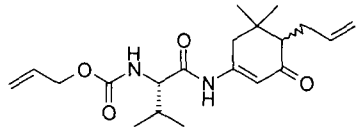 (diastereomers **A** & **B**)	0.086 g, 79 %; δ_H (250 MHz, MeOD) 0.90 (3H, d, *J* = 6.9, CH($C^AH_3C^BH_3$), **A** & **B**), 0.93 (3H, s, C($C^AH_3C^BH_3$), **A** & **B**), 0.94 (3H, d, *J* = 6.9, CH($C^AH_3C^BH_3$), **A** & **B**), 1.02 (3H, s, C($C^AH_3C^BH_3$), **A** & **B**), 2.08-2.35 (4H, m, $CHCH_2$, $CH(CH_3)_2$, $CH_2C(CH_3)_2$, **A** & **B**), 4.10-4.19 (1H, m, NHC*H*, **A** & **B**), 3.96-4.03 (2H, m, CH_2CH=CH_2, **A** & **B**), 4.52 (2H, d, *J* = 5.3, $CHCH_2CH$=CH_2, **A** & **B**), 5.13-5.31 (1H, m, CH_2CH=CH_2, **A** & **B**), 5.56 (1H, d, *J* = 7.7, N*H*, **A** & **B**), 5.76-5.99 (2H, m, CH_2CH=CH_2, $CHCH_2CH$=CH_2, **A** & **B**), 6.66 (1H, s, NHC=C*H*CO, **A**), 6.68 (1H, s, NHC=C*H*CO, **B**); MS ES (+ve) m/z 363.2 $(M+H)^+$, 361.2 $(M-H)^-$.
91	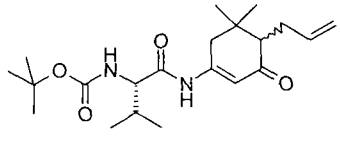 (diastereomers **A** & **B**)	0.075 g, 66 %; δ_H (250 MHz, $CDCl_3$) 0.86 (3H, d, *J* = 7.2, CH($C^AH_3C^BH_3$), **A** & **B**), 0.90 (3H, d, *J* = 7.2, CH($C^AH_3C^BH_3$), **A** & **B**), 0.91 (3H, s, C($C^AH_3C^BH_3$), **A** & **B**), 1.00 (3H, s, C($C^AH_3C^BH_3$), **A** & **B**), 1.39 (9H, s, $C(CH_3)_3$, **A**), 1.40 (9H, s, $C(CH_3)_3$, **B**), 1.98-2.06 (1H, m, $CH(CH_3)_2$, **A** & **B**), 2.13-2.30 (3H, m, $CH_2C(CH_3)_2$, $CHCH_2$), 3.90-4.05 (1H, m, NHC*H*, **A** & **B**), 4.86-4.99 (2H, m, $CHCH_2CH$=CH_2), 5.43 (1H, d, *J* = 5.0, N*H*, **A** & **B**), 5.85-5.94 (1H, m, $CHCH_2CH$=CH_2), 6.60 (1H, s, NHC=C*H*CO, **A** & **B**), 8.50 (1H, s, br, N*H*, **A** & **B**); MS ES (+ve) m/z 379.3 $(M+H)^+$, 377.3 $(M-H)^-$.

84	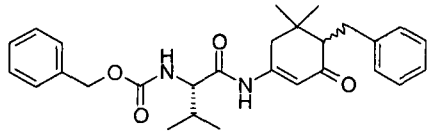 (diastereomers **A** & **B**)	0.104 g, 75 %. Analysis same as **5.2.35**.
92	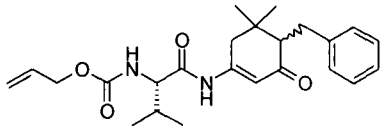 (diastereomers **A** & **B**)	0.089 g, 72 %; δ_H (250 MHz, $CDCl_3$) 0.94 (3H, d, J = 6.9, CH($C^AH_3C^BH_3$), **A** & **B**), 0.97 (3H, d, J = 6.9, CH($C^AH_3C^BH_3$), **A** & **B**), 1.02 (3H, s, C($C^AH_3C^BH_3$), **A** & **B**), 1.12 (3H, s, C($C^AH_3C^BH_3$), **A** & **B**), 2.12-2.23 (1H, m, C*H*(CH_3)$_2$), **A** & **B**), 2.38-2.46 (3H, m, CH_2C(CH_3)$_2$, C*H*CH_2Ph, **A** & **B**), 2.68 (1H, dd, J = 7.2, 14.1, CHCH^AH^BPh, **A** & **B**), 3.02 (1H, dd, J = 8.4, 14.1, CHCH^AH^BPh, **A** & **B**), 4.06 (1H, dd, J = 6.5, 7.2, NHC*H*, **A** & **B**), 4.58 (2H, d, J = 5.6, CH_2CH=CH_2, **A** & **B**), 5.20-5.36 (3H, m, CH_2CH=CH_2, N*H*, **A** & **B**), 5.86-5.93 (1H, m, CH_2C*H*=CH_2, **A** & **B**), 6.54 (1H, s, NHC=C*H*CO, **A**), 6.56 (1H, s, NHC=C*H*CO, **B**), 7.14-7.22 (5H, m, Ar-*H*, **A** & **B**), 8.16 (1H, s, br, N*H*, **A** & **B**); MS ES (+ve) m/z 413.3 $(M+H)^+$, 411.2 $(M-H)^-$.
93	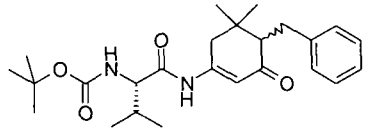 (diastereomers **A** & **B**)	0.102 g, 80 %; δ_H (250 MHz, $CDCl_3$) 0.87 (3H, d, J = 6.6, CH($C^AH_3C^BH_3$), **A** & **B**), 0.88 (3H, d, J = 6.6, CH($C^AH_3C^BH_3$), **A** & **B**), 0.90 (3H, s, C($C^AH_3C^BH_3$), **A**), 0.91 (3H, s, C($C^AH_3C^BH_3$), **B**), 1.00 (3H, s, C($C^AH_3C^BH_3$), **A**), 1.01 (3H, s, C($C^AH_3C^BH_3$), **B**), 1.37 (9H, s, C(CH_3)$_3$, **A**), 1.38 (9H, s, C(CH_3)$_3$, **B**), 1.98-2.06 (1H, m, C*H*(CH_3)$_2$, **A** & **B**), 2.16-2.34 (3H, m, CH_2C(CH_3)$_2$, C*H*CH_2Ph), 2.61 (1H, dd, J = 7.4, 14.1, CHCH^AH^BPh, **A**), 2.63 (1H, dd, J = 7.4, 14.1, CHCH^AH^BPh, **B**), 2.96 (1H, dd, J = 8.0, 14.1, CHCH^AH^BPh, **A**), 2.97 (1H, dd, J = 8.0, 14.1, CHCH^AH^BPh, **B**), 3.90-4.05 (1H, m, NHC*H*, **A** & **B**), 5.43 (1H, d, J = 5.0, N*H*, **A** & **B**), 6.60 (1H, s, NHC=C*H*CO, **A** & **B**), 7.05-7.16 (5H, m, Ar-*H*, **A** & **B**), 8.50 (1H, s, br, N*H*, **A** & **B**); δ_C (63 MHz, DEPT, $CDCl_3$) 17.9 (CH($C^AH_3C^BH_3$), **A** & **B**), 19.3 (CH($C^AH_3C^BH_3$), **A** & **B**), 23.2 (C($C^AH_3C^BH_3$), **A** & **B**), 28.3 (C(CH_3)$_3$, **A** & **B**), 28.9 (C($C^AH_3C^BH_3$), **A** & **B**), 30.5 (*C*H(CH_3)$_2$, **A** & **B**), 31.1 (*C*H_2Ph, **A**), 31.3 (*C*H_2Ph, **B**), 35.9 (*C*(CH_3)$_2$, **A**), 36.0 (*C*(CH_3)$_2$, **B**), 42.1 (NHC*C*H_2C(CH_3)$_2$, **A**), 42.3 (NHC*C*H_2C(CH_3)$_2$, **B**), 58.8 (C*H*CH_2Ph, **A**), 58.9 (C*H*CH_2Ph, **B**), 60.7 (NH*C*H, **A** & **B**), 80.4 (*C*(CH_3)$_3$, **A** & **B**), 111.1 (NHC=C*H*CO, **A** & **B**), [125.6 (CH), 128.1 (CH), 128.8 (CH), 5C, *Ar*-H, **A** & **B**], 141.3 (CH_2*Ph*, **A**), 141.6 (CH_2*Ph*, **B**), 150.8 (NH*C*=CH, **A** & **B**), 156.4 (*C*ONH, **A** & **B**), 171.6 (NHCH*C*O, **A** & **B**), 201.0

		(NHC=CH*C*O, **A**), 201.1 (NHC=CH*C*O, **B**); MS ES (+ve) m/z 429.3 $(M+H)^+$, 427.3 $(M-H)^-$.
83	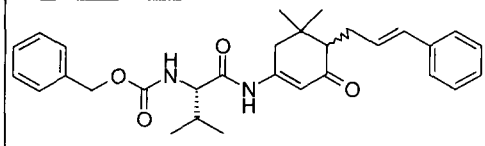 (diastereomers **A** & **B**)	0.105 g, 72 %. Analysis same as **5.2.34**.
94	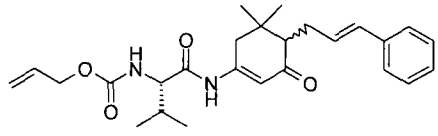 (diastereomers **A** & **B**)	0.090 g, 68 %; δ_H (250 MHz, $CDCl_3$) 0.92 (3H, d, J = 6.8, CH($C^AH_3C^BH_3$), **A** & **B**), 0.96 (3H, d, J = 6.8, CH($C^AH_3C^BH_3$), **A** & **B**), 0.98 (3H, s, C($C^AH_3C^BH_3$), **A** & **B**), 1.08 (3H, s, C($C^AH_3C^BH_3$), **A** & **B**), 2.15-2.49 (6H, m, C*H*CH_2CH=CH, C*H*$_2$C$(CH_3)_2$, C*H*$(CH_3)_2$, CHC*H*$_2$CH=CH, **A** & **B**), 4.09-4.12 (1H, m, NHC*H*, **A** & **B**), 4.59 (2H, d, J = 5.8, CH_2CH=C*H*$_2$, **A** & **B**), 5.22-5.35 (3H, m, C*H*$_2$CH=CH_2, N*H*, **A** & **B**), 5.87-5.95 (1H, m, CH_2C*H*=CH_2, **A** & **B**), 6.20-6.35 (2H, m, CH_2C*H*=C*H*Ph, **A** & **B**), 6.61 (1H, s, NHC=C*H*CO, **A** & **B**), 7.41-7.57 (5H, m, Ar-*H*, **A** & **B**), 7.97 (1H, s, br, N*H*, **A** & **B**); MS ES (+ve) m/z 439.3 $(M+H)^+$, 437.3 $(M-H)^-$.
95	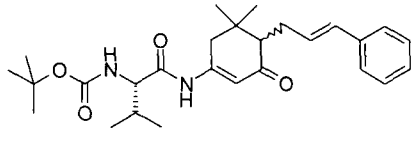 (diastereomers **A** & **B**)	0.113 g, 83 %; δ_H (250 MHz, MeOD) 0.93 (3H, d, J = 6.9, CH($C^AH_3C^BH_3$), **A** & **B**), 0.95 (3H, d, J = 6.9, CH($C^AH_3C^BH_3$), **A** & **B**), 1.05 (3H, s, C($C^AH_3C^BH_3$), **A** & **B**), 1.11 (3H, s, C($C^AH_3C^BH_3$), **A** & **B**), 1.42 (9H, s, C(C*H*$_3)_3$, **A** & **B**), 2.12-2.45 (6H, m, C*H*CH_2CH=CH, C*H*$_2$C$(CH_3)_2$, C*H*$(CH_3)_2$, CHC*H*$_2$CH=CH, **A** & **B**), 3.92-3.96 (1H, m, NHC*H*, **A** & **B**), 6.15-6.39 (2H, m, CH_2C*H*=C*H*Ph, **A** & **B**), 6.74 (1H, s, NHC=C*H*CO, **A** & **B**), 7.13-7.30 (5H, m, Ar-*H*, **A** & **B**), 7.90 (1H, s, br, N*H*, **A** & **B**); MS ES (+ve) m/z 477.3 $(M+Na)^+$, 453.4 $(M-H)^-$.
96	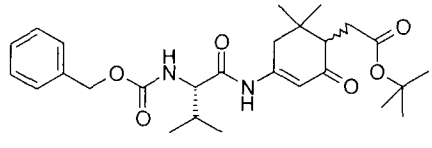 (diastereomers **A** & **B**)	0.114 g, 78 %; δ_H (250 MHz, $CDCl_3$) 0.84 (3H, d, J = 2.5, CH($C^AH_3C^BH_3$), **A**), 0.91 (3H, d, J = 2.5, CH($C^AH_3C^BH_3$), **B**), 0.93 (3H, s, C($C^AH_3C^BH_3$), **A** & **B**), 0.96 (3H, d, J = 6.8, CH($C^AH_3C^BH_3$), **A**), 0.99 (3H, d, J = 6.8, CH($C^AH_3C^BH_3$), **B**), 1.03 (3H, s, C($C^AH_3C^BH_3$), **A** & **B**), 1.45 (9H, s, C(C*H*$_3)_3$, **A** & **B**), 2.07-2.24 (2H, m, C*H*$^AH^BC(CH_3)_2$, CHC*H*$^AH^B$), 2.54-2.67 (2H, m, CHCH^AH^B, CH^AH^BC$(CH_3)_2$), 2.83 (1H, dd, J = 4.6, 8.0, C*H*CH_2, **A** & **B**), 4.09-4.12 (1H, m, NHC*H*, **A** & **B**), 5.09 (2H, s, PhC*H*$_2$O, **A**), 5.10 (2H, s, PhC*H*$_2$O, **B**), 5.40 (1H, d, J = 8.6, N*H*, **A**), 5.77 (1H, d, J = 8.6, N*H*, **B**), 6.59 (1H, s, NHC=C*H*CO, **A** & **B**), 7.32 (5H, s, Ar-*H*, **A**), 7.35 (5H, s, Ar-*H*, **B**), 8.39 (1H, s, br, N*H*, **A**), 8.42 (1H, s, br, N*H*, **B**); δ_C (63 MHz, DEPT, DMSO) 17.2 (CH($C^AH_3C^BH_3$), **A**) 17.7

		(CH($C^AH_3C^BH_3$), **B**), 18.9 (CH($C^AH_3C^BH_3$), **A**), 19.2 (CH($C^AH_3C^BH_3$), **B**), 21.1 (C($C^AH_3C^BH_3$), **A & B**), 27.8 (C(CH_3)$_3$, **A & B**), 28.7 (C($C^AH_3C^BH_3$), **A & B**), 30.4 ($CH_2CO_2C(CH_3)_3$, **A & B**), 30.9 ($CH(CH_3)_2$, **A & B**), 35.6 ($C(CH_3)_2$, **A & B**), 43.5 ($NHCCH_2C(CH_3)_2$, **A & B**), 52.6 ($C(CH_3)_2CH$, **A & B**), 58.7 (NHCH, **A & B**), 66.9 (OCH_2Ph, **A**), 67.3 (OCH_2Ph, **B**), 80.3 ($C(CH_3)_3$, **A & B**), 111.3 (HNC=CHCO, **A & B**), [127.9 (CH), 128.0 (CH), 128.1 (CH), 128.3 (CH), 128.4 (CH), 128.5 (CH), *Ar*-H, **A & B**], 135.6 (OCH_2Ph, **A**), 135.7 (OCH_2Ph, **B**), 151.4 (NHC=CH, **A & B**), 156.3 (CONH, **A & B**), 156.9 (CONH, **A & B**) 175.4 (NHCHCO, **A & B**), 199.6 (NHC=CHCO, **A & B**); MS ES (+ve) m/z 487.3 $(M+H)^+$, 485.3 $(M-H)^-$.
97	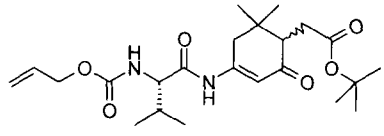 (diastereomers **A & B**)	0.080 g, 61 %; δ_H (250 MHz, $CDCl_3$) 0.84 (3H, d, J = 6.2, CH($C^AH_3C^BH_3$), **A & B**), 0.88 (3H, s, C($C^AH_3C^BH_3$), **A & B**), 0.91 (3H, d, J = 6.2, CH($C^AH_3C^BH_3$), **A & B**), 1.04 (3H, s, C($C^AH_3C^BH_3$), **A & B**), 1.47 (9H, s, C(CH_3)$_3$, **A & B**), 2.02-2.17 (2H, m, $CH^AH^BC(CH_3)_2$, $CHCH^AH^B$, **A & B**), 2.50-2.62 (2H, m, $CH^AH^BC(CH_3)_2$, $CHCH^AH^B$, **A & B**), 2.70 (1H, dd, J = 4.5, 7.9, $CHCH_2$, **A & B**), 4.09-4.12 (1H, m, NHCH, **A & B**), 4.59 (2H, d, J = 5.8, $CH_2CH=CH_2$, **A & B**), 5.20-5.32 (3H, m, $CH_2CH=CH_2$, NH, **A & B**), 5.86-5.96 (1H, m, $CH_2CH=CH_2$, **A & B**), 6.50 (1H, s, NHC=CHCO, **A & B**), 8.30 (1H, s, br, NH, **A & B**); MS ES (+ve) m/z 437.4 $(M+H)^+$, 435.4 $(M-H)^-$.
98	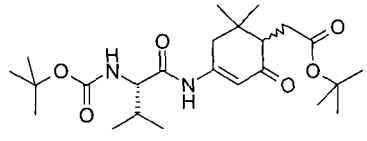 (diastereomers **A & B**)	0.079 g, 58 %; δ_H (250 MHz, $CDCl_3$) 0.82 (3H, d, J = 7.0, CH($C^AH_3C^BH_3$), **A & B**), 0.90 (3H, s, C($C^AH_3C^BH_3$), **A & B**), 0.94 (3H, d, J = 7.0, CH($C^AH_3C^BH_3$), **A & B**), 1.01 (3H, s, C($C^AH_3C^BH_3$), **A & B**), 1.50 (9H, s, C(CH_3)$_3$, **A & B**), 1.55 (9H, s, C(CH_3)$_3$, **A & B**), 2.00-2.16 (2H, m, $CH^AH^BC(CH_3)_2$, $CHCH^AH^B$, **A & B**), 2.48-2.60 (2H, m, $CH^AH^BC(CH_3)_2$, $CHCH^AH^B$, **A & B**), 2.68-2.73 (1H, m, $CHCH_2$, **A & B**), 4.01-4.09 (1H, m, NHCH, **A & B**), 5.54 (1H, d, J = 7.0, NH, **A & B**), 6.47 (1H, s, NHC=CHCO, **A & B**); MS ES (+ve) m/z 453.4 $(M+H)^+$, 451.4 $(M-H)^-$.

5.2.38 5,5-dimethyl-3-(L-phenylalanine methyl ester)-cyclohex-2-enone (99)

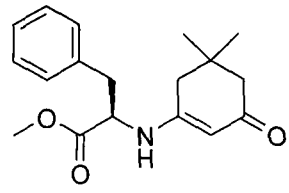

L-phenylalanine methyl ester hydrochloride (0.31 g, 1.43 mmol) was added to a stirring suspension of dimedone (0.2 g, 1.43 mmol) in glacial acetic acid (0.25 ml) and toluene (20 ml). The reaction mixture was heated to reflux for 2 hours and water removed azeotropically using Dean-Stark apparatus. After cooling to room temperature the solvent was evaporated *in vacuo* and the residue redissolved in EtOAc (10 ml), washed with water (5 ml) then saturated $NaHCO_3$ solution (5 ml) and dried ($MgSO_4$). Flash column chromatography on silica gel using 3 % methanol in dichloromethane as eluent afforded a yellow oil (0.41 g, 97 %); δ_H (250 MHz, $CDCl_3$) 0.94 (3H, s, $C(C^A\mathit{H}_3C^BH_3)$), 0.96 (3H, s, $C(C^AH_3C^B\mathit{H}_3)$), 2.06 (2H, s, $C\mathit{H}_2C(CH_3)_2$), 2.08 (2H, s, $C\mathit{H}_2C(CH_3)_2$), 3.05 (2H, dd, J = 5.7, 13.8, $CHC\mathit{H}_2Ph$) 3.63 (3H, s, $OC\mathit{H}_3$), 4.22-4.29 (1H, m, $C\mathit{H}CH_2Ph$), 4.86 (1H, d, J = 7.8, N*H*), 5.02 (1H, s, NHC=C*H*CO), 6.91-6.95 (3H, m, Ar-*H*), 7.14-7.18 (2H, m, Ar-*H*); δ_C (63 MHz, DEPT, $CDCl_3$) 28.8 ($C(\mathit{C}^AH_3C^BH_3)$), 28.9 ($C(C^A\mathit{H}_3C^BH_3)$), 33.5 ($\mathit{C}(CH_3)_2$), 37.5 ($\mathit{C}H_2Ph$), 44.1 ($NC\mathit{C}H_2C(CH_3)_2$), 50.8 ($C(CH_3)_2\mathit{C}H_2C{=}O$), 53.2 ($OCH_3$), 56.3 ($C\mathit{H}CH_2Ph$), 97.4 (NC=*C*HCO), [128.0 (CH), 129.3 (CH), 129.8 (CH), 5C, *Ar*-H], 135.7 ($OCH_2\mathit{Ph}$), 161.4 (N*C*=CH), 172.1 ($\mathit{C}OOCH_3$), 198.0 (NC=CH*C*O); HRMS FAB (+ve) m/z 302.1749, $C_{18}H_{24}NO_3$ requires 302.1756.

5.2.39 5,5-dimethyl-3-(L-valine methyl ester)-cyclohex-2-enone (100)

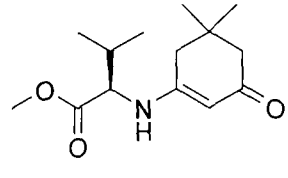

Experimental procedure 5.2.38 was followed using *L*-valine methyl ester hydrochloride (0.24 g, 1.43 mmol) and dimedone (0.2 g, 1.43 mmol) in glacial acetic

acid (0.25 ml) and toluene (20 ml). Flash column chromatography on silica gel using 3 % methanol in dichloromethane as eluent afforded a yellow solid (0.33 g, 92 %); R_f 0.17 (3 % MeOH in DCM); δ_H (300 MHz, $CDCl_3$) 0.93 (3H, d, J = 6.9, $CH(C^AH_3C^BH_3)$), 1.01 (3H, d, J = 6.9, $CH(C^AH_3C^BH_3)$), 1.06 (3H, s, $C(C^AH_3C^BH_3)$), 1.07 (3H, s, $C(C^AH_3C^BH_3)$), 2.11-2.22 (1H, m, $CH(CH_3)_2$), 2.18 (2H, s, $CH_2C(CH_3)_2$), 2.25 (2H, s, $CH_2C(CH_3)_2$), 3.76 (3H, s, OCH_3), 3.91 (1H, dd, J = 5.1, 8.0, NHCH), 5.07 (1H, s, NHC=CHCO), 5.15 (1H, d, J = 8.0, NH); δ_C (75 MHz, DEPT, $CDCl_3$) 18.7 ($CH(CH_3C^BH_3)$), 18.9 ($CH(C^AH_3CH_3)$), 28.4 ($C(CH_3C^BH_3)$), 28.5 ($C(C^AH_3CH_3)$), 31.2 ($CH(CH_3)_2$), 33.0 ($C(CH_3)_2$), 43.8 ($NCCH_2C(CH_3)_2$), 50.5 ($C(CH_3)_2CH_2C$=O), 53.2 (OCH_3), 60.7 (NHCH), 96.7 (NC=CHCO), 162.1 (NC=CH), 172.2 ($COOCH_3$), 197.4 (NC=CHCO); MS ES (+ve) 254.0 $(M+H)^+$.

5.2.40 5,5-dimethyl-3-(L-tyrosine methyl ester)-cyclohex-2-enone (101)

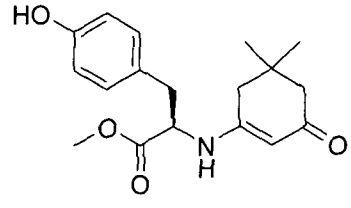

L-tyrosine methyl ester hydrochloride (0.33 g, 1.43 mmol) was added to a stirring suspension of dimedone (0.2 g, 1.43 mmol) in glacial acetic acid (0.25 ml) and toluene (20 ml). The reaction mixture was heated to reflux for 5 hours and water removed azeotropically using Dean-Stark apparatus. After cooling to room temperature the solvent was evaporated *in vacuo* and the residue redissolved in EtOAc (10 ml), washed with water (5 ml) then saturated $NaHCO_3$ solution (5 ml) and dried ($MgSO_4$). Flash column chromatography on silica gel using 1 % methanol in ethyl acetate as eluent afforded a white solid (0.20 g, 74 %); R_f 0.42 (3 % MeOH in EtOAC); δ_H (300 MHz, $CDCl_3$) 1.06 (3H, s, $C(C^AH_3C^BH_3)$), 1.08 (3H, s, $C(C^AH_3C^BH_3)$), 2.14-2.27 (4H, m, $CH_2C(CH_3)_2$, $C(CH_3)_2CH_2$), 2.24 (2H, s, $CH_2C(CH_3)_2$), 2.95 (1H, dd, J = 5.4, 14.1, C^AHC^BHPh), 3.06 (1H, dd, J = 5.4, 14.1, C^AHC^BHPh), 3.74 (3H, s, OCH_3), 4.22-4.29 (1H, dd, J = 5.4, 7.0, NHCH), 5.16 (1H, s, NHC=CHCO), 5.23 (1H, br, d, J = 6.9, NH), 6.79 (2H, d, J = 8.8, Ar-H), 6.86

(2H, d, J = 8.8, Ar-*H*), 7.14-7.18 (2H, m, Ar-*H*); δ_C (75 MHz, DEPT, $CDCl_3$) 28.3 ($C(C^AH_3C^BH_3)$), 28.5 ($C(C^AH_3C^BH_3)$), 33.1 ($C(CH_3)_2$), 36.4 (CH_2Ph), 43.8 ($NCCH_2C(CH_3)_2$), 50.1 ($C(CH_3)_2CH_2C{=}O$), 52.9 (OCH_3), 56.3 ($CHCH_2Ph$), 96.5 ($NC{=}CHCO$), [116.1 (*C*H), 130.5 (*C*H), 4C, *Ar*-H], 125.9 (OCH_2Ph), 130.6 (*Ph*OH), 156.6 ($NC{=}CH$), 171.8 ($COOCH_3$), 198.5 ($NC{=}CHCO$); MS ES (+ve) 254.0 $(M+H)^+$.

5.2.41 (6,6-dimethyl-4-methoxy-2-oxo-cyclohex-3enyl)-acetic acid (102)

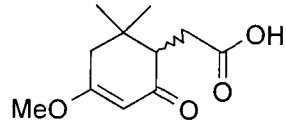

Trifluoroacetic acid (9.2 ml, 0.09 mol) was added to a solution of **46** (2.56 g, 0.009 mol) and triethylsilane (3.79 ml, 0.02 mol) in DCM (20 ml) and the solution stirred at room temperature for 2 hours. The DCM was evaporated *in vacuo* and the residue redissolved in EtOAc (15 ml) and washed with water (5 ml) then dried ($MgSO_4$). The EtOAc solution was concentrated *in vacuo* to give pale yellow oil. Flash column chromatography on silica gel using 50 % ethyl acetate in petroleum ether 40-60 as eluent afforded a white solid (1.64 g, 81 %); δ_H (250 MHz, CDCl3) 0.87 (3H, s, $C(C^AH_3C^BH_3)$), 1.12 (3H, s, $C(C^AH_3C^BH_3)$), 2.16 (1H, d, J = 17.4, $CH^AH^BC(CH_3)_2$), 2.31 (1H, dd, J = 1.9, 14.3, $CHCH^AH^BCO_2H$), 2.57 (1H, dd, J = 1.1, 17.4, $CH^AH^BC(CH_3)_2$), 2.70-2.84 (1H, m, $CHCH^AH^BCO_2H$, $CHCH_2$), 3.70 (3H, s, CH_3O), 5.40 (1H, d, J = 1.1, $CH_3OC{=}CHCO$), 9.31 (1H, 2, br, $COOH$); δ_C (63 MHz, DEPT, $CDCl_3$) 20.9 ($C(C^AH_3C^BH_3)$), 28.7 ($C(C^AH_3C^BH_3)$), 29.6 ($CHCH_2$), 35.6 ($C(CH_3)_2$), 44.2 ($CH_2C(CH_3)_2$), 52.5 ($C(CH_3)_2CH$), 55.7 (CH_3O), 100.6 ($CH_3OC{=}CHCO$), 175.9 (CO_2H), 178.1 (CH_3OC), 199.3 ($CH_3OC{=}CHCO$); HRMS EI (+ve) m/z 212.1048, $C_{11}H_{16}O_4$ requires 212.1048; mp 115-117°C.

5.2.42 (6,6-dimethyl-4-methoxy-2-oxo-cyclohex-3enyl)-acetyl-L-valinyl methyl ester (103)

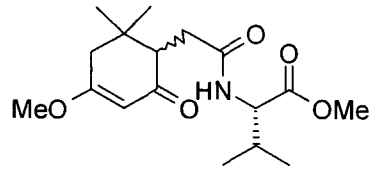

(diastereomers **A** & **B**)

PyBOP (0.489 g, 0.94 mmol), DIPEA (0.16 ml, 1.88 mmol) and **102** (0.200 g, 0.94 mmol) were dissolved in DCM (10 ml) and stirred at room temperature. After 5 minutes, *L*-valine methyl ester hydrochloride (0.158 g, 0.94 mmol), was added and the solution stirred at room temperature. After 2 hours the DCM was evaporated *in vacuo* and the residue redissolved in EtOAc (10 ml). The solution was washed with 1M $KHSO_4$ solution (2 ml), water (2 ml), saturated $NaHCO_3$ solution (2 ml), water (2 ml), dried ($MgSO_4$) and the solvent removed *in vacuo* to give a yellow oil. Flash column chromatography on silica gel using 40 % ethyl acetate in petroleum ether 40-60 as eluent afforded a viscous yellow oil (0.21 g, 74 %); δ_H (250 MHz, $(CD_3)_2CO$) 0.80 (3H, s, $C(C^AH_3C^BH_3)$, **A**), 0.81 (3H, s, $C(C^AH_3C^BH_3)$, **B**), 0.87 (3H, d, J = 6.8, $CH(C^AH_3C^BH_3)$, **A** & **B**), 0.90 (3H, d, J = 6.8, $CH(C^AH_3C^BH_3)$, **A** & **B**), 1.03 (3H, s, $C(C^AH_3C^BH_3)$, **A**), 1.04 (3H, s, $C(C^AH_3C^BH_3)$, **B**), 2.02-2.21 (3H, m, $CH^AH^B(CH_3)_2$, $CHCH_2$, **A** & **B**), 2.48-2.75 (3H, m, $CH^AH^B(CH_3)_2$, $CH(CH_3)_2$, $CHCH_2$, **A** & **B**), 3.62 (3H, s, CH_3O, **A**), 3.63 (3H, s, CH_3O, **B**), 3.66 (3H, s, CH_3O, **A**), 3.67 (3H, s, CH_3O, **B**), 4.32 (1H, d, J = 5.7, NHCH, **A** & **B**), 5.27 (1H, d, J = 1.6, $CH_3OC{=}CHCO$, **A**), 5.28 (1H, d, J = 1.6, $CH_3OC{=}CHCO$, **B**); δ_C (63 MHz, DEPT, $(CD_3)_2CO$) 17.7 ($CH(C^AH_3C^BH_3$, **A** & **B**), 18.8 ($CH(C^AH_3C^BH_3$, **A** & **B**), 20.8 ($C(C^AH_3C^BH_3$, **A** & **B**), 28.2 ($C(C^AH_3C^BH_3$, **A** & **B**), 30.7 ($CHCH_2$, **A** & **B**), 30.7 ($CH(CH_3)_2$, **A** & **B**), 35.7 ($C(CH_3)_2$, **A**), 35.9 ($C(CH_3)_2$, **B**), 44.0 ($CH_2C(CH_3)_2$, **A** & **B**), 49.0 (CO_2CH_3, **A** & **B**), 52.7 ($CHCH_2$, **A**), 52.9 ($CHCH_2$, **B**), 55.6 (CH_3O, **A** & **B**), 57.6 (NHCH, **A** & **B**), 100.5 ($CH_3OC{=}CHCO$, **A** & **B**), 172.3 (CONH, **A**), 172.4 (CONH, **B**), 172.9 (CO_2CH_3, **A**), 173.0 (CO_2CH_3, **B**), 175.6 (CH_3OC, **A**), 175.8 (CH_3OC, **B**), 198.9 ($CH_3OC{=}CHCO$, **A**), 199.0 ($CH_3OC{=}CHCO$, **B**); HRMS EI (+ve) m/z 325.1893, $C_{17}H_{27}NO_5$ requires 325.1889.

5.2.43 *2-(6,6-dimethyl-4-methoxy-2-oxo-cyclohex-3-enyl)-N-((S)-1-phenyl-ethyl)-acetamide (104)*

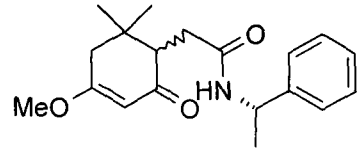

(diastereomers **A** & **B**)

Experimental procedure 5.2.42 was followed using PyBOP (0.435 g, 0.7 mmol), DIPEA (0.15 ml, 1.4 mmol), **71** (0.150 g, 0.7 mmol) and (S)-α methyl benzylamine (0.09 ml, 0.7 mmol) in DCM (10 ml). Flash column chromatography on silica gel using 50 % ethyl acetate in petroleum ether 40-60 as eluent afforded a yellow oil (0.181 g, 82 %); δ_H (250 MHz, CH_3OD); 1.00 (3H, s, $C(C^AH_3C^BH_3)$, **A** & **B**), 1.21 (3H, s, $C(C^AH_3C^BH_3)$, **A** & **B**), 1.53 (3H, d, J = 7.0, CH_3, **A**), 1.54 (3H, d, J = 7.0, CH_3, **B**), 2.31 (1H, d, J = 17.4, $CH^AH^BC(CH_3)_2$, **A** & **B**), 2.37 (1H, dd, J = 4.5, 15.1, $CHCH^AH^B$, **A** & **B**), 2.31 (1H, d, J = 17.4, $CH^AH^BC(CH_3)_2$, **A** & **B**), 2.67 (1H, d, J = 17.4, $CH^AH^BC(CH_3)_2$, **A** & **B**), 2.73 (1H, dd, J = 7.9, 15.1, $CHCH^AH^B$, **A** & **B**), 2.94 (1H, dd, J = 4.5, 7.9, $CHCH_2$, **A** & **B**), 3.81 (3H, s, CH_3O, **A**), 3.82 (3H, s, CH_3O, **B**), 5.04-5.16 (1H, m, NHC*H*, **A** & **B**), 5.46 (1H, d, J = 1.3, CH_3OC=*C*HCO, **A** & **B**), 7.30-7.50 (5H, m, Ar-*H*, **A** & **B**), 8.43 (1H, d, J = 7.6, N*H*, **A** & **B**); δ_C (63 MHz, DEPT, CH_3OD) 21.6 ($C(C^AH_3C^BH_3$, **A** & **B**), 22.5 (CH_3, **A**), 22.6 (CH_3, **B**) 28.9 ($C(C^AH_3C^BH_3$, **A** & **B**), 32.3 ($CHCH_2$, **A** & **B**), 36.8 ($C(CH_3)_2$, **A** & **B**), 44.8 ($CH_2C(CH_3)_2$, **A** & **B**), 50.0 (NHCH, **A** & **B**), 53.9 ($CHCH_2$, **A** & **B**), 56.4 (CH_3O, **A** & **B**), 101.0 (CH_3OC=*C*HCO, **A** & **B**), [127.1 (CH), 127.8 (CH), 129.3 (CH), 5C, *Ar*-H, **A** & **B**], 145.1 ($CH(CH_3)Ph$, **A**) 145.2 ($CH(CH_3)Ph$, **B**), 174.5 (*C*ONH **A** & **B**), 178.5 (CH_3OC **A** & **B**), 202.4 (CH_3OC=CH*C*O **A** & **B**); HRMS EI (+ve) m/z 315.1833, $C_{19}H_{25}NO_3$ requires 315.1889.

5.2.44 5,5-dimethyl-3-methoxy-6-(2-(2-methyl-piperidin-1-yl)-2-oxo-ethyl)-cyclohex-2-enone (105)

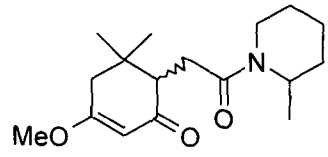

Experimental procedure 5.2.42 was followed using PyBOP (0.186 g, 0.3 mmol), DIPEA (0.06 ml, 0.6 mmol), **71** (0.064 g, 0.3 mmol) and 2-methyl piperidine (0.04 ml, 0.3 mmol) in DCM (10 ml). Flash column chromatography on silica gel using 50 % ethyl acetate in petroleum ether 40-60 as eluent afforded a yellow oil (0.069 g, 79 %); MS ES (+ve) m/z 294.1 $(M+H)^+$.

5.2.45 6-allyl-3-(N-benzyloxycarbonyl-D-valinyl-amino)-5,5-dimethyl-cyclohex-2-enone (106)

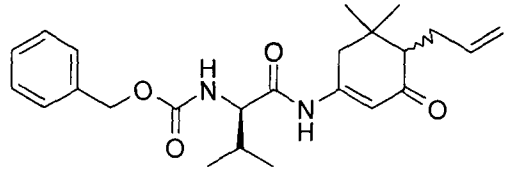

(diastereomers **A** & **B**)

Experimental procedure 5.2.33 was followed using *N*-benzyloxycarbonyl-D-valine (0.210g, 0.84 mmol), PyBroP (0.391 g, 0.84 mmol), DMAP (0.205 mg, 1.68 mmol) and **78** (0.100 g, 0.56 mmol) in DCM (10 ml). Flash column chromatography on silica gel using 30 % ethyl acetate in petroleum ether 40-60 as eluent afforded a white solid (0.206 g, 89 %); δ_H (250 MHz, CH_3OD) 0.97 (3H, d, J = 6.8, $CH(C^AH_3C^BH_3)$, **A** & **B**), 0.99 (3H, d, J = 6.8, $CH(C^AH_3C^BH_3)$, **A** & **B**), 1.02 (3H, s, $C(C^AH_3C^BH_3)$, **A** & **B**), 1.05 (3H, s, $C(C^AH_3C^BH_3)$, **A** & **B**), 2.17-2.36 (6H, m, $CH(CH_3)_2$, $CH_2C(CH_3)_2$, $CHCH_2CH{=}CH_2$, $CHCH_2CH{=}CH_2$, **A** & **B**), 3.34-3.39 (1H, m, NHCH, **A** & **B**), 4.95-5.03 (2H, m, $CHCH_2CH{=}CH_2$, **A** & **B**), 5.20 (2H, s, $PhCH_2O$, **A** & **B**), 5.28 (1H, d, J = 7.1, br, NH, **A** & **B**), 5.83-5.87 (1H, m, $CHCH_2CH{=}CH_2$, **A** & **B**), 6.53 (1H, s, $NHC{=}CHCO$, **A**), 6.55 (1H, s, $NHC{=}CHCO$,

B) 7.23-7.33 (5H, m, Ar-*H*, **A** & **B**), 7.76 (1H, s, br, N*H*, **A** & **B**); δ_C (63 MHz, DEPT, MeOD) 18.4 (CH($C^AH_3C^BH_3$), **A** & **B**), 19.6 (CH($C^AH_3C^BH_3$), **A** & **B**), 24.6 (C($C^AH_3C^BH_3$), **A** & **B**), 28.8 (C($C^AH_3C^BH_3$), **A** & **B**), 30.7 (CH_2CH=CH_2, **A** & **B**), 30.8 (CH$(CH_3)_2$, **A** & **B**), 36.2 (C$(CH_3)_2$, **A** & **B**), 41.7 (NHCCH_2C$(CH_3)_2$, **A** & **B**), 57.1 (C$(CH_3)_2$CH, **A** & **B**), 61.8 (NHCH, **A** & **B**), 67.7 (OCH_2Ph, **A** & **B**), 110.8 (HNC=CHCO, **A** & **B**), 115.9 (CH_2CH=CH_2, **A** & **B**), [128.7 (CH), 129.0 (CH), 129.6 (CH), 5C, *Ar*-H, **A** & **B**], 136.2 (OCH_2*Ph*, **A** & **B**), 137.4 (CH_2CH=CH_2, **A** & **B**), 151.2 (NHC=CH, **A** & **B**), 156.8 (CONH, **A** & **B**), 170.9 (NHCHCO, **A** & **B**), 203.1 (NHC=CHCO, **A** & **B**) HRMS FAB (+ve) m/z 412.2363, $C_{24}H_{32}N_2O_4$ requires 412.2362.

5.2.46 6-allyl-3-(N-benzyloxycarbonyl-L-leucyl-amino)-5,5-dimethyl-cyclohex-2-enone (107)

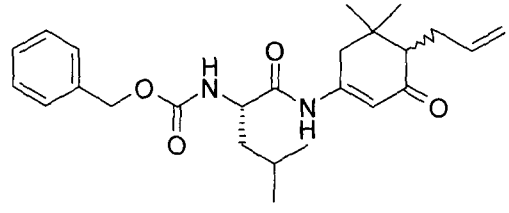

(diastereomers **A** & **B**)

Experimental procedure 5.2.33 was followed using N-benzyloxycarbonyl-L-leucine (0.111 g, 0.42 mmol), PyBroP (0.195 g, 0.42 mmol), DMAP (0.102 mg, 0.84 mmol) and **78** (0.050 g, 0.28 mmol) in DCM (3 ml). Flash column chromatography on silica gel using 30 % ethyl acetate in petroleum ether 40-60 as eluent afforded a white solid (0.104 g, 87 %); R_f 0.77 (50 % EtOAc in petroleum ether 40-60); δ_H (250 MHz, $CDCl_3$) 0.85-1.06 (12H, m, CH(CH_3)$_2$, C(CH_3)$_2$, **A** & **B**), 1.51-1.67 (3H, m, CH_2CH$(CH_3)_2$, CH_2CH$(CH_3)_2$, **A** & **B**), 2.07-2.39 (5H, m, CH_2C$(CH_3)_2$, CHCH_2CH=CH_2, CHCH_2CH=CH_2, **A** & **B**), 4.10-4.16 (1H, m, NHC*H*, **A** & **B**), 4.91-5.02 (2H, m, CHCH_2CH=CH_2, **A** & **B**), 5.11 (2H, s, PhCH_2O, **A** & **B**), 5.63-5.81 (2H, m, N*H*, CHCH_2C*H*=CH_2, **A** & **B**), 6.56 (1H, s, NHC=C*H*CO, **A** & **B**), 7.28-7.35 (5H, m, Ar-*H*, **A** & **B**), 8.40 (1H, s, br, N*H*, **A** & **B**); δ_C (63 MHz, DEPT, $CDCl_3$) 22.1 (CH($C^AH_3C^BH_3$), **A** & **B**), 23.2 (CH($C^AH_3C^BH_3$), **A** & **B**), 24.7

($C(C^AH_3C^BH_3)$, **A & B**), 24.9 ($CH(C^AH_3C^BH_3)$, 29.0 ($C(C^AH_3C^BH_3)$, **A & B**), 30.3 ($CH_2CH{=}CH_2$, **A & B**), 30.9 ($CH_2CH(CH_3)_2$, **A & B**), 35.8 ($C(CH_3)_2$, **A & B**), 41.7 ($NHCCH_2C(CH_3)_2$, **A & B**), 57.2 (NHCH, **A & B**), 67.3 ($PhCH_2$, **A & B**), 111.2 (NHC=CHCO, **A & B**), 115.9 ($CH_2CH{=}CH_2$, **A & B**), [128.4 (CH), 128.8 (CH), 128.9 (CH), 5C, *Ar*-H, **A & B**], 137.9 ($PhCH_2O$, **A & B**), 137.2 ($CH_2CH{=}CH_2$, **A & B**), 151.8 (NHC=CH, **A & B**), 152.4 (CONH, **A & B**), 171.9 (NHCHCO, **A & B**), 202.2 (NHC=CHCO, **A & B**); MS ES 427.0 $(M+H)^+$, 425 $(M-H)^-$.

5.2.47 6-allyl-3-(N-benzyloxycarbonyl-L-isoleucyl-amino)-5,5-dimethylcyclohex-2-enone (108)

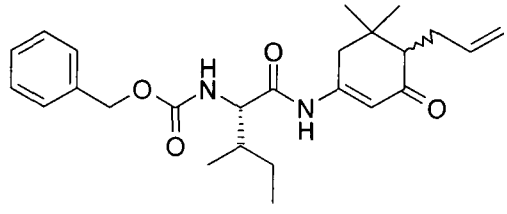

(diastereomers **A & B**)

Experimental procedure 5.2.33 was followed using N-benzyloxycarbonyl-L-isoleucine (0.111 g, 0.42 mmol), PyBroP (0.195 g, 0.42 mmol), DMAP (0.102 mg, 0.84 mmol) and **78** (0.050 g, 0.28 mmol) in DCM (3 ml). Flash column chromatography on silica gel using 30 % ethyl acetate in petroleum ether 40-60 as eluent afforded a white solid (0.099 g, 83 %); R_f 0.78 (50 % EtOAc in petroleum ether 40-60); δ_H (250 MHz, $CDCl_3$) 0.80-0.93 (6H, m, ($CH(CH_3)CH_2CH_3$), **A & B**), 0.95 (3H, s, $C(C^AH_3C^BH_3)$, **A & B**), 1.04 (3H, s, $C(C^AH_3C^BH_3)$, **A & B**), 1.22-1.40 (2H, m, ($CH(CH_3)CH_2CH_3$), 1.88-2.39 (6H, m, $CH_2C(CH_3)_2$, $CHCH_2CH{=}CH_2$, $CHCH_2CH{=}CH_2$, $CH(CH_3)CH_2CH_3$, **A & B**), 4.10-4.16 (1H, m, NHCH, **A**), 4.29-4.31 (1H, m, NHCH, **B**), 4.91-5.02 (2H, m, $CHCH_2CH{=}CH_2$, **A & B**), 5.09 (2H, s, $PhCH_2O$, **A & B**), 5.63-5.81 (2H, m, NH, $CHCH_2CH{=}CH_2$, **A & B**), 6.53 (1H, s, NHC=CHCO, **A**), 6.54 (1H, s, NHC=CHCO, **B**), 7.26-7.35 (5H, m, Ar-H, **A & B**), 8.53 (1H, s, br, NH, **A & B**); δ_C (63 MHz, DEPT, $CDCl_3$) 10.9 ($CH(CH_3)CH_2CH_3$, **A**), 11.4 ($CH(CH_3)CH_2CH_3$, **B**), 14.1 ($CH(CH_3)CH_2CH_3$, **A**), 15.4 ($CH(CH_3)CH_2CH_3$, **B**), 24.0 ($C(C^AH_3C^BH_3)$, **A & B**), 24.4 $CH(CH_3)CH_2CH_3$, **A & B**), 28.5

($C(C^AH_3C^BH_3)$, **A & B**), 30.3 ($CH_2CH=CH_2$, **A & B**), 35.4 ($C(CH_3)_2$, **A & B**), 36.9 ($CH(CH_3)CH_2CH_3$), 41.1 ($NHCCH_2C(CH_3)_2$, **A & B**), 56.6 ($CHCH_2Ph$, **A & B**), 67.2 (NHCH, **A & B**), 67.3 ($PhCH_2$, **A & B**), 110.7 (NHC=CHCO, **A & B**), 115.4 ($CH_2CH=CH_2$, **A & B**), [127.8 (CH), 128.2 (CH), 128.5 (CH), 5C, *Ar*-H, **A & B**], 135.9 ($PhCH_2O$, **A & B**), 137.2 ($CH_2CH=CH_2$, **A & B**), 150.8 (NHC=CH, **A & B**), 151.1 (CONH, **A & B**), 171.1 (NHCHCO, **A & B**), 201.8 (NHC=CHCO, **A & B**); MS ES 427.0 $(M+H)^+$, 425 $(M-H)^-$.

5.2.48 6-allyl-3-(N-α-benzyloxycarbonyl-N-ε-tert-butoxycarbonyl-L-lysyl-amino)-5,5-dimethyl-cyclohex-2-enone (109)

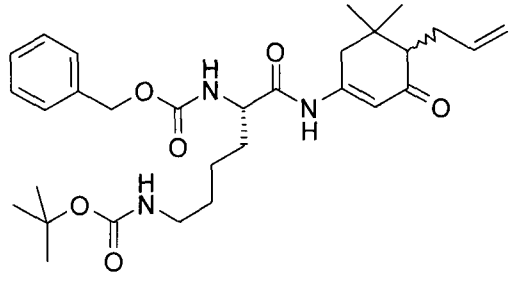

(diastereomers **A & B**)

Experimental procedure 5.2.33 was followed using *N*-α-benzyloxycarbonyl-*N*-ε-*tert*-butoxycarbonyl-L-lysine (0.171g, 0.45 mmol), PyBroP (0.391 g, 0.45 mmol), DMAP (0.073 mg, 0.60 mmol) and **78** (0.054 g, 0.30 mmol) in DCM (10 ml). Flash column chromatography on silica gel using 50 % ethyl acetate in hexane as eluent afforded a white solid (0.143 g, 88 %); δ_H (250 MHz, MeOD) 0.99 (3H, s, $C(C^AH_3C^BH_3)$, **A & B**), 1.06 (3H, s, $C(C^AH_3C^BH_3)$, **A & B**), 1.40 (9H, s, $C(CH_3)_3$, **A & B**), 1.62-1.81 (4H, m, $(CH_2)_2$, **A & B**), 2.05-2.50 (7H, m, $CHCH_2CH=CH_2$, $CH_2C(CH_3)_2$, $CHCH_2CH=CH_2$, CH_2, **A & B**), 2.97-3.02 (2H, m, CH_2, **A & B**), 4.06-4.16 (1H, m, NHCH, **A & B**), 5.06 (2H, s, $PhCH_2O$, **A & B**), 5.75-5.85 (1H, m, $CHCH_2CH=CH_2$), 6.67 (1H, s, NHC=CHCO, **A**), 6.69 (1H, s, NHC=CHCO, **B**), 7.24-7.34 (5H, m, Ar-H, **A & B**); δ_C (63 MHz, DEPT, MeOD) 22.3 ($(CH_2)_2$, **A & B**), 24.7 ($C(CH_3)_2$, **A & B**), 29.6 (CH_2, **A & B**), 30.5 ($CH_2CH=CH_2$, **A & B**), 30.8 ($C(CH_3)_3$, **A & B**), 31.8 (CH_2, **A & B**), 35.5 ($C(CH_3)_2$, **A & B**), 41.0 ($NHCCH_2C(CH_3)_2$, **A & B**), 57.3 ($C(CH_3)_2CH$, **A & B**), 58.1 (NHCH, **A & B**), 67.7 ($PhCH_2O$, **A**), 67.8 ($PhCH_2O$, **B**),

110.9 (HNC=*C*HCO, **A** & **B**), 116.0 (CH_2CH=*C*H_2, **A** & **B**), [128.0 (CH), 128.6 (CH), 128.7 (CH), 5C, *Ar*-H, **A** & **B**], 138.1 (OCH_2*Ph*, **A** & **B**), 138.7 (CH_2*C*H=CH_2, **A** & **B**), 151.2 (NH*C*=CH, **A** & **B**), 156.8 (*C*ONH, **A** & **B**), 158.7 (*C*ONH, **A** & **B**), 171.2 (NHCH*C*O, **A** & **B**), 202.1 (NHC=CH*C*O, **A** & **B**); MS ES (+ve) m/z 542.4 $(M+H)^+$, 564.4 $(M+Na)^+$.

5.2.49 6-allyl-3-(N-benzyloxycarbonyl-L-prolyl-amino)-5,5-dimethyl-cyclohex-2-enone (110)

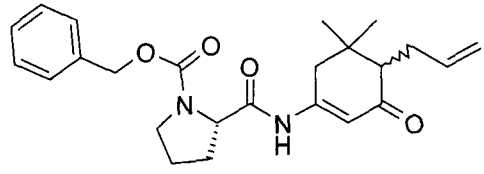

(diastereomers **A** & **B**)

Experimental procedure 5.2.33 was followed using *N*-benzyloxycarbonyl-L-proline (0.209g, 0.84 mmol), PyBroP (0.391 g, 0.84 mmol), DMAP (0.205 mg, 1.68 mmol) and **78** (0.100 g, 0.56 mmol) in DCM (10 ml). Flash column chromatography on silica gel using 40 % ethyl acetate in hexane as eluent afforded a white powder (0.196 g, 85 %); δ_H (360 MHz, $CDCl_3$) 0.99 (3H, s, C($C^AH_3C^BH_3$), **A** & **B**), 1.07 (3H, s, C($C^AH_3C^BH_3$), **A** & **B**), 1.85-2.35 (9H, m, $CH_2C(CH_3)_2$, $CHCH_2CH=CH_2$, $CHCH_2CH=CH_2$, $(CH_2)_2$, **A** & **B**), 3.35-3.52 (CH_2, **A** & **B**), 4.45 (1H, d, J = 7.4, $CH(CH_2)_3$, **A** & **B**), 4.94-5.22 (4H, m, $PhCH_2O$, $CHCH_2CH=CH_2$, **A** & **B**), 5.81-5.89 (1H, m, $CH_2CH=CH_2$, **A** & **B**), 6.59 (1H, s, NHC=C*H*CO, **A** & **B**), 7.36-7.40 (5H, m, Ar-*H*, **A** & **B**), 9.20 (1H, s, N*H*, **A** & **B**); δ_C (90 MHz, DEPT, $CDCl_3$) 24.0 (C($C^AH_3C^BH_3$), **A** & **B**), 24.1 (CH_2, **A** & **B**), 26.4 (CH_2, **A** & **B**), 28.5 (C($C^AH_3C^BH_3$), **A** & **B**), 30.4 ($CHCH_2CH=CH_2$), 41.2 ($NHCCH_2C(CH_3)_2$, **A**), 41.4 ($NHCCH_2C(CH_3)_2$, **B**), 56.7 (*C*HCH_2Ph, **A** & **B**), 60.9 (NH*C*H, **A** & **B**), 67.7 ($PhCH_2O$, **A** & **B**), 110.4 (NHC=C*H*CO, **A** & **B**), 115.3 ($CHCH_2CH=CH_2$), [127.8 (CH), 128.2 (CH), 128.5 (CH), 5C, *Ar*-H, **A** & **B**], 135.9 (*Ph*CH_2O, **A** & **B**), 137.3 ($CHCH_2CH=CH_2$), 151.2 (NH*C*=CH, **A** & **B**), 157.1 (*C*ONH, **A** & **B**), 169.9 (NHCH*C*O, **A** & **B**), 201.6 (NHC=CH*C*O, **A** & **B**); MS ES 411.2 $(M+H)^+$.

5.2.50 *(4-(N-benzyloxycarbonyl-L-valinyl-amino)-6,6-dimethyl-2-oxo-cyclohex-3-enyl)-acetic acid (111)*

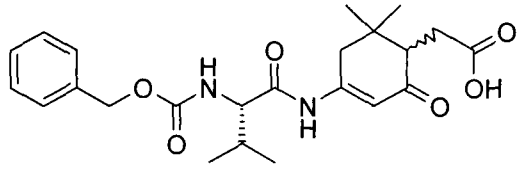

(diastereomers **A** & **B**)

Trifluoroacetic acid (0.05 ml, 0.067 mmol) was added to a solution of **47** (0.06 g, 0.12 mmol) and triethylsilane (0.06 ml, 0.36 mmol) in DCM (3 ml) and the solution stirred at room temperature for 2 hours. The DCM was evaporated *in vacuo* and the residue redissolved in EtOAc (5 ml) and washed with water (1 ml) then dried ($MgSO_4$). The EtOAc solution was concentrated *in vacuo* to give pale yellow oil. Flash column chromatography on silica gel using 50 % ethyl acetate in petroleum ether 40-60 as eluent afforded a white solid (0.043 g, 83 %); δ_H (250 MHz, $CDCl_3$) 0.91 (3H, d, J = 6.8, CH($C^AH_3C^BH_3$), **A** & **B**), 0.95 (3H, d, J = 6.8, CH($C^AH_3C^BH_3$), **A** & **B**), 0.98 (3H, s, C($C^AH_3C^BH_3$), **A** & **B**), 1.08 (3H, s, C($C^AH_3C^BH_3$), **A** & **B**), 2.11-2.52 (6H, m, C*H*CH_2CO_2H, C*H*$(CH_3)_2$, CHC*H*$_2CO_2H$, C*H*$_2C(CH_3)_2$, **A** & **B**), 4.09-4.12 (1H, dd, J = 4.3, 4.5, NHC*H*, **A** & **B**), 5.10 (2H, s, PhC*H*$_2$O, **A** & **B**), 5.56 (1H, d, J = 7.5, N*H*, **A** & **B**), 6.58 (1H, s, NHC=C*H*CO, **A**), 6.61 (1H, s, NHC=C*H*CO, **B**) 7.25-7.29 (5H, m, Ar-*H*, **A** & **B**), 8.26-8.32 (1H, s, br, CO_2H), 8.75 (1H, s, br, N*H*, **A** & **B**); δ_C (63 MHz, DEPT, $CDCl_3$) 18.0 (CH($C^AH_3C^BH_3$), **A** & **B**), 19.1 (CH($C^AH_3C^BH_3$), **A** & **B**), 23.6 (C($C^AH_3C^BH_3$), **A** & **B**), 28.6 (C($C^AH_3C^BH_3$), **A** & **B**), 30.4 (CH_2CO_2H, **A** & **B**), 31.0 ($CH(CH_3)_2$, **A** & **B**), 35.6 ($C(CH_3)_2$, **A** & **B**), 42.4 (NHC$CH_2C(CH_3)_2$, **A** & **B**), 55.5 ($C(CH_3)_2CH$, **A** & **B**), 60.9 (NHCH, **A** & **B**), 67.1 (PhCH_2O, **A** & **B**), 110.9 (HNC=CHCO, **A** & **B**, [128.0 (CH), 128.2 (CH), 128.4 (CH) 5C, *Ar*-H, **A** & **B**], 137.7 (*Ph*CH_2, **A** & **B**), 151.8 (NHC=CH, **A** & **B**), 156.7 (CONH, **A** & **B**), 171.2 (NHCHCO, **A** & **B**), 175.5 (CO_2H), 201.7 (NHC=CHCO, **A** & **B**); HRMS FAB (+ve) m/z 431.2188, $C_{23}H_{31}N_2O_6$ requires 431.2812.

5.2.51 *3-(N-benzyloxycarbonyl-L-valinyl-amino)-6-(2,3-dihydroxy-propyl)-5,5-dimethyl-cyclohex-2-enone (112)*

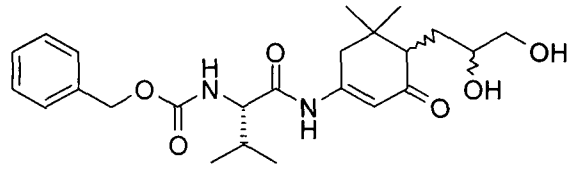

(diastereomers **A** & **B**)

N-Methylmorpholine-*N*-oxide (0.053 g, 0.44 mmol) and osmium tetroxide (0.028 ml, 0.02 mmol) were added to stirred solution of **25** (0.093 g, 0.22 mmol) in acetone (4 ml) and water (1 ml) at 0°C. The reaction mixture was allowed to warm to room temperature and stirred for 2 hours. TLC analysis showed some starting material remaining so further osmium tetroxide (0.028 ml, 0.02 mmol) was added and stirred for 2 hours. The solvent was removed *in vacuo* and the residue redissolved in EtOAc (10 ml) then washed with saturated $Na_2S_2O_3$ solution (5 ml), water (5 ml), dried ($MgSO_4$) and the solvent removed *in vacuo* to give a light brown oil (0.082 g, 84 %); HRMS FAB (+ve) m/z 447.2496, $C_{24}H_{35}N_2O_6$ requires 447.2495.

5.2.52 *(4-(N-benzyloxycarbonyl-L-valinyl-amino)-6,6-dimethyl-2-oxo-cyclohex-3-enyl)-acetaldehyde (113)*

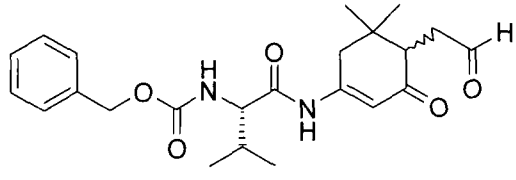

(diastereomers **A** & **B**)

A solution of sodium periodate (0.072 mg, 0.33 mmol) in water (1 ml) was added to a sturred slurry of silica (1 g) in DCM (3 ml) followed by a solution of **51** (0.10 g, 0.22 mmol) in DCM (2 ml). The reaction mixture was stirred at room temperature for 2 hours then filtered, the silica residue then washed with DCM (2 x 2 ml). The combined DCM solution was evaporated *in vacuo* to give a brown oil (0.080 g, 87 %); δ_H (250 MHz, $CDCl_3$) 0.79 (3H, s, $C(C^A\!H_3C^BH_3)$, **A** & **B**), 0.86 (3H, d, J = 7.0,

$CH(C^AH_3C^BH_3)$, **A & B**), 0.89 (3H, d, J = 7.0, $CH(C^AH_3C^BH_3)$, **A & B**), 0.98 (3H, s, $C(C^AH_3C^BH_3)$, **A & B**), 2.14-2.65 (6H, m, $CHCH_2COH$, $CH(CH_3)_2$, $CHCH_2COH$, $CH_2C(CH_3)_2$, **A & B**), 4.04-4.12 (1H, m, br, NHC*H*, **A & B**), 5.02 (2H, s, $PhCH_2O$, **A & B**), 5.56 (1H, d, br, J = 3.0, N*H*, **A & B**), 6.62 (1H, s, NHC=C*H*CO, **A & B**) 7.25-7.30 (5H, m, Ar-*H*, **A & B**), 8.52 (1H, s, br, CO*H*); δ_C (63 MHz, DEPT, $CDCl_3$) 17.9 ($CH(CH_3C^BH_3)$, **A & B**), 19.3 ($CH(C^AH_3CH_3)$, **A & B**), 21.2 ($C(CH_3C^BH_3)$, **A & B**), 29.0 ($C(C^AH_3CH_3)$, **A & B**), 30.5 ($CH(CH_3)_2$, **A & B**), 35.6 ($C(CH_3)_2$, **A & B**), 37.9 ($CHCH_2COH$), 43.6 ($NHCCH_2C(CH_3)_2$, **A & B**), 51.6 ($CHCH_2COH$, **A & B**), 61.6 (NHCH, **A & B**), 67.7 ($PhCH_2O$, **A & B**), 110.8 (NHC=C*H*CO, **A**), 110.9 (NHC=C*H*CO, **B**), [127.9 (CH), 128.3 (CH), 128.4 (CH), 128.6 (CH), 5C, *Ar*-H, **A & B**], 135.8 ($PhCH_2O$, **A & B**), 152.3 (NHC=CH, **A & B**), 157.1 (CONH, **A & B**), 171.4 (NHCHCO, **A & B**), 199.4 (COH, **A & B**), 201.4 (NHC=CHCO, **A & B**); HRMS FAB (+ve) m/z 415.2231, $C_{23}H_{31}N_2O_5$ requires 415.2233.

5.2.53 6-allyl-3-(L-valinyl-amino)-5,5-dimethyl-cyclohex-2-enone (114)

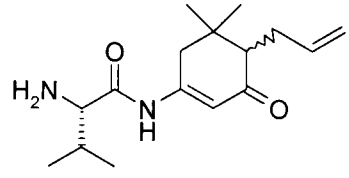

(diastereomers **A & B**)

Iodotrimethylsilane (0.54 ml, 3.78 mmol) was added to a stirred solution of **82** (1.3 g, 3.15 mmol) in MeCN (10 ml) at room temperature. After 30 minutes, MeOH (3 ml) mixed with aq. 2M HCl (1 ml) was added and the solution stirred for 10 minutes. The solvent was then evaporated *in vacuo* and the residue redissolved in EtOAc (20 ml) and washed with saturated $NaHCO_3$ solution (2 x 5 ml). The EtOAc layer was then extracted with dilute acetic acid (30 %, 3 x 5 ml), the combined aqueous layer evaporated *in vacuo* to yield a white solid (0.737 g, 84 %); δ_H (250 MHz, MeOD) 1.00 (3H, d, J = 7.0, $CH(C^AH_3C^BH_3)$, **A & B**), 1.03 (3H, s, $C(C^AH_3C^BH_3)$, **A & B**), 1.07 (3H, d, J = 7.0, $CH(C^AH_3C^BH_3)$, **A & B**), 1.09 (3H, s, $C(C^AH_3C^BH_3)$, **A & B**), 2.07-2.51 (6H, m, br, $CH_2C(CH_3)_2$ $CH(CH_3)_2$, $CHCH_2CH=CH_2$, $CHCH_2CH=CH_2$, **A & B**), 3.50-3.64 (1H, m, NH_2CH, **A & B**), 4.96-5.03 (2H, m, $CHCH_2CH=CH_2$, **A &**

B), 5.73-5.84 (1H, m, $CHCH_2CH{=}CH_2$, **A** & **B**), 6.72 (1H, s, NHC=C*H*CO, **A**), 6.76 (1H, s, NHC=C*H*CO, **B**); δ_C (63 MHz, DEPT, DMSO) 17.5 ($CH(C^AH_3C^BH_3)$, **A** & **B**), 19.1 ($CH(C^AH_3C^BH_3)$, **A** & **B**), 21.1 ($C(C^AH_3C^BH_3)$, **A** & **B**), 28.8 ($C(C^AH_3C^BH_3)$, **A** & **B**), 31.9 ($CH_2CH{=}CH_2$, **A** & **B**), 31.9 ($CH(CH_3)_2$, **A** & **B**), 36.5 ($C(CH_3)_2$, **A** & **B**), 41.7 ($NHCCH_2C(CH_3)_2$, **A** & **B**), 57.1 ($C(CH_3)_2CH$, **A** & **B**), 60.4 (NH_2CH, **A** & **B**), 111.2 (HNC=CHCO, **A** & **B**), 116.0 ($CH_2CH{=}CH_2$, **A** & **B**), 137.7 ($CH_2CH{=}CH_2$, **A** & **B**), 151.4 (NHC=CH, **A** & **B**), 156.8 (CONH, **A** & **B**), 169.9 (NHCHCO, **A** & **B**), 201.7 (NHC=CHCO, **A** & **B**); MS ES 279.0 $(M+H)^+$, 277.0 $(M-H)^-$

5.2.54 Reductive amination array (1x9) synthesis

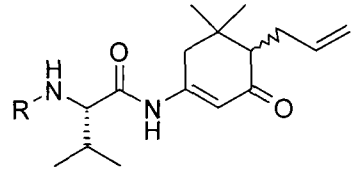

Table 5.3 Reagents

Reagent	No.Moles in stock solution (mmol)	MeOH stock sol. volume (ml)	No. Moles Dispensed (mmol)	MeOH Volume Dispensed (ml)
ligand **114**	1.1	9.0	0.12	1.0
aldehyde	-	-	0.10	-
PS-CBH	-	-	0.20	-
benzaldehyde resin	-	-	0.20	-

The reagents were prepared as in table 5.2. The ligand **114** solution (1.0 ml) was manually dispensed into each of the 9 tubes being used in the MiniBlock. The aldehyde derivatives were manually added to the individual MiniBlock tubes followed by 4Å molecular sieves, the MiniBlock was then shaken on the Shaking and Washing Station for 1 hour. The Miniblock was removed from the shaker station and (polystyrylmethyl)trimethylammonium cyanoborohydride was manually added to

each of the 9 tubes being used, the MiniBlock was then shaken overnight. The Miniblock was removed from the shaker and 4-benzyloxybenzaldehyde polystyrene resin was added and the MiniBlock shaken overnight. The MiniBlock was drained into a 48 well plate, the crude solutions were then subject to purification using the Biotage Parallex Flex preparative HPLC system.

Table 5.4 Array products

Ligand	Structure	Yield and Analysis
115	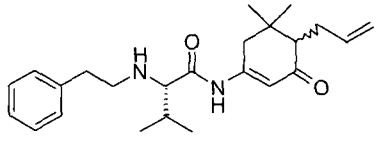 (diastereomers **A** & **B**)	0.021 g, 54 %; δ_H (250 MHz, $CDCl_3$) 0.99-1.09 (12H, m, $CH(CH_3)_2$, $C(CH_3)_2$, **A** & **B**), 2.12-2.43 (6H, m, $CH(CH_3)_2$, $CH_2C(CH_3)_2$, $CHCH_2CH{=}CH_2$, $CHCH_2CH{=}CH_2$, **A** & **B**), 3.01-3.17(4H, m, br, $Ph(CH_2)_2NH$, **A** & **B**), 4.33-4.35 (1H, m, br, NHC*H*, **A** & **B**), 4.91-5.03 (2H, m, $CHCH_2CH{=}CH_2$, **A** & **B**), 5.78-5.89 (1H, m, $CHCH_2CH{=}CH_2$, **A** & **B**), 7.09-7.31 (6H, m, Ar-*H*, NHC=C*H*CO, **A** & **B**), 10.01 (1H, s, br, N*H*); MS ES (+ve) m/z 383.1 $(M+H)^+$.
116	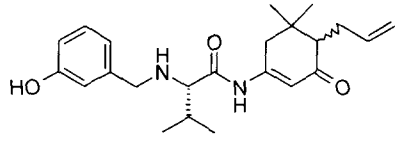 (diastereomers **A** & **B**)	0.020 g, 52 %; δ_H (250 MHz, MeOD) 0.98-1.08 (12H, m, $CH(CH_3)_2$, $C(CH_3)_2$, **A** & **B**), 2.07-2.37 (6H, m, $CH(CH_3)_2$, $CH_2C(CH_3)_2$, $CHCH_2CH{=}CH_2$, $CHCH_2CH{=}CH_2$, **A** & **B**), 3.42-3.44 (2H, m, $ArCH_2NH$, **A** & **B**), 3.65-3.72 (1H, m, NHC*H*, **A** & **B**), 4.07-4.23 (2H, m, $ArCH_2NH$, **A** & **B**), 5.01-5.13 (1H, m, $CHCH_2CH{=}CH_2$, **A** & **B**), 5.74-5.85 (1H, m, $CHCH_2CH{=}CH_2$), 6.76 (1H, s, NHC=C*H*CO, **A**), 6.78 (1H, s, NHC=C*H*CO, **B**), 6.96-7.01 (2H, m, Ar-*H*, **A** & **B**), 7.19-7.26 (1H, m Ar-*H*, **A** & **B**), 7.37-7.41 (1H, m, Ar-*H*, **A** & **B**); MS ES (+ve) m/z 385.1 $(M+H)^+$.
117	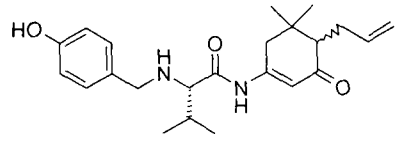 (diastereomers **A** & **B**)	0.021 g, 53 %; δ_H (250 MHz, MeOD) 0.99-1.08 (12H, m, $CH(CH_3)_2$, $C(CH_3)_2$, **A** & **B**), 2.09-2.34 (6H, m, $CH(CH_3)_2$, $CH_2C(CH_3)_2$, $CHCH_2CH{=}CH_2$, $CHCH_2CH{=}CH_2$, **A** & **B**), 3.40-3.43 (2H, m, $ArCH_2NH$, **A** & **B**), 3.66-3.74 (1H, m, NHC*H*, **A** & **B**), 4.10-4.24 (2H, m, $ArCH_2NH$, **A** & **B**), 5.04-5.15 (1H, m, $CHCH_2CH{=}CH_2$, **A** & **B**), 5.78-5.87 (1H, m, $CHCH_2CH{=}CH_2$), 6.81 (1H, s, NHC=C*H*CO, **A** & **B**), 6.96-7.01 (2H, m, Ar-*H*, **A** & **B**), 7.19-7.26 (2H, m Ar-*H*, **A** & **B**); MS ES (+ve) m/z 385.1 $(M+H)^+$.

118	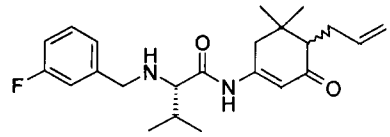 (diastereomers **A** & **B**)	0.023 g, 60 %; δ_H (250 MHz, MeOD) 1.00-1.07 (12H, m, CH(CH_3)$_2$, C(CH_3)$_2$, **A** & **B**), 2.07-2.14 (1H, m, CHCH$_2$CH=CH$_2$, **A** & **B**), 2.21-2.48 (5H, m, CH(CH$_3$)$_2$, CH_2C(CH$_3$)$_2$, CHCH_2CH=CH$_2$, **A** & **B**), 3.76-3.79 (1H, m, NHCH, **A** & **B**), 4.10-4.25 (2H, m, ArCH_2NH, **A** & **B**), 4.92-5.00 (1H, m, CHCH$_2$CH=CH_2), 5.73-5.85 (1H, m, CHCH$_2$CH=CH$_2$), 6.61 (1H, s, NHC=CHCO, **A**), 6.63 (1H, s, NHC=CHCO, **B**), 7.16-7.40 (4H, m, Ar-H, **A** & **B**); MS ES (+ve) m/z 387.1 $(M+H)^+$, 409.0 $(M+Na)^+$.
119	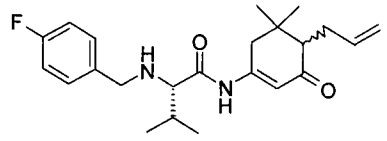 (diastereomers **A** & **B**)	0.021 g, 54 %; δ_H (250 MHz, MeOD) 0.99-1.06 (12H, m, CH(CH_3)$_2$, C(CH_3)$_2$, **A** & **B**), 2.07-2.13 (1H, m, CHCH$_2$CH=CH$_2$, **A** & **B**), 2.23-2.40 (5H, m, CH(CH$_3$)$_2$, CH_2C(CH$_3$)$_2$, CHCH_2CH=CH$_2$, **A** & **B**), 3.76-3.81 (1H, m, NHCH, **A** & **B**), 4.17-4.23 (2H, m, ArCH_2NH, **A** & **B**), 4.94-5.02 (1H, m, CHCH$_2$CH=CH_2), 5.72-5.83 (1H, m, CHCH$_2$CH=CH$_2$), 6.59 (1H, s, NHC=CHCO, **A**), 6.61 (1H, s, NHC=CHCO, **B**), 7.11-7.18 (2H, m, Ar-H, **A** & **B**), 7.42-7.53 (2H, m, Ar-H, **A** & **B**); MS ES (+ve) m/z 387.1 $(M+H)^+$, 409.0 $(M+Na)^+$.
120	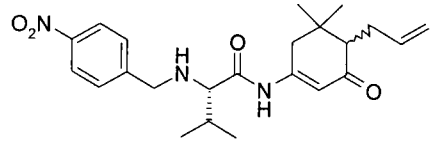 (diastereomers **A** & **B**)	0.026 g, 62 %; δ_H (250 MHz, MeOD) 0.97-1.08 (12H, m, CH(CH_3)$_2$, C(CH_3)$_2$, **A** & **B**), 2.05-2.12 (1H, m, CHCH$_2$CH=CH$_2$, **A** & **B**), 2.23-2.46 (5H, m, CH(CH$_3$)$_2$, CH_2C(CH$_3$)$_2$, CHCH_2CH=CH$_2$, **A** & **B**), 3.84-3.88 (1H, m, NHCH, **A** & **B**), 4.34 (2H, dd, J = 4.3, 13.2, ArCH_2NH, **A** & **B**), 4.94-5.03 (1H, m, CHCH$_2$CH=CH_2), 5.72-5.83 (1H, m, CHCH$_2$CH=CH$_2$), 6.57 (1H, s, NHC=CHCO, **A**), 6.69 (1H, s, NHC=CHCO, **B**), 7.56 (1H, d, J = 8.7, Ar-H, **A** & **B**), 7.72 (1H, d, J = 8.7, Ar-H, **A** & **B**), 8.21 (1H, d, J = 8.7, Ar-H, **A** & **B**), 8.26 (1H, d, J = 8.7, Ar-H, **A** & **B**); MS ES (+ve) m/z 436.1 $(M+Na)^+$.
121	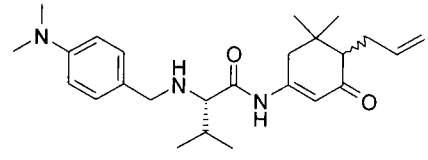 (diastereomers **A** & **B**)	0.022 g, 53 %; δ_H (250 MHz, MeOD) 0.94-1.04 (12H, m, CH(CH_3)$_2$, C(CH_3)$_2$, **A** & **B**), 2.03-2.46 (6H, m, CH(CH$_3$)$_2$, CH_2C(CH$_3$)$_2$, CHCH_2CH=CH$_2$, CHCH$_2$CH=CH$_2$, **A** & **B**), 2.93 (3H, s, (CH_3)$_2$N, **A**), 2.94 (3H, s, (CH_3)$_2$N, **B**), 3.78-3.82 (1H, m, NHCH, **A** & **B**), 4.17-4.23 (2H, m, ArCH_2NH, **A** & **B**), 4.97-5.05 (1H, m, CHCH$_2$CH=CH_2), 5.69-5.86 (1H, m, CHCH$_2$CH=CH$_2$), 6.51 (1H, s, NHC=CHCO, **A**), 6.53 (1H, s, NHC=CHCO, **B**), 6.81 (2H, d, J = 7.3, Ar-H, **A** & **B**), 7.32 (2H, d, J = 7.3, Ar-H, **A** & **B**); MS ES (+ve) m/z 412.1 $(M+H)^+$.

122	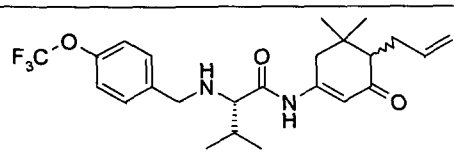 (diastereomers **A** & **B**)	0.027 g, 59 %; δ_H (250 MHz, MeOD) 0.98-1.06 (12H, m, CH(CH_3)$_2$, C(CH_3)$_2$, **A** & **B**), 2.06-2.13 (1H, m, C*H*CH_2CH=CH_2, **A** & **B**), 2.27-2.39 (5H, m, C*H*(CH_3)$_2$, CH_2C(CH_3)$_2$, CHCH_2CH=CH_2, **A** & **B**), 3.84 (1H, dd, J = 1.3, 4.6, NHC*H*, **A** & **B**), 4.19-4.30 (2H, m, ArCH_2NH, **A** & **B**), 4.95-5.04 (1H, m, CHCH$_2$CH=CH_2), 5.73-5.85 (1H, m, CHCH$_2$C*H*=CH_2), 6.61 (1H, s, NHC=C*H*CO, **A**), 6.62 (1H, s, NHC=C*H*CO, **B**), 7.30 (2H, d, J = 8.7, Ar-*H*, **A** & **B**), 7.61 (2H, d, J = 8.7, Ar-*H*, **A** & **B**); MS ES (+ve) m/z 453.1 $(M+H)^+$.
123	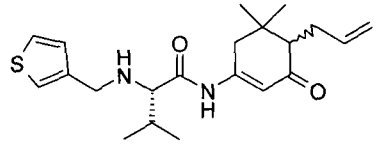 (diastereomers **A** & **B**)	0.017 g, 46 %; δ_H (250 MHz, $CDCl_3$) 1.00 (3H, d, J = 6.9, CH($C^AH_3C^BH_3$), **A** & **B**), 1.02 (3H, d, J = 6.9, CH($C^AH_3C^BH_3$), **A** & **B**), 1.07 (3H, s, C($C^AH_3C^BH_3$), **A** & **B**), 1.09 (3H, s, C($C^AH_3C^BH_3$), **A** & **B**), 2.08-2.41 (6H, m, C*H*(CH_3)$_2$, CH_2C(CH_3)$_2$, C*H*CH_2CH=CH_2, CHCH_2CH=CH_2, **A** & **B**), 4.02 (1H, dd, J = 2.0, 4.5, NHC*H*, **A** & **B**), 4.40-4.48 (2H, m, CHCH$_2$CH=CH_2), 4.93-5.02 (3H, m, ArCH_2, N*H*, **A** & **B**), 5.73-5.84 (1H, m, CHCH$_2$C*H*=CH_2), 6.64 (1H, s, NHC=C*H*CO, **A**), 6.66 (1H, s, NHC=C*H*CO, **B**), 7.06 (1H, d, J = 5.1, Ar-*H*, **A**), 7.08 (1H, d, J = 5.1, Ar-*H*, **B**), 7.24-7.26 (1H, m, Ar-*H*, **A** & **B**), 7.56 (1H, d, J = 5.1, Ar-*H*, **A**), 7.57 (1H, d, J = 5.1, Ar-*H*, **B**); MS ES (+ve) m/z 375.0 $(M+H)^+$.

5.2.55 Attempted preparation of 6-allyl-3-(N-fluorescein-thiourea-L-valinyl-amino)-5,5-dimethyl-cyclohex-2-enone

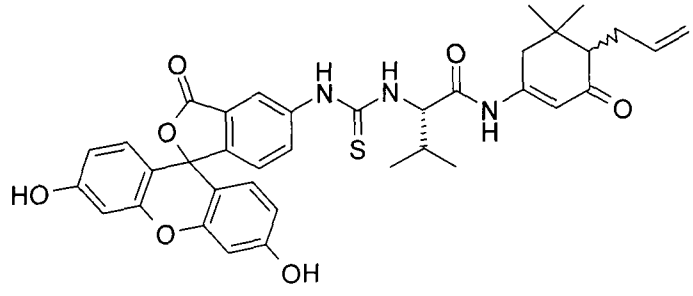

Fluorescein isothiocyanate isomer 1 (0.056 g, 0.14 mmol) and **61** (0.040 g, 0.14 mmol) were dissolved in DMF (1 ml) and stirred at room temperature for 1 hour. Water (2 ml) and EtOAc (2 ml) were added, the aqueous layer separated and extracted with EtOAc (2 x 3 ml). The combined organic layers were dried ($MgSO_4$) and evaporated *in vacuo* to give a yellow oil. TLC analysis (50 % EtoAc in

petroleum ether 40-60) indicated the presence of two distinct compounds. One corresponded to fluorescein isothiocyante (R_f 0.6), this was supported by mass spectroscopy (MS ES 390 $(FITC+H)^+$, 388 $(FITC-H)^-$). Analysis by mass spectroscopy of the second compound (R_f 0.4) indicated a mass of 487 (M-**23**).

5.2.56 6-allyl-3-(N-dansyl-L-valinyl-amino)-5,5-dimethyl-cyclohex-2-enone (126)

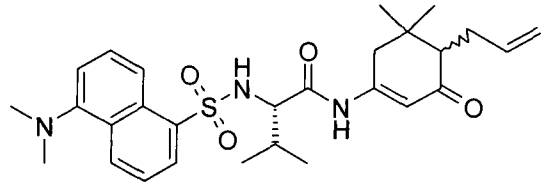

(diastereomers **A** & **B**)

Dansyl-L-valine cyclohexylammonium salt (0.125 g, 0.36 mmol) was dissolved in EtOAc (5 ml) and washed with 2M $KHSO_4$ solution (3 x 3 ml) to remove the cyclohexylamine. The combined aqueous layers were washed with EtOAc (5 ml), the organic phases combined and the solvent evaporated *in vacuo* to give a yellow oil. The oil was dissolved in DCM (2 ml) and PyBroP (0.168 g, 0.36 mmol) and DMAP (0.088 g, 0.72 mmol) were added. The solution was stirred at room temperature for 5 minutes then **78** (0.045 g, 0.25 mmol) was added. After 1 hour the DCM was evaporated *in vacuo* and the residue redissolved in EtOAc (5 ml) and water (2 ml). The organic layer was separated and washed with 1M $KHSO_4$ solution (2 ml), water (2 ml), saturated $NaHCO_3$ solution (2 ml), water (2 ml), dried ($MgSO_4$) and the solvent removed *in vacuo* to give a yellow oil. Flash column chromatography on silica gel using 30 % ethyl acetate in petroleum ether 40-60 as eluent afforded a yellow solid (0.101 g, 79 %). δ_H (250 MHz, $CDCl_3$) 0.67 (3H, d, J = 6.8, $CH(C^AH_3C^BH_3)$, **A**), 0.68 (3H, d, J = 6.8, $CH(C^AH_3C^BH_3)$, **B**), 0.77 (3H, d, J = 6.8, $CH(C^AH_3C^BH_3)$, **A** & **B**), 0.83 (3H, s, $C(C^AH_3C^BH_3)$, **A**), 0.84 (3H, s, $C(C^AH_3C^BH_3)$, **B**), 0.93 (3H, s, $C(C^AH_3C^BH_3)$, **A**), 0.94 (3H, s, $C(C^AH_3C^BH_3)$, **B**), 1.88-2.25 (6H, m, $CH(CH_3)_2$, $CHCH_2CH{=}CH_2$, $CHCH_2CH{=}CH_2$, $CH_2C(CH_3)_2$, **A** & **B**), 2.86 (6H, s, $N(CH_3)_2$, **A** & **B**), 3.67 (1H, dd, J = 5.2, 7.7, NHC*H*, **A** & **B**), 4.91-5.00 (2H, m, $CHCH_2CH{=}CH_2$, **A** & **B**), 5.64-5.84 (2H, m, N*H*, $CHCH_2CH{=}CH_2$, **A** & **B**), 6.14 (1H, s, NHC=C*H*CO, **A**), 6.17 (1H, s, NHC=C*H*CO, **B**), 7.19 (1H, d, J = 7.5, Ar-*H*,

A & B), 7.49 (1H, dd, *J* = 7.4, 8.5, Ar-*H*, **A & B**), 7.60 (1H, dd, *J* = 7.5, 8.6, Ar-*H*, **A & B**), 7.91 (1H, s, N*H*, **A**), 7.94 (1H, s, N*H*, **B**), 8.23 (1H, d, *J* = 7.4, Ar-*H*, **A**), 8.24 (1H, d, *J* = 7.4, Ar-*H*, **B**), 8.32 (1H, d, *J* = 8.6, Ar-*H*, **A & B**), 8.53 (1H, d, *J* = 8.5, Ar-*H*, **A & B**); δ_C (90 MHz, DEPT, $CDCl_3$) 17.1 (CH($C^AH_3C^BH_3$), **A**), 17.2 (CH($C^AH_3C^BH_3$), **B**), 18.7 (CH($C^AH_3C^BH_3$), **A**), 18.9 (CH($C^AH_3C^BH_3$), **B**), 23.7 ($C(C^AH_3C^BH_3)$, **A**), 24.0 ($C(C^AH_3C^BH_3)$, **B**), 28.3 ($C(C^AH_3C^BH_3)$, **A**), 28.4 ($C(C^AH_3C^BH_3)$, **B**), 30.1 ($CH_2CH{=}CH_2$, **A**), 30.3 ($CH_2CH{=}CH_2$, **B**), 30.6 ($CH(CH_3)_2$, **A & B**), 35.1 ($C(CH_3)_2$, **A**), 35.2 ($C(CH_3)_2$, **B**), 40.5 ($NHCCH_2C(CH_3)_2$, **A & B**), 40.8 ($NHCCH_2C(CH_3)_2$, **B**), 45.2 ($N(CH_3)_2$, **A**), 45.3 ($N(CH_3)_2$, **B**), 56.5 ($C(CH_3)_2CH$, **A**), 56.6 ($C(CH_3)_2CH$, **B**), 63.1 (NHCH, **A & B**), 110.3 (HNC=CHCO, **A**), 110.4 (HNC=CHCO, **B**), 115.2 (*Ar*-H, **A**), 115.3 (*Ar*-H, **B**), 115.4 ($CH_2CH{=}CH_2$, **A**), 115.5 ($CH_2CH{=}CH_2$, **B**), 118.0 (*Ar*-H, **A & B**), 123.0 (*Ar*-H, **A & B**), 128.8 (*Ar*-H, **A**), 128.9 (*Ar*-H, **B**), 129.4 ($(CH_3)_2NC$, **A**), 129.5 ($(CH_3)_2NC$, **B**), 130.2 (*Ar*-H, **A & B**), 131.3 (CSO_2, **A**), 133.4 (CSO_2, **B**), 137.2 ($CH_2CH{=}CH_2$, **A**), 137.4 ($CH_2CH{=}CH_2$, **B**), 150.9 (NHC=CH, **A**), 151.0 (NHC=CH, **B**), 169.7 (NHCHCO, **A & B**), 201.8 (NHC=CHCO, **A**), 201.9 (NHC=CHCO, **B**); HRMS EI (+ve) m/z 512.2580, $C_{28}H_{37}N_3O_4S$ requires 512.2583.

References

(1) L. A. Carpino, E. -S. Mansour, D. Sadat-Aalaee, *J. Org. Chem.*, **1991**, *56*, 2611.

(2) C. M. Stevens, R. Watanabe, *J. Am. Chem. Soc.*, **1950**, *72*, 725.

(3) N. Berry, M. Davey, L. Harwood, *Synthesis*, **1986**, 476.

(4) T. Nishio, Y. Omote, *Synthesis*, **1980**, *12*, 1013.

(5) P.G.Baraldi, D. Simoni, S. Manfredini, *Synthesis*, **1983**, 903.

(6) M. Azzaro, S. Geribaldi, B. Videau, *Synthesis*, **1981**, 880.

(7) G. Sennyey, G. Barcelo, J. -P. Senet, *Tetrahedron Lett.*, **1987**, *28*, 5809.